Self-Evaluation

FY2006 Contractor Performance Evaluation and Measurement Plan

For

Management and Operation of the

Stanford Linear Accelerator Center

Volume 1, Science and Technology, Goals 1.0 – 3.0

SUBMITTED TO THE U.S. DEPARTMENT OF ENERGY

OCTOBER 27, 2006

Table of Contents

Executive Summary

The principal mission of SLAC is to perform excellent science using cutting edge instruments. Our original mission was to perform excellent science in particle physics and particle accelerator technology design and development. In the 1970s that mission expanded to include the first photon science experiments with the development of SPEAR. Our mission has since expanded to include particle astrophysics and ultrafast science as well as advanced computing, especially for ultrafast transmission, storage and analysis of the vast data sets collected by the experimental instruments at SLAC. The following sections describe the work at SLAC in more detail, highlighting the accomplishments of the past fiscal year, FY2006. As ever, our mission continues to be to perform outstanding science, as well as computing, technology and engineering development.

The self-evaluation covers goals 1.0 – 3.0 from Appendix B, Contractor Performance Evaluation and Measurement Plan from the contract for the management and operations of SLAC. In the attached reports SLAC is proud of its scientific accomplishments and believes its high grades are well justified. The grades are as follows

Goal 1.0, Provide of Efficient and Effective Mission Accomplishments: A
Goal 2.0, Provide for Efficient and Effective Design, Fabrication, Construction and Operations of Research Facilities: B+
Goal 3.0, Provide Effective and Efficient Science and Technology Program Management A

Detailed Evaluation

Goal 1.0, Provide of Efficient and Effective Mission Accomplishments:

ELEMENT	Letter Grade	Numerical Score	Objective Weight (HEP)	Total Points	Total Points
1.0 Provide of Efficient and Effective Mission Accomplishments:					
1.1 Science and Technology Results Provide Meaningful Impact on the Field	A	4.0	30%	1.2	
1.2 Provide Quality Leadership in Science and Technology	A	4.0	30%	1.2	
1.3 Provide and Sustain Science and Technology Outputs that Advance Program Objectives and Goals	Pass	4.3	30%	1.29	
1.4 Provide for Effective Delivery of Science and Technology	Pass	4.3	10%	.43	
				Performance Goal 1.0 Total	4.09

Goal 2.0, Provide for Efficient and Effective Design, Fabrication, Construction and Operations of Research Facilities

ELEMENT	Letter Grade	Numerical Score	Objective Weight (HEP)	Total Points	Total Points
2.0 Provide for Efficient and Effective Design, Fabrication, Construction and Operations of Research Facilities					
2.1 Provide Effective Facility Designs as Required to Support Laboratory programs.	B+	3.4	20%	0.68	
2.2 Provide Effective and Efficient Construction of Facilities	B+	3.4	0%	0.0	
2.3 Provide Efficient and Effective Operation of Facilities	B+	3.4	80%	2.72	
2.4 Effective Utilization of Facilities to Grow and Support the Laboratory's Research Base	B+	3.4	0%	0.0	
				Performance Goal 2.0 Total	3.40

Goal 3.0, Provide Effective and Efficient Science and Technology Program Management

ELEMENT	Letter Grade	Numerical Score	Objective Weight (HEP)	Total Points	Total Points
3.0 Provide Effective and Efficient Science and Technology Program Management					
3.1 Provide Effective and Efficient Stewardship of Scientific Capabilities and Program Vision.	A	4.0	40%	1.6	
3.2 Provide Effective and Efficient Science and Technology Project/Program Planning and Management	A	4.0	40%	1.6	
3.3 Provide Efficient and Effective communications and Responsiveness to Customer Needs	A	4.0	20%	0.8	
				Performance Goal 3.0 Total	4.0

1. FY06 PROGRESS FOR PEP-II by John Seeman, Michael Sullivan, and Uli Wienands

General statements: PEP-II is a particle beam accelerator which collides 1722 bunches of electrons with 1722 bunches of positrons in two countercirculating storage rings to produce continuous luminosity to make B mesons in the BaBar physics detector. It is called a B-Factory. Each bunch contains about 100 billion particles. Each bunch collides on every turn of the accelerator or about 136,300 times per second.

Construction and installation of PEP-II was completed within budget in early July 1998. First collisions were observed in late July 1998 that was two months ahead of the final PEP-II DOE construction milestone. The BaBar detector was installed in May 1999. PEP-II has been delivering luminosity to BaBar nearly continuously over the past seven years. PEP-II exceeded its design luminosity (3×10^{33} $cm^{-2}s^{-1}$) in October 2000 by achieving 3.30×10^{33} $cm^{-2}s^{-1}$. Through steady progress, PEP-II has now exceeded, on August 16, 2006, over four times its design luminosity reaching 1.207×10^{34} $cm^{-2}s^{-1}$. The peak integrated luminosity in 24 hours has reached 911 pb^{-1} which is seven times the design of 130 pb^{-1} per day.

End of PEP-II Run 5a in early FY2006: The end of Beam Run 5a was from October 1 through 10 where PEP-II delivered luminosity to BaBar and did extra accelerator studies to increase the peak luminosity. This beam run in early FY2006 achieved several milestones for the PEP-II program. PEP-II exceeded 3.3 times its design luminosity on October 9, 2005, by achieving 1.003×10^{34} $cm^{-2}s^{-1}$. This luminosity level corresponds to giving BaBar over 1 million new particle physics events every day! This very high luminosity was reached using 1732 bunches with 2940 mA of positrons and 1740 mA of electrons, both record beam currents at the time. The vertical and horizontal beam sizes at the interaction region were about 4.0 by 125 microns, respectively. Furthermore, PEP-II delivered 728 pb^{-1} in one day to BaBar in early October 2004.

Installation period October 10 through November 15, 2005: There was an installation period for PEP-II where several new components were installed or upgraded and the overall accelerator safety systems were recertified. The original vacuum chambers in PEP-II (arcs and straights) were designed to handle twice the LER current and four times the HER current. However, to reach these higher currents the interaction region vacuum chambers need upgrading. Two of these chambers were exchanged. Several NEG pumps were removed from LER interaction region vacuum chambers which were being heated by beam Higher Order Modes (HOMs). All safety systems were checked.

PEP-II Operation: The operation of PEP-II collider (Run 5b) started in mid-November 2005, and ran until August 18, 2006. Over 100 fb^{-1} of data on and near the Upsilon 4S resonance were delivered to BaBar in FY2006.

The luminosity increases over the past year have come from several factors. Reducing βy^*s from 11 to about 10 mm increased the luminosity by about 10%. The bunch spacing has been changed from the "By-2" (a bunch every second RF bucket) with mini-gaps to a full "By-2" without mini-gaps. This configuration has only one gap of about 15 missing bunches which is used as an abort gap. This "By-2" spacing has some (anticipated) parasitic crossing effects but the adverse affects were measured to be below a few percent in the luminosity, consistent with our beam-beam

computer simulations. The new bunch spacing allowed more bunches to be collided which also allowed the beam currents to be increased with constant bunch current. The higher beam currents with the new RF stations are now about 2950 mA in the LER and 1900 mA in the HER. Both of these currents are world records for electron and positron storage rings. The betatron tunes were optimized near the half integer reducing the effects of the beam-beam interaction.

Much work has gone into improving the optical magnet lattice for both rings. This work has improved the machine performance by reducing the "beta" errors around the rings. The horizontal tunes have been moved closer to the half integer resonance allowing even higher beam-beam tune shifts. As a result, the specific luminosity (luminosity divided by the product of the beam currents) was at an all time high and was the cause of the most significant gain in the luminosity this past year. The optics-lattice group has done an excellent job.

Trickle injection was a great improvement for PEP-II in FY2004 and continued to improve in FY2005 and FY2006. An example of a good day with trickle injection is shown in the first figure below. Trickle injection for positrons uses about ten injection pulses per second from the linac, resulting in the positron current being stable to about 0.1%. The HER injection of electrons is about five Hz. The SLAC linac was designed to allow up to 40 injected positron pulses and also 40 electron pulses each second in any order, although fewer pulses are in fact actually needed. Thus, PEP-II has true trickle injection with very steady currents and steady luminosity. BaBar records better than 98% of the data in the trickle running mode. The PEP-II and BaBar groups are all very pleased with this improvement. All data taking is now with continuous injection.

There were five interrupting events in Run 5b: four of which needed vacuum intervention. 1) A gap ring for a vacuum flange in the Low Energy Ring (LER) in PEP-II Region 4 started to arc with the higher positron beam current. This gap ring was changed, fixing the problem. 2) The high power bellows near the Q2 magnet shared between the HER and LER ring in the interaction region developed an arc near the HOM absorbing tiles and the associated "Omega" RF seal. These two bellows were removed and a new Omega seal used to fix the problem was designed, built, and installed. 3) At high current two Beam Position Monitor (BPM) button heads in the LER physically dropped off near the interaction region. This problem has been seen before in FY2005 and has been carefully controlled since then. These button heads were successfully removed. For a global cure, all the LER BPMs in the interaction region and the dipole arcs will be replaced or removed during the Fall 2006 down, completely fixing this problem. 4) At high current an expansion bellows unit and three Omega seals in the High Energy Ring (HER) were damaged. These related problems are being addressed during the Fall 2006 down. 5) Finally, on August 18 during an accelerator machine studies period, a special bunch pattern (By-4) was used to study high bunch charge beam-beam effects and caused overheating in a cable near the transverse feedback kicker, subsequently causing a small cable fire. The fire was promptly and safety extinguished. The cause of the cable heating is now understood and will be fixed before the next run starts in January 2007.

The beam run in the FY2006 achieved new records in all performance milestones for the PEP-II program. PEP-II exceeded 4 times its design luminosity this year (August 16, 2005) by achieving 1.207×10^{34} $cm^{-2}s^{-1}$. This very high luminosity was reached using 1722 bunches with 2900 mA of positrons and 1875 mA of electrons, both record beam currents. The vertical and horizontal beam sizes at the interaction region were about 3.8 by 130 microns, respectively. Furthermore, PEP-II

delivered 911 pb^{-1} in one day to BaBar in July 2006. This rate is 7 times the design delivered luminosity per day of 130 pb^{-1}/day. Thus, the luminosity delivery efficiency is excellent. The total integrated luminosity delivered to BaBar in FY2006 was 100.3 fb^{-1}, bringing a total so far of 410 fb^{-1} for the life of PEP-II.

The achievements of FY2006 for PEP-II can be seen in the nine figures below. The first figure shows a good day with trickle injection, stable beam currents and steady luminosity. The next figure shows the peak luminosity in each month since PEP-II started up with BaBar in May of 1999. Note that the PEP-II luminosity passed 1.2 x $10^{34}/cm^2/s$ on August 16, 2006. The next figure shows the daily integrated luminosity indicating PEP-II can deliver solidly over 800 pb^{-1} per day. The next figure shows the daily average luminosity each month with August 2006 being by far the best month. The next figure shows the monthly integrated luminosity for PEP-II since the collider started operation FY1999. Over 19.3 fb^{-1} has been delivered to BaBar in a 30 day period in July 2006. The next plot shows the total integrated luminosity with time over Run 5a and Run 5b indicating a total of 153.8 fb^{-1} over that time. The following plot shows the total integrated luminosity since May 1999 indicating that PEP-II has delivered to BaBar over 410 fb^{-1}. The next table shows the operational records of PEP-II, highlighting our peak luminosity of over 1.2 x $10^{34}/cm^2/s$. The final chart shows our integrated luminosity and run time statistics for the four fiscal quarters of FY2006.

PEP-II installation in August and September 2006: PEP-II entered a shut-down-maintenance period August 21, 2006, to do safety related activities in the tunnels and to install new hardware for increasing the luminosity. There are about a dozen projects associated with increased luminosity. New HER Q4L, Q4R, and Q5R vacuum chambers in the interaction region will be installed to improve the HER vacuum pressure with beam current and BaBar backgrounds. New LER vacuum chamber Q4R&L and Q5R&L will be installed to allow high beam currents. A beam spoiler will be reworked upstream of the LER abort dump to protect the vacuum window from cracking from high peak currents. A tenth HER RF station is being installed to increase the ring's current capability to over 2 A. New beam position monitor (BPM) units will be installed in the LER dipole arcs to improve their high current capabilities. A HER vacuum transition chamber will be changed with a higher power unit. A higher power expansion bellows will be installed near a collimator in LER in PEP-II Region 10 which is in a higher HOM power region. New power supplies are being added to the HER ring to allow the betatron tunes to be increased to shorten the bunch length, which allows a smaller vertical beta in the interaction region increasing the luminosity. All of these tasks are planned to be completed in the August through December 2006 shut-down. The restart of PEP-II is anticipated for early January 2007.

PEP-II DOE Performance Measure: The DOE HEP integrated luminosity measure for FY2006 for PEP-II was 100 fb^{-1}. The actual integrated luminosity delivered by PEP-II in FY 2006 was 100.3 fb^{-1} which meets the goal.

Figures for PEP-II performance in FY2006:

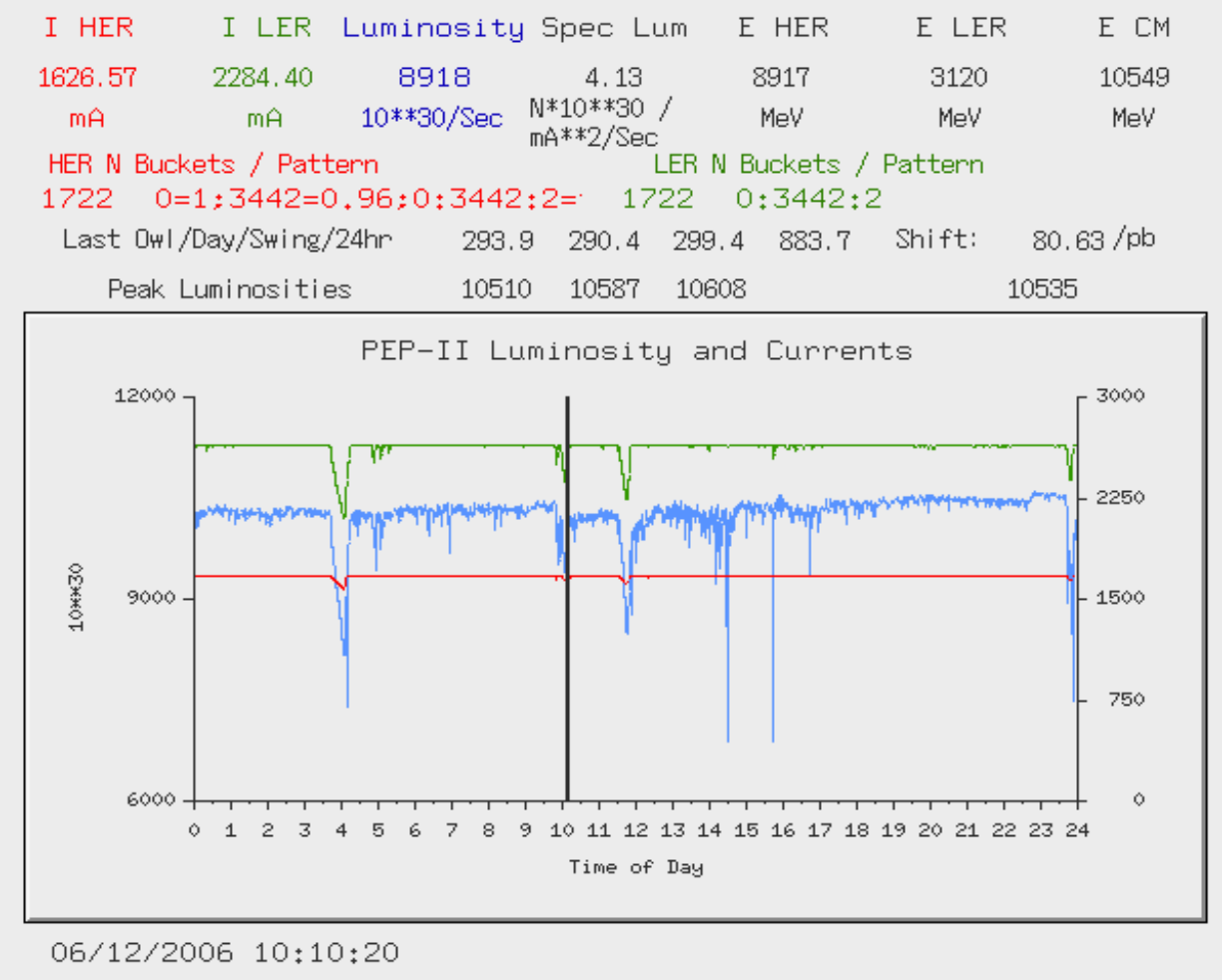

PEP-II beam currents and luminosity for 24 hours in July 2006 showing the stability of continuous (trickle) injection and very high average luminosity approaching 1.1 x 10^{34}.

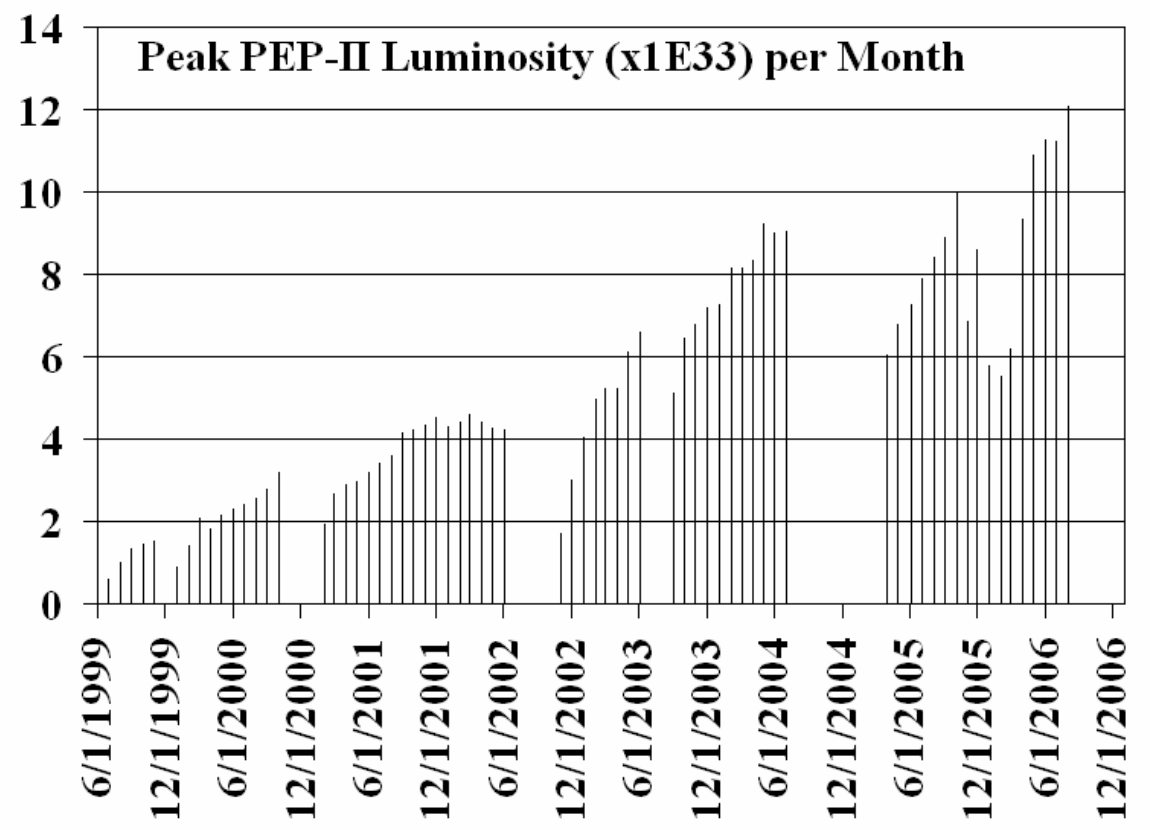

PEP-II peak luminosity in each month since May 1999.

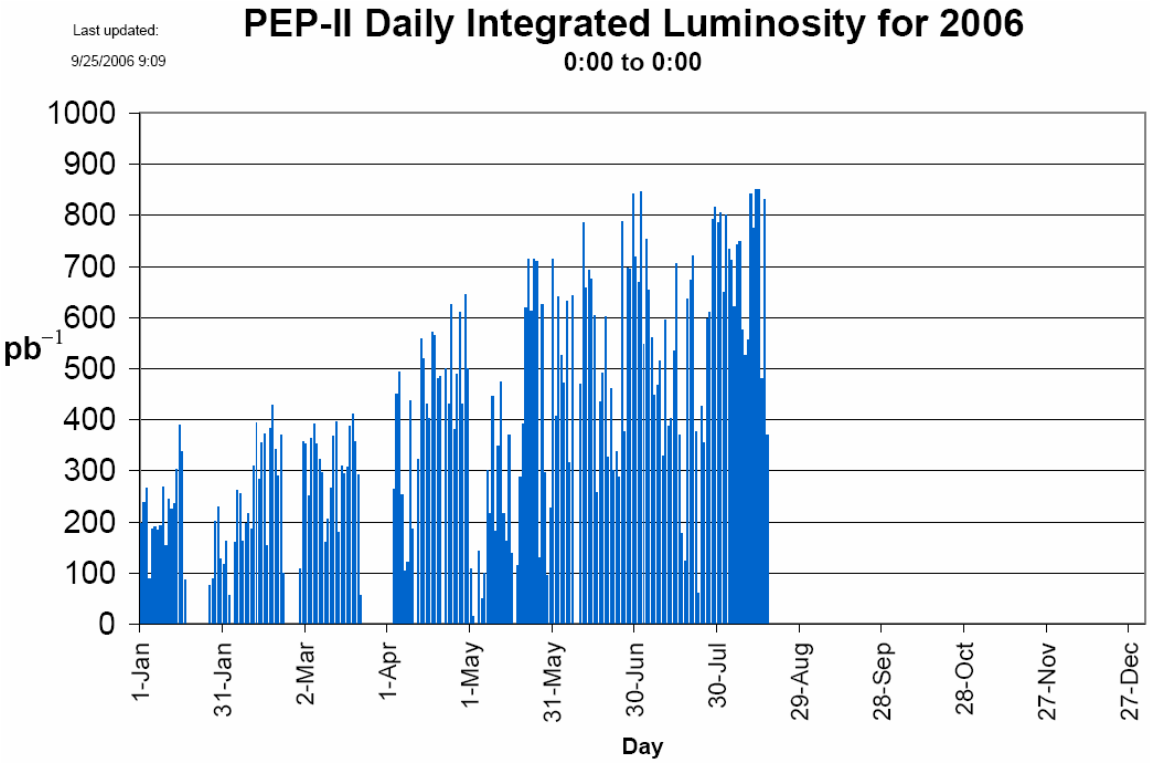

PEP-II Daily Integrated Luminosity for CY2006 showing very strong progress.

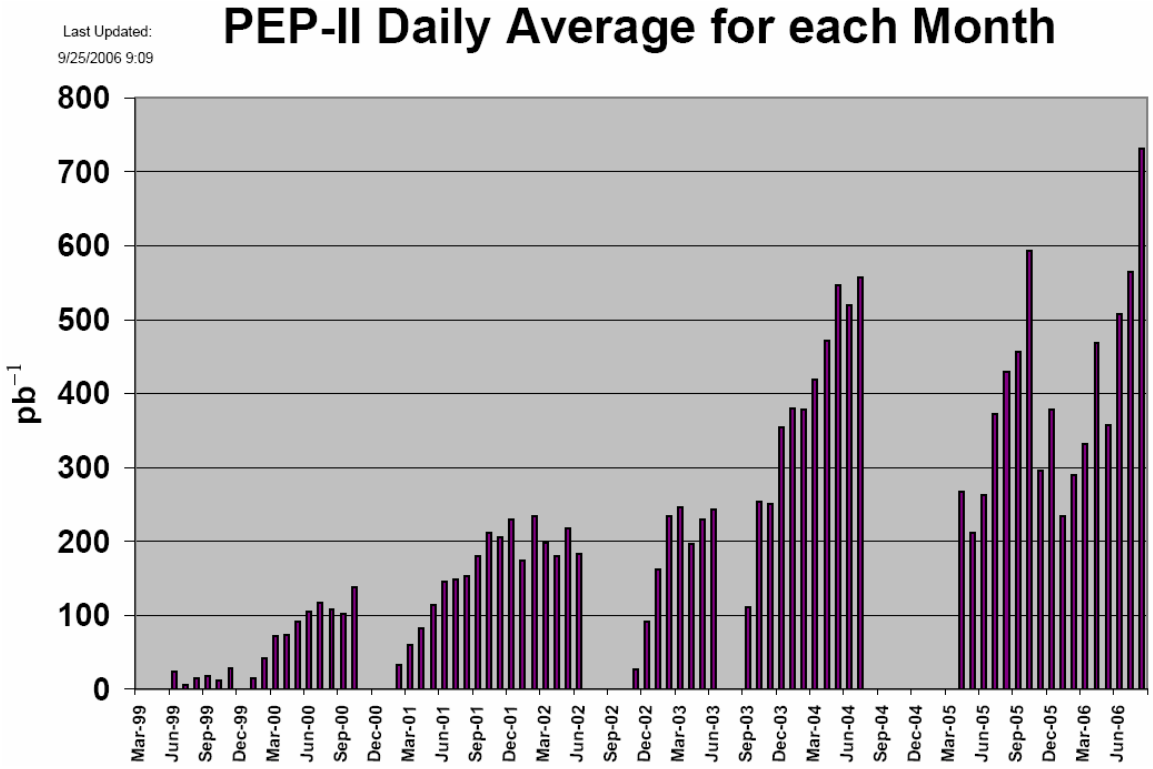

PEP-II Daily average integrated luminosity for each month showing strong improvement at the end of the Run 5b.

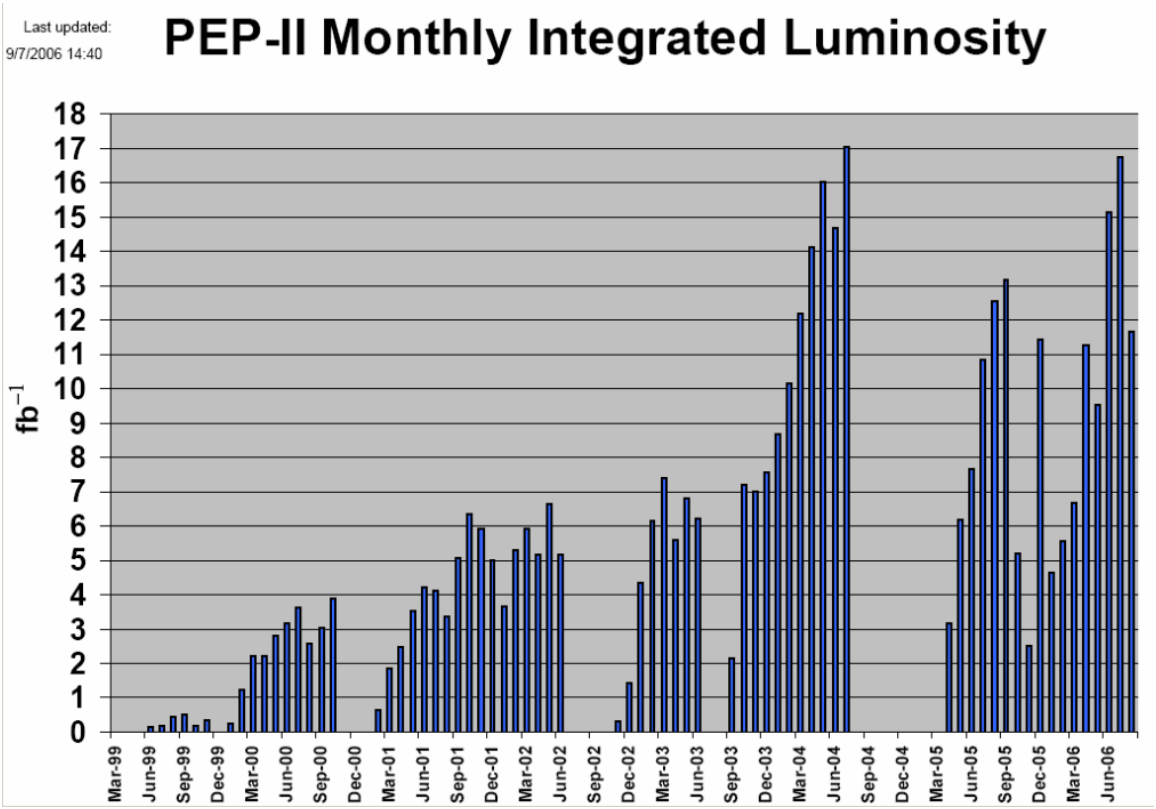

PEP-II integrated luminosity per month showing steady improvement.

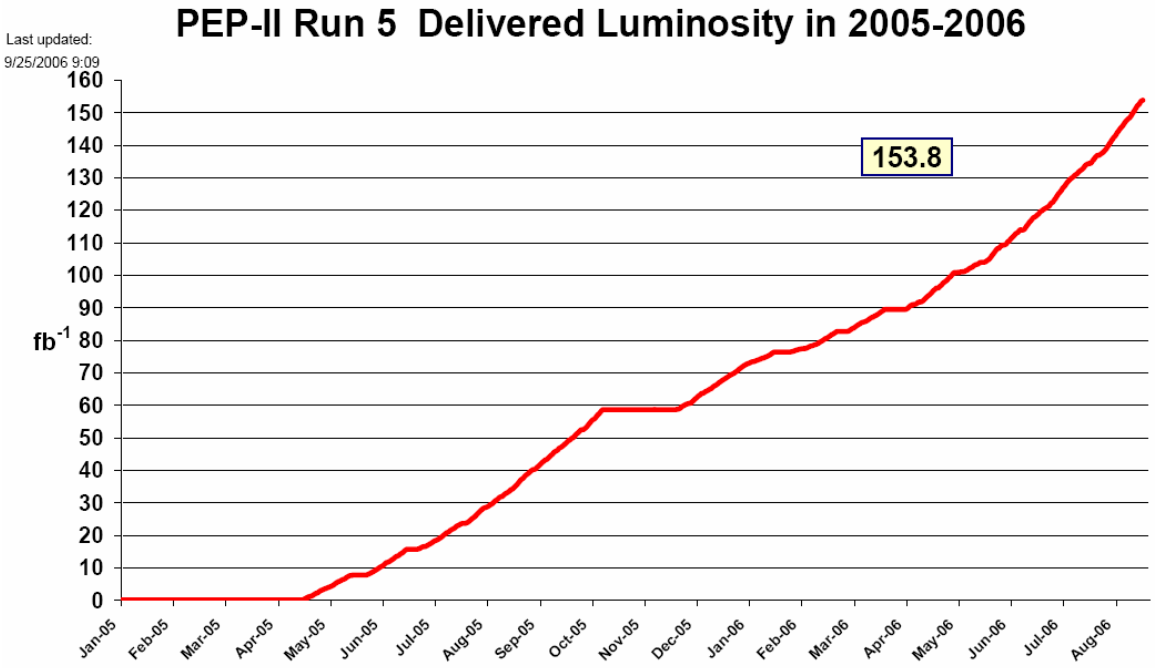

PEP-II accumulated integrated luminosity during FY2006.

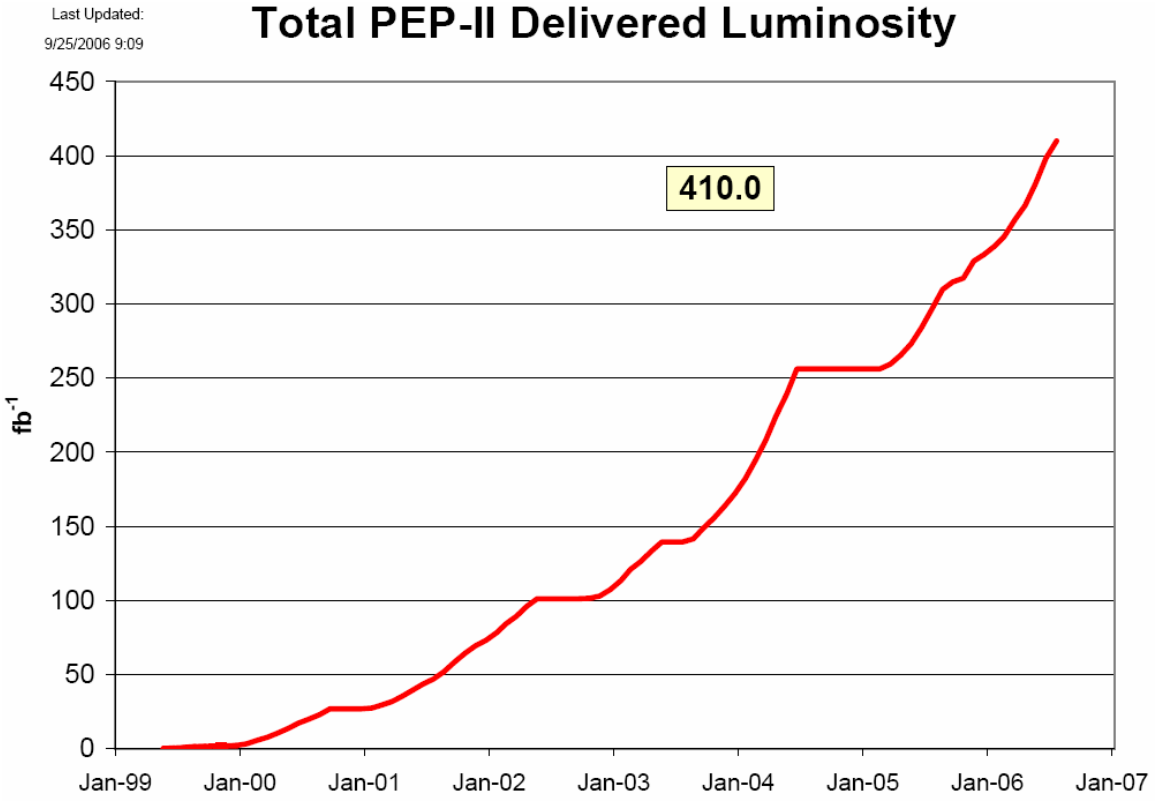

PEP-II accumulated integrated luminosity since May 1999.

PEP-II Records

Last update:
August 18, 2006

Peak Luminosity

12.069×10^{33} $cm^{-2}sec^{-1}$ **August 16, 2006**

1722 bunches 2900 mA LER 1875 mA HER

Integration records of delivered luminosity

Best shift (8 hrs, 0:00, 08:00, 16:00)	**339.0** pb^{-1}	**Aug 16, 2006**
Best 3 shifts in a row	**910.7** pb^{-1}	**Jul 2-3, 2006**
Best day	**849.6** pb^{-1}	**Aug 14, 2006**
Best 7 days (0:00 to 24:00)	**5.385** fb^{-1}	**Jul 27-Aug 3, 2006**
Best week (Sun 0:00 to Sat 24:00)	**5.111** fb^{-1}	**Jul 30-Aug 5, 2006**
Peak HER current	**1900** mA	**Aug 15, 2006**
Peak LER current	**2995** mA	**Oct 10, 2005**
Best 30 days	**19.315** fb^{-1}	**Jul 19 – Aug 17, 2006**
Best month	**17.036** fb^{-1}	**July 2004**

Total delivered

410 fb^{-1}

PEP-II overall performance records

FY2006 Totals - PEP run	BaBar	PEP Mach. Dev.	Tuning & Injection	Unsched. Down	Sched. Off	Total hours	Data delivered to BaBar (fb-1)	Data recorded BaBar (fb-1)
Q1 hours	789.9	46.9	299.5	155.8	891.9	2184	19.1	18.4
Q2 hours	1077.6	86.3	280.1	272.3	466.7	2183	16.8	16.6
Q3 hours	1316.8	14.8	255.9	465.5	131	2184	35.9	35.4
Q4 hours	817.2	27.4	118.3	205.1	1016	2184	28.5	27.6
FY2006 Total hours	4001.5	175.4	953.8	1098.7	2505.6	8735	100.3	98.0
(% of total hrs.)	45.8%	2.0%	10.9%	12.6%	28.7%			
Exclude All Sched. Off (% of Sched. On hrs.)	64.2%	2.8%	15.3%	17.6%		6229.4		

2. FY06 PROGRESS IN BABAR AT PEP-II by Hassan Jawahery, Gregory P. Dubois-Felsmann, and Bill Wisniewski

Overview

Over this past year, the *BABAR* experiment has continued its pursuit of heavy flavor physics generating a spectacular array of new results in topics ranging from time-dependent and direct *CP* asymmetries in decays of B mesons, rare and semileptonic *B* decays, charm and tau physics. The experiment has also produced a number of new results from the study of electron-positron annihilation at Center-of-Mass (CM) energies near the Y(4S) resonance, as well as CM energies well below the Y(4S) via initial state radiation reaction. BaBar also reported the first observation of a rare two-photon annihilation process. The detector continues to perform extremely well, with an operational efficiency of 97%. Since the start of running in October 1999, *BABAR* has accumulated an integrated luminosity of 349 fb^{-1} on the $\Upsilon(4S)$ resonance, corresponding to 384 million *B*-meson pairs, and an additional 37 fb^{-1} taken 40 MeV below the resonance. During the Run 5 that ended on August 21, 2006 the detector recorded an integrated luminosity of 148.6 fb^{-1}. The analysis of the BaBar data has so far yielded 242 papers, published or submitted for publication. The collaboration submitted 114 papers to the International Conference on High Energy Physics in Moscow (ICHEP 2006), which were summarized in 24 invited presentations by BaBar collaborators, including two plenary talks by Roger Barlow of University of Manchester, and Robert Kowalewski of University of Victoria. These presentations covered the full spectrum of heavy flavor physics that is reachable at the Y(4S) resonance with the B factories. Clearly, PEP-II and *BABAR* have been highly productive in recording, reconstructing, analyzing and simulating data, more than fulfilling expectations for the promise for exciting physics from the project.

BABAR Physics Highlights

The *BABAR B* physics program, based on this enormous data sample, encompasses three main goals: (1) study of CP violation in B meson decays and tests of the CKM paradigm through measurement of a complete set of *CP*-violating asymmetries and CP conserving observables in *B* meson decays; (2) search for the effects of physics beyond the Standard Model, through a systematic exploration of rare decay processes; and (3) detailed studies to elucidate the dynamics of processes involving heavy quarks. The first two goals focus on testing the Standard Model, measuring its parameters, and searching for the effects of new physics, while the third goal is designed to build a solid foundation by elucidating the interplay between electroweak and strong interactions in heavy-quark processes.

During the past year, substantial progress has been made in all three areas. A large number of measurements have been updated with the full data sample leading to more precise measurements. In addition a number of new observations and measurement were reported. A new improved measurement was presented of sin2β, the time-dependent CP violation parameter in B decays into charmonium modes, including $B^0 \to J/\psi K_S^0$ and $B^0 \to J/\psi K_L^0$. In Figure 1, is shown the decay time evolution of the event sample, as well as the time-dependence of the measured CP asymmetry, the amplitude of which is related to the CP parameter sin2β. The new BaBar measurement $\sin 2\beta = 0.710 \pm 0.034 \pm 0.019$ and the measurement reported by the Belle Collaboration at the KEKB machine, $\sin 2\beta = 0.642 \pm 0.031 \pm 0.017$, with an average of

$\sin 2\beta = 0.672 \pm 0.026$ represents the most precisely determined parameter of the CKM matrix. The consistency of the sin2β measurement with indirect constraints on this parameter from interpretations of other observables in the K meson, charm and B decays (see Figure 2 below), has now led to the conclusion that the CKM matrix is the primary mechanism responsible for the observed CP violating effects in nature. In addition to providing a powerful test of the CKM mechanism, the sin2β measurment from the charmonium modes serves as a benchmark for the measured CP asymmetries in penguin dominated decay channels, which are sensitive to the effects of New Physics.

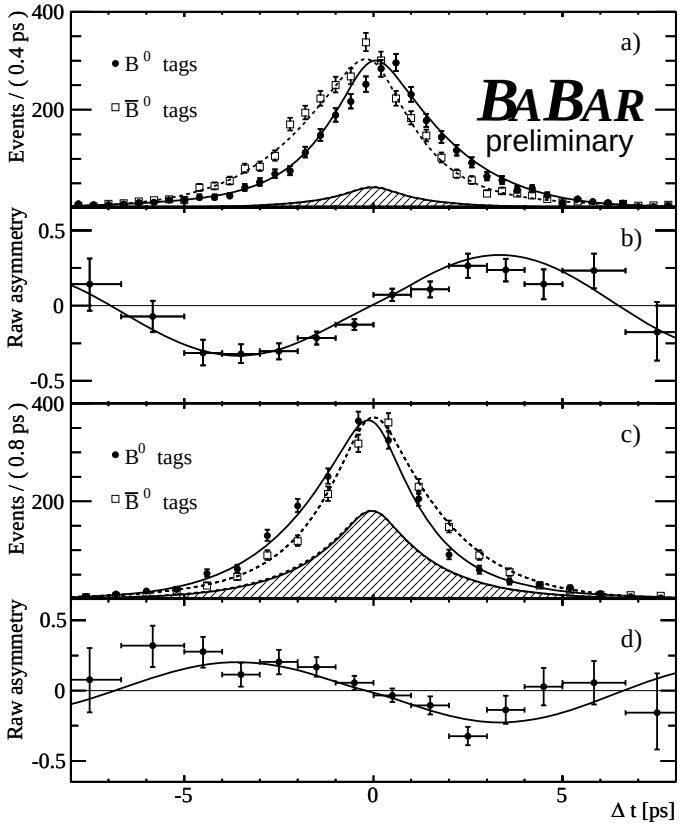

Figure 1: a) Distribution of flavor tagged candidate B^0 and $\overline{B}^0$ decays in final states $J/\psi K_s^0, \psi(2S)K_s^0$ $\chi_{c1}K_s^0$, and $\eta_c K_s^0$, b) time dependence of the CP raw asymmetry. Figures c) and d) are the corresponding distributions for the CP conjugate mode $J/\psi K_L^0$.

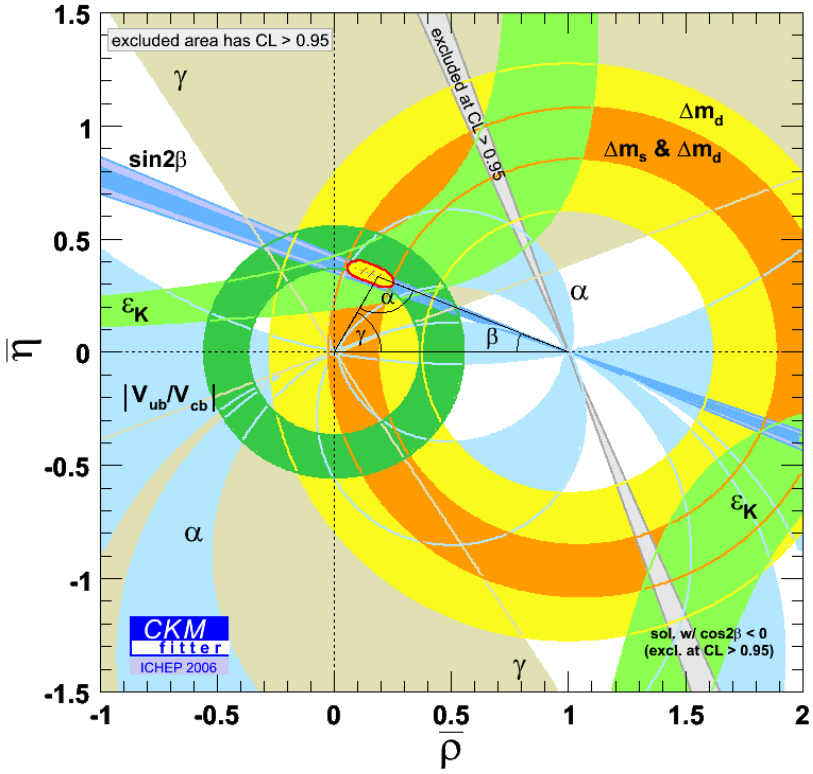

Figure 2: Compilation of indirect and direct measurements of the unitarity triangle (UT). The plot shows the allowed region for the apex of UT, obtained from indirect constraints from ε_K from *CP* violation in kaon decays, $|V_{ub}/V_{cb}|$ and Δm_d, Δm_s from rare *B* decays and mixing. The allowed region from *CP* violating measurements in *B* decays (the overlap of the blue regions) is consistent with the indirect constraints on UT.

From the outset, a major goal of the BaBar experiment has been to perform a test of the CKM paradigm by over-constraining the CKM unitarity triangle. This requires a complete set of measurements of the three angles α, β and γ, and the sides of the unitarity triangle. With the increasing size of the available data sample, determination of the angles α and γ, which require measurements of the rates and CP asymmetries in a large set of rare processes, have now become possible. The angle α is related to time-dependent asymmetries in two-body modes involving $b \to u$ transitions such as $B^0 \to \pi^+\pi^-$, $B^0 \to \rho\pi$, and $B^0 \to \rho^+\rho^-$. However, the additional complication for many of these channels is the significant contribution of a second important decay mechanism, involving a so-called penguin diagram. The presence of the penguin diagram introduces a theoretical uncertainty (Δα) in extraction of the angle α, which can ultimately be removed when precise measurements are performed of the rates and CP asymmetries of all isospin partners of the primary decays. An indicator of the size of the penguin contribution in each case is the ratio of branching fractions such as, $\frac{B(B\to\pi^0\pi^0)}{B(B\to\pi^+\pi^-)}$, and $\frac{B(B\to\rho^0\rho^0)}{B(B\to\rho^+\rho^-)}$, which in lieu of a full set of measurements, provide constraints on the magnitude of Δα. In the B→ππ system, where the full set of isospin partners has now been measured, albeit some with large experimental uncertainties, the penguin contributions are shown to be large, providing only a very loose bound on the penguin

pollution- $|\Delta\alpha_{\pi\pi}|<.40^{o}$ at 90% c.l. A major advance in the determination of the angle α was made by the discovery at BaBar that the decay mode $B^0 \to \rho^0\rho^0$ is highly suppressed compared to the decay $B^0 \to \rho^+\rho^-$, thus indicating a comparatively small contamination from the penguin amplitude in this channel, with a constraint of ~11^{o} on $|\Delta\alpha_{\rho\rho}|$. BaBar also observed that the decay $B^0 \to \rho^+\rho^-$ is essentially a pure *CP* eigenstate, thus allowing for a clean determination of time-dependent CP asymmetries in this mode. A further important development in the study of this channel this year, has been the first evidence by *BaBar* of the decay $B^0 \to \rho^0\rho^0$. At the ICHEP 2006, the BaBar collaboration also presented an update of time –dependent CP asymmetry measurements in $B^0 \to \rho^+\rho^-$ channel. The observed Δt distributions for tagged samples of $B^0 \to \rho^+\rho^-$ candidates and the corresponding visible asymmetry are shown in Figure 3. Combined with results on decays $B^0 \to \rho^0\rho^0$ and $B^+ \to \rho^+\rho^0$, an isospin analysis of the $\rho\rho$ modes has been performed constraining the angle α in the range $\in [84,114]^{O}$. Combining all information on α, including constraints from decays B→ππ and B→ρπ and measurements from the Belle collaboration, the CKM fitter group finds $\alpha = \left[93 \pm^{11}_{9}\right]^{O}$ (see Figure 4). The observation of the decay $B^0 \to \rho^0\rho^0$ opens the possibility of measuring time-dependent CP asymmetry in this channel, which in future will allow for significant reduction of the theoretical uncertainties in this channel.

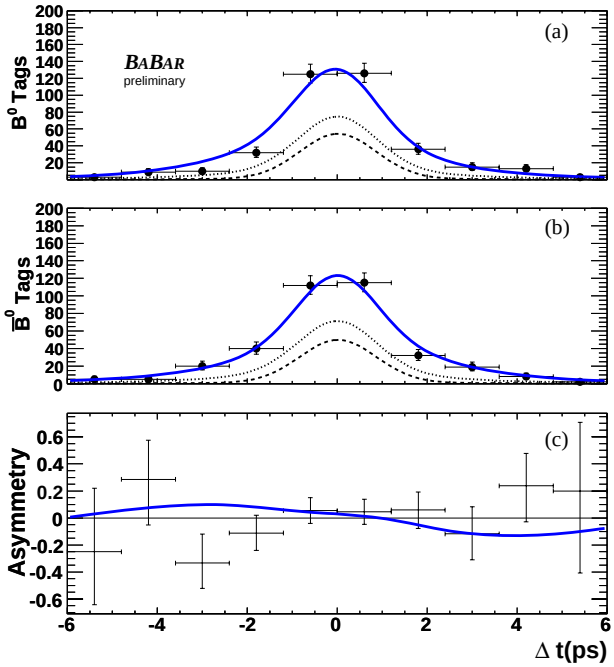

Figure 3: Δt distribution for events enriched in $B^0 \to \rho^+\rho^-$ signal events for B^0-tagged (upper) and $\overline{B}^0$-tagged (middle) events. The dashed line represents the sum of backgrounds and the solid line the sum of signal and backgrounds. The time-dependent *CP* asymmetry is shown in the lower panel along with the projected fit result.

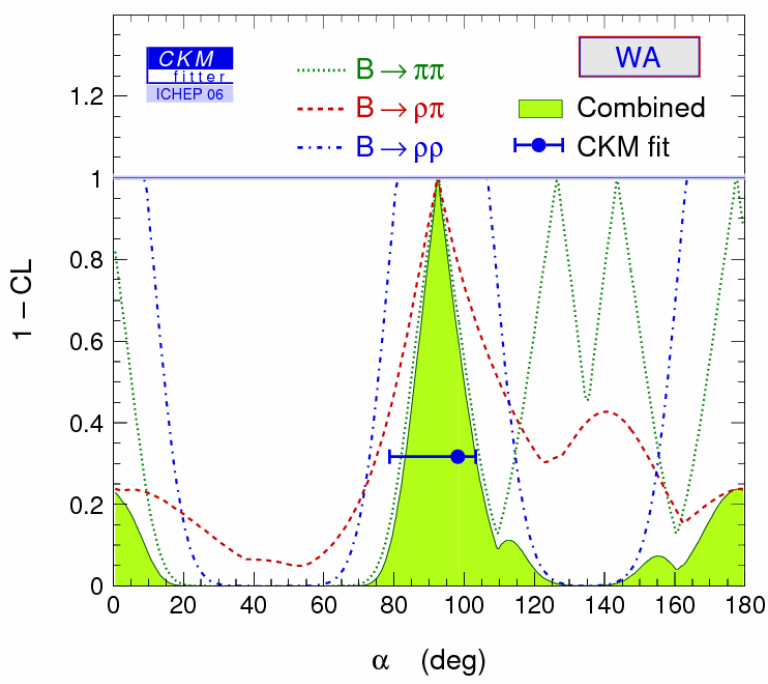

Figure 4: Combined *BABAR* result (shaded region) for direct determination of the unitarity angle α, based on measurements of *CP* asymmetry in $B \to \pi\pi$, $B \to \rho\pi$, and $B \to \rho\rho$. The point with error bars is the predicted value for α from indirect measurements of CKM matrix elements.

Studies have also continued on measurements of the angle γ. These involve measurements of the rates and direct CP violation in decay modes such as $B^- \to D^{(*)0} K^{(*)-}$, which receives contributions from two competing diagrams, one of which depends on the phase γ through the b→u transition. In situations where the D meson is observed in a final state that is common to both the D^0 and $\overline{D}^0$ meson, interference between the two contributing diagrams can result in direct CP violation. A number of techniques have been pursued in identifying the appropriate decay final states for this measurement, including observation of D decays in CP eigenstates (the GLW method) or through doubly Cabibbo-suppressed decays (the ADS method). Alternatively, the D^0 decay is identified in a common multibody final state such as $D^0 \to K^0_S \pi^+ \pi^-$ (the GGSZ method), requiring a Dalitz analysis of the final state. The GGSZ analysis is emerging as the most promising approach for measurements of γ. The current BaBar analysis yields a measurement of $\gamma = 92 \pm 41 \pm 11 \pm 12(\text{deg})$, where the 1st and 2nd errors are the statistical and systematic uncertainties respectively, and the last error is the uncertainty due to imperfect treatment of the resonance structure of the three body final state (the so-called Dalitz error). In all cases, the sensitivity to the phase γ depends on the ratio r_B of the suppressed to dominant decay mechanism, which must be determined from the data along with the angle γ. Measurements using all three methods have been updated with the full data over the past year.

Over the past year r studies have continued of the BaBar data aimed at improving the measurements of the sides of the CKM unitarity triangle, in particular measurements of the magnitudes of the CKM elements $|V_{cb}|$, and $|V_{ub}|$. Progress on this front increasingly depends on

improved knowledge of the dynamics of the B meson decays and on the ability to disentangle the weak and strong interaction effects. The measurement of the $|V_{cb}|$ has already reached an accuracy of about 2%, thanks to significant advances in measurements of the properties of semileptonic B decays as well as the radiative b→sγ process. The combined analysis of b→clν and b→sγ processes provides, in addition to $|V_{cb}|$, information on parameters of B decay dynamics, including the b quark mass and the b quark Fermi motion in the B meson system, which are important for extraction of $|V_{ub}|$ from charmless semileptonic decays. Two sets of analyses have been carried out for determination of $|V_{ub}|$: (1) measurement of the partial rate for inclusive charmless semileptonic decay b→ulν in a region of phase-space that minimizes the contamination from the dominant b→clν decays; and (2) measurement of the differential decay rates in exclusive decays such as B→πlν and B→ρlν. In both approaches, significant theoretical uncertainties are involved in extraction of $|V_{ub}|$ from the measured decay rates. The systematic uncertainties in the two methods are however, complementary, hence in principle a comparison between the two sets of measurements will provide an important cross-check on the two approaches. A compilation of these results is shown in Figure 5. Inclusive measurements have already reached a precision of ~7%, whereas the exclusive results have an overall accuracy of ~20%. A useful comparison of the two sets of measurements therefore awaits improvement measurements from exclusive modes, which may indeed be possible if the promised improved knowledge of the form factors from Lattice QCD is achieved.

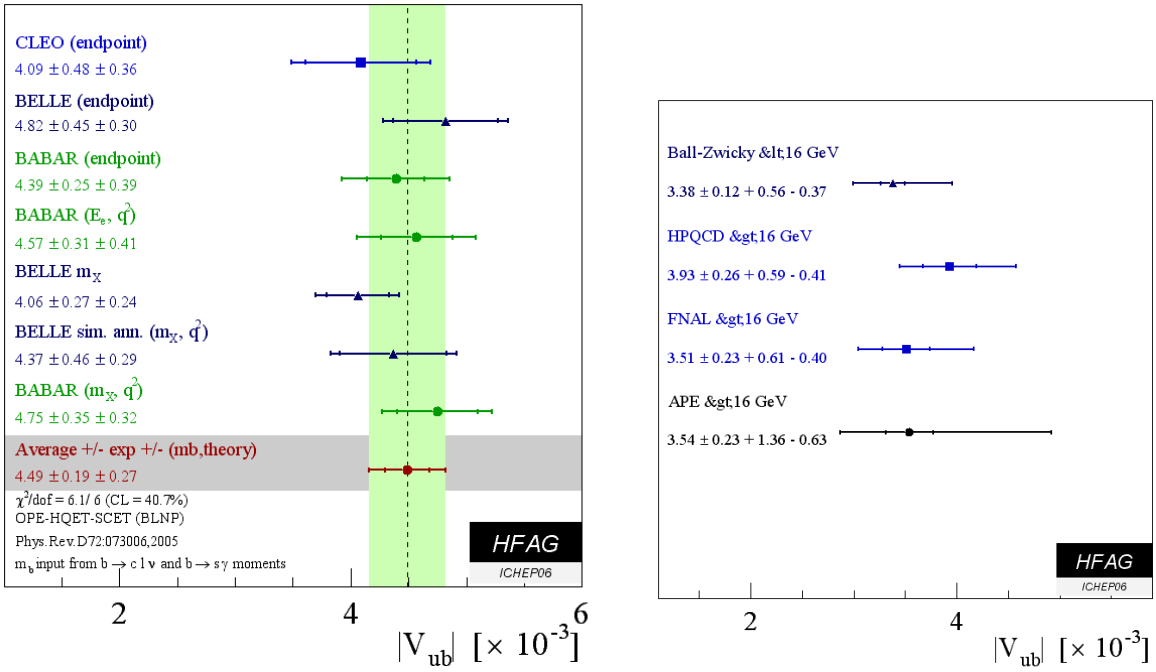

Figure 5: Compilation of available measurements of the quark mixing element $|V_{ub}|$ using the inclusive and exclusive charmless semileptonic B decays. The combined statistical and theoretical error on present world average is ~7% for measurements from inclusive decays and ~20% from exclusive decays.

In the past year, one of the most important events in heavy flavor physics was the observation of $B_s^0 \Leftrightarrow \overline{B}_s^0$ oscillation by the CDF and D0 experiments at Tevatron, leading to a measurement of

the mass difference Δm_s. The ratio $\Delta m_d/\Delta m_s$ provides a measurement of the ratio $|V_{td}/ V_{ts}/$ to an accuracy of ~4%, including theoretical uncertainties. A measurement of $|V_{td}/V_{ts}/$ can also be obtained from the ratio $B(B\rightarrow d\gamma)/B(b\rightarrow s\gamma)$, involving a complementary set of theoretical uncertainties. At the ICHEP 2006, BaBar presented measurements of the branching ratios $B(B^+\rightarrow\rho^+\gamma)$, $B(B^0\rightarrow\rho^0\gamma)$, and a limit on the branching ratio $B(B^0\rightarrow\omega\gamma)$. Figure 6 shows the distribution of the beam-constrained mass for the candidate samples, indicating clear signals at the B mass. An estimate of the ratio of the CKM elements $|V_{td}/V_{ts}/$ is obtained from the ratio of branching ratios $B(B\rightarrow(\rho/\omega)\gamma)/ B(B\rightarrow K^*\gamma)$. A compilation of the results from BaBar and Belle and comparison with the value extracted from measurements of B^0 mixing is shown in Figure 7. The consistency of $|V_{td}/V_{ts}|$ extracted from mixing measurements and the radiative decays, when comparable accuracies have been achieved, is an important test of the internal consistency of the Standard Model. Whereas the mixing measurement is essentially close to its ultimate accuracy, significant improvements are still expected in measurements of the radiative decays from future B factory data. This will remain an important area of BaBar physics to watch in the next few years.

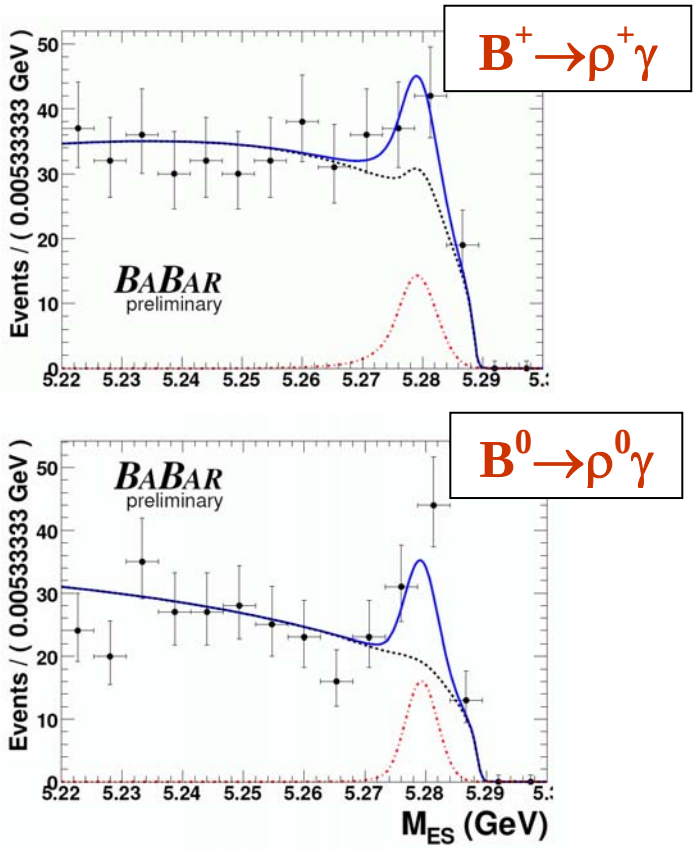

Figure 6: Distribution of $B^+ \rightarrow \rho^+\gamma$ and $B^0 \rightarrow \rho^0\gamma$ candidates in beam-constrained mass M_{ES}. For each plot the signal fraction is enhanced by selection on other variables used in the fit to the entire candidate sample. The points are data, the solid line is the total Probability Distribution Function (PDF) used in the fit to the data and the dark (light dot-dashed) line is the background (signal) only PDF.

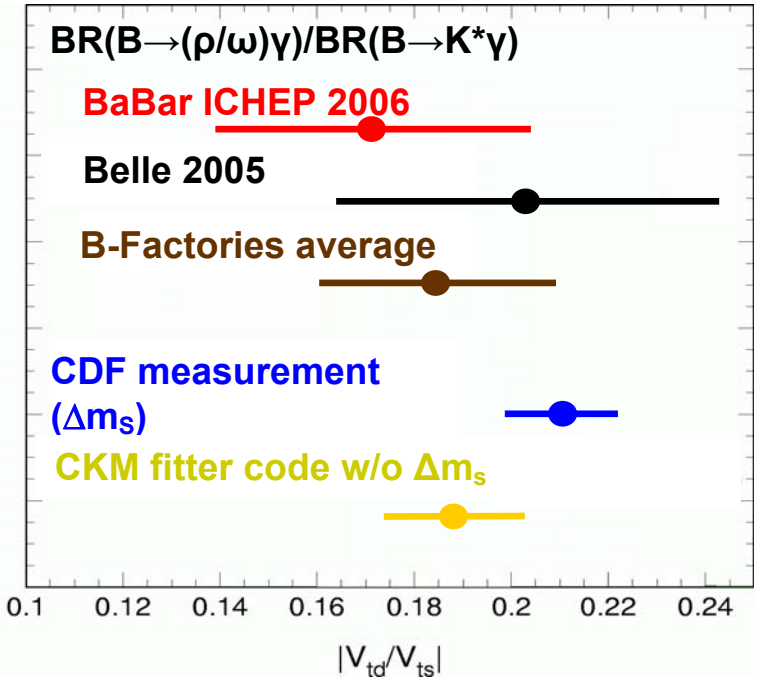

Figure 7: Compilation of all experimental results on $|V_{td}/V_{ts}|$.

As already noted, the CKM unitarity triangle is a convenient summary of knowledge of the charge weak sector of the Standard Model. From a suite of measurements of *CP* violation in kaon decays, the *B* lifetime and V_{cb} from semileptonc $b \to c\ell\nu$ decays, and Δm_d and Δm_s from B_d^0 and B_s^0 mixing, it is possible to infer indirectly the shape of the unitarity triangle and the location of its apex. The plot in Figure 2 shows with the 90% CL allowed region the present knowledge of the unitarity triangle as inferred from this suite of indirect constraints. Measurements of *CP* violation in *B* decays allows determination of the interior angles α, β, and γ and comparison of the preferred region with that from indirect measurements.. As can be seen, the fit to the direct *CP* violation measurements shows an allowed region that is both comparable in size to and consistent with that from the indirect measurements.

A key element of the BaBar physics program is searching for the effects of New Physics through rare decays of B mesons. A relatively clean set of observables sensitive to the effects of New Physics are time-dependent CP violating parameters in the so-called $b \to s\bar{s}s$ penguin diagrams containing virtual quarks and vector bosons. While such modes, including $B^0 \to \varphi K^0$, $B^0 \to \eta' K^0$ and a number of related channels, should show the same *CP* asymmetry as the benchmark charmonium result for $\sin 2\beta$, they are also sensitive to new physics at high mass scales beyond those directly produced by present-day experiments. *BABAR* reported a comprehensive set of results on *CP* violation studies in these channels at ICHEP 2006 in Moscow, based on most of the data collected by BaBar up to the conference. Most of the results have now been updated with the full data set of Runs 1-5 and are in preparation for submissions to journals. A particularly noteworthy result is the measurement of CP violation in the decay $B^0 \to \eta' K^0$, which represents the first observation of time-dependent CP violation in a charmless decay.

Figure 8 shows examples of kinematic variables used in selection of $B^0 \to \eta' K_s^0$ decays, and the distribution of the time-evolution and visible CP asymmetry of the sample.

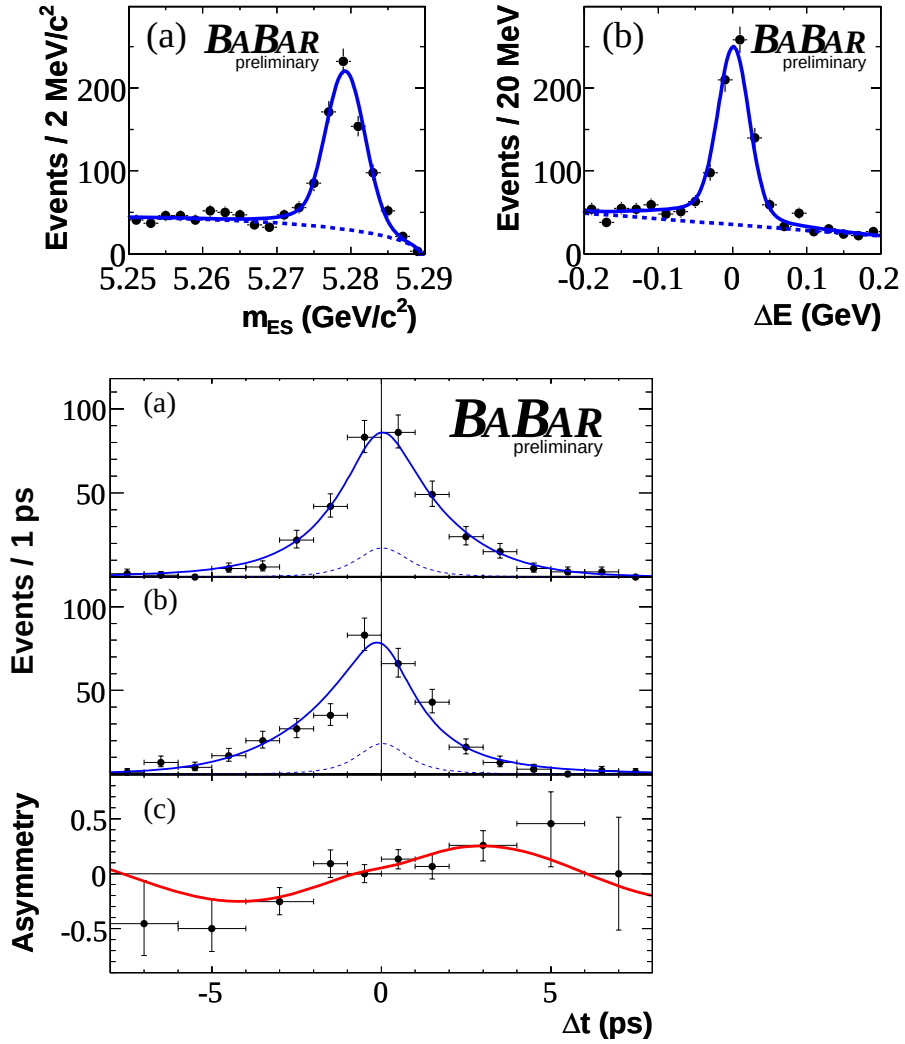

Figure 8: Distribution for the energy-substituted mass m_{ES} and energy difference $\Delta E = E - E_{beam}$ for a sample of $B^0 \to \eta' K_s^0$ (upper) signal events, Δt distributions for B^0-tagged (lower (a)) and $\overline{B}^0$-tagged (lower (b)) events, and visible asymmetry (lower (c)) with overlaid fit results.

A full compilation of measurements of *CP* asymmetries in $b \to s\bar{s}s$ penguin modes is shown in Figure 9, including the results presented by the Belle collaboration. The average value 0.52 ± 0.05 for the product of the amplitude of the sine (S_f) term in the time-dependent asymmetry and the *CP* eigenvalue for the final state (η_{CP}) should be equal to the well-measured value of $\sin 2\beta = 0.672 \pm 0.026$. Intriguingly, this is not the case at present, with a discrepancy at the level of 2.5 standard deviations. Clearly this remains a result to watch in the future as more data is

accumulated, since a difference between the charmonium and penguin modes is exactly the kind of signature one would expect from new physics beyond the Standard Model.

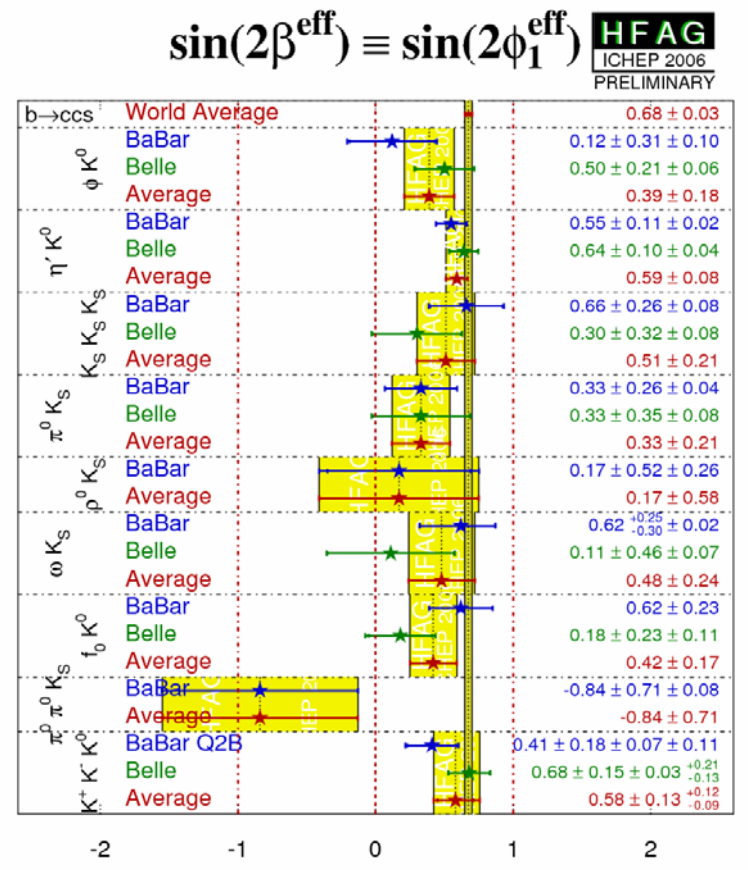

Figure 9: Compilation of fit results for the amplitude of the sine (S_f) term in the time-dependent asymmetry multiplied by the *CP* eigenvalue for the final state (η_{CP}) as obtained for various $b \to s\bar{s}s$ channels by *BABAR* and Belle. The average over the eight channels, 0.52 ± 0.05, is about 2.5 standard deviations below the precision measurement of $\sin 2\beta$ obtained in the charmonium modes, $\sin 2\beta = 0.672 \pm 0.026$.

BaBar's ability to search for New Physics effects extends to rare processes in decays of charmed mesons and tau lepton. In the charm sector, a major effort is underway to measure the $D^0 \Leftrightarrow \overline{D}^0$ oscillation frequency which, contrary to the neutral B system, is highly suppressed in the Standard Model; typical theoretical estimates of the D mixing rate are in the range O(10^{-6}- 10^{-4}). Observation of D mixing even at the current level of experimental sensitivity would represent a departure from the Standard Model and a sign of New Physics contributions. The mixing process is parameterized in terms of the quantities: $x = \Delta m / \Gamma$ and $y = 2\Delta\Gamma / \Gamma$, which respectively measure the mass and lifetime differences of the two CP eigenstates in the neutral D system. The mixing rate is defined as $R_M = (x^2 + y^2)/2$ and is extracted from the time evolution of flavor-tagged D^0 decays. BaBar has presented results on D mixing rate by examining D^0 decays into CP-even eigenstates, semileptonic D decays and the decay $D^0 \rightarrow K^- \pi^+$. In the past year the BaBar

collaboration presented new results using decay final channels, $D^0 \rightarrow K^- \pi^+ \pi^0$ and $D^0 \rightarrow K^- \pi^+ \pi^- \pi^+$, based an analysis of the Run 1-4 data sample (230 fb^{-1}). These analyses yield a measurement of the mixing rate $R_M = (0.020^{+0.011}_{-0.010})\%$, leading to an upper bound of R_M<0.042% at 95% confidence level. This analysis rules out the hypothesis of no mixing at 2.1% confidence level. Clearly, this measurement will continue to be of great interest and its evolution with the future data will be closely watched.

Finally, it should be noted that physics reach of the *B* Factory program spans a broad range of topics in heavy flavor physics, including beauty, charm, and tau physics, through a variety of production mechanisms, including e^+e^- annihilation, two-photon, and initial-state radiation events. Among the highlights of BaBar results, outside the weak interaction physics described above, has been the ongoing discovery of members of strange charm meson (D_s) family, high-mass states decaying to charm or charmonium mesons and lately an excited charm baryon state. At the ICHEP 2006 conference in Moscow, the BaBar collaboration presented the first observation of an excited charm baryon (css) (Ω_c^*) in the radiative decay $\Omega_c^0 \gamma$, using the run 1-4 data set of 230 fb^{-1}. Figure 10 shows the invariant mass distributions of $\Omega_c^* \rightarrow \Omega_c^0 \gamma$ candidates, for four decay channels of Ω_c baryon that were reconstructed in this analysis. The combined set yields a 5.2 σ signal for an excited charm baryon state at a mass difference $M_{\Omega_c^*} - M_{\Omega_c^0} = 70.8 \pm 1.0 \pm 1.1 \;\; MeV$.

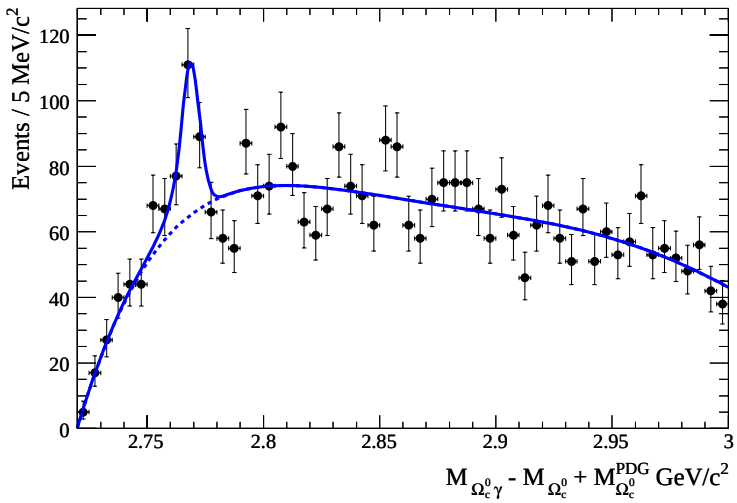

Figure 10: The invariant mass distribution of $\Omega_c^* \rightarrow \Omega_c^0 \gamma$ candidates. Here $M_{\Omega_c^0 \gamma}$ is the reconstructed invariant mass of the Ω_c^* candidate and $M_{\Omega_c^0}$ is the reconstructed mass of Ω_c^0.

At the ICHEP meeting, the BaBar collaboration also presented new results from further investigation of the Y(4260) state (seen in $J/\psi \pi^+ \pi^-$), discovered at BaBar in 2005 in initial-state radiation events and a new structure seen in $\psi(2S)\pi\pi$. The Y(4260) state, has now been confirmed by the CLEO experiment at CESR and the Belle experiment at KEKB. These states are the latest in a series of new structures observed in the past few years at the B factories, which include hybrid states, molecules, as well as conventional charmonium states. Interpretation of these states is the subject of a lively debate in the community and is likely to lead to important insights in QCD dynamics.

In summary, the analysis of BaBar data has so far led to major findings, including establishment of the CKM matrix as the primary mechanism responsible for observed CP violating effects in nature. In the next two years, the experiment is poised to increase its data sample by a factor of 2.5 with a very rich physics prospect. A key goal of the program is to search for the effects of new

physics, through a large number of observables. In addition, a major legacy of the experiment is expected to be precision determination of the charge weak sector of the Standard Model, which will serve as a benchmark for testing predictions of models of new physics in the LHC era.

BABAR Detector

The *BABAR* Detector completed the second half of its fifth data run on 21 August 2006. BaBar recorded 148.6 fb^{-1} in total during Run 5 (Figure D1). This data was recorded with 97% efficiency. Two components contribute to the ~3% inefficiency: downtime due to equipment failure, which has averaged about 1.7% for Run 5, and dead time due to inefficiencies in the data acquisition system. Downtime due to equipment failure has been minimized because of the robustness of the detector design and construction, the emphasis on quick repair by the system experts, and the attention of the personnel on shift acquiring the data. Minimization of dead time has been, and continues to be, a key focus of effort for the experiment. Many of the upgrades that have recently come to fruition have dealt with minimization of dead time in the face of ever-increasing luminosity. Luminosity is now four times design. The data acquisition system (DAQ) will need to cope with luminosities seven times design, prompting increased attention to backgrounds by the Machine Detector Interface group (MDI), to DAQ bottlenecks in all the detector systems, and to event selection (triggering).

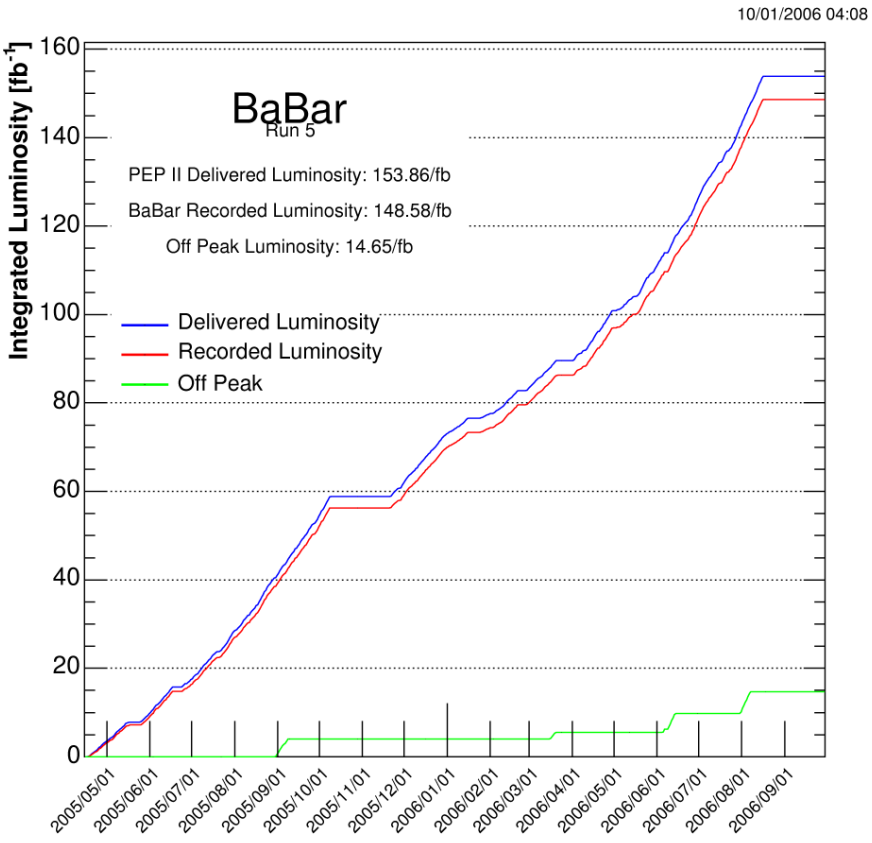

Figure D1. *BABAR* integrated luminosity (Run 5)

The five-week October down period that began the 2006 fiscal year, provided a brief interruption in Run 5 to address a couple of accelerator and safety issues. Advantage was taken of this time to install in the detector the Drift Chamber (DCH) electronics upgrade, as well as to prepare for the Instrumented Flux Return (IFR) upgrade work that began at the end of Run 5.

The *BABAR* Machine Detector Interface group continues to understand detector backgrounds using the detailed Monte Carlo simulation (GEANT4) of the interaction region that it developed. The MDI group has developed online tools for determining the horizontal and longitudinal beam size at the interaction point, as well for measuring the crossing angle of the beams at the IP, on a real time basis. This has proved to be very useful to the machine physicists and accelerator operators. *BABAR* members contributed heavily to the process of identifying the location of IR region gas burst instability using the detector's background devices (radiation sensing PIN diodes) in conjunction with PEP-II's vacuum measuring devices.

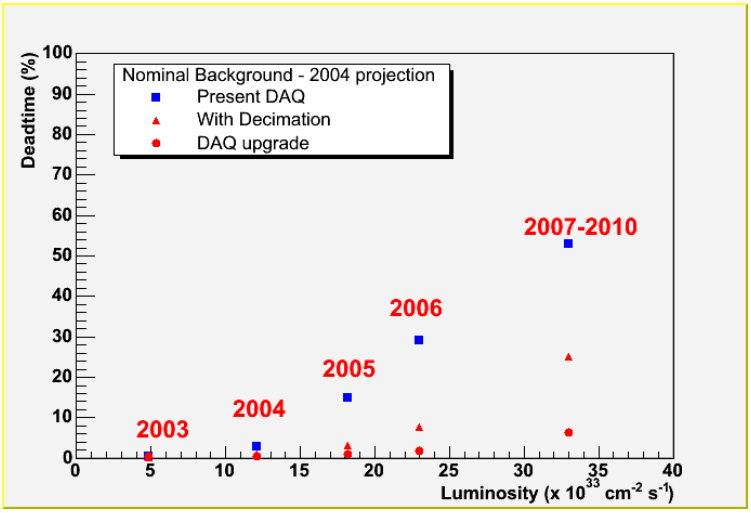

Figure D2: Dead-time due to DCH readout. Blue squares show extrapolation of original front end electronics; red triangles show extrapolation with phase 1 upgrade; red circles show extrapolation with phase 2 upgrade.

For the past couple of years the Drift Chamber team has focused on upgrading the front-end readout electronics. Beam related backgrounds clog the data pathway from the on-detector electronics to the off-detector readout modules, producing readout dead time (Figure D2). Fragments produced in the interaction of radiative bhabha event electrons and positrons with beam line elements dominate these backgrounds that grow with luminosity. The fix for this problem has been implemented in two steps. In the first phase, the programmable array front end chips were reprogrammed to send half of the waveforms. This reduced the readout dead time during Run 5a to acceptable levels (i.e., of order a per cent or less), although the limits of this implementation were apparent in dead-time increases that accompanied unusually high backgrounds.

In the second phase, the feature extraction algorithms, which are currently executed in the off-detector readout modules, were moved into modern programmable array chips located in the on-detector electronics. The new electronics board, which uses a modern field programmable gate array and programmable read-only memories, was installed during the October 2005 shutdown. This board supports downloading new feature extraction algorithms. Run 5b was thus begun using

the algorithms of the first phase. By mid-February, the off-detector feature extraction algorithms had been downloaded to the new on-detector electronics boards and were in routine use. A weakness of this new system is its sensitivity to radiation- induced upsets because of its location next to the beam line. This is mitigated by frequently reloading the algorithms while checking data consistency and integrity. Dead time dropped on installation of the feature extraction algorithms. Dead time at the highest luminosity projected through the lifetime of the experiment will remain acceptably small.

The Silicon Vertex Tracker (SVT) has performed well during the past year. Effort has been devoted to developing software tools that allow readout of sections of the SVT that have been isolated by local chip damage. Studies are in process to understand the future rate limitations of the SVT DAQ, and ways to mitigate these limitations. Possible mitigations include full readout of chips from both ends, which reduces the amount of data flowing through individual readout chips; frequent adjustment of thresholds to limit radiation damage induced effects that increase the number of noise hits; shrinking the readout time window to reduce the data transmitted; and increasing the clock rate of the readout, if this is possible. It is hoped that the first three of these will reduce the size of the readout stream enough to make the fourth unnecessary. Success here will limit dead time to acceptable levels for the lifetime of the experiment.

The DIRC, which uses Cherenkov light to identify charged particle species, has performed well this year. The Electromagnetic Calorimeter has performed without problems. Effort continued to be focused this year on improvements to the electromagnetic shower reconstruction code and calibration scheme. The improvements are now ready for use.

The Forward Endcap Resistive Plate Chambers (RPCs) performed efficiently during the fifth data run. The additional steel added during last year's down has decreased beam-related background rates in the outer layers of the forward end cap by over a factor of three. This has permitted all layers to be utilized, allowing the realization of the full benefits of the summer 2002 upgrade: increased μ identification efficiency with improved π rejection. In order to decrease the sensitivity to backgrounds of portions of the RPCs closest to the beam line, which increase directly with future luminosity improvements, electronics have been developed to operate the RPCs in avalanche mode, rather than streamer mode. Prototype electronics were installed during the October shutdown in three RPCs to test this scheme. These electronics performed well, lowering the charge seen by the RPCs by a factor of 5. Efficiency has increased for these RPCs while occupancy levels have remained acceptable. Improvements in efficiency for the regions closer to the beam line can be seen in Figure D3. Studies where water vapor is introduced into the RPC gas have been successfully completed. This boosts the RPC efficiency and has been implemented in all forward end-cap chambers.

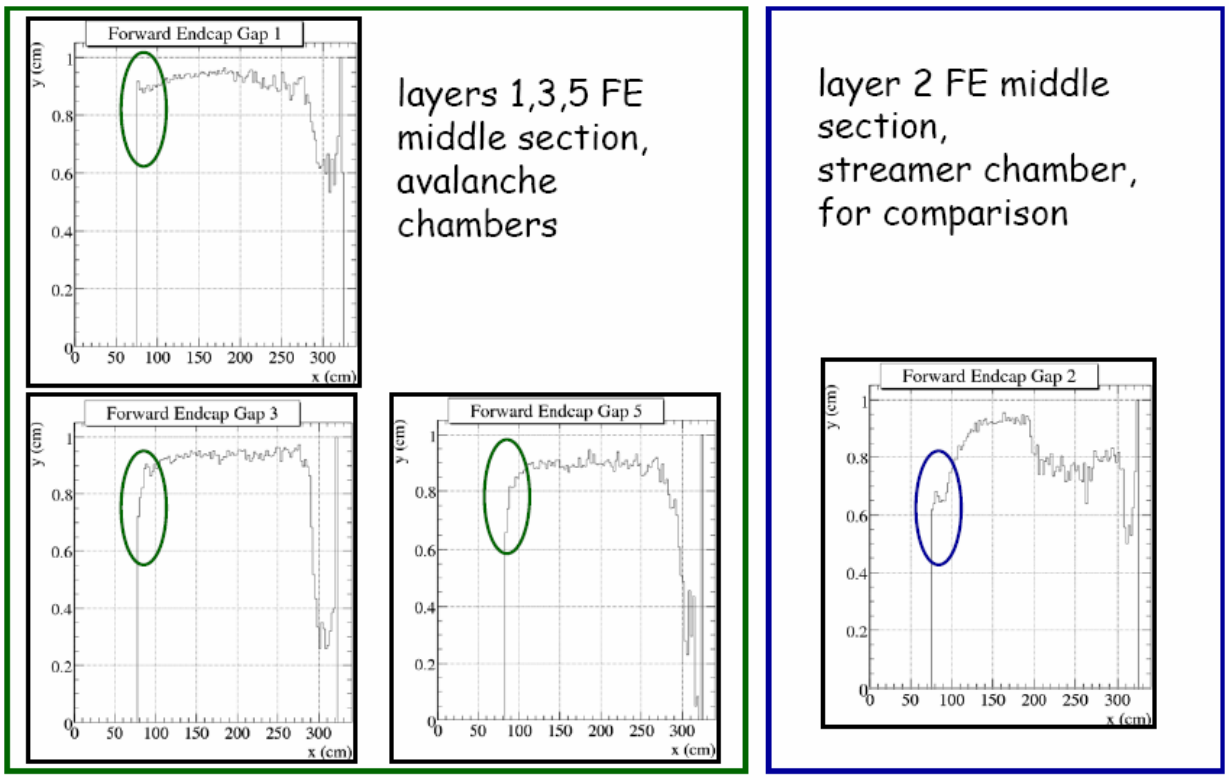

Figure D3. Efficiency across end-cap RPC layers. The left part of the figure shows chambers that have been fitted with preamplifiers and run in avalanche more. The right part of the figure shows a chamber not modified. The circles call attention to the regions closer to the beam line where higher backgrounds limit performance. Performance is clearly enhanced in the chambers run in avalanche mode.

In December 2002 the collaboration selected Limited Streamer Tubes (LSTs) as the replacement technology for the RPCs of the barrel portion of the IFR. Installation of twelve layers of LSTs into the top and bottom sextants of the barrel IFR was completed in mid-October 2004. Brass 7/8" absorber replaces the barrel RPCs in six layers in these sextants to improve the π/μ rejection ratio. The barrel LSTs have performed well during Run 5. The performance improvements can be seen in Figure D4.

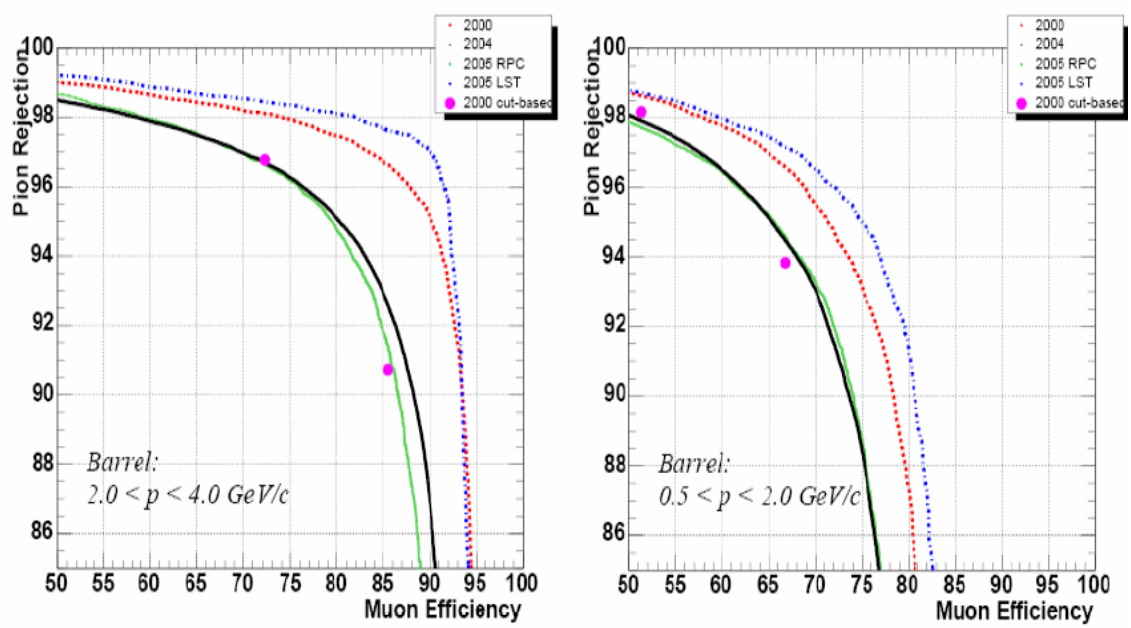

Figure D4. Improvements in efficiency for identification of muons and rejection of pions are shown as a function of time. The contrast between barrel sextants equipped with RPCs (green line) and the sextants with LSTs (dotted blue) is stark. Comparing the LSTs with the performance of the RPC system when it was new (red dots) shows that the IFR upgrade with LSTs and additional brass provides improved performance compared to the initial performance (and design) of the detector.

Figure D5: LSTs being prepared for installation in autumn 2006.

The LSTs for the remaining four sextants of the barrel IFR have been under continuous test since 2004 (Figure D5). Design and fabrication of tooling for the installation of the remaining four sextants of the barrel IFR was completed just in time for the shut-down that started at the end of Run 5 and continues until January 2007. Installation of the first of these four sextants was completed at the end of FY2006 (Figs. D6, D7).

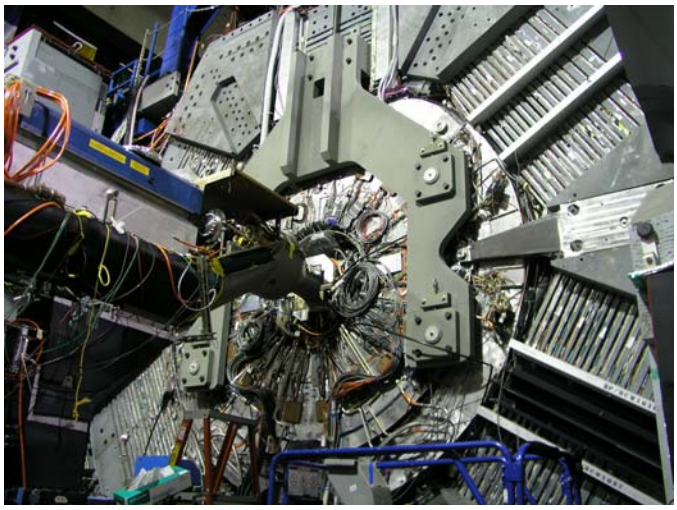

Figure D6. Front end of the detector with EMC load transfer fixture (yoke: inverted y frame hanging from top of detector).

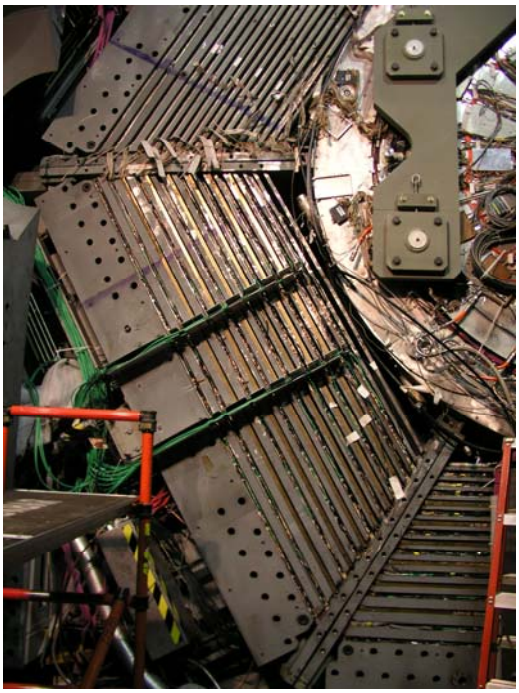

Figure D7. The first of four sextants (left, diagonal) of LSTs and brass have been installed.

The trigger has been upgraded to handle higher luminosity. Additional information from the DCH is used to ensure that events originate close to the interaction point along the beam line. The upgraded system has performed well during Run 5. Long-standing sources of dead time have been eliminated from the trigger system. Investigations into effects on the efficiency of accepting key

final states are in progress at this time. They are aimed at tightening trigger conditions to limit DAQ dead time, should this become necessary, as luminosity increases.

PEP-II is continuing to operate in the "trickle-injection" mode first introduced during Run 4. The modifications introduced to the data acquisition system to support this are working well, and the data acquisition system is being steadily refined to handle the increasing luminosity. As a result, *BABAR* continues to maintain its record of recording for physics analysis approximately 97% of the data produced by the accelerator.

During FY06, approval and funding were received from the *BABAR* International Finance Committee for an upgrade of the event building, filtering, and quality monitoring farm in the online system, and work began on this as soon as data-taking ended in August. The cluster of sixty Intel/Linux servers that had supported these tasks since 2002 is being replaced with a new group of fifty Sun AMD/Linux servers with dual dual-core Opteron processors, while the Cisco network switch that supports event building is being replaced with an upgraded version. These changes are necessary to support the higher event rates and larger events that are expected to come with the beam current and luminosity increases of the next two years of *BABAR*'s running.

Computing

The new Computing Model deployed by *BABAR* at the end of 2003, based on the storage of event data in an ensemble of ROOT files rather than in an Objectivity/DB object-oriented database, has continued to work well and contribute to the experiment's ability to perform many parallel analyses on very recently acquired data. *BABAR* computing continues to be carried out across six major "Tier A" sites – SLAC, CC-IN2P3 in France, RAL in the UK, GridKa in Germany, and Padova and CNAF-Bologna in Italy – as well as a larger network of university- and lab-based simulation production sites, all coordinated from SLAC.

During the previous year, the move to the new computing model was completed with the first comprehensive reprocessing of the *BABAR* data sample entirely within the new model. All of the data from Runs 1-4 were reprocessed with the same software release used for the new data from Run 5, in the course of which it proved possible to recover several fb^{-1} of data that had previously had problems of various sorts. For the 126 fb^{-1} of data from Runs 1-3, originally reconstructed within the Objectivity-based model and converted to the ROOT data format of the new model, this was the first reconstruction directly to ROOT files.

In conjunction with the reprocessing, new simulated data samples covering the whole of *BABAR* running were also generated. In the course of this "SP8" Monte Carlo simulation cycle, thus far over nine billion simulated events have been produced, with about two billion remaining to generate, a task that should be complete at the end of 2006. A substantial fraction of the simulated data is now being generated using "Grid"-based computing systems in the UK and Italy, and this fraction is expected to increase in the future.

Many of the results presented at the ICHEP 2006 conference were based on the reprocessed data sample, demonstrating the success of the effort. Data from Run 5 were included in physics analyses within ten days of their being acquired in IR-2, following reconstruction, data quality check, and skimming. Because of the reprocessing, for the past year data have been processed and simulated at over twice the rate at which new data were being acquired from the detector,

demonstrating that the data production pipeline is already capable of dealing with the higher rates expected in the next two years.

In the course of normal data processing, events acquired from the online computing system are first passed through a calibration procedure hosted at SLAC, updating the calibration database with the latest conditions of the hardware systems. The raw data are then transferred to the Tier-A center at Padova (Padua), where one of several available PC-based Linux farms are used to apply an initial physics filter and actually reconstruct the events. (Additional farms at Padova are available for performing reprocessing of other data in parallel with the reconstruction of newly acquired events.) Typically within 24 hours of data acquisition, both steps are complete and the data shipped back to SLAC for a quality assurance evaluation. The resulting fast access to physics quality data both ensures a continuous monitoring of detector performance and permits data to enter analysis soon after it is acquired.

Following initial reconstruction in Padova, all data are passed through a skim process, which applies over 200 separate physics preselections to the data sample and allows much faster and efficient physics analysis of the full data sets. These selections vary in selectivity over four orders of magnitude, allowing many analyses to work with datasets much smaller than the full unselected sample. Specific selections of the data are made uniquely available at individual *BABAR* Tier-A sites at SLAC and in Europe. One of the major goals of the new computing model has been achieved, in that the length of time required to produce a skim from the complete data sample is now short enough that it is possible to demonstrate the capability for central production of new skims several times per year. During Run 5 three separate skim cycles were carried out, with a fourth now just beginning. This enhances the group's ability to quickly attack new areas of physics interest.

This ability to make highly efficient use of acquired data – the high precision and sensitivity achieved per unit of luminosity – outlined above in the discussion of physics results – has been further enhanced by the reprocessing and by the flexibility of the computing model.

The reprocessing, resimulation, and skimming in FY06 have produced approximately 400 TB of data, all of which is stored for archival purposes in the HPSS mass storage system at SLAC. Specific skims, as noted above, are kept on disk at their assigned Tier-A sites, including SLAC.

Current *BABAR* software releases are now virtually free of direct dependencies on Objectivity for the nonevent databases that are still required, and Objectivity is required at run time for only one of these databases – the "conditions database". The work remaining to completely eliminate Objectivity even in that one remaining application is proceeding rapidly at this time and is expected to be complete in early 2007. The complete elimination of Objectivity will allow reducing cost and complexity for establishing the *BABAR* computing environment at new sites, from universities to laptops.

In preparing for Run 6, improvements are being introduced to track reconstruction which can be applied to the new data acquired in FY07 and beyond, as well as retroactively to the results of the recent reprocessing, thanks to the enhanced "mini" event data format from the revised computing model. Initial indications are that this will lead to further improvements in physics productivity and precision in the coming year.

BABAR Future Plans

The goal of the experiment is to accumulate a full sample of 1000 fb^{-1} by September 2008. The collaboration and the laboratory have explored the physics case for this rich *B* physics program, with many important new results that can be anticipated by quadrupling the sample currently used for analysis. The program rests on two main scientific goals. The first is to provide precision measurements of the weak interaction couplings of beauty quarks that will test at a fundamental level the Standard Model of particle physics through a series of over-constraining measurements. The couplings of quarks to the weak interaction, *i.e.,* the elements of the quark mixing matrix, are as basic to the theory as the quark masses. The *B* Factory will substantially improve the precision of our knowledge of both the magnitude of these couplings and the single complex phase that appears to describe all observed matter-antimatter differences, which are referred to as *CP*-violating asymmetries. Over the next three years, additional independent measurements of the quark couplings will achieve a threshold of precision that will, for the first time, allow these new methods to provide further stringent consistency tests. The combination of existing and new constraints will provide a powerful test of the Standard Model.

The second goal is to study *CP* violation and rare decays in beauty, charm, and tau decays for indirect evidence of New Physics beyond the Standard Model. Such searches are possible only because of the ever increasing precision with which the Standard Model can be understood, thereby providing a benchmark against which the additional effects of New Physics can be distinguished. Searches for New Physics are of fundamental interest if either convincing new effects are seen or limits can be substantially improved. In general, *CP* violation and rare processes are sensitive to New Physics at high mass scales through their quantum contributions to penguin diagrams, which may involve virtual production of particles from either the Standard Model or New Physics. If there are deviations from the Standard Model, a first exciting look will be given at the properties of New Physics even before it is directly observed at the LHC. However, if no deviations are seen, the *B* Factory program will still provide all important evidence to rule out whole classes of theoretical explanations for new phenomenon discovered at the LHC. The *B* Factory and the LHC are thus complementary tools in the search for New Physics, with the *B* Factory providing a powerful legacy of constraints on the nature of any New Physics directly produced at the LHC.

3.0 FY06 PROGRESS IN THE PARTICLE ASTROPHYSICS PROGRAM by Roger Blandford

The Kavli Institute for Particle Astrophysics and Cosmology (KIPAC) has completed its third full academic year. The KIPAC faculty has been joined by Professor Risa Wechsler who works in the area of cosmic structure formation and by Panofsky Fellow Saurabh Jha, whose work focuses on supernovae and their use as cosmological probes.

As of Oct 2006 there are 18 postdoctoral researchers in KIPAC. The new recruits are Marcelo Alvarez, Andres Escala, Stelios Kazantzidis, Masamune Oguri and Lukasz Stawarz. KIPAC continues to hire the very best young scientists, working across the wide range of topics under the

KIPAC mandate. (This year's hires were selected from an outstanding field of approximately 120 applicants.) Over 30 graduate students are now associated with the group and morale among students and postdoc members is very high. At the administrative level, Ziba Mahdavi has joined the group. The current KIPAC membership can be found at http://www-group.slac.stanford.edu/kipac/.

The six postdoc members who came to the end of their time at KIPAC in the past year have all moved on to prestigious positions. Anatoly Spitkovsky has moved to Princeton University as Assistant Professor in the Department of Astrophysical Sciences. Andrei Frolov has moved on to Simon Fraser University as Assistant Professor in the Department of Physics. John Peterson has moved on to Purdue University as Assistant Professor of Physics. Masao Sako has moved to the University of Pennsylvania as Assistant Professor of Physics and Astronomy. Phil Marshall is the TABASGO Fellow at UC Santa Barbara. Ted Baltz has taken up a staff scientist position at SLAC. Three grad students have moved on to postdoc positions at other universities. The success rate in the job market for KIPAC student and postdoctoral members is clearly very high.

KIPAC has become well-integrated into the SLAC-campus physics community. Joint astrophysics seminars take place on Thursday afternoons, the venue alternating between campus and SLAC; these are well attended. There is good coordination with other lecture series at SLAC and on campus. There are twice-weekly KIPAC `morning teas,' one on campus and one at SLAC, where recent papers and `hot topics' are discussed and short research presentations are made by group members and visitors. Attendance at these meetings typically varies between 50 and 70. KIPAC has achieved the goal of providing a lively and open scientific forum, connecting SLAC with campus. Further outreach has also occurred into the Bay Area astrophysics community.

Administratively, the KIPAC-Physics department has been running smoothly. More than 80 individuals are now associated with KIPAC Physics, with 27 individuals receiving partial or full funding support through the department (6 faculty, 7 staff, 8 postdocs and 6 students). The various subdepartments of KIPAC-Physics have continued to operate efficiently within their FY06 budgets.

The new Fred Kavli Building has been a tremendous success. The open design of the building has enhanced the spirit of lively, open discussion and has fostered further collaboration and the sense of `team' within the Institute. The new Physics-Astrophysics Building on campus will be completed in early October 2006 and bring further opportunities.

The scientific program at KIPAC is diverse with wide-ranging efforts on observational, theoretical, computational and experimental fronts.

Given the nature of modern particle astrophysics and cosmology, this maximizes the opportunity for significant progress. In addition to the work directly related to major projects, reported below, over 100 scientific papers, including conference proceedings, have been written by KIPAC members over the past year and a comparable number of talks has been delivered. Major research concentrations include, in no particular order:

- cosmological studies of clusters of galaxies, combining observations made using X-ray, optical and radio telescopes.
- projects in weak and strong gravitational lensing as well as microlensing, investigations of particle dark matter
- studies of dark matter, dark energy and cosmological parameters
- participation in the Sloan Digital Sky Survey, particularly in the discovery and analysis of supernovae
- participation in radio observations of the sources likely to be studied by GLAST
- modeling of pulsars, especially the recently discovered double pulsar
- modeling of gamma ray bursts
- numerical simulations of the growth of structure in the early universe
- analysis of microwave background observations
- calculations of atomic transitions for use in X-ray astronomy
- new ideas in black hole astrophysics
- studies of astrophysical jets, accretion and galaxy formation.

KIPAC looks forward to further growth over the coming year.

GLAST

The Gamma-ray Large Area Space Telescope, GLAST, is a satellite-based experiment under construction to measure the cosmic gamma-ray flux in the energy range 20 MeV to >300 GeV, with supporting measurements for gamma-ray burst (GRB) transients in the energy range 10 keV to 30 MeV. With a sensitivity that is more than a factor of 30 greater than that of the EGRET detector on the previous Compton GRO mission, GLAST will open a new and important window on a wide variety of high-energy phenomena, including super-massive black holes and active galactic nuclei, GRBs, supernova remnants and cosmic ray acceleration, and searches for new phenomena such as super-symmetric dark matter annihilations, Lorentz invariance violations and big-bang particle relics. The GLAST launch is scheduled for late 2007.

The Large Area Telescope (LAT) is the primary science instrument on GLAST. The LAT collaboration is a novel teaming of particle physicists and high energy astrophysicists.
The collaboration now numbers 86 scientific members, 85 affiliated members and 23 postdocs and many graduate students (5 currently at SLAC-Stanford). The LAT Principal Investigator (PI) and Spokesperson is Professor Peter Michelson (Stanford and SLAC). The LAT has been developed in a partnership between NASA and the DOE, with substantial contributions from Italy, Japan, France and Sweden. The LAT project is managed at SLAC.

The LAT collaboration had a 3-day meeting in Stockholm in August 2006, preceded by splinter meetings of many of the 9 science groups organized in the collaboration, and followed by a one-day science symposium on gamma-ray bursts.

The integration of all 16 towers, the Anti-coincidence Detector and data acquisition electronics onto the LAT support grid was completed at SLAC in May 2006. The LAT was then trucked to the Naval Research Laboratory in Washington, DC for environmental testing, including vibration,

acoustic, electromagnetic interference and thermal-vacuum testing. These tests verified that the LAT successfully operated after being subjected to launch-like stresses and the expected temperature extremes of on-orbit operating conditions. After a successful post-test review on 15 September 2006, the LAT arrived at General Dynamics C4 Systems in Gilbert, AZ on 18 September 2006 ready to be integrated onto the GLAST spacecraft. The development of the LAT flight software is nearing completion. The final launch-ready version of the software will be installed on the LAT in November, before initial testing of the integrated GLAST. The integration and test of GLAST will last approximately 9-10 months at General Dynamics before GLAST is transported to Cape Canaveral for launch.

Preparations for the operation of the LAT continue at SLAC. The LAT Instrument Science Operations Center (ISOC) at SLAC will operate the LAT in conjunction with the GLAST Mission Operations Center (MOC) and GLAST Science Support Center (GSSC) at NASA Goddard Space Flight Center, and will process LAT detected event data and provide reduced data to NASA and the LAT collaboration. Most of the ISOC staff have been consolidated into the Central Lab Annex building at SLAC. Construction has started on the LAT ISOC Operations Facility in the Central Lab Annex, comprising an operations control room, office area for operations staff, and a dataflow lab housing a full-scale replica of the LAT flight electronics and eventually the flight-spare detectors. The construction of the Operations Facility is scheduled for completion in January 2007.

Data Challenge 2 (DC2) was held during March-June 2006, following on from DC1 in 2004. DC2 used a simulation of 55 days of LAT data generated using 200,000 CPU hours on 400 CPUs in the SLAC computer farm. DC2 provided end-to-end testing of instrument simulation, event reconstruction and science analysis tools including pulsar timing, GRB detection, and the analysis pipeline for generating the LAT source catalog.

From July to September of 2006 a beam test was conducted at CERN in the Swiss-French border, using spare modules of the LAT assembled into a mechanical support grid. The test article, hereafter calibration unit (CU), consists of 2 complete LAT towers (tracker, calorimeter and tower electronics module), a third calorimeter and tower electronics module, a trigger module, and 5 plastic scintillator tiles from the anti-coincidence detector. Data were collected in the CERN PS beam line during the months of July and August using low-energy beams (up to 10 GeV) of photons (tagged and untagged), electrons, positrons and hadrons. Data were collected with the CU in the SPS beam line in early September using beams of photons, electrons and hadrons at several energies up to 280 GeV. Further data taking with the LAT CU will be conducted with heavy ion beams at GSI/Germany in November.

Work to understand the LAT acceptance, proton rejection, and response functions using ground Cosmic Ray data and beam test data is ongoing. Preparations at SLAC are ongoing in three broad areas of GLAST science.

1. Dark Matter and New Physics
2. Particle Interactions and Acceleration in Astrophysical Sources
3. Relativistic Outflows.

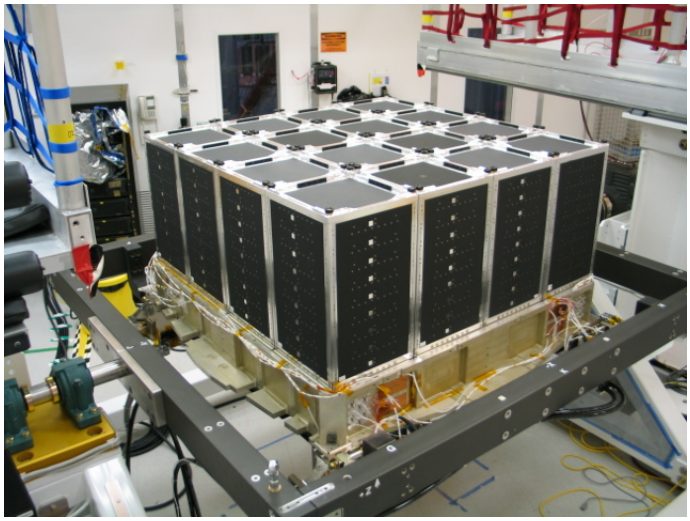

Figure 1. 16 towers installed on the LAT

Figure 2. The LAT in the thermal-vacuum chamber at NRL

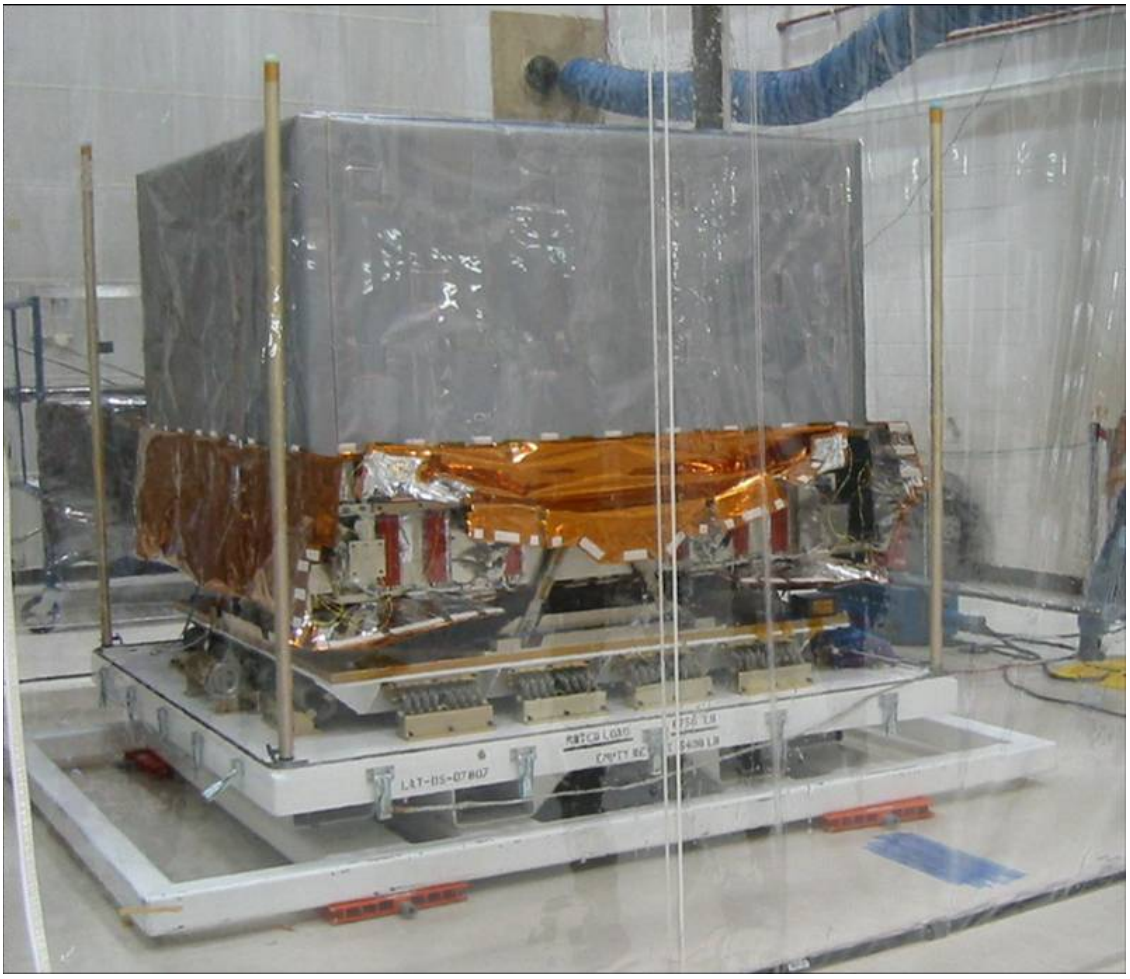

Figure 3. The LAT ready to ship to General Dynamics for integration onto GLAST

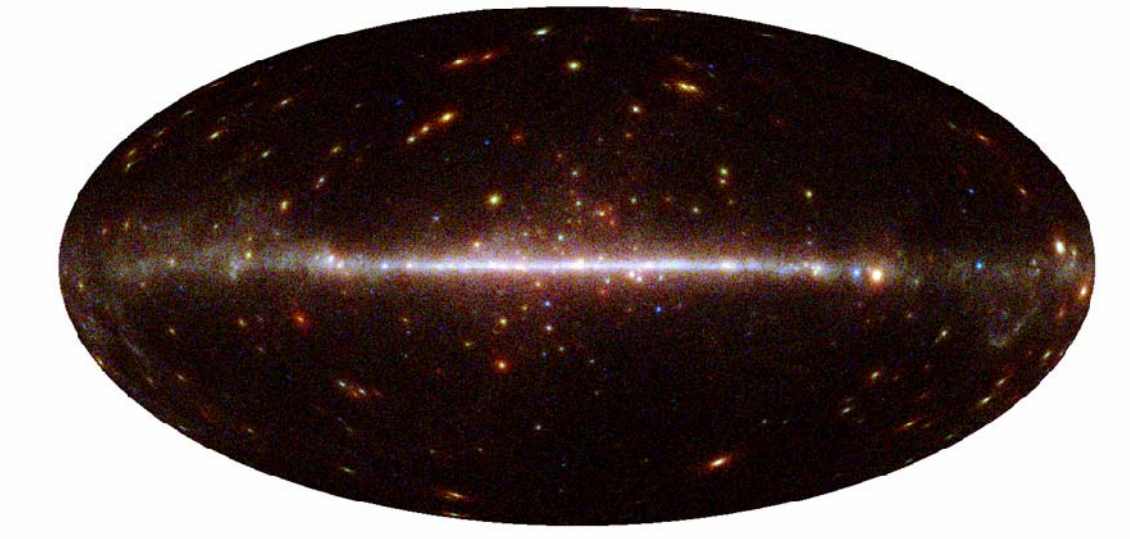

Figure 4. Sky map of gamma rays detected by the LAT in the Data Challenge 2 simulation.

Figure 5. The Calibration Unit (CU) used for the beam test at CERN.

LSST

The prime goal of LSST is a precision measure of the nature of dark energy though a suite of techniques using a homogeneous imaging data set. Central of these is weak lens shear of galaxy shapes to z=3 by mass at z<3, giving a unique probe of dark energy. This will be done through a combination of deep-wide multiband imaging data over 20,000 sq.deg. in a weak lensing survey of unprecedented sensitivity x volume and quality. By measuring the gravitational lens distorted shapes of billions of galaxies as a function of angle on the sky and photometric red shift out to z=3, and using galaxy P(k) from these same data together with WMAP and Planck data, LSST will constrain six eigenmodes of the dark energy equation of state parameter. The shear power spectra and 3-point correlations depend on the growth function and angular diameter distances, which are both sensitive to the equation of state of dark energy. The technique used in these forecasts is lensing tomography with the auto- and cross-power spectra of the lensing shear. LSST will also measure with record precision: baryon acoustic oscillations, hundreds of thousands of SNe, and clusters of galaxies — three additional cosmological diagnostics providing independent constraints on dark energy.

LSST will be a large, wide-field ground-based telescope designed to obtain sequential images of the entire visible sky every few nights. The optical design involves a 3-mirror system with an 8.4 m primary, which feeds three refractive correcting elements inside a camera, providing a 10 square degree field of view sampled by a 3 gigapixel focal plane array. The total effective system throughput, AΩ = 318 m 2 deg2, is nearly two orders of magnitude larger than that of any existing facility. The survey will yield contiguous overlapping imaging of 20,000 – 23,000 square degrees of sky in 6 optical bands covering the wavelength regime 350–1100 nm.

A collaboration led by SLAC is building the LSST camera which is a wide-field optical (0.35-1 μm) imager designed to provide a 3.5 degree FOV with better than 0.2 arcsecond sampling. The camera includes a filter mechanism and shuttering capability. It is positioned in the middle of the telescope where cross-section area is constrained by optical vignetting and heat dissipation must be controlled to limit thermal gradients in the optical beam. The fast, f/1.2 beam will require tight tolerances on the focal plane mechanical assembly. SLAC personnel occupy several leadership

positions within the project. Steven Kahn is the Deputy Director of the LSST project overall, and is the Lead Scientist for the Camera. Kirk Gilmore is the Camera Project Manager. Roger Blandford, the Director of KIPAC, is a member of the LSST Corporation Board of Directors.

During the past year, substantial progress has been made on the camera development. Camera body/cryostat modeling as well as overall metrology is currently being developed by SLAC designers and engineers. The current level of design is leading to several years of R&D that will include extensive prototyping of the major components of the camera. Part of the prototyping effort is motivated by retiring the risk associated with state of the art components.

The LSST Camera focal plane contains a large array of imagers. The challenge is the development of imagers which meet LSST's specifications on pixel size, QE, flatness, dead area and readout speed. All the specifications have been achieved in previously used CCD arrays; the development task involves integrating all the required features into a single sensor. The LSST sensor working group, which includes members of the LSST at SLAC team, currently has several vendors under contract to develop study sensors that will help determine the final operating characteristics of the science detectors.
LSST's fast optics produce a very narrow depth of field which requires that the focal plane be flat within 10 μm. The R&D program for the LSST camera will focus on understanding the best techniques to employ to keep the focal plane flat to the high precision tolerances required. Initial studies will include the development of various motion control scenarios to actively maintain flatness of the raft (3x3 detector array) under a variety of thermal and mechanical conditions.

LSST filters present special fabrication challenges to achieving spatially uniform passband characteristics necessary to do <1% photometry. These include achieving the necessary thermal and mechanical stability. A development program spearheaded by SLAC personnel is currently under way with the ultimate goal of fabricating a full-scale prototype which demonstrates the necessary performance characteristics over the full field.

In terms of scientific investigations, science collaboration groups have been formed to address the issues associated with the major scientific projects of the LSST. These Science Collaborations will work closely with the LSST Project as it builds the telescope, camera, and software, and will be expected to play a substantial role in the scientific commissioning of the project. The major input of the science collaboration groups will help identify and resolve key scientific issues. KIPAC is heavily represented on most of the collaborations.

A camera face-face meeting was held at SLAC in FY06 and was attended by 48 LSST personnel with 37 people from partner institutions and 11 people from SLAC. SLAC also hosted an LSST simulations workshop and operations simulator workshop in FY06.

Below is an image of the LSST camera body with the cryostat. The raft tower contains the detector and the electronics. The diameter of the L1/L2 housing is about 1.7 meters.

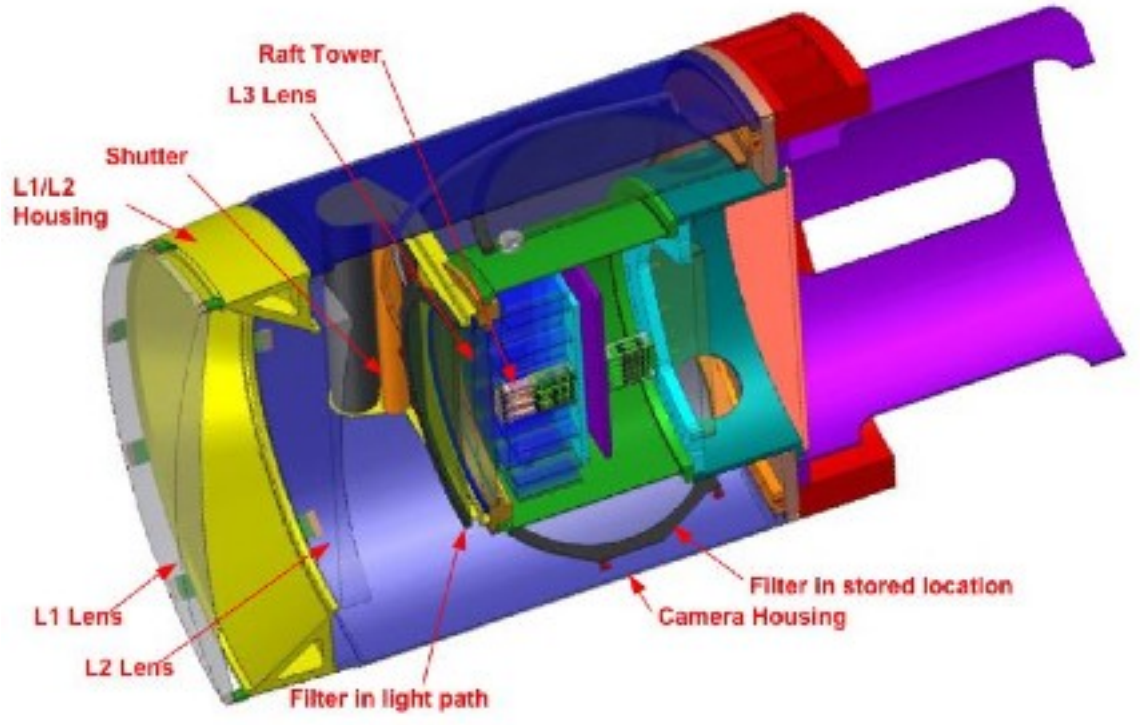

SNAP

The Supernova Acceleration Probe (SNAP) is a proposal for a space-based wide-field telescope designed to study the physics of dark energy using calibrated Type 1a supernovae as standard candles. The mission will also enable weak lensing studies with high precision over moderate angular scales. The SNAP design includes a large focal plane tiled with both visible-light and infrared-imaging sensors, as well as a visible/IR spectrograph suitable for following up detected supernovae.

SLAC/Stanford proposed to join the SNAP collaboration in August of 2003. That application was formally approved in March 2004. Within the collaboration, SLAC is responsible for the design and development of the SNAP Instrument Control Unit (ICU) and the focal plane guiding system. SLAC scientists also provide significant support of the strong lensing abilities of the SNAP telescope.

The ICU performs electronic supervision of the entire SNAP instrument, executes the science mission, manages the operation of instrument mechanisms and thermal controls, and controls the flow of commands and data between the focal plane electronics, mass memory and spacecraft. This effort is led by Gunther Haller who has been hosting semimonthly electronics exchange (elex) meetings between SLAC, FNAL and LBL. The SNAP mission desires to have all focal plane components maintained at a common temperature without thermal control on each device. Over the last year the ICU team have been studying of the thermal properties of the focal plane and developing communications protocols between the warm electronics and the cold focal plane components. The level 3 electronic requirements document and on deck component layout studies are being developed.

The focal plane guiding system will allow the SNAP observatory to track its science fields to an accuracy of better than 20 milliarcseconds. SNAP intends to use a new technical approach, consisting of four asynchronously operated imaging devices, controlled by a central processor. This system will collect sufficient photons to generate an appropriate error signal for the spacecraft pointing system. By operating the sensors asynchronously, the integration time for each device can be tailored to the number and brightness of stars available with the field of view. This approach was simulated and compared with worst-case star field density and shown to meet the accuracy requirements. In collaboration with Lockheed Martin LLC, Bill Craig, Kevin Reil and Johnny Ng have been developing a test-bed prototype to confirm the pointing requirements. Studies using this test-bed should be completed over the next year.

SLAC scientists have also played a significant role in formulating the detailed scientific program for SNAP, especially with regard to strong lensing investigations. The SNAP database should reveal a large number of new strong lenses. Measurements of the properties of these lensed images will yield a number of interesting constraints on cosmological models. SLAC scientists including Phil Marshall, Roger Blandford, Masao Sako [see 2005-01-16 New Astronomy Reviews 49 387 (2005)], have provided support for strong lensing science from SNAP. Currently, in support of the scientific promise of SNAP, studies of existing data in the HST ACS archive are underway. Information on their search for lenses in this existing data can found in http://arxiv.org/abs/astro-ph/0607239.

Computing

KIPAC members have strong research programs spanning much of high energy astrophysics and cosmology including gamma-ray, X-ray and radio astronomy, modeling of gamma-ray bursts, active galactic nuclei, pulsars and supernova remnants. Generic, high energy astrophysics processes, such as relativistic shock waves and particle acceleration are also being studied. Most of these scientific programs require high performance computing and this has been a major feature of KIPAC's plans since its inception. Data handling, data analysis and numerical modeling activities are driving this development. In 2006, major efforts included searching the Hubble Space Telescope database for gravitational lenses and cosmic strings, analysis of X-ray observational rich clusters of galaxies, numerical modeling of the kinetic structure of supersonic and relativistic shock fronts, determining the properties and consequences of the first stars to form in the universe and modeling the production of gamma-ray bursts during the collapse of massive stars. A more complete tour of computational activities at KIPAC is available on the web at: http://www-group.slac.stanford.edu/kipac/comp_physics.htm.

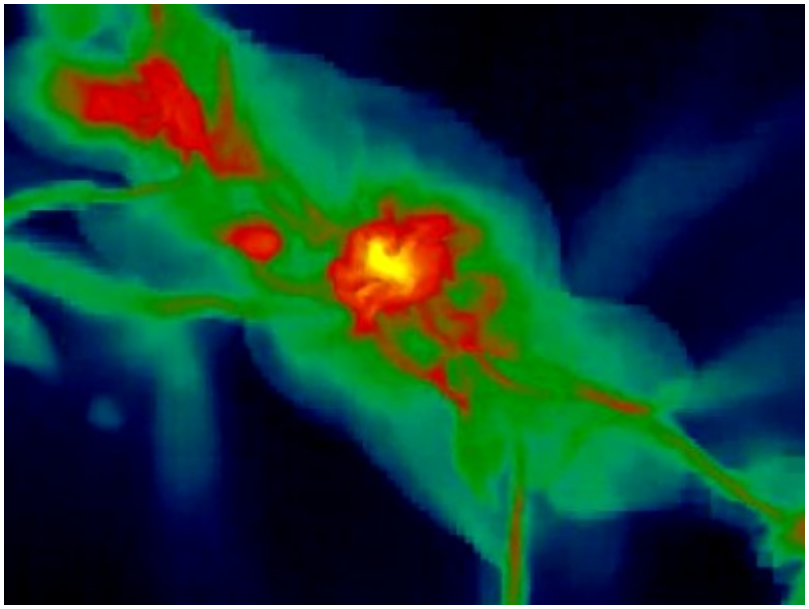

Using adaptive mesh refinement cosmological hydrodynamics calculations the collapse of primordial gas is followed over 25 orders of magnitude in density with a maximal dynamic range of 1015. Simulations are being carried out on the KIPAC, 72 processor SGI Altix supercomputer.

To support these activities KIPAC has established a computing department with 2006 as its first full year. Development has begun of a sustained computing program comprising four elements: processing cycles, data/storage management, visualization, and personnel.

Current processing capability includes a 72-processor SGI Altix SMP system, KIPAC's 12-node set of Apple compute servers, access to the Advanced Computation Department's myrinet clusters for MPI jobs, SLAC's batch servers, and individual users' desktops. These resources have been used aggressively to carry out many projects but to date, computing capability has been a source of limitations. These systems will be augmented with a 64-node cluster in late 2006 specifically tailored for numerical astrophysics computations. Additionally, KIPAC's SGI Altix is being upgraded with additional memory specifically to facilitate cosmological simulations that require larger dynamic range.

This year (2006) development began of a long term "Data Lifecycle Management" program which includes tiered storage and planned growth. KIPAC purchased 30 TB of storage and plan for approximately constant annual costs[1] to keep up with increasing demand. An implementation is currently being tested of a high performance storage system to support the compute cluster environment where I/O performance can be a significant enabling factor in scientific output.

Visualization capabilities have also been developed in 2006 with prototype 3-D projection and 2-D tiled display systems suitable for software development and modest data interaction. Use of these facilities includes creating three-dimensional movies, using multiscreen displays of high dimensional parameter spaces and exploring new methods to exhibit three-dimensional vectors like magnetic field. The strong graphical content of observational and theoretical astrophysics and cosmology makes it ideal for education and public outreach.

[1] As cost per unit storage decreases

With the move into the Fred Kavli Building in mid 2006, the process of building personnel resources and communication mechanisms has been enhanced. Five FTEs are currently resident at KIPAC and SLAC's Scientific Computing and Computing Services (SCCS) group supporting computing. Regular meetings are held with SCCS twice per month and an external review of our computing plan was held in March 2006. An expert in scientific visualization is being recruited to join KIPAC. Additionally, substantial use is made of our SU campus location at kipac.stanford.edu to host KIPAC-specific computing documentation and group communications.

As the year closes, negotiations with vendors are in progress to obtain a low-latency compute cluster with 64 nodes (each with 4 cpu cores), 512 GB total memory and 10 TB of parallel disk storage. KIPAC staff are collaborating with SCCS to develop the specialized configurations needed for numerical astrophysics. Staff are also working closely with SCCS to design and integrate this new system with the existing storage and visualization capabilities. This system will augment substantially the existing research programs and provide a significant capability to the incoming group of postdocs.

Other Activities

NuSTAR

NuSTAR is a satellite-based instrument to image hard X-ray radiation from celestial sources. This experiment is led by Caltech (Fiona Harrison, PI), but with a substantial involvement of KIPAC scientists (W. Craig, G. Madejski, R. Blandford) in addition to participants from JPL, UCSC, and Columbia University. The technical approach is via the use of multilayer grazing incidence optics focusing hard X-rays onto pixilated CdZnTe detectors. This approach dramatically reduces the particle- and Cosmic X-ray background, resulting in at least a 100-fold sensitivity improvement over any previous instruments. The science goals of the mission are: to study the production of heavy elements in supernovae; to determine the origin of the celestial hard X-ray background (where most of its energy is detected); and to provide for a tool to study relativistic jets in celestial sources via simultaneous observations with the GLAST satellite (also involving SLAC personnel).

This instrument was selected by NASA via a competitive process for the extended definition study in the Explorer program, with the goal of launch in 2009. Unfortunate budgetary constraints at NASA led to the termination of funding for the project. However, since this experiment was the top-rated astrophysics mission in the Explorer class, and the science objectives remain extremely compelling, it is anticipated that it will be either reinstated, or will be highly competitive in the next Announcement of Opportunity, expected next year. The NuSTAR team is fully committed to its success.

Even if NASA chooses not to be involved in the sensitive exploration of the hard X-ray sky, there is a highly competitive international program with similar goals. The most viable is the Japanese-led mission NeXT, which is identified as the next high energy astrophysics effort of the Japanese Space Agency JAXA. With the intended launch of 2012-2013, NeXT will include an imaging hard X-ray instrument similar in design to NuSTAR, but also will include detectors sensitive in soft X-ray, and soft gamma-ray bands. KIPAC scientists are part of the NeXT collaboration, and

fully intend to participate, since such work is likely to enhance the scientific return of the GLAST (and LSST!) projects.

PoGO
PoGO is a balloon-borne hard X-ray polarimeter that consists of well-type phoswich scintillation counters to study polarization of hard X-ray flux from celestial sources. PoGO is funded by a Stanford Campus fund in the US, the Warrenburg Foundation in Sweden (PI is Mark Pearce of the Royal Institute of Technology), three grants from Grants-in-Aid in Japan (PI's are Jun Kataoka of Tokyo Institute of Technology, Yasushi Fukazawa of Hiroshima University and Tune Kamae as a professor emeritus of University of Tokyo). A proposal was also submitted to NASA, which is being reviewed right now.

A beam test has been completed using synchrotron light to study the performance and another beam test using proton beam to study the effect of cosmic rays. Developments of detector elements, readout electronics, data acquisition system, gondola and pointing system are on track for the first balloon flight in 2009 spring.

4. FY2006 SELF-APPRAISAL FOR DOE: ILC DEPARTMENT AND NLCTA by Nan Phinney and ILC Staff

4.1 The ILC Department at SLAC
The SLAC ILC group is internationally recognized for its expertise. SLAC has been a leader in linear collider development for over 25 years. SLAC built and operated the first linear collider, the SLC, and used that experience to produce an integrated, comprehensive design for a linear collider based on warm rf technology for the accelerating structures. SLAC has accelerator physics expertise in *all* subsystems of the collider from the sources to the Interaction Regions (IR). With the adoption of the superconducting rf technology for the ILC in 2004, this expertise has been refocused on developing a design based on cold rf technology.

SLAC continues to be a major contributor to linear collider development through its broad expertise and unique test facilities. Over the years, significant R&D has been performed on all of the subsystems of the 'warm' X-band design and both the 'warm' design and ILC design share many common features. Less than 25% of the cost of the superconducting design is in the superconducting cavities or cryomodules – the rest of the collider is based on normal-conducting technology similar to that which SLAC has studied extensively. SLAC is applying the major advances that were made for the X-band design to the ILC. The activities in or supported by the SLAC ILC program address 14 of the 15 critical R2 items identified in the ILC Technical Review Committee (TRC) report from 2003 – many of these issues are important to resolve as part of an international Reference Design Report (RDR).

In addition, the SLAC accelerator complex provides facilities capable of supporting a wide range of ILC R&D. An L-band rf test facility is being developed in End Station B, which benefits from the existing infrastructure of the NLC Test Accelerator (NLCTA). This facility will provide long-term testing of klystrons and modulators, and rf power for coupler and normal-conducting structure testing. The NLCTA beam and beam-line support full power structure testing with beam. Modifications are being made to produce an ILC-type bunch for instrumentation development.

End Station A has been reconfigured as a test beam facility for experiments with collimators, IR instrumentation, and detector components. Two successful runs were completed in FY06. This is the only experimental area with access to multi-GeV high quality electron beams. Prototype vacuum chambers utilizing various electron cloud suppression techniques are being installed for testing in PEP-II.

The rest of this section will describe the ILC Department participation in the ILC GDE, participation in Reviews and Conferences, and Department safety issues. In the following sections, the close-out of the X-band R&D program, the L-band R&D program, and the Accelerator Design programs will be described. Following this will be short sections describing the operation of the NLC Test Accelerator (NLCTA) which the ILC Department operates to support advanced accelerator R&D as well as ILC R&D and participation in the LHC Accelerator Research Program (LARP) in the form of advanced beam collimators which were spun off from the NLC R&D program.

4.1. a. ILC GDE Activities

The ILC Global Design Effort (GDE), which reports to the International Linear Collider Steering Committee of the International Committee for Future Accelerators, was formed in 2004. Barry Barish was appointed director in March 2005, and shortly thereafter he formed an Executive Committee with three regional directors and three accelerator physicists, Tor Raubenheimer (SLAC) for the Americas, Nick Walker (DESY) for Europe, and Kaoru Yokoya (KEK) for Asia. Three regional cost engineers and three conventional facilities engineers were also selected.

The rest of the GDE members were appointed and met for the first time at the Snowmass 2005 workshop, and several more have been added later to fill gaps in expertise. In addition to Raubenheimer, SLAC has 9 members of the GDE including Chris Adolphsen, Tom Himel, Tom Markiewicz, Ewan Paterson, Nan Phinney, Marc Ross, Andrei Seryi and John Sheppard. The GDE director also formed three boards, all of which have SLAC participation: the Change Control Board with Tom Markiewicz, the R&D Board with Tom Himel and Marc Ross, and the Design Cost Board with Ewan Paterson and Nan Phinney. Tom Markiewicz also chaired a committee to select EDMS tools.

The major GDE task for 2005 was to develop the Baseline Configuration Document for the ILC. Key decisions were taken at the Snowmass workshop and these were further developed and finalized for a GDE meeting in Frascati in December, 2004. The SLAC ILC group played a major role in formulating the shape and content of both the Snowmass and Frascati meetings. In both cases, SLAC ILC Department members made significant contributions to the overall meeting structure, with many SLAC ILC members as conveners of global or working groups..

The major task for 2006 is to develop a complete design for the ILC with a preliminary cost estimate, documented in a Reference Design Report (RDR) by the end of calendar 2006. Again SLAC ILC physicists are playing a major role in this effort. For the RDR, a matrix of Area, Global and Technical System groups was formed, with leaders from all 3 regions. SLAC physicists are system leaders for 5 of the 6 Area Systems (Axel Brachmann-Electron Source, John Sheppard-Positron Source, Peter Tenenbaum-Ring to Main Linac, Chris Adolphsen-Main Linac, Andrei Seryi-Beam Delivery). They are also leaders of several Technical or Global groups (Tom Himel-Operations & Availability, Fred Asiri-Installation, Ray Larsen-RF Sources, Marc Ross-

Instrumentation, Tom Markiewicz-Dumps & Collimators). In addition, Ewan Paterson is the Systems Integration Engineer. Tor Raubenheimer and Ewan Paterson are members of the RDR Management team and Nan Phinney is chief editor for the RDR Report.

There have been three full GDE meetings in FY06. The first was in Frascati, Italy, December 7-9, 2005, just after a Tesla Technology Collaboration meeting. The 2nd was in Bangalore, India Mar 9-11 2006 together with the international LCWS. The third was in Vancouver, Canada July 19-22, 2006 together with the ALCPG workshop. SLAC ILC physicists played a major role in formulating the shape and content of these GDE meetings. In addition, there were meetings of the RDR Area leaders in January at KEK and in February at FNAL and of the RDR Management in August at KEK. Most of the Area, Technical and Global groups have regular three-region teleconferences, often augmented by a face-to-face meeting between full GDE meetings. The three Boards, the RDR Management and the Executive Committee also have weekly teleconferences.

4.1. b. Reviews and Meetings

The ILC group has participated actively in the national and international community through reviews and meeting participation.

From October 17-21, 2005, the Nanobeams Workshop was held in Kyoto, Japan. SLAC ILC members served on the program committee and as working group convenors.

In December 2005, an Availability Mini-Workshop was held Dec 1-2 at Groemitz, Germany where SLAC ILC staff made presentations. This was followed by the Tesla Technology Collaboration and 2nd GDE meetings in Frascati.

In February, SLAC hosted an ATF-2 collaboration meeting on Feb 3-4.

In March, many SLAC ILC members attended the 3rd GDE meeting Mar 9-13 in Bangalore, India, along with satellite GDE Executive Committee, Change Control Board, R&D Board and Design Cost Board meetings.

In April, SLAC ILC physicists made presentations on several key areas of the ILC program at the Apr 4-6 DOE Review and Apr 7-9 MAC meeting, both held at FNAL.

In May, SLAC hosted the second meeting of the Linear Collider Forum of the Americas on May 1-2.

EPAC 2006, the biennial international particle accelerator conference, was held in Edinburgh, Scotland in June 2006. ILC staff submitted more than a dozen papers and gave two invited talks.. In addition, ILC staff members were active in the program committee for the conference.

The SLAC ILC group also played a major role in formulating the shape and content of the three ILC GDE Meetings at Frascati in December 2005, at Bangalore, India in March 2005 and at Vancouver in July 2006. SLAC ILC Department members made significant contributions to the overall meeting structure and to leadership of area, technical and global groups.

In August, SLAC ILC engineers also attended Linac'06 where they made presentations on the modulator systems that we are developing.

In September, SLAC ILC Physicists made presentations at the second ILC MAC Meeting Sep 20-22 at KEK. They participated in meetings Sep 23-24 of the Executive Committee, RDR Management, R&D Board, Design Cost Board, and Linac working groups. On Sep 25-28, SLAC physicists joined the Tesla Technology Collaboration meeting also at KEK. SLAC also hosted the 9th International Workshop on Accelerator Alignment Sept 25-29.

SLAC ILC members also participated in many other conferences and workshops where they presented papers and shared plans with colleagues without actual linear collider experience and without the depth and breadth of research that backs the SLAC ILC team. Other workshops held at SLAC include an ongoing series on ATCA technology as a possible basis for standardization of ILC electronics.

4.1. c. Collaborations

The ILC Department has a long history of collaboration with KEK and within the US with LLNL, LBNL, FNAL and BNL. Additional collaborations are ongoing with Queen Mary University of London, Oxford University, the Rutherford Appleton Laboratory, the Daresbury Laboratory and DES, and with the French laboratories CEA Saclay and CEA Orsay.

Collaboration at DESY includes work on benchmarking reliability and availability codes and working on the Tesla Test Facility (TTF). Members of the ILC Department also used concepts and technology developed for the X-band program to measure the higher-order mode (HOM) signals from the TESLA cavities. Such HOM detectors may prove important to align the cavities in the ILC. At DESY's request, the ILC group built a set of 40 of these detectors which were installed at the TTF. Ongoing R&D is using these detectors to understand the internal deformation of the 9-cell cavities. Finally, SLAC has formally joined the TTC and MOUs have been exchanged.

The ILC Department has a long-standing collaboration with KEK on ATF and on rf technology. During FY2006, the SLAC group has worked on three main projects with KEK and has received roughly 400k$ of US-Japan funding. Much of the effort focused on the development of the ATF-2 which would prototype the ILC beam delivery system utilizing the extremely low emittance beam from the ATF damping ring. Specifically, activities in FY2006 include development of an ultrafast kicker for testing at ATF, testing of a new technology for the ATF ring BPMs, design of the ATF-2 beamline, and the development of an rf BPM system for the ATF-2. The ILC Department has had a physical presence at KEK working on the ATF damping ring that averaged roughly one FTE. An MOU with KEK on the ATF which covers operation of the ATF and the international construction of the ATF-2 has been finalized. Ewan Paterson of SLAC chairs the ATF-2 International Collaboration Board and Tor Raubenheimer and Andrei Seryi of SLAC are members of the ATF-2 Technical Board.

The End Station A Test Facility, which has been developed to test prototypes of IR beam diagnostics and IR design concepts using the high energy SLAC beam, is a collaboration between SLAC and US and UK universities. Most of the specific experimental proposals have at least one spokesperson from a university in either the UK or the US.

4.1.d. Safety

At SLAC and in the ILC Department, concern for safety is an integral part of our culture. All personnel review and update their JHAMs annually or when work activities change, and they complete all other safety courses recommended by their supervisors. Work authorization procedures at the NLCTA, a major test facility operated under the ILC Program, have been used as a model for other facilities at SLAC. The ILC Conventional Facilities engineers continue to contribute to the lab-wide effort implementing risk mitigation measures. ILC engineers and physicists participate in the various Citizens' Committees such as Radiation Safety and Earthquake Safety.

4.2. X-band rf R&D

With the ITRP decision of the superconducting technology for the ILC in August, 2004, the SLAC X-band program was put on hold. In FY2005, the ILC group chose to continue some of the X-band (11.4 GHz) structure testing in a program to wrap-up the 15-year-long structure development effort, and to provide useful information for future high gradient applications. In FY2006, the research using existing high gradient X-band structures continued at a low level, and was funded by SLAC as part of the newly created US Collaboration on High Gradient Research program.

The program at NLCTA included the operation of an X-band structure at a lower water cooling temperature to determine whether this would reduce the breakdown rate, as might be expected if breakdowns are related to migration of surface contaminants. However, no significant difference in breakdown rate was seen when operating at the normal structure cooling water temperature of 110 F and the reduced temperature of 60 F. Various vacuum venting experiments were also performed on another structure and showed that purging with nitrogen or venting to either filtered or unfiltered tunnel air had minimal impact on high gradient operation. However when the structure was heated to ~ 160 °C and vented to filtered air, the breakdown rate increased substantially and never fully recovered after a week of rf processing. Presumably, this slow recovery was the result of an oxide layer that formed on the inner surfaces (such layers have been observed in some structures, and are likely the result of small vacuum leaks during brazing or baking).

The accelerator structure used in the water temperature test was longer (75 cm) than the standard NLC high gradient designs (60 cm) that were developed, and performed as well as the best of them (about 25 had been tested). It achieved a breakdown rate of 0.2 per hour during 75 MV/m, 60 Hz operation with 400 ns NLC-like pulses. Its performance would allow for a higher gradient operation than the 65 MV/m unloaded value that had been adopted for the NLC.

4.3. L-band rf

The ILC superconducting linacs require low cost, high efficiency and high reliability rf sources that generate 10 MW, 1.6 ms, 5 Hz pulses of L-band (1.3 GHz) rf power and distribute it to 24 accelerator cavities. Six ILC rf system related programs based at SLAC are described below. SLAC is the center for the ILC Americas rf system development, which includes all elements in the main linacs between the 'wall plug' and the cavity couplers, and the normal-conducting injector accelerators.

4.3.a. Modulator

The ILC baseline modulator is a pulse transformer type with an LC 'bouncer' circuit for droop compensation. Although several of the baseline pulse transformer modulators have been built and operated without major reliability problems, they have very large and heavy oil-filled transformers, and the switching is done at the low voltage (10 kV), high current (1.6 kA) end, which increases the losses. The goal of the SLAC modulator program is to evaluate alternative designs that could reduce the modulator size, weight and cost while increasing reliability and energy efficiency.

The ILC alternate modulator choice is a Marx Generator design, and a prototype is being developed at SLAC. For this approach, a series of capacitors are slowly charged in parallel, and discharged in series to form the pulse. No transformer is used and all switching is done at the lower load current (130 A). The modulator consists of a series of 12 kV main cells (large circuits boards mounted on a common backplane) and 900 V vernier cells for regulation and droop compensation. These circuits are summed to produce the required 120 kV, 1.6 ms flat pulses at 5 Hz. Its modular design lends itself to high reliability (extra cells are included to automatically replace ones that fail), and to mass production assembly techniques, which should provide significant cost savings (~ 40%) over the baseline design. The fabrication of a full-scale prototype is nearly complete and initial testing is expected in the next month. One of the cells has been operated at full specification and shown to survive a shorted load.

Another design being evaluated at SLAC is the SNS High Voltage Converter Modulator, which employs a high efficiency, 20 kHz switching circuit in a compact layout. A production unit on loan from SNS has been installed and brought into operation at the SLAC L-band Test Stand (see Section 3.f.). Its main drawback is that droop compensation has yet to be successfully implemented. The unit at SLAC may eventually be modified to produce flat pulses for 10 MW klystron testing. Yet another modulator being considered is a direct switch unit being developed by Diversified Technologies through SBIR funds. It uses a multiplier circuit to produce the full voltage, which is then applied by a direct solid-state switching element to the klystron. As in the Marx approach, the pulse transformer is avoided, and as in the baseline design, droop is compensated with a bouncer circuit. The first unit is due to be delivered to SLAC at the end of 2006 for evaluation.

4.3.b. Klystrons

The existing ILC high power rf source prototypes consist of three vendor-produced 10 MW Multiple Beam Klystrons (MBKs) that were built in a collaboration with DESY. These designs achieve high efficiency (~ 65%) by using six or seven beams to reduce the space charge forces that limit rf bunching (single beam tubes typically have 40% - 45% efficiencies). However, these prototypes have not yet proven robust or have not been tested long enough to fully qualify them. The SLAC Klystron Group is instead investigating the merits of a new class of sources known as Sheet Beam Klystrons (SBKs). In these tubes, a flat beam is used to reduce the space charge forces, which should produce an efficiency similar to that of the MBKs.

In FY2006, SLAC funded the design effort for the SBK, and the ILC group has proposed for FY2007 that two prototype SBKs be built at SLAC in the next two years. This effort has benefited from the Klystron Group's recent design and fabrication efforts that led to successful beam transport in a 91 GHz SBK (no commercial SBKs exist at any frequency). The ILC prototypes,

which will be ‘plug compatible’ with the MBKs, will have a 40:1 beam aspect ratio and will utilize permanent magnets for focusing (reducing the ILC power consumption by about 4 MW).

Much work has been done over the past year in perfecting 3-D klystron simulations using recently developed software modeling packages for the gun, beam transport and rf power formation and extraction. The basic SBK rf design is complete and the first prototype could be fabricated by the fall of 2007. Future plans also call for acquiring and long-term testing second generation, 10 MW MBKs.

4.3.c. Rf Distribution

To distribute the rf power from a klystron to the cavities in the ILC linacs, the baseline design is to have a series of tap-offs along a waveguide that runs parallel to the beam line. There would be a circulator in each cavity feed line followed by a three-stub tuner to allow control of the cavity phase and Qext. Currently the DESY rf distribution systems use off-the-shelf components that are not necessarily optimized for this application. Also, delivering the same power to each cavity is inefficient with the ~ 5 % rms spread in cavity operating gradients that is expected (i.e., the worst cavity limits the gradients of the others).

At SLAC, four changes to the rf distribution design are being considered. The circulators would be eliminated as they are a big cost item, and the cavities would instead be powered in pairs using 3-dB hybrids. This would still isolate the cavities, but would allow some power (< 1%) to return to the klystron in the event of an rf fault in a single cavity or coupler, which should be benign. A second change would be to use a variable tap-off system to feed the cavity pairs. One proposal is to have rotatable, polarized TE11 circular waveguide sections between the cavities whose orientation would be adjusted (one time only) after the relative cavity performance was measured. Another cost cutting measure is to replace the 3-stub tuner with a simpler phase shifter that would be adjusted once the system is set up, and would not require further changes. Finally, with the large number of waveguide flanges, a means of welding the waveguides together is being sought to reduce cost and improve reliability. At present, an rf design for a variable tap-off system has been completed and some initial waveguide welding tests have been done. The plan next year is to assemble an eight cavity feed system for the first FNAL cryomodule. It would incorporate these proposed changes if they prove practical to implement and robust in high power tests at SLAC (circulators would be supplied for the initial cryomodule operation to ensure full cavity isolation).

4.3.d. Coupler

The power coupler designs for the ILC superconducting cavities are complex devices due to the required cleanliness, high power rf operation, temperature gradients (300 K to 2 K), vacuum isolation (with two rf windows) and tunability requirements. The current ILC baseline design (TTF3) works reasonably well, but the couplers can take up to a few days to rf process.

To understand what limits the processing, Brian Rusnak from LLNL, in collaboration with SLAC, has been examining the coupler design and its performance. From this study, a series of tests has been planned to power various coupler parts including sections with and without bellows, and sections with and without windows. In FY06, significant progress was made in developing components for the coupler test stand. An overall design concept was configured and an L-band waveguide-to-coaxial transition was designed that would accommodate the SLAC L-band window and the installation of components needed for the tests. The test stand imposed significant

constraints on the rf components and how they interconnect. Since the goal of the experiment is to measure gas loads during rf conditioning from individual coupler components, it is important that all rf electrical connections be robust and repeatable to avoid anomalous arcing and heating. A further complication comes from the need to reconfigure the experiment multiple times, and requires that both the inner and outer conductor connections to be easily separable, robust, and repeatable. Finally, the design of the inner conductor connections must ensure that adequate thermal conductivity is maintained.

Currently all of the coupler test stand parts are being fabricated in the SLAC shops. Commissioning the test stand using a straight, stainless-steel coaxial line should take place early in FY2007 using the L-band source that was constructed in the End Station B (see Section 3.f.). Afterwards, additional components will be fabricated at SLAC and purchased from CPI, and processed in the same way as DESY TTF-3 coupler components. They will be used in a series of tests to identify those features (e.g., bellows or widows) contributing to the long coupler conditioning times. The results will also be compared with multipactoring simulations by the SLAC ACD group to see how well this phenomenon can be predicted (see Section 4.d.).

4.3.e. L-Band Normal Conducting Accelerator Structures

After the ILC linac technology recommendation was made, the NLC structure group turned its attention from X-band structures to the normal-conducting cavities that are required for the ILC position source. They have developed an improved version from the DESY approach for the positron accelerator that will be located just after the target. A five cell prototype was designed in FY2005 and fabrication of the cells began last November. Since then, a full set of drawings (over 100) was generated for the five-cell cavity, surrounding solenoid magnet, high power rf vacuum windows, supports and cooling system. The solenoid was acquired from Boeing this summer as a gift to Stanford. The magnet was made by Thales for L-band klystrons, and could be used with our klystrons if needed. The fabrication of the cavity has been very slow due to the low priority of ILC work in the Klystron Shop relative to work on klystrons for PEP II and an rf gun for LCLS. So far, the inner half cells have been machined, brazed in pairs and re-machined: they still require tuning before they are assembled with the end cells, which are still being machined.

In the next month, the rf vacuum windows should be completed and at least two of them high power tested (four are being built: one for the structure, one spare and two for the coupler test stand). The cooling system should be also assembled and tested at the required 100 gpm flow rate with 45 °C temperature-regulated water (a preliminary test was done at 50 gpm earlier in the year). The 5 MW rf power source (all components from the LLRF system to the connecting waveguide) should also be in place and ready for operation (see Section 3.f.). Unfortunately, the structure itself will probably not be available for test until at least December. After it is installed, it will be processed to 15 MV/m with 1 ms pulses at 5 Hz, and the absolute gradient and its uniformity during the pulse measured by accelerating a single bunch from the NLCTA injector at different times relative to the rf pulse. The cavity will also be operated in a 0.5 T solenoidal magnetic field, as required in the ILC, to see if its performance is affected

4.3.f. L-band Test Station

To gain experience with L-band sources and rf components at SLAC, construction of an L-band test stand was started in FY2005 at the Next Linear Collider Test Accelerator (NLCTA). For this facility, a 140 kV converter-style modulator was borrowed from SNS, and an SDI-legacy, 10 MW,

160 kV, short-pulse klystron was purchased from Titan. Also, a 500 W drive amplifier, WR650 waveguide, loads, directional couplers and high-power circulators were acquired, and an EPICS-based low-level rf system configured.

The modulator was first tested using a resistor load, and then used to power the klystron at 120 kV. In March, this source produced 3.3 MW, 1 ms rf pulses at 5 Hz, which is the peak power expected at this voltage. The power was used to test a high power circulator and waveguides that were pressurized (3 bar) with nitrogen (instead of SF6) to suppress rf breakdown. Arcing at the waveguide flanges was observed and has since been eliminated by machining the flange mating surfaces flatter (to < 1 mil) to reduce any gaps.

The step-up transformers and resonant circuit capacitors in the modulator were then modified to allow higher current (90 A) operation with a newly acquired 5 MW, 128 kV Thales 2104C klystron (this tube has been the 'workhorse' for testing at DESY and FNAL). This modification was contracted to the group at LANL that designed the modulator, and it took longer to implement and was more difficult to make work than had been anticipated (for a given configuration, modulator only works reliably within a narrow range of load impedances). Nonetheless, the upgraded modulator with the new klystron has recently produced 4.9 MW, 1 ms pulses at 5 Hz, limited only by modulator charging supply voltage (a parallel HV water load is used to fine tune the modulator load impedance). One shortcoming of the SNS modulator is that the HV droop compensation system was never made to work reliably and so is disabled. In our case, the rf power droops by 10% during a 1 ms pulse. However, when operating below saturation, the rf drive system can be used to compensate for this decrease, as is done at SNS.

As configured, the L-band Test Stand will provide power to two experimental test areas. One will be used to rf process coupler sections (see Section 4.3.d.) and other rf components, and the other will be located in the NLCTA beam enclosure to test prototype positron accelerator cavities (see Section 3.e.). During the next month, the waveguide transport system to these test areas should be completed and the full control system for rf processing should be commissioned. In FY2007, if the new modulators that are being developed do not perform well, the SNS modulator may again be modified to allow operation of ILC prototype 10 MW klystrons (at 120 kV, 130 A).

4.4. ILC Accelerator Design and R&D

SLAC has more than 20 years of experience with the design of a linear collider and has quickly moved to play a leading role in the design of essentially all components of the machine except the cryomodules and cryogenics. The ILC group is actively developing designs for the electron and positron sources, the damping rings, the bunch compressors, the beam delivery and machine-detector interface. In the main linacs, in addition to work on the L-band rf power sources described elsewhere, the effort includes optics and simulations and superconducting quadrupole measurements. The availability simulation developed for the US Technology Options study has been expanded and used as a tool to study various configuration options. SLAC is also involved in developing diagnostics, controls and high-availability hardware. The conventional facilities group is actively collaborating with FNAL to develop site criteria and US candidate sites.

4.4.a. Electron Source

SLAC now has more than 25 years developing and operating polarized electron sources and 15 years experience with the polarized electron source developed for the SLC. The present polarized

source program includes R&D on the photo-injector source laser system and DC polarized electron gun, photocathode development and design of the injector beam lines up to 5 GeV, which is the beam energy required for injection into the ILC damping ring. The baseline design for the ILC adopted at Snowmass 2005 was based on the SLC source. Such an electron source will fulfill the ILC requirements in terms of bunch charge, but a laser system with the required wavelength of 780 nm +/- 20 nm that can generate the required pulse train is challenging and a feasibility demonstration is needed.

During FY 06, a facility for the laser development program was established. This facility will to combine the laser system and electron gun to facilitate a 'proof of principle' of the source. A conceptual design of the laser system is complete that consists of a mode-locked oscillator, electro-optical bunch train generation and amplification. The laser system will be based on Ti:Sapphire technology. Amplification of the pulse train will be achieved by using Diode Pumped Solid State (DPSS) pump lasers.

SLAC continues to have an active program on polarized photocathode research. This program resulted in cathodes capable of routinely delivering polarization well over 90% for the E158 experiment. The present program at the Cathode Test Laboratory is focused on reoptimizing the cathode parameters for the ILC bunch train format and on further improvements in available quantum efficiency and polarization. Work in FY06 investigated de-polarization processes, such as internal charge scattering, that prevent P>90% in GaAs-type cathodes. An SBIR collaboration with Saxet, Inc. aimed at forward-biasing the emitting layer to reduce the electron drift time. GaAs/InGaP strained-superlattice structures have been investigated to explore superlattice materials with a lower spin relaxation rate. An SBIR collaboration with SVT Associates was started to develop robust photocathodes based on GaN for polarized gun applications.

Beam line simulations have been completed starting from the electron gun through the trans-relativistic region of the bunching system up to the damping ring injection point. The simulations established a physical beam line layout and the required magnet system. These simulations provide the basis for developing a model for cost analysis of the polarized electron injector in interaction with other area, technical and global systems groups. First results were discussed at the GDE meeting at the Vancouver Linear Collider Workshop in July 2006.

4.4.b. Positron Source

SLAC has had a long-standing program of R&D on the design of a conventional positron source and, in FY2005, this was expanded to include design of an undulator-based source. The SLAC positron source program in FY06 included accelerator design as well as R&D activities. The ILC positron source includes the undulator based production source, a conventional 10% intensity "keep alive" backup source, and the associated 5 GeV booster linac and requisite transport lines.

SLAC has taken the leadership role in coordinating the world wide activities for the BCD and RDR design efforts in FY06. In FY07, this will evolve into the design and R&D in support of the Technical Design Report (TDR). SLAC has been co-leader of the ILC GDE RDR effort and is the US ILC wbs level 2 manager for positron work. To accomplish these tasks (BCD, RDR, and TDR), SLAC is defining the goals and working closely with US and international collaborators, notably from ANL, LBNL, LLNL, UCB, and Cornell. as well as from KEK, DESY-Hamburg, DESY-Zeuthen, Liverpool U., Durham U., CCLRC Daresbury and CCLRC RAL.

The bulk of the design effort was spent in refining the Baseline Configuration Document (BCD) by the end of calendar 2005 and then was spent developing the Reference Design Report (RDR) configuration, inventory, and cost model. Significant ongoing effort is directed towards cost and design optimization for the RDR. The goal of present ILC positron RDR activities are directed towards writing the text and cost estimate by the end of calendar 2007.

To accomplish the RDR tasks, a full design model for the ILC positron source has been developed with all major components identified, specified, and costed. This work is based on positron production, capture, transport, and acceleration modeling developed at SLAC. The costing effort was accomplished by coordinating, collecting, and collating the efforts of the various ILC GDE Technical and Global groups. The initial results of the costing efforts were presented and discussed at the GDE meeting in Vancouver in July 2006. Coordination of the TDR work has begun and a first international meeting for this effort has been organized by SLAC to be held at RAL Oxford during the last week of FY06.

The R&D activities included ongoing data analysis and post experiment component calibration for the E166 experiment. Initial studies have begun on the determining the feasibility of utilizing a strong (~7 T) dc solenoid in conjunction with a spinning target for efficient positron collection. An R&D program for FY07-09 has been developed in support of the TDR requirements. This program will be overseen by SLAC and carried out in collaboration with both US and international partners.

4.4.c. Damping Rings

Large acceptance is an important requirement for the position damping ring. Significant progress has been made in improving and understanding the dynamic aperture of the damping rings. First, by carefully studying the nonlinearity in wigglers, we have found that well designed wigglers, such as the superconducting wigglers used in CESR, were not a limiting factor for the machine acceptance. Second, we concluded that rings with a large degree of symmetry have better dynamic aperture. As a result, 6-km rings with a twelve-fold symmetry were chosen to replace the 17-km TESLA dog-bone damping rings. Finally, a baseline lattice with adequate acceptance was established. Although this work was carried out by an international collaboration including ANL, LBNL, KEKB and Cornell, SLAC has provided a leading and vital role.

From the experience in the existing B-Factories: PEP-II and KEKB, collective instabilities due to electron cloud are likely to become a severe performance limitation in the positron damping ring. Based on the simulation, two positron rings are required to separate adjacent bunches enough to avoid the head-tail instability. SLAC has continued a large R&D effort to find a way to mitigate effects of electron cloud. A grooved vacuum chamber with diagnostics has been designed and manufactured. The chamber is scheduled to be installed in PEP-II before the end of this year. Measurements with position beam are expected in the next year. The success of this R&D is crucial since the decision was recently taken to eliminate one of the positron rings as a cost reduction measure.

SLAC continues to play an important role in the design of the ILC damping rings and development of the related technical subsystems. We continue to collaborate with our colleagues

worldwide to complete the design. Urgent tasks include developing a realistic impedance model, evaluating classical instabilities, and developing a fast injection and extraction kicker.

The SLAC-LLNL Kicker development continued with investigation of fast switches to improve rise and fall times of the kicker. In addition the prototype kicker tested at ATF was modified with additional driver cards to increase output voltage and provide a short flat top. This unit can now achieve over +/-9 kV bipolar pulses and is being returned to ATF for further tests. Meanwhile after trying tests of a new MOSFET with integrated driver that offered no improvement, a new circuit was developed with a push-pull circuit to achieve less than 2 ns rise and fall times, for a total base pulse width of 4.1 ns. This is acceptable for the 6 km ring if after-pulse ripple can be sufficiently clean. Some newer devices with inherently faster speed are also being tested.

SLAC is also collaborating on testing a new device, a Drift Snap Recovery Diode, DSRD, that showed almost 1 ns rise and fall for a multi kV pulse, with some pre-and after-baseline effects. This is under an SBIR program. A workshop has been organized by the Damping Ring group to discuss all these developments. FY07 plans include construction of a new prototype that meets all specifications including full power operation at +/-10kV, 3 MHz CW.

4.4.d. Ring to Main Linac

The SLAC ILC group has taken the lead in the design and cost estimation of the Ring to Main Linac (RTML) transfer line. In collaboration with physicists from DESY and Cornell University, a complete optics design for the RTML, including all necessary pulsed extraction systems, instrumentation, and other beamline elements was completed. The RTML includes the SLAC/LBNL/LEPP design for a two-stage bunch compressor which was developed in 2005, but with a number of improvements to reduce its total length and cost. A cost estimate for the "as designed" RTML was developed by the worldwide ILC GDE in the spring and early summer of 2006. Since that time the SLAC group has developed and proposed a number of design changes which could potentially reduce the system cost, and has participated in developing a "Central Damping Ring" design for the ILC which would require significant changes in the RTML.

Additionally, a collaboration between SLAC, FNAL, and Cornell University has been exploring the beam dynamics issues of the RTML. These studies have so far concentrated on the static tuning of the beamline (i.e., using the beam instrumentation to eliminate emittance growth induced by static misalignments and errors of the beamline components), with additional studies on the longitudinal stability requirements of the bunch compressors. Several members of this collaboration attended the Low Emittance Transport (LET) workshop at CERN in February of 2006. In the last few weeks, studies have begun to explore whether the RTML is subject to instabilities which have historically been regarded as relevant only to storage rings (for example, the Fast Beam-Ion Instability).

Future work on the RTML will focus on further improvements and refinements in the design, with a goal of completing a fully optimized design by the end of FY07; completion of the static emittance preservation and instability studies; and work on dynamic and multi-system studies of beam dynamics, in collaboration with the worldwide LET team.

4.4.e. Main linacs

A number of key linac design decisions were made in FY2006, most notably, the overall linac configuration has been chosen: 1 quad per rf station, which has 3 cryomodules, a vertically curved linac to allow the entire linac to lie roughly on a gravitational equipotential, with 1.2 km insertions for the positron undulator on the electron side and for the timing adjustment system on the positron side. High priority activities for FY2007 are to: wrap up the last few decisions required for the production linac lattices (mainly related to dispersion matching and other details); produce final production versions of the electron and positron linac lattices; and transition the simulation work to the production lattices.

A workshop on Low Emittance Transport (LET) was held early in FY2006. At that time, the aforementioned vertically curved lattice was adopted for main linac studies, and agreement was reached on a set of simulation tests which would be used to "certify" the basic beam dynamics properties of a code before it was accepted for use in linac studies. All of the codes currently in use have been certified in this manner. Since the LET workshop, studies of the main linac have demonstrated that there is an incremental penalty in emittance dilution for the use of a vertically-curved linac as compared to a laser-straight version. This penalty is sufficiently small that the vertically-curved version has been accepted as the baseline configuration. For the first time, a simulation result produced by one group was reproduced, in full detail, by a separate group with a completely independent simulation code base.

In FY2007 work will continue in all these areas, both area-by-area and in an integrated approach. The goals of the effort will be: to demonstrate with 90% confidence that the emittance budget of the ILC can be achieved; to demonstrate multiple steering and alignment algorithms which can be used in each area; and to have at least 1 independent verification of each simulation result before it is accepted as a valid demonstration for these purposes.

In addition to the LET studies, physicists from the Advanced Computing Department (ACD) and Beam Physics Group at SLAC made a good start in FY2006 at understanding a number of issues related to wakefields in the ILC linac cavities, and multipactoring in the high power cavity couplers. They used both analytical models and computer simulations to study the characteristics of the cavity dipole modes (e.g. their external Q values, polarization, frequency spread and mode splitting), and the severity of multipacting in the TTF3 coupler bellows. The cavity simulations show that elliptical dipole modes will be generated with purely symmetrical cavity cells, although they are unlikely to be present in the ILC linacs due to the azimuthal asymmetries introduced during the cavity manufacturing process.

The main goals for this group in the FY2007 are to (1) develop a model of the cavity shape distortions that will explain the variations observed in the lowest-band dipole mode properties, (2) use this model to verify that the spectrum of (R/Q)*Qext for lowest band modes will not produce significant beam breakup in the ILC Linacs, (3) extend this analysis to trapped modes over multiple cavities for frequencies up to ~8 GHz, which will require massively parallel computer processing and (4) complete the multipacting evaluation of the TTF-3 coupler and suggest design changes to reduce this phenomenon.

The main focus of linac design R&D in FY2006 was on proving beam-based quad alignment techniques that are required to preserve the small emittances in the ILC linacs. The simplest technique proposed requires that the alignment of the magnetic center of each quad be first

measured relative to the electrical center of the nearby BPM. This involves changing the quad strength and recording the resulting beam kick. To achieve the desired accuracy, the quad magnetic center cannot move by more than a few microns when the field strength is changed by 20%. The large aperture of ILC Linac quads (78 mm) may make achieving this stability difficult, especially if high gradient magnets with coil-defined fields are used. The beam-based alignment procedures also require large aperture beam position monitors (BPMs) with micron-level resolution.

The goal at SLAC is to develop a SC quad and BPM that meet these requirements. To this end, a TELSA SC linac quad prototype was obtained (on loan) from DESY this year along with gas-filled-type leads to power it (100 A produces 60 T/m in the 0.66 m long magnet). The quad was built by the CIEMAT group in Spain and tested initially in a vertical Dewar at DESY. At SLAC, the design of a warm-bore cryostat for this quad was started in FY2005 and finished this spring (keeping the magnet stable vibrationally at the submicron level while allowing contraction of the support system during cool-down is not trivial). The cryostat is now under construction and is about 80% complete (the quad was recently inserted in the He vessel). The power supply and quench protection circuit for the magnet was assembled and the gas-filled lead assembly tested in a dewar at full current. The magnet will be tested at the SLAC Magnetic Measurement Lab using liquid He and N2 supplied by 2000 liter portable dewars. The parts for the cryogenic supply system have been purchased and are being assembled. Also, a rotating coil system was built that will allow the position of the quad magnetic center to be monitored at the sub-micron level as the magnetic field is varied (the design of this system is based on that developed for the normal-conducting NLC quads). Finally, accelerometers were purchased that will be used to monitor the vibration of the quad relative to base on which the cryostat will be supported (the measurements will be done in collaboration with FNAL).

In a parallel program, a slotted-waveguide-style, S-band (2.9 GHz), cavity BPM was designed, and three prototypes constructed and tested at End Station A at SLAC. These BPMs have a 36 mm aperture, which is about half of the nominal ILC size. This choice makes testing this design concept simpler, and it would be advantageous to adopt this aperture size for the ILC. The BPM geometry naturally suppresses monopole mode signals, and it was carefully designed so the neighboring modes are well separated in frequency. A low cavity Qext was chosen (~ 500) to allow clean bunch-to-bunch signal separation in the ILC (the signal drops to 0.2% of its initial level after 337 ns, the nominal ILC bunch separation). The prototype BPMs preformed well in beam tests with 29 GeV, 300 micron-long single bunches of 1.5e10 electrons. Resolutions of 400-800 nm were achieved when down-mixing the signals to 73 MHz and digitizing them at 100 MHz. These resolutions are better than that required in the ILC linacs.

4.4.f. Beam Delivery System

SLAC is playing a leading role in the international collaboration on the design of the Beam Delivery System (BDS), including development of required hardware, instrumentation and test facilities. SLAC played a key role in the technical evaluation of the baseline configuration and in the cost estimation of the beam delivery. As a result, it was suggested that the BDS would have improved performance and 15% lower cost if the baseline configuration were changed to 14mrad crossing angle in both IRs. This configuration was analyzed from both the physics and technical perspective and was adopted as a new baseline. SLAC continues to play a key role in all accelerator physics aspects of the BDS design.

SLAC is further enhancing its role in coordination of the worldwide BDS development activities, providing feedback and guidance for technical specifications and design as well as in developing a coordinated plan for the R&D and design work distribution between global partners. The global plans for the next three years of BDS R&D leading to an Engineering/Technical Design Report will attempt to utilize the expertise in the Americas as well as in worldwide collaborating labs and universities.

The experimental studies to support a reliable BDS design are being conducted at End Station A at SLAC (described below) and will later be conducted at ATF-2 at KEK. The ATF-2 is being constructed by an international collaboration. It will use the uniquely small emittance ATF beam to achieve a beam size of about 35 nm, develop methods of tuning and maintaining a small beam size for an extended duration, and eventually stabilize the beam with nanometer precision. In FY2006, SLAC built a prototype High Availability power supply which was adopted for the ATF-2. SLAC also contributed to the development of BPM electronics and the magnet system for the ATF-2 proposal. In FY07 and beyond, SLAC will continue contributing in-kind hardware for construction and will be involved in the pre-commissioning evaluation of ATF-2 hardware.

4.4.g End Station A Test Facility for Prototypes of Beam Diagnostics and IR Design
The SLAC Linac can deliver to End Station A (ESA) a high-energy test beam with similar beam parameters as for the International Linear Collider (ILC) for bunch charge, bunch length and bunch energy spread. ESA beam tests run parasitically with PEP-II with single damped bunches at 10Hz, beam energy of 28.5 GeV and bunch charge of (1.5-2.0)·1010 electrons. Four experiments were approved and took data in FY06. A 5-day commissioning run was performed in January 2006, followed by a 2-week run in April and a 2nd 2-week run in July. These tests included measurements of collimator wakefield kicks from 8 sets of collimators (T-480); measurements of the electronic and mechanical stability of bpms for a bpm energy spectrometer (T-474); commissioning of a quartz fiber detector for a synchrotron stripe energy spectrometer (T-475); characterizing the performance of prototype beam position monitors (BPMs) for the ILC Linac (part of T-474), and a study of background effects for the IP feedback BPMs (T-488). Beam tests were also performed to characterize beam-induced electro-magnetic interference (EMI) along the ESA beamline and to study an EMI failure mode in the electronics for the SLD vertex detector; and bunch length diagnostics were tested that have applicability for ILC and LCLS.

The ILC test beam program in ESA is described in SLAC-PUB-11988 (also available as EUROTeV-Report-2006-060), which was prepared for a paper and poster contribution at EPAC06. Two other papers and posters were also contributed to EPAC06 for T-480 and T-488. There are 22 institutions collaborating on the ILC test beam program in ESA. More details of the ILC test beam program in ESA in FY06 can be found in this DOE self-assessment document in the section on Test Beams. Analysis of the data taken in FY06 is ongoing. The program will continue in FY07 with the addition of a magnetic chicane, undulator magnet and new BPMs for the energy spectrometer tests (T-474 and T-475), new collimators for wakefield measurements (T-480) and a new bunch length measurement experiment using Smith-Purcell radiation (T-487).

4.4.h Diagnostics and Controls
The most important ILC beam diagnostics are for precision, ultra-high-resolution measurements of position, transverse profile and longitudinal profile. Development of these devices has long been

recognized as a high priority for linear collider R&D and SLAC has maintained a leading role in this effort. The most useful test facility for the development of precision position and (transverse) profile monitors is the KEK ATF which routinely produces the lowest emittance beam available worldwide. During the last year the SLAC group, supported by groups from LLNL, LBNL, Cornell University and a group of UK universities, have installed hardware and instrumentation that allows the position of the precision beam monitors to be linked to other beamline components. The 'optical anchor' hardware will be used for ILC energy spectrometry. The SLAC group at ATF also supports the effort, lead by the UK, to deploy a laser-based beam profile monitor with resolution better than 1 micron. In the last year, the system was successfully used for initial precision scans of the damped ATF beam.

For longitudinal profile measurements, the SLAC group has developed a world record precision longitudinal monitor based on a high-power S-band deflecting structure. The device was tested in FY2005 at the DESY Tesla Test Facility and showed resolution of 10 microns. In 2006, this monitor was used to provide a basic understanding of the transport of extremely short bunches and for the first time provided 'slice emittance' and longitudinal correlated energy spread measurements. Finally, in support of the superconducting rf cavity development at DESY, the SLAC group has developed a signal-processing system that allows the interpretation of the higher order mode signals generated in the cavity for beam position monitoring. The system was used in 2006 to provide critical offset information with 30 micron indicating the placement of the niobium cavities inside the cryostat. The system was adapted to provide accurate beam to RF phase measurements with a resolution of 0.1 degrees.

In 2006 controls efforts continued with the GDE Controls Collaboration to refine all Baseline Conceptual Design (BCD) models begun at Snowmass, defining system architectures for both hardware and software, and developing first order cost models for all components down to the interfaces of controls with front end instrumentation and major technical subsystems. Integrated with this effort was an evaluation of a commercial modular computing standard called ATCA which features the critical High Availability features that ILC requires to be a successful machine. This system also provided the cost model for the core control system, multiprocessing farm and Low Level RF instrumentation for the Main Linac.

4.4.i. Operations and Availability

The availability simulation developed at SLAC and reported in 2005 has continued to play an invaluable role in guiding the overall machine design. As options continue to be proposed, such as going to a 1 tunnel design from the present 2 tunnel plan or putting both damping rings in the same tunnel, the performance implications are evaluated with the simulation. Simulation results also have determined where High Availability R&D programs are needed.

With the basis of performance now understood, major progress was made in 2006 in advancing designs for controls, power supply systems, diagnostics processors, controls and Marx modulators. The latter is a lower cost more reliable alternate to the baseline design that is being developed. Evaluation of the ATCA core processor and gigabit switching fabric network system has begun in collaboration with the University of Illinois (Urbana). HA power supplies consisting of n+1 redundant DC-DC converters in current-shared operation, such that a module can fail with no interruption to the machine, were demonstrated. A bulk supply redundant system was also demonstrated, and conceptual design of the critical diagnostic controller was started. For the Marx,

redundant IGBT charging and switching on the base 12kV cells became operational, and a special diagnostic controller that could float at high voltage was developed and is operational. Commercial contacts are continuing to grow including vendor seminars, presentations to subgroups of the Linear Collider Forum of America, seminars, product evaluations of ATCA, and evaluation of redundant highly reliable DC-DC converter power system components built for the computer server industry.

Within the ILC the high availability program has taken firm root among the collaborating laboratories. The proposal to interest other mega-projects in high availability modular standards is ongoing. Formal papers on the subject were given at the Nuclear Science Symposium in 2004 and a seminar in 2005, Real Time Conference in 2005 (Plenary talk)

4.4.j. Conventional Facilities Design and Installation

The SLAC Conventional Facilities (CF), partnering with the FNAL-CF engineers, identified several potential locations for the ILC alignment in northeast Illinois. They assessed each location considering not only cost of the construction and installation phase of the project, but the environmental impacts as well as eventual impact on the long term operations of the ILC. Results were analyzed, reviewed, and amended into the global site assessment matrix. As results of this effort, a Sample Site for the Americas region was identified.

The baseline configuration layout as well as a complete description for the CF portion of the ILC was developed by a collaboration of SLAC, Fermilab, Japanese and European engineers working closely with the Area System leaders. In addition to baseline choices, alternate configurations were also established that may have cost benefits. These efforts were complete in time for inclusion into the Baseline Configuration Document (BCD) in December, 2004.

Subsequent to the adoption of the BCD, a concept design and associated cost estimate for the ILC Conventional Construction was developed. This effort included many 3-D visualization drawings which facilitated a top-level assessment of the major choices, as well as a set of concept designs that could provide cost effective, safe underground and surface facilities. This initial design and cost estimate was completed in FY06 and will form the basis for the Reference Design Report expected by the end of 2006.

In addition, SLAC has devoted a major effort in initiating, organizing and setting-up a complete and comprehensive cost model plan for the ILC Installation Global System in collaboration with the Asian and European engineers. The SLAC Installation group being also partner in the Conventional Facilities Group has tried to coordinate and to integrate the installation effort with the CF work as well as with the other Regional Technical and Area Teams. A first cut installation cost estimate for ILC was completed in FY06.

4.5. NLCTA Operations

During FY2006, the focus of the ILC effort at NLCTA was on the development of L-band rf power systems. The primary effort was to develop a 5 MW rf source as described in ILC Section 4.3.f above. Planning work also began for removing a large shielding wall in End Station B to provide space for two new rf stations that will be used to do long-term testing of the Marx and DTI modulators using either a water load or 10 MW klystrons as they become available.

The ILC group also worked to maintain the NLCTA as an operating linac to be used for advanced accelerator R&D. To this end, the 8-pack modulator, which was contaminated with beryllium, was decommissioned and was replaced with a newer 2-pack modulator, which was tested initially in the Power Conversion Department Building in FY2004. The 2-pack modulator will not deliver as much power as the 8-pack but it will still accelerate the beams to roughly 300 MeV. This modulator will be recommissioned at NLCTA within the next month, and the 8-pack rf source used to test advanced SLED pulse compression techniques (SLC operating budget funds).

As discussed in Section 4.2, high gradient R&D using existing X-band accelerator structures continued in FY2006, funded by SLAC as part of the US Collaboration on High Gradient Research program. For this work, the Station 2 X-band rf source was mainly used. Also, members of the Accelerator Technology Research Group at SLAC used the Station 1 rf source to study rf breakdown in a molybdenum waveguide for the high gradient program.

In FY2005, the NLCTA was modified to provide beam for the SLAC E-163, a 'Laser Acceleration at NLCTA' experiment. See Section 6.1 for further detail

4.6. LHC Accelerator Research Program (LARP) Collimators

The LHC collimator R&D program developed out of a request from CERN to study the applicability to the LHC of the ‘consumable’ collimator technology that was developed for the NLC. As the project became better defined, it was added to the US LHC Accelerator Research Proposal. All funding for this program flows through LARP, although the program is administered out of the ILC Department, where the technological concepts originated and the people driving the effort are located.

The LHC collimation system will be installed in two phases. The first phase devices are carbon-jaw collimators that can survive the direct impact of up to 8 nominal-intensity bunches, a rare but regularly foreseen accident condition. The system will have adequate efficiency and low enough impedance for start-up luminosity of 10% nominal design or 1x1033 cm-2s-1. A system based on metal collimators with improved efficiency and lower impedance must be devised and installed before the LHC can reach the full design luminosity of $1x10^{34}$ $cm^{-2}s^{-1}$.

The ILC Department has proposed to design and prototype these so-called LHC Phase II collimators as an extrapolation of the design that was developed and prototyped for the NLC. The basic concept is one that replaces classic rectangular jaws with cylindrical jaws that can rotate to present a fresh surface to the beam if the surface is damaged in an accidental beam abort. Relative to the NLC design, the LHC jaws must be longer, of a smaller diameter and each provided with ~12 kW of water cooling.

In FY2005, tracking studies, energy deposition studies, and finite element analyses were used to determine the optimal design of the collimators. This information, together with relevant 3-D CAD design drawings, was assembled into a conceptual design report for a first collimator prototype.

In FY2006 the conceptual design was independently reviewed. It was recommended that before proceeding with construction we increase our engineering manpower and further develop the

design of the mechanisms to a) support the collimator jaws, b) prevent them from intruding into the beam if thermally distorted, and c) rotate the jaws after damaging asynchronous beam aborts. In response, two FTEs were added to the engineering team and the design developed that elegantly addressed all the concerns of the reviewers.

In late FY2006 two rounds of short test jaws were constructed to verify machining, brazing and assembly procedures and drawings made for the first full size collimator jaw. Additionally a clean room was prepared and equipped with resistive heaters, thermocouples, capacitive monitors and a data acquisition system. In FY2007 it is planned to build and test the thermo-mechanical properties of this full length jaw and to build a full two-jaw vacuum compatible mechanical prototype with all the mechanisms required for jaw support and adjustment.

5.A FY06 PROGRESS: ACCELERATOR TECHNOLOGY RESEARCH DEPARTMENT by Sami Tantawi

The Accelerator Technology Research Department has worked on a wide variety of topics this past year. The work has four main directions: performance enhancement of current accelerators at SLAC such as PEP-II; research and design for near future facilities such as ILC; upgrades to PEP-II or LCLS; and research in fundamental aspects of accelerator and beam physics. Selected topics from ATR are discussed below.

1.1.1. **Electronics Research.** Electronics Research combines SLAC staff with Stanford graduate students in Applied Physics and Electrical Engineering to provide both accelerator physics and technology skills for accelerator projects. The group's hardware and software instability control systems have been implemented at labs in the US, Europe and Asia. During the year the group has presented results through nine journal publications, at the CERN LLRF Workshop, and at the European Particle Accelerator Conference. John Fox taught two Stanford courses in Applied Physics and Dmitry Teytelman was an organizer for the CERN LLRF workshop. The group currently includes four full-time SLAC staff and two Stanford graduate students.

1.1.2.

The group has been central in efforts to better understand the interactions of the PEP-II rf systems, with their complex impedance-reducing feedback architectures, and the longitudinal dynamics of the machine. These efforts are broad and include simulation modeling as well as extensive machine physics studies. In a parallel effort, the group continues to measure and control the HOM coupled bunch instabilities in PEP-II via the broadband coupled bunch feedback systems.

In 2005/2006 instability control activities were increased at LNF-INFN (DAFNE) and a series of studies was begun at KEK-B and the ATF. FY2005/2006 also brought some new activity related to LCLS in the form of dynamics modeling for the LLRF control of the rf gun, and in review functions for the LCLS LLRF development.

PEP-II Activities

In 2006, focus was continued on high current configuration and stability of the rf systems through machine physics experiments, nonlinear numeric simulation and analytical studies. In 2006 PEP-II ran at record currents and luminosity, and the increases in PEP-II currents (to 1860 mA HER and 3A LER) have been possible because of the group's development and commissioning of the

Low Group Delay Woofer in 2005 (the capabilities of the original rf system implementation were exceeded with 2006 operating currents). Additionally, a new configuration technique was developed for the PEP-II rf stations that trades-off growth rates for station stability, and this "comb rotation" technique is a significant new approach to allow high current operation

Another PEP-II research area involves techniques to linearize the high power klystrons. In 2005/2006 the group developed prototypes of this nonlinear processing channel through installation of four prototypes in the LER. This year focused on a machine development effort to understand the linearizer interaction with the complex LLRF systems. These linearizers are a mix of RF circuitry plus a digital processor used for gain compensation to keep the closed-loop frequency response stable. This project is led by Dan Van Winkle.

Photo of the prototype linearizers, incorporating 476 MHz rf circuitry and digital compensation control techniques.

These linearizer efforts led to successful demonstration of the technology and operation as a test in the PEP-II LER. One of the most valuable aspects of the project involved the close ties with the modeling and simulation of low-mode dynamics, and understanding the impact of a linearized klystron in the LLRF system helped lead to higher-current operational configurations needed for the 3A operation of LER.

The figure shows the time-domain output of a PEP-II klystron without the linearizer (the gain of the klystron is modulated by power supply ripple). The second figure shows the action of the linearizer in fixing the small-signal gain, so that the modulation of gain from the high-voltage power supply is greatly reduced. This improved linearity in small-signal gain increases the effectiveness of the direct and comb loop impedance control loops in the LLRF systems.

Instability Control Systems (coupled-bunch feedback systems)
High-speed signal processing systems development has continued, and this last year the detailed circuit and signal processing system designs for a 1.5 GSample/s feedback processing channel moved forward. This new architecture is of direct applicability to PEP-II and other collider needs, and can implement either longitudinal (downsampled) or transverse (non-downsampled) processing systems. It represents a significant advance in the processing speed and density previously achieved. The initial development has been done in conjunction with Dr. Makoto Tobiyama of KEK, and has progressed to include a significant funding component under the US-Japan Cooperative Program in High Energy Physics. A one-fourth capacity processing prototype (the Gproto) was developed by Dmitry Teytelman as a proof of concept demonstrator. This Gproto system has the capability to run transverse or longitudinal coupled-bunch feedback algorithms at a 500 megasample/s rate.

Two GProto channels have been fabricated and in 2005/2006 commissioned at DAFNE (for transverse e+ control), PEP-II (transverse LER control), KEK-B (transverse control) and ATF (longitudinal control). A design for an integrated iGP was completed in September 2006 - this control channel is in fabrication for use at several facilities. Based on the operating experience

from these 500 megasample/s iGp channels there are plans in place to construct the full speed (1.5 gigasample/s) GBoard channels in future years

Power Spectrum of multibunch beams in the ATF, showing the effectiveness of the iGp longitudinal feedback control.

The figure shows the impact of longitudinal control at the ATF (KEK) using the GProto channel. The ATF is particularly directed at developing low-emittance beams for ILC studies, and studies in November 2005 and April 2006 included studies of noise structures on the beam as well as studies of the beam emittance as a function of longitudinal motion. The figure shows that the iGp reduces the longitudinal motion by over two orders of magnitude.

Plot of LER vertical RMS motion in KEKB LER as a function of system gain

A study of transverse motion and coupled-bunch instability in the KEKB LER has continued. The figure shows a study of residual RMS vertical beam motion as a function of system gain. Over the range of gain shown the beam is always stable, but an increase of transverse residual motion with increasing gain shows the noise limits of the detection channel, and helps find an optimal operating point to have adequate damping margins without increasing the transverse beam size.

PEP-II Modeling Effort

Modeling to study the dynamics of the rf systems in PEP-II is necessary to predict the behavior of the systems at upgraded currents, and to evaluate possible new control techniques or new control hardware for future low-level rf systems.

The rf system and accelerator dynamics simulation is a nonlinear time domain simulation which models the direct and comb loop behavior in the rf systems, as well as the interaction of the high current beam with the rf cavities and high power klystrons. This model has been expanded to allow the simulation of the HER ring with 2 and 4 cavity rf stations. The essential elements of the nonlinear time domain model are shown in the figure.

.The simulation model can be used to predict instability growth rates and modal patterns. By simulating existing conditions, and comparing the results to actual machine operating data, the validity of the model has been verified. The model can then be used to predict higher-current operation of the machine, and evaluate new operating configurations, and stability margins for future operating points.

The figure below shows the predicted modal growth rates for the PEP-II LER at 2.5 A. The model is in excellent agreement with the measurements of the LER machine. The next figure shows the expected growth rates for operating currents up to 3 A, with several possible rf station configurations shown. These predictive models help to develop new LLRF configurations required at higher currents in advance of the physical machine being available at these operating points.

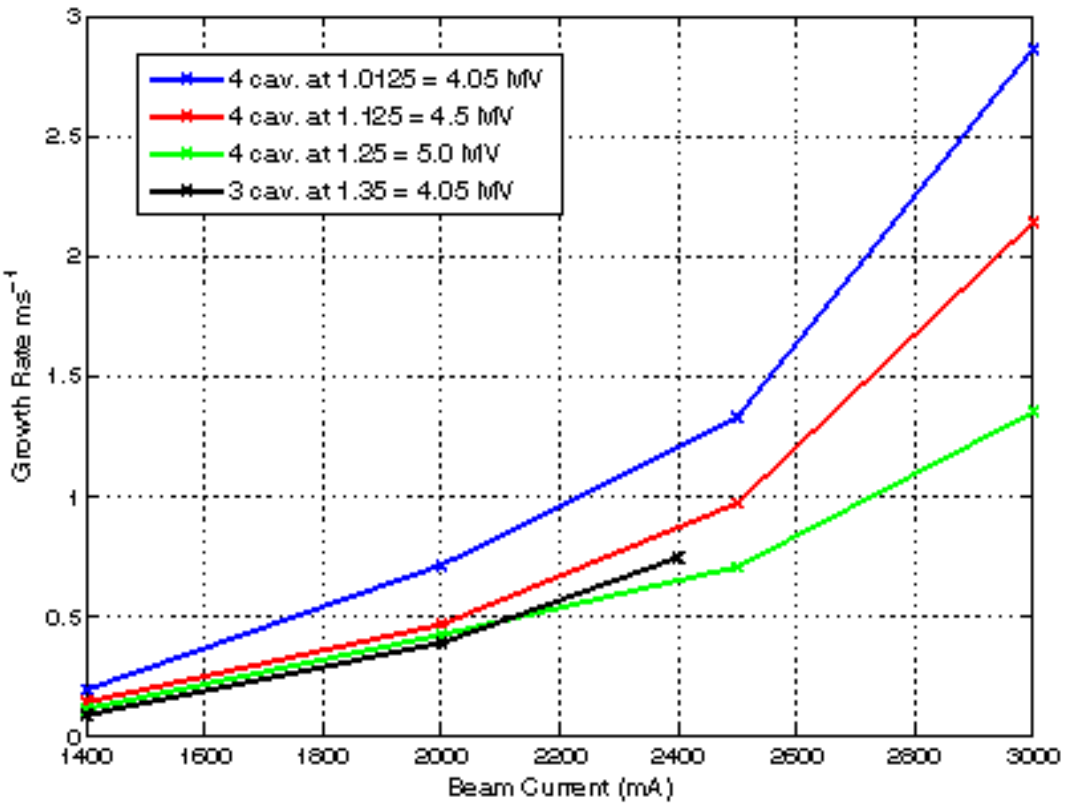

The figure above shows the estimated growth rates in the LER for several different gap voltage and station configurations.

Study of "comb rotation" configuration technique in the LER, with simulation results compared with physical measurements

The impact of the "comb rotation" technique can be seen in the figure above, which compares the simulation results with the measurements of the PEP-II LER. There is agreement between the model and the physical system for the most unstable mode, as well as the overall shape of the curves. A configuration change of roughly ten degrees in the comb filter reduces the instability growth rates by a factor of three. This technique resulted from the insights into the physics gained from the simulation effort. In summer 2006 this comb rotation technique was implemented in the LER as part of the high current commissioning, and was central in reaching the 3A record.

LCLS Contributions

In 2005/2006 the group led two separate LCLS LLRF system reviews, highlighting design options and helping the LCLS project focus efforts on critical technology questions.

Claudio Rivetta contributed to the LCLS project by modeling the rf gun cavity stability and frequency tuning. These efforts helped the LCLS group specify the necessary components and performance of the temperature control loops for the cavity cooling, as well as estimate the rejection of outside disturbances. His initial study proposes the necessary control algorithms for LCLS commissioning.

The figure shows the block diagram of the rf gun, with temperature control loops and rf system loops. The dynamics of the system is driven by both, and there are slow dynamics (in the water control system) and thermal dynamics in the rf heating of the cavity. The regulator which controls the rf excitation also drives the system response.

The figure shows the expected transient response for the RF gun as the RF power is initially applied. The system responds with perturbations in cavity center frequency, then stabilizes at the desired operating frequency. The cavity amplitude and phase are additionally controlled via feedback through the LLRF system.

Accelerator Structures

The mission of Rf Structures group is to design, engineer, and test a variety of accelerator structures with superior properties in high rf efficiency, good Higher Order Mode (HOM) suppression and high gradient performance. These activities span design theory and practice, simulation, structure related beam dynamics studies, fabrication technology, microwave measurements, structure characterization and high power experiments. Accelerator R&D programs at SLAC are supported including the ILC, LCLS and others.

Accelerator Structures Work

1). Accelerator structures for the ILC positron source and electron source

Progress has been made toward an improved alternative design for L-Band normal conducting accelerating system for the ILC positron source and electron source including both standing wave (SW) and traveling wave (TW) sections. The schematic layout of the accelerator system for the ILC positron source is shown below.

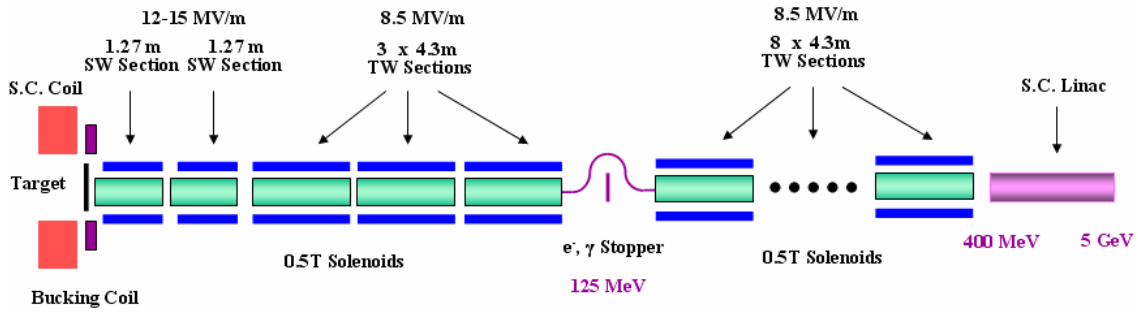

Schematic layout of the ILC positron source.

There are two types of accelerator structures: the11-cell SW structure for capturing positrons and the 4.3 m 3π/4 mode TW structure. The following tables show their basic rf parameters.

Table 1 Parameters of 1.3 m SW structure

Structure Type	Simple π Mode
Cell Number	11
Aperture 2a	60 mm
Q	29700
Shunt impedance r	34.3 MΩ/m
E0 (8.6 MW input)	15.2 MV/m

Table 2 Parameters of 4.3 m TW structure

Structure Type	TW 3π/4 Mode
Cell Number	50
Aperture 2a	46 mm
Attenuation τ	0.98
Q	24842 - 21676
Group velocity Vg/c	0.62% – 0.14%
Shunt impedance r	48.60 – 39.45 MΩ/m
Filling time Tf	5.3 μs
Power Dissipation	8.2 kW/m
E0 (10 MW input)	8.5 MV/m

The simple π mode SW structure with 11 cells is designed for high gradient (15 MV/m) positron capturing. The advantages are more effective cooling, higher shunt impedance with larger aperture (60 mm), lower rf pulse heating, apparent simplicity and cost saving. The mode and amplitude stability for this type of structure has been calculated theoretically to be feasible.

In order to optimize the rf efficiency, the "phase advance per cell" has been used as a knob for designing large aperture, constant gradient 4.3 m TW structures. The advantages are lower pulse heating, easy installation for long solenoids, no need for rf reflection protection (circulators), apparent simplicity and cost saving.

Some extensive PARMELA simulations have been conducted for the beam dynamics using various accelerating gradients and structure combination.

2). L-Band 5-cell SW test accelerator section for the positron capture structure

In order to gain fabrication experience and to make high power tests at full gradient and pulse length with an existing 5 MW peak power L-band klystron, a 5-cell L-band test structure was designed with a coupler cell at one end and all necessary features for a positron capture section. Due to the low priorities in the machine shops, the structure fabrication schedule has been much delayed. Hopefully, this will be completed by the end of 2006 and the test can be started in the early 2007.

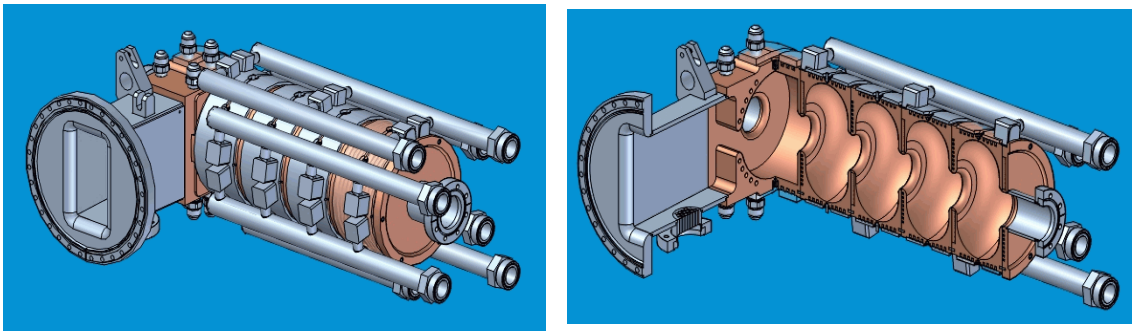

Figure 2. A 5-cell L-band SW accelerator section for the positron capturing.

Figure 3. Some of the subassemblies for the 5-cell SW structure: a completed unit cell (left), a half cell to be brazed on the input coupler (middle), L-band rf window (right).

3). Three S-Band BPMs have been tested for the ILC main linac beam diagnostics. The measurements showed the TM_{11} mode working frequencies were accurate with 2856 + 1-3 MHz and two orientations were balanced with frequency difference $\Delta|f_x-f_y|<0.75$ MHz. The loaded Q_L value was close to the designed value with 420 – 550. The cross coupling between x/y pick-ups was better than -40db.

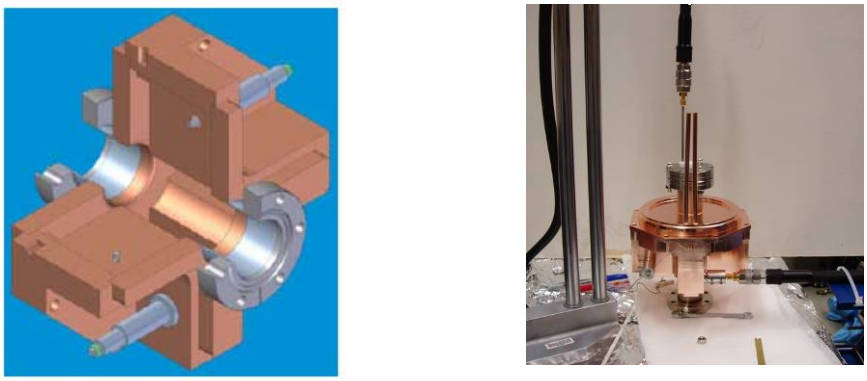

Figure 4. S-Band BPM for the ILC main linac: the cutaway view (left) and microwave measurement set-up (right).

4). Rf design of a Higher Order Mode (HOM) polarized rf gun for the ILC

The ILC requires a polarized electron beam. The ILC injector system can be simplified and made more efficient if a GaAs-type cathode can be combined with a low emittance rf gun. Compared with existing rf guns, this type of cathode is known to be extremely sensitive to vacuum, contaminations, and back bombardment by electrons and ions. Careful studies have been made of a new rf design for an L-band normal conducting (NC) rf gun for the ILC polarized electron source. This design incorporates a higher order mode (HOM) structure, with much-improved conductance for vacuum pumping on the cathode. Computer simulations have been used to optimize the rf parameters with three principal goals: first to minimize the required rf power; second to reduce the peak surface field relative to the field at the cathode in order to suppress field-emitted electron bombardment, third to minimize the maximum surface magnetic field for

reduction of pulse heating and ease of cooling. The beam properties have also been simulated initially using PARMELA.

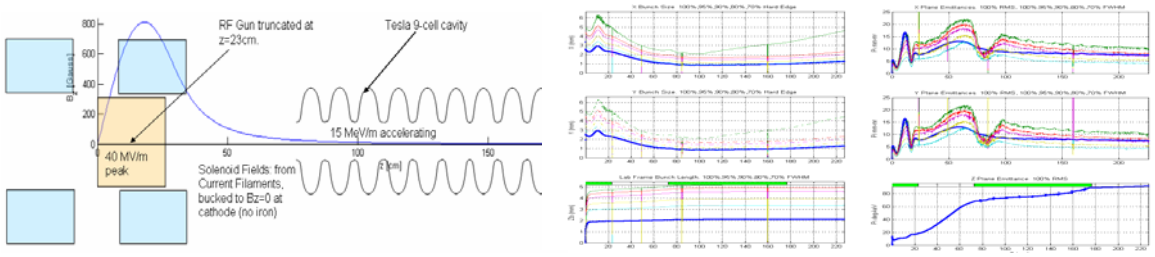

Figure 5. Layout of the polarized rf gun system (left) and beam dynamics simulation (right).

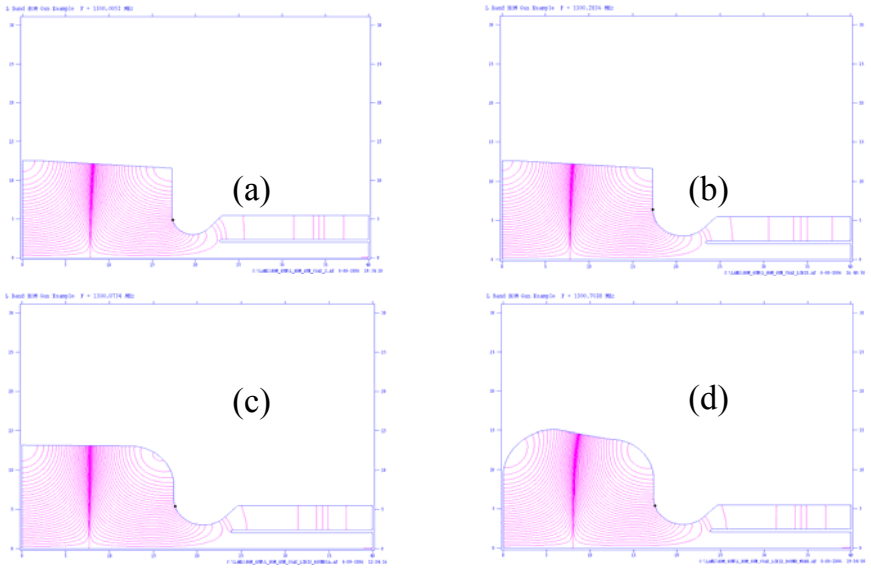

Figure 6. Design examples for an HOM rf gun: (a) with an output iris radius of 2.4 mm; (b) with an output iris radius of 3.4 mm; (c) with a rounding radius of 5 cm on the outer cell wall at the output end; and (d) with an additional rounding radius of 6 cm.

2) Accelerator Structures Work for the LCLS Project

Accelerator structures work for the LCLS began with the 2004 LCLS Injector RF Technical Review.

1). Tuning and characterization of the LCLS rf gun

The rf performance of the first LCLS rf gun has been thoroughly studied including the frequencies of the 0-mode and π-mode, quality factor as a function of the cathode tightening torques, the electrical field distribution along the gun axis, coupling coefficient and so on. The tuning was done by machining a tuning ring in the cathode cell based on careful microwave measurements and calculations.

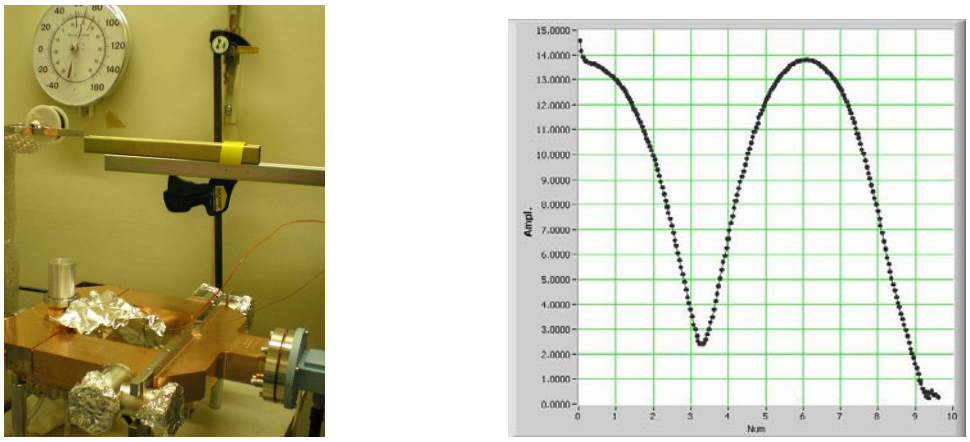

Figures 7. A bead drop microwave measurement set-up for the electrical field distribution (left) and a plot showing a perfect balanced field in cathode cell and coupling cell (right).

By using bead pull technology and precise frequency measurements for various cathode curvatures, complete tuning curves – the ratio of the fields in cathode cell and coupling cell as a function of mode spacing between the 0-mode and π-mode frequencies - as shown in the right plot in Figure 8 - have been obtained and studied. The round red dot is the perfect working point in the present and future reference for cathode replacement. This work not only contributed to the LCLS project for producing a superior quality rf gun, it also gained some important knowledge for its operation as well as the design of the next generation of the LCLS rf gun.

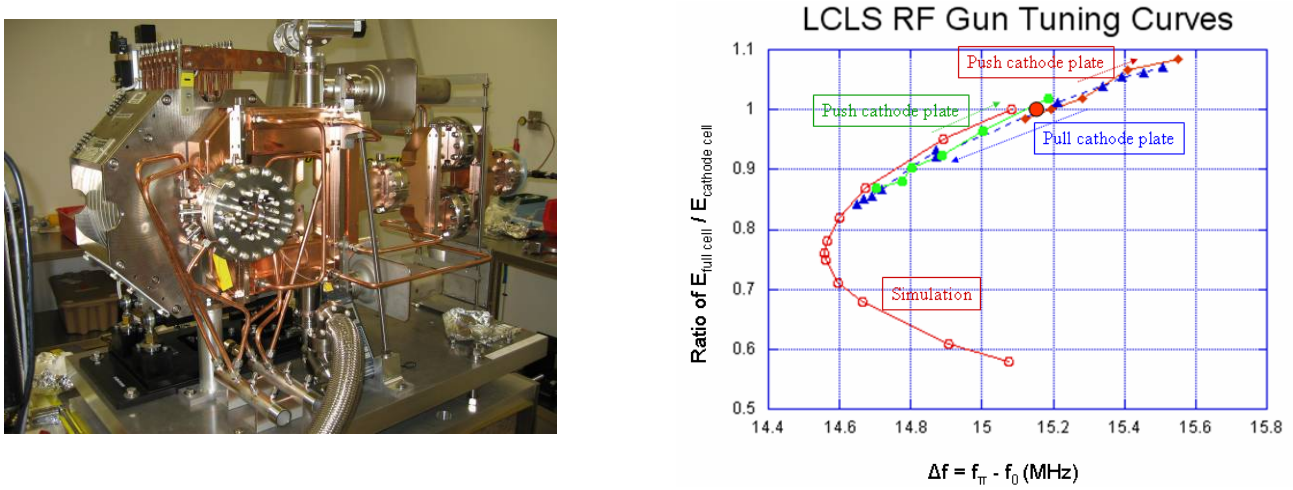

Figure 8. The final assembly of the first LCLS RF gun after microwave tuning, characterization and test probes calibration (left) and the tuning curves (right).

2). In addition to measurement, retuning and evaluation of two 9.5 ft S-band accelerator sections for the new LCLS beam line, two candidates were selected for booster sections from six 10-foot S-band accelerator sections. The front ends were modified with new double input waveguides and 5 new cells. The tuning and characterization are complete. They are now baking and will soon be ready for installation. A deflector section was also tuned for the beam length measurement.

Figure 9. Microwave measurement set-up for an S-band TW booster section (left) and a deflector for the beam length measurements for the LCLS (right).

3. Other research related to accelerator structures

1). Wire-based structure experimental method

Progress continues to be made in wire measurement for accelerator studies. This method can quickly and inexpensively analyze the wakefield suppression properties of accelerator structures. An improved control program has been developed to move a brass wire using microstepping motors and data acquisition. Also, we are still analyzing the recorded S-parameters for interpreting them to deduce the impedances of the monopole band as well as the impedance of higher dipole mode bands.

2). MicroLinac

Work continues on the MicroLinac, which is a small, standing wave (SW) linac. It is intended as a low-cost radiography source with dosage larger than 100 Ci. This linac could be used in place of radioactive sources, which can potentially be used for "dirty bombs." The preliminary operation showed too much of the unwanted rf phase drift due to the rf power transfer, leading to the beam energy reduction and low capture efficiency. Now, design studies are under way for an alternative traveling wave structure.

High Gradient Program

During this fiscal year a dedicated high-gradient program was initiated at SLAC. This program is part of the new US collaborative initiative on high gradient research. The purpose of this collaboration is to perform research to determine the gradient potential of normal-conducting, rf-powered particle beam accelerators, and to develop the necessary accelerator technology to achieve those high gradients. Harnessing the momentum of the concluded NLC/JLC development programs and working in conjunction with the ongoing CLIC studies, the collaboration will explore the possibility of pushing the useable acceleration gradient from the 65 MV/m reliably achieved in NLC structures up towards 180 MV/m or higher. Advancing the state-of-the-art in this area is essential to the realization of a post-ILC, multi-TeV linear collider using two-beam rf power generation.

This research and development effort includes studying the rf breakdown phenomenon itself, both theoretically and experimentally. This effort aims to establish a better understanding of the frequency scaling of the limiting gradient, as well as its dependence on material, surface preparation, structure design, pulsed heating, etc. It will explore the high gradient barriers due to choices made in linear collider programs to date. The experimental side of this effort will entail the upgrade of test facilities and the development of new high-power rf sources specifically designed for high gradient testing. The final goal is to produce and successfully test at very high gradient an accelerator structure suitable for use in a multi-TeV two-beam linear collider.

The high-gradient research initiative began with a two-day workshop in July 2005, which was organized by SLAC. The workshop spawned a nationwide collaboration consisting of several participating institutions, including universities and government laboratories, each of which submitted one or more proposals for work related to the goals of this initiative. These participants all have histories of contributions to the fields of accelerator design and/or high power rf R&D. Each institution brings its own capabilities, facilities and academic/scientific missions to the service of the collaboration and will be funded for participation through their normal DOE grants. These institutions form the initial collaboration; however, the make up of the collaboration may change based on each institution's funding and goals.

After the initial meeting, several activities under the leadership of SLAC scientists continued to strengthen this collaboration

- **a.** On September 9, 2005, S. Tantawi gave a talk at LBNL and discussed their planned studies.
- **b.** Second collaboration meeting at the University of Maryland, November 18, 2005.
- **c.** The 2006 Advanced Accelerator Concepts workshop had a working group on High Gradient RF Research chaired by S. Tantawi (SLAC) and co-chaired by V. Dolgashev (SLAC).

SLAC hosts this collaboration. Its experimental facilities will be available to collaborators for experiments supported through this collaboration. The program at SLAC will have three principal elements:

1) Enhancement of the experimental facilities,
2) SLAC's experimental program, and
3) SLAC's theoretical program.

Experimental Areas

Rf breakdown studies are still in their infancy. Very little is known either about the theory of surface breakdown at microwave frequencies or about the effect of geometries and the response of simple materials, let alone alloys and composites. The initial program is characterized by intensive experimental efforts. This program has to address the basic physics of breakdown phenomena. Because of its exploratory nature, a large number of experiments addressing different aspects of geometrical change and material variations are needed. Hence, priorities have to be given to establish experimental facilities capable of operating with a high enough repetition rate. Also, as recent experiments show, the frequency scaling of rf breakdown is not well understood. Therefore, it is necessary to carry out experiments at different frequencies. To do this, a variety of high frequency rf sources is required, some of which will need to be developed. In addition to studying breakdown phenomena in existing accelerating structures, it is necessary to have experimental facilities to test novel structures.

Existing Experimental Areas

Generally speaking, any high gradient rf structure reaches its limits after a period of high power processing. The nature of this processing is an open question. However, it is known that most structures more than double their initial gradient after processing. Also, the initial gradient that the structure can handle is poorly correlated with the final gradient after processing. This initial gradient correlates well with the surface processing and machining of the surface, while the final gradient is usually a function of material and geometry. Therefore, the processing time depends on the preparation and surface treatment. Although a system where this processing time goes to zero would be ideal, the potential for reduced or no processing time for a particular geometry or a material can not be ascertained without processing.

In any high vacuum system, a typical installation procedure will take about 3 days to complete. At X-band, the processing of copper structures typically takes about 3 days at 60 Hz, with close to 1,000 breakdowns. Refractory metals, on the other hand, take close to 4 weeks, with close to 100,000 breakdowns. Thus, an experimental program aimed at exploring the problem in a systematic way requires several test stands and the ability to change and test structures relatively quickly. The test stands need to be able to run at high repetition rate (~60 Hz).

At the moment, the only place in the US capable of doing tests at frequencies at S-band or above is SLAC. Ideally, SLAC should serve as the primary experimental site for the collaboration. At X-band, SLAC has three stations at the NLCTA and one station at the Test Lab capable of producing uncompressed pulses of ~80 MW, and each of these stations has an associated pulse compressor. There are an additional two stations, each capable of producing up to 50 MW, but with no associated pulse compressor. The capabilities of these stations vary, and they are not all capable of supporting all types of experiments. In effect, there are four useful experimental stations. Even if they are all dedicated to this program (at the moment not one is dedicated to this program), and assuming an average of 4 weeks/experiment for processing and characterization and a running time of 40 weeks/year, only 40 experiments would be completed per year, barely enough to do all the systematic studies needed. The rate of 40 weeks of running time and 4 weeks per experiment assumes that these stations are all equipped with data acquisition systems and monitors and that there are enough scientists and staff to service the stations and to conduct the experiments. Clearly this is not currently the case. As things stand, during the NLC development time, the NLCTA was capable of supporting about 10 experiments/year. The Test Lab supported about 3 experiments/year. Hence, the first order of business is to enhance the capabilities of these test stands:

1. The pulse compression system has been redesigned so that one can change the compression ratio from 1 to about 4 or 8, depending on the station, without breaking vacuum. This will reduce the time between experiments and will lower the cost of installations. The installation cost is one of the big cost drivers, because it is labor intensive.
2. To minimize the amount of vacuum work, windows are being built before and after the device under test. This will also minimize the cost and time.
3. The general infrastructure for diagnostics is being redesigned so that experiments can run in parallel.

The programs/users that these stands will serve, for the first year, are:

1. SLAC's experiments on geometries and materials, in particular single and multiple cell traveling-wave structures, single and multiple cell standing-wave structures, distributed coupling structures and waveguide structures.
2. Finish SLAC's series of experiments on NLC structures; test CERN structures.
3. Test Omega-P's structures
4. Test MIT structures (Scaled versions of most 17 GHz structures should be fabricated and tested at 11.4 GHz to understand frequency scaling).
5. Test structures manufactured by KEK.
6. Test and compare materials at ANL.
7. Test structures proposed by HRC, but at 11.4 GHz rather than 17 GHz.

RF Sources at High Frequencies

A. Gyrotron Development

High power rf sources at high frequency, 11.4GHz < f < 30GHz, are not available. These are needed to study one of the most fundamental issues in high gradient research, frequency scaling of breakdown limits. At these high frequencies, a klystron is not the device of choice. Gyrotrons are more suitable, because they are fast-wave devices, in which microwave power is produced in the circuits with sizes on the order of a wavelength and above. Gyrotron oscillators and amplifiers have a long history of success at frequencies from 8-10 GHz up to 100-200 GHz. Usually, gyrotron oscillators are simply called gyrotrons, while gyroklystrons are amplifier forms of these devices. Fundamentally, the development of amplifiers is much more difficult than the development of oscillators. In accelerator applications, amplifiers are traditionally needed for two reasons: synchronizing several devices and manipulating phase for a pulse compression system. However, for high gradient studies of single structures, raw power is all that is needed. Also, developments in active pulse compression make it possible to compress an oscillator signal.

Under the US High Gradient Collaboration, development was proposed of a gyrotron oscillator at SLAC in collaboration with other institutes. The oscillator comprises the following elements:

1- A modulator.
   I. The modulator already exists at SLAC.
2- A magnet, which can be either a superconducting magnet for millimeter-wave radiation or water-cooled solenoid for frequencies up to 20-30 GHz,
3- A magnetron injection gun (MIG)
   I. The MIG can be electrically designed as a collaboration between SLAC, the University of Maryland, MIT and CPI
   II. The mechanical design of the MIG could be done at SLAC.
4- Two microwave circuits to be installed on top of the gun, one at 30 GHz and the other at ~22 GHz.
   I. The microwave circuit design can be done in collaboration between SLAC, University of Maryland, MIT, CCR and CPI
   II. Manufacturing could be done at SLAC or at outside shops. The necessary machining is not demanding..
5- Active pulse compressors for the two frequencies. These can be developed within SLAC.

The system can be installed near the ASTA bunker and operated there for high gradient studies at high frequency. This is the shortest route to providing a workhorse for high gradient studies at high frequencies, which could serve the worldwide research community. It is also the most economical route to designing and building these devices

B. Active Pulse Compression

Active pulse compression at high frequencies (11.4 GHz < f < 91 GHz) can be readily achieved with the use of laser triggered bulk effect semiconductor switches. With the advances made in this field during recent years, one can project an inexpensive active pulse compression system at 30 GHz, which can be powered by either an oscillator or an amplifier. The development of such a system would be the shortest path to an operational test stand at 30 GHz. It could be used with CLIC's CTF-3 facility to compress the output of the extraction linacs. Fast changes of the output of these linacs are not easily attained, and a pulse compressor that can work without a phase-flip is the key device to make a useful test stand at CERN. Also building a gyrotron oscillator is far easier than building a gyroklystron amplifier, and, as stated above, this will provide the needed compression system for such an oscillator. Such a system has been designed and is now under construction.

SLAC's Experimental Program

The program is aimed at:

1) The study of the basic physics of rf breakdown, and
2) Studying and testing novel accelerator structures, including CERN and KEK structures.

Basic Physics Experimental Studies

There are three basic vehicles for these studies:

1. Traveling-wave single cell accelerator structures, see Figure 1,
2. Single-cell standing-wave accelerator structures,
3. Waveguide structures

Figure 1. a) "single-cell" traveling-wave and standing-wave test accelerator structures and b) a "single-cell" structure with demountable low-field couplers attached.

The single-cell, traveling-wave accelerator structures employ a new concept recently developed at SLAC. In these structures, a single cell which is a true representative of a cell of a long accelerator structure, is inserted between matching geometries that mimic the response of a long accelerator structure. This matching geometry has much lower fields though than the accelerator cell. In this manner, one retains as much as possible the elements of a real accelerator structure while testing a structure that is much simpler and is amenable to simulation and modeling.

Demountable couplers were added to these structures. The concept was invented at SLAC and this type of coupler has been proven to be reliable and tolerant of high power operations. This greatly reduces the cost of testing different structures, because the couplers are reusable. These three types of structures will be used to study both geometrical effects and materials. At the moment, four couplers and nine different structures are ready for testing. They have different material combinations and geometries. This represents the start of these studies. More structures must be created; in particular, structures made from chromium and if possible beryllium, are needed. Theoretical modeling at SLAC has shown that these materials should have superior performance, even better than the commonly sought after refractory metals. It is very important to test these to gain an insight into the theory of breakdown. If indeed the behavior of materials can be predicted, one can start on the road to the engineering of materials for high gradient rf.

SLAC's Theoretical Program

SLAC has been investigating theoretical and modeling aspects of the breakdown process. A simulation of the post breakdown phenomenon has been tested against experimental results with success for some waveguide geometries (See Figure 2) and accelerating structures.

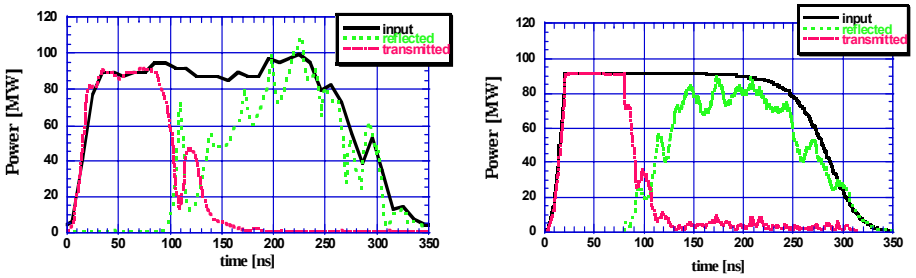

Figure 2: Incident reflected and transmitted rf power for a breakdown in the waveguide. a) a measurement of a typical breakdown in the preprocessed waveguide. b) 3D Particle-in-Cell simulations of the breakdown event.

Modeling of breakdown currents and the induced kick to an accelerated beam has been performed at SLAC. A unique theory for the breakdown threshold and the effect of the material properties has been put forward by P. Wilson. This effort is closely coupled to the experimental program. Most of the innovations and directions of the experimental program are driven by theory and the possibility of modeling. At this stage the modeling work will be directed toward creating a multiphysics simulation environment that will include electron-ion beam simulation in presence of electromagnetic fields, simulation of interaction of the beams with materials, and then transient thermomechanical analysis of the beam-material interaction. Using this environment, structure materials, geometries and circuits will be analyzed and compared with the experimental data.

5. B. FY06 PROGRESS: ACCELERATOR RESEARCH DEPARTMENT-B (ARDB)

5.B. 1 NLCTA AND E-163 by Eric Colby

The NLC Test Accelerator (NLCTA) is operated by the ILC Department in support of ILC R&D and advanced accelerator R&D including X-band structure testing and laser acceleration experiments. The operating funds for the NLCTA come from the SLAC operating budget.

NLCTA Operations

During FY2006, the focus at the NLCTA has been on L-band power source development and the commissioning of an experimental facility for SLAC experiment E-163, Laser Acceleration at the NLCTA. High Gradient RF work was also carried out on X-band components, as described above in Section 4.5.

A high-power L-band modulator, on loan from the Spallation Neutron Source at Oak Ridge National Laboratory, has been fully installed and tested in End Station B. The klystron has been successfully operated for hundreds of hours into an rf load at powers of up to 4.8 MW. Construction of rf waveguide distribution and laboratory facilities for a dedicated coupler test stand has begun. Preparations for installing a full-power L-band positron capture cavity have also begun.

Commissioning of the facilities for E-163 continued, with extensive studies to improve the quantum efficiency of the cathode, and commissioning of the full injector beamline and diagnostics up to the extraction point completed. Installation of the experiment beamline and its associated controls also progressed. Approval to operate E-163 is expected in early FY2007, and final commissioning will proceed thereafter.

NLCTA Schedule

The NLCTA accelerator ran routinely in support of the E-163 and X-band programs. The L-band program, not yet coupled to the NLCTA beamline, operated independently. Budget cuts in mid-FY2006 necessitated halving the operating hours for the remainder of year.

In FY2007, the NLCTA will operate approximately 1,000 hours in support of E-163, including commissioning of the extraction beamline. The L-band positron cavity will be installed and operated for approximately 1,000 hours. A prototype Marx-bank modulator will be installed and testing will commence.

NLCTA Safety

The NLCTA implementation of the DOE Integrated Safety and Environmental Management System (ISEMS) continues to be singled out by laboratory management as “exemplary,” and demonstrating “best practice among DOE labs.” The ISEMS practice at NLCTA includes weekly 7:30 AM “tailgate” meetings to review the scope, hazard controls, and approval of work in End Station B, and two weekly operations meetings at 9:30 AM to provide longer-term planning and coordination of activities in the End Station. The NLCTA SAD was revised to include the expanded facilities for E-163 and L-band research and approval of the new SAD is pending.

5.B.2 EXPERIMENT "E-167: PLASMA WAKEFIELD ACCELERATION by Mark Hogan

The E-167 Plasma Wakefield Acceleration Experiment was the continuation of an experimental program to study all aspects of beam-driven plasma wakefield acceleration. The experiments were performed by a UCLA, USC, SLAC/AARD collaboration using the unique high energy, high peak current, short pulse SLAC beams. There have been eighteen experimental runs (as experiments E157, E162, E164, E164X and E167) utilizing over sixteen months of beam time from June 1999 through April 2006. The E157, E162, E164(X) data have been analyzed, and the results have been published in eighteen papers in peer-reviewed journals.

Data from experiments E164 and E164X were analyzed in FY05, and the results were published in an article featured on the cover of *Physical Review Letters*.

M. J. Hogan, et al., "Multi-GeV Energy Gain in a Plasma Wakefield Accelerator," *Physical Review Letters* **95,** 054802, 2005.

In this paper, which has been widely recognized as a milestone in the development of plasma accelerators, it was shown that accelerating gradient in excess 27 GeV/m were sustained for 10 cm of plasma length resulting in energy gains of 2.7 GeV. The energy aperture of the beamline downstream of the plasma limited the energy gain and plasma length in E164 and E164X. That aperture restriction was identified and removed, and in the first E167 run in August 2005 energy gains of more than 10 GeV were observed using a 30-cm-long plasma. The experiments demonstrating this new world-record energy gain were in progress just when the previous results in Hogan *et al*. were being published and widely cited.

One of the major goals of plasma accelerator research for high energy physics applications is to demonstrate the ability to sustain ultrahigh accelerating fields associated with relativistic plasma wakes over a length long enough to at least double the energy of a real collider beam. Although a small fractional increase (10%) in the energy of beam electrons had been shown to occur over a10-cm-long plasma, that this could be extended to energy doubling over a meter scale was by no means clear. This is because such an extension transitions from a regime in which the beam has no time to distort, deplete or go unstable to a regime in which it is significantly depleted and deformed via the long interaction. This depletion is important because without it there can never be high-energy transfer efficiency from the drive electron beam to the wake. Without such a high efficiency the overall energy budget of a future hybrid collider that utilizes a conventional accelerator as a driver for a plasma accelerator would not make sense.

The final E167 run, carried out with the highest energy electron beam available in the world today, showed that instability is not a limitation. In April 2006, the collaboration demonstrated that an 85-cm-long plasma could double the energy of some of the incoming electrons from 42 to 85 GeV. These results have been submitted for publication and are out for review.

In addition to the acceleration, wsome of the properties of a new phenomenon have been observed and measured, accelerated electrons that originate from the plasma at high gradients. Analysis of the data from the April 2006 experiment and further plasma accelerator developments will be major activities in FY07.

6. FY06 PROGRESS IN ADVANCED COMPUTATIONS by Kwok Ko

In FY06, the codes **T3P** (wakefields) and **Track3P** (multipacting) with extensive benchmarking, joined **Omega3P** (eigensolver) and **S3P** (scattering matrix) to form a comprehensive suite of parallel electromagnetic codes developed under SciDAC. Close to maturity is the parallel 2D PIC code **Pic2P** for rf gun simulation and under development is a parallel 3D code **Gun3P** for beam formation and transport in sheet beam klystrons. Using these codes, a majority of ACD's efforts in the past year has turned to accelerator applications such as the ILC, PEP-II, Advanced Accelerator Concepts and the LCLS. Highlights from these simulations follow.

Transients and Cavity Deformations in the ILC TDR Cavity

The temporal electromagnetic field behavior in the ILC baseline TDR (TESLA) cavity due to a beam transit was simulated with **T3P** to obtain useful information on the transients in the cavity and the 3D effects from the couplers (input and HOM) on the short range wakefields. Figure 1 shows two snapshots in time of the magnetic fields (image current) on the cavity wall induced by the transiting beam: the first set of pictures from before the beam enters the cavity and the second set after the beam has passed. Performed on NERSC's Seaborg, the **T3P** simulation parameters were: 1.75M quadratic elements (10M DOFs) requiring 173 GB on 1024 processors and 47 minute per ns of beam travel.

1.2.
1.3.
1.4.

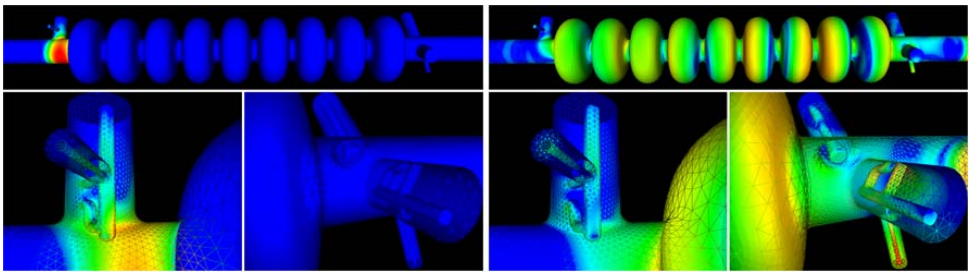

Figure 1: Snapshots of **T3P** magnetic field contours on the wall surface of the TDR cavity and couplers before beam enters main cavity (Left set) and after exiting output end beampipe (Right set).

Each of the two dipole bands in the TDR cavity consists of 9 pairs of modes as the mode degeneracy is split by the input and HOM couplers. Figure 2 shows the comparison between the **Omega3P** results from the ideal cavity and the measurement of 8 cavities in a DESY cryomodule for the sixth pair in the second band. It is observed that for the measured data: (1) the splitting of the mode pair is larger; (2) the mode pair is mostly shifted to lower frequencies; and (3) their Qe's are scattered towards the high side. The Qe increase would be problematic if they exceed the beam stability limit. The differences between simulation and measurement can be attributed to cavity deformations. An effort has begun to determine the cavity shape by solving an inverse problem using the TESLA data as input parameters.

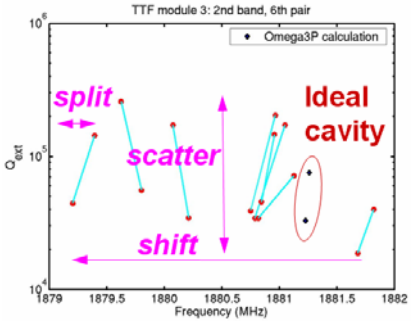

Figure 2: Comparison between ideal cavity results from **Omega3P** and measurements from 8 different TESLA cavities in an actual cryomodule, showing differences in mode splitting, mode frequencies and damping.

Mode Damping in the ILC Low-loss Cavity and the 3.9 GHz Crab Cavity

The Low-Loss cavity design (Figure 3) is being considered as a possible upgrade to the baseline TDR cavity for the ILC main linac. Based on a different cell shape, it has 20% lower cryogenic loss plus higher gradient (via a smaller cavity iris) over the TESLA design. Additionally, the end pipes where the couplers are located are larger than the cavity iris to allow for adequate coupling to the input coupler plus more effective HOM damping. Using the HOM coupler from the TESLA cavity directly, **Omega3P** analysis found that the first mode in the third dipole band does not meet the beam stability requirement of Qe < 10^5. A high fidelity mesh consisting of 0.53M quadratic elements (3.5M DOFs) was used to model the cavity. This provides sufficient resolution for modifying the end groups to improve the HOM damping. By adjusting the end-pipe radius, the HOM coupler azimuthal location, and the loop shape and configuration (Figure 3 colored inserts), the Qe of the dangerous third band mode was reduced to below the stability threshold. The **Omega3P** simulations were performed on NERSC's Seaborg with a direct solver, requiring 300 GB memory on 512 processors and one hour of runtime per dipole band. Comparison between original and new damping results is shown in Figure 4.

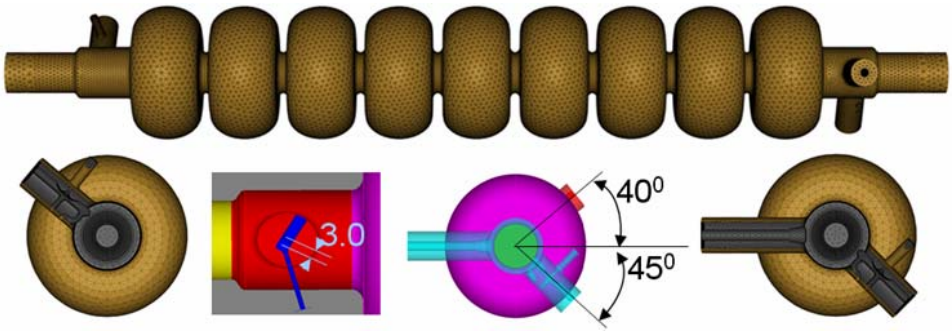

Figure 3: Mesh models of the LL cavity including the end groups and with the modifications of the HOM loop orientation and the coupler location shown in colored inserts.

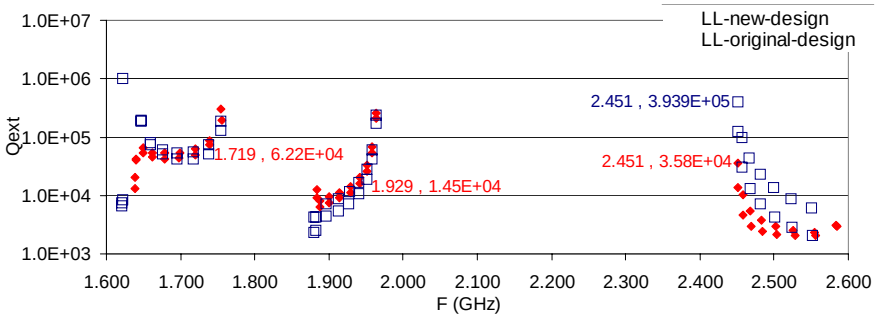

Figure 4: Qe versus frequency for the LL cavity with TESLA HOM coupler (in blue) and SLAC's improved design (in red).

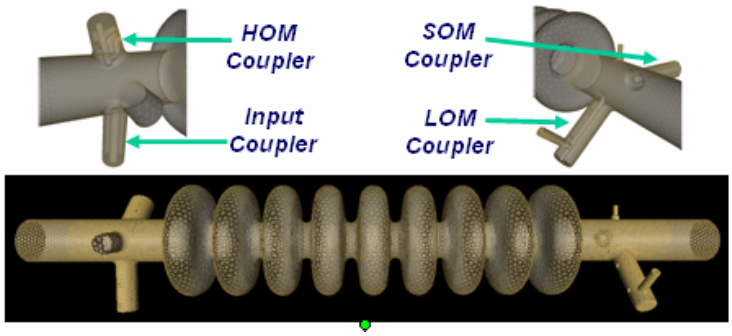

Figure 5: Mesh model of the FNAL design of the ILC crab cavity showing input, LOM, SOM and HOM couplers.

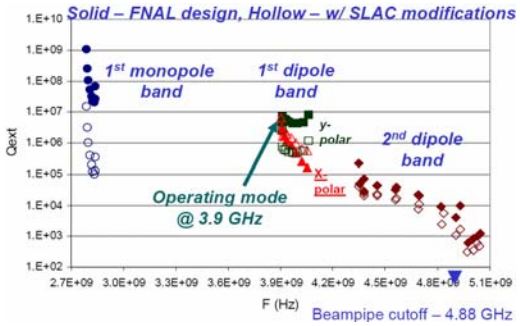

Figure 6: Mode damping improvements in the ILC crab cavity after 1st SLAC modifications.

The crab cavity employs the first deflecting mode to rotate the beam bunches to achieve higher luminosity at the ILC interaction point. The existing FNAL design has been simulated and preliminary modifications have been made to the computational model (Figure 5) to provide improved damping results (Figure 6).

Multipacting and Notch Filter Sensitivity in the ILC ICHIRO Cavity

Researchers at KEK are devoting a large effort to high gradient cavity R&D for the ILC with the focus on the ICHIRO cavity which evolved from the LL cavity design. In single cell tests, the ICHIRO design established a record gradient of 54 MV/m while 9-cell ICHIRO cavities (Figure 7) are having difficulties reaching gradients greater than 30 MV/m. The ICHIRO cavity differs from the LL design in the enlarged end-tube at the input end. Using **Track3P** multipacting activity in the transition from the enlarged end-tube to the beam pipe was revealed from simulation (Figure

7). The calculated MP levels are found to be in good agreement with X-ray barriers observed in the experiment (Figure 8). Work is underway to redesign the cavity to circumvent this problem.

Figure 7: (Left) 9-cell ICHIRO cavity prototype under high power tests at KEK with enlarged end-tube shown on the input end to the left, (Right) MP trajectory in the transition from enlarged end-tube to beam pipe.

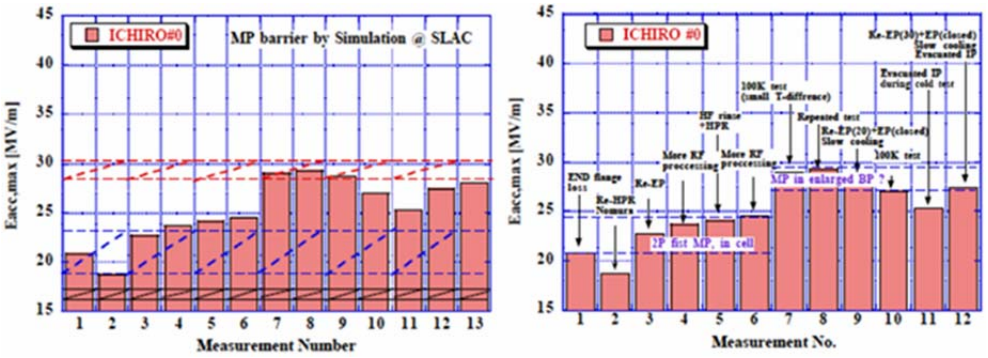

Figure 8: (Left) MP barriers in 9-cell ICHIRO cavity calculated with Track3P, (Right) MP barriers measured on ICHIRO prototype (K. Saito, KEK).

The notch filter in the TESLA HOM coupler is designed to reject the fundamental mode power while allowing damping of all HOMs. To study its sensitivity and detuning effect due to change in notch gap dimensions, two calculations were carried out. First the tuning curves of the HOM coupler for three different notch gap dimensions were computed with **S3P** to find the response around the fundamental mode frequency of 1.3 GHz (Figure 9) and a sensitivity of 0.11 MHz per micron was obtained. Next, the fundamental mode was computed for the cavity complete with HOM couplers set at the three different notch gap dimensions. A comparison of the fields in the HOM couplers from the fundamental mode in the three cases is shown in the table in Figure 9. While the notch gap fields vary little in all cases, the Qe of the mode is reduced by orders of magnitude when the notch filter is tuned far off the notch frequency at 1.3 GHz. This could lead to large amounts of power flowing through the feed-through and could result in excessive heating if proper cooling is not factored into the design.

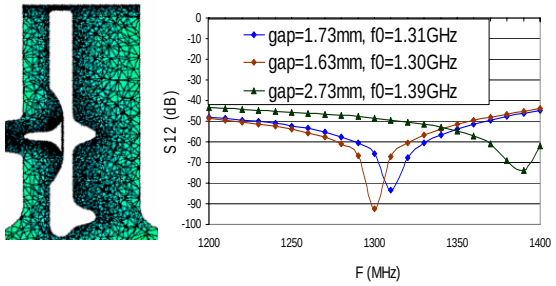

Notch gap (mm)	Notch gap field (MV/m)		Antenna tip Field (MV/m)		Qext of HOM port @1.3GHz	
	Up-stream	Down-stream	Up-stream	Down-stream	Up-stream	Down-stream
1.63	16.9	5.0	0.8	0.2	6.1e+9	1e+12
1.73	16.5	4.9	1.4	0.4	5.2e+8	9.e+9
2.73	13.3	3.9	6.1	3.0	1.4e+7	1.7e+8

Figure 9: (Left) Detailed mesh in the ICHIRO HOM coupler showing mesh density in the notch gap and near the antenna tip, (Middle) tuning curves of HOM coupler with three different notch gaps near 1.3 GHz, (Right) Field values in the notch gap and at the antenna tip for three different notch gap dimensions and the corresponding Qe.

Multipacting Studies for the ILC TTF III Input Coupler

Track3P simulations are being performed to investigate the effect of multipacting on the processing of the ILC TTF III input coupler. A model of the coupler is shown in Figure 9 (Left). Initial studies have been focusing on the region around the cold bellows as depicted in light blue in the model. The operating power level is between 300 and 400 kW. Simulations results reveal multipacting activities near 360 kW power level with multipacting particles impacting the coax outer wall but none within the bellows. The distribution of impact particles shown in Figure 9 (Middle) reflects the electric field profile along the coax which has a standing wave component on the upstream side of the bellows but remains a purely traveling wave on the downstream side. A typical particle trajectory on the upstream side is displayed in Figure 9 (Right) and it represents a fifth-order multipacting. Work is continuing to determine if the multipacting barrier persists beyond 20 impacts and the simulation will be extended to include the entire coupler geometry.

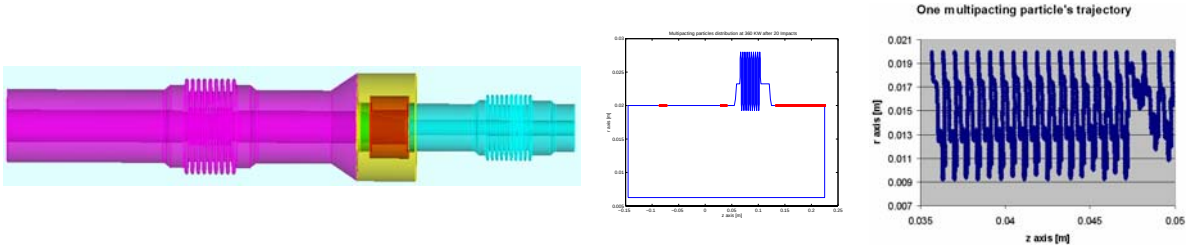

Figure 9: (Left) Model of the TTF III input coupler, (Middle) impacts of multipacting particles along the outer wall of coax, (Right) a typical particle trajectory with impacts close to the cold bellows on the upstream side.

Trapped Modes in ILC Multicavity Structures

First studied at DESY, the superstructure design for the ILC combines two or more cavities through weakly coupled beam pipes into a single unit. The goal is to reduce the number of input couplers and increase the packing fraction which reduces the linac length. One concern with superstructures is the presence of trapped modes between cavities. Figure 10 shows a two-cavity superstructure model and a HOM trapped between the cavities as computed by Omega3P. The

ILC GDE has expressed strong interest in computing the wake fields for an ILC RF unit consisting of 3 cryomodules with 8 TDR cavities each. As a first step, a four-cavity structure which is relevant to KEK's STF cryomodule is being modelled. The simulation parameters on NLCF's Phoenix are: 2.52M quadratic elements (15.2 M DOFs) requiring 280 GB on 1000 CPUs and 23 hours of runtime for 2 eigenmodes. The solution method used was Second Order Arnoldi with restarted GMRES and multilevel preconditioner. One of the modes with high fields in between the cavities is shown in Figure 11. Rough estimates of the computational requirements for modelling the entire ILC RF unit are 20-30 M quadratic elements (100M – 200M DOFs) and several thousand modes. This challenging simulation will require petascale computing resources and advances in scalable eigensolver algorithms as well as parallel refinement techniques. Efforts in these two computational science research areas are in progress under SciDAC.

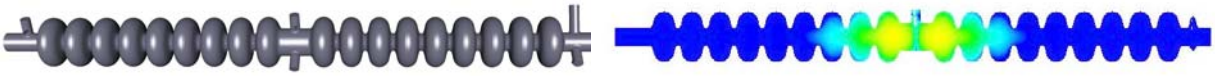

Figure 10: Two-cavity superstructure model and a trapped mode found by **Omega3P.**

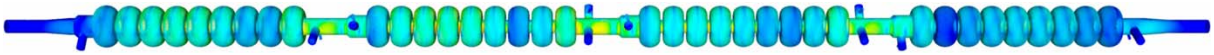

Figure 11: One **Omega3P** computed HOM in the ILC 4-cavity structure with strong fields between cavities.

Broadband Impedance of PEP-II LER BPM

During PEP-II operation some BPMs in the LER lost the buttons due to poor thermal contact. There was a request to find out through simulation the effect of the missing buttons on the ring's broad band impedance. This problem is very difficult for structured grid codes like **MAFIA** to solve accurately because of the elliptical vacuum chamber and the fine details in the BPM. Figure 12 shows a high fidelity model of the geometry for the vacuum chamber as well as the BPM with and without buttons. Using **T3P** on NERSC's Seaborg, the mesh resolution was increased till the wakefields converged. The results for the short-range wakefields are shown in Fig 12 which compares the case with buttons to that without buttons indicating the difference is not significant. The PEP-II has since operated normally even with some missing buttons in a number of LER BPMs.

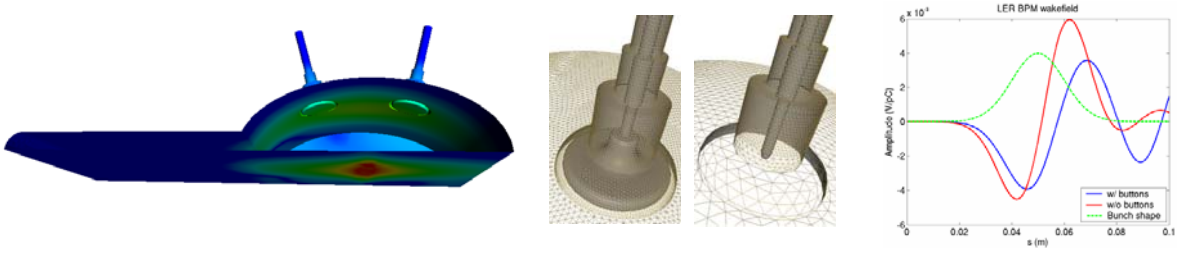

Figure 12: (Left) Upper-half model of the PEP-II LER vacuum chamber with two BPMs and showing the beam down the axis, (Middle) Mesh of the BPM with and without button, (Right) Comparison of short-range wakefields in the two cases.

Wakefields in the MIT Photon-Band-Gap (PBG) Structure

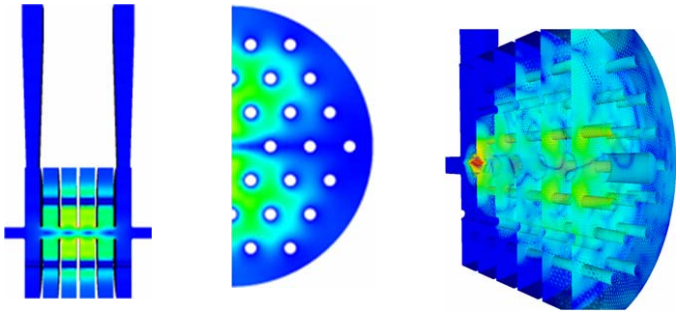

Figure 13: (Left) A dipole mode at 23 GHz computed by **Omega3P** with Qe = 131, (Right) wakefields generated by a beam using **T3P.** Absorbing boundaries are imposed at the outer wall in both cases.

ACD is collaborating with MIT and STAR, Inc on a SBIR project to advance the R&D on the Photon-Band-Gap (PBG) structure as a promising Advanced Accelerator Concept. The PBG is, by design, a single mode structure in which all HOMs are not confined and therefore can escape from the structure once generated by the beam. MIT has fabricated a 17 GHz PBG structure which demonstrated that it can provide 35 MV/m accelerating field-gradient in beam tests. The role of simulation is to verify the effectiveness of the PBG concept in damping HOMs. For the MIT 17 GHz structure, both time and frequency domain simulations were carried out. Figure 13 (Left) shows one HOM computed with **Omega3P** that has a Qe of 131 so is heavily damped. The wakefields due to a transit beam modeled with **T3P** is shown in Figure 13 (Right) where no high fields inside the structure were seen after some time. In both **Omega3P** and **T3P** simulations absorbing boundaries were imposed at the outer wall of the PBG structure.

RF Gun Simulation for the LCLS

In the past year, ACD has devoted a significant effort to the development of a parallel particle-in-cell capability which is based on conformal grids and higher-order finite elements for superior geometry representation and higher field accuracy. There is strong interest in such a code from the rf gun community because of the growing need for high brightness, low emittance beams in next generation FELs and light sources. The initial focus is on the 2D code, **Pic2P,** with the LCLS rf gun as the target application. To our knowledge, **Pic2P** is the first successful implementation of self-consistent particle-field interaction on an unstructured grid. Based on first principles, the code contains all pertinent physics effects such as space charge, retardation and wakefields. Figure 14 (left) shows the highly unstructured mesh of the LCLS rf gun with mesh densities concentrated along the beam path. The particle bunch as accelerated by the driven cavity mode and the scattered fields generated by the beam in its interaction with the gun cavity are shown in Figure 14 (middle) and Figure 14 (right) respectively, This is the first time that the wakefields in the LCLS rf gun have been calculated accurately. The effect, though, is relatively small, accounting for about a 6% change in the transverse emittance. The comparison of the normalized RMS transverse emittance between **Pic2P, MAFIA** and **PARMELA** for different bunch charge is summarized in Figure 15 (left). There is excellent agreement between **Pic2P** and **MAFIA** although **Pic2P** requires far less computational resources to reach the same convergence. Figure 15 (right) shows the parallel speedup presently achieved by **Pic2P** and the good scalability makes it viable to use the code as a design tool as the computing time can be reduced to the same order as **PARMELA**'s while providing all the correct physics as a PIC code can. Work has begun on the 3D version (**PIC3P**) which will be an invaluable tool for commissioning the LCLS gun.

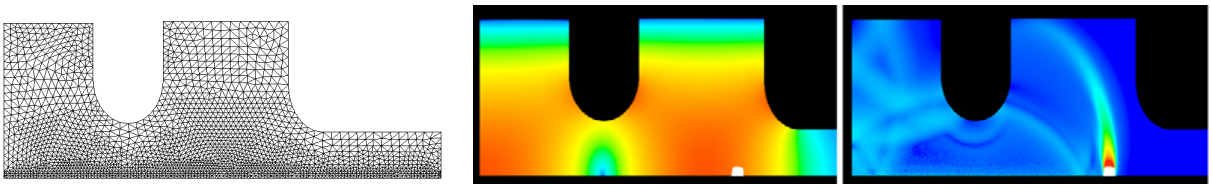

Figure 14: (left) Mesh of the LCLS rf gun, (middle) Particle bunch accelerated by operating mode as modeled by **Pic2P,** (right) scattered fields generated by the beam in its interaction with the RF gun cavity.

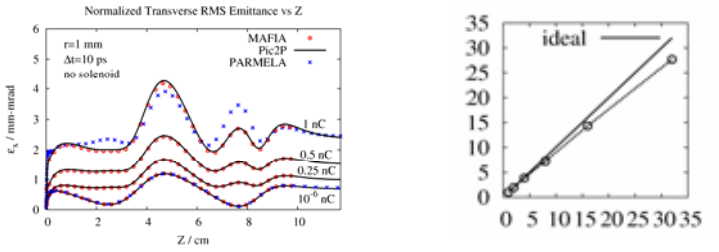

Figure 15: (left) Comparison of the normalized transverse RMS emittance for different bunch charges between **MAFIA, Pic2P** and **PARMELA,** (right) parallel speedup of current implementation of **Pic2P.**

7. FY06 HIGH POLARIZATION ELECTRON SOURCE/ACCELERATOR MATERIALS DEVELOPMENT by Bob Kirby and Takashi Maruyama

The **Surface and Materials Science Dept**. (SMS) contributes to SLAC's accomplishments in a number of areas, by using vacuum and materials expertise to support the development of novel electron sources, detectors and accelerating structures. Current areas of focus include a high polarization-high current electron source for the ILC, metal photocathodes for the LCLS photo-injector, and surface-analytical research and development on methods for suppressing collective electron instabilities in high current positron/proton storage rings.

SMS engages in a continuing research collaboration with Linear Collider Detector Group, the Accelerator Technology Group's Sources and Polarization Group, and the University of Wisconsin on the development of **high-polarization high-current semiconductor electron sources**, originally for E-122, then for the SLC and End Station A experiments, and currently for the ILC. After several years of DOE SBIR programs, strained-superlattice photocathodes based on GaAsP and GaAs have been developed in collaboration with SVT Associates, who grow such wafers using molecular-beam-epitaxy (MBE). The strained superlattice structures consisting of very thin quantum well layers alternating with lattice-mismatched barrier layers are excellent candidates for achieving higher polarization. Due to the difference in the effective mass of the heavy- and light-holes, a superlattice exhibits a natural splitting of the valence band, which adds to the strain-induced splitting. In addition, each of the superlattice layers is thinner than the critical thickness for strain relaxation. Spin polarization as high as 86% is reproducibly observed with the quantum efficiency (QE) exceeding 1%.

Although the GaAsP/GaAs strained-superlattice structure is considered as the leading candidate for the ILC polarized electron source, the polarization appeared saturated at about 85% and is independent of the valence band energy splitting. This is a strong indication of a spin-depolarization mechanism in the GaAsP/GaAs structure. To characterize the spin-depolarization mechanism, three structures are under investigation:

1) Biased photocathodes – The spin depolarization apparently takes place during transport in the conduction band and in the band bending region. By applying a bias voltage, the electron drift velocity can be controlled and the band bending can be altered. The bias across the device is achieved through a metallic grid photolithographically grown atop the emitting GaAs surface and a back contact to the substrate GaAs. Supported by a DOE STTR Phase II program, spin-polarized photoemission from metal-gridded cathodes has been investigated in collaboration with Saxet Surface Science. When the surface is positively biased, the QE increases as much as 100% as a result of the lower vacuum level. The polarization is also observed to increase by 5% ($\Delta Pe/Pe$).

2) AlInGaAs/GaAs strained-superlattice structure – The aluminum content determines the formation of a barrier in the conduction band, while adding indium leads to conduction band lowering, so that the conduction band offset can be completely compensated by an appropriate choice of the aluminum and indium contents. As a result, a higher vertical electron mobility and a lower spin relaxation rate can be achieved. The structure has been investigated in collaboration with a St. Petersburg Technical University group. Polarization as high as 90% has been observed from two wafers. However, such a high polarization does not seem to be reproducible partly because the quaternary structure is more difficult to grow. Furthermore, the high polarization can be observed only when the cathode heat-cleaning temperature is significantly lower than the standard 600°C. The low temperature heat-cleaning technique using atomic hydrogen source will be investigated.

3) InGaP/GaAs strained-superlattice structure – This is a structure similar to the GaAsP/GaAs strained-superlattice structure, but with the GaAsP barrier layers replaced by InGaP. The GaAs layers are quantum wells and continue to be strained. The spin-orbit interaction in InGaP is three times smaller than in GaAsP, and the spin depolarization is expected to be smaller. Since the band gap energy in InGaP is larger than in GaAsP, higher QE is also expected. Five wafers have been grown through a DOE SBIR Phase I program, and cathode characterization is in progress.

Electron cloud disruption of positively-charged beams is a significant problem in high-current positron and proton rings, and is expected to be a problem in the LHC main ring and the **ILC positron Damping Ring**. Heating by very low energy secondary electrons endangers the LHC beam chamber cryogenic budget. SMS's X-ray photoelectron spectrometer (XPS) makes secondary electron yield (SEY) measurements down to 10 eV primary electron energy. In FY06, secondary yield and XPS surface chemical valence measurements continued on yield-suppressing coatings on grooved surfaces of aluminum (Al). Particularly interesting was grooving plus TiN coating, which have a cumulative yield-lowering effect. Various grooving profiles were measured, bare or with TiN coating, with coated values less than one, before electron conditioning (which lowers the yield further during ring commissioning).

Ion bombardment of the coatings from beam- and surface-ionized residual gas was measured using an ion gun with H_2 and N_2 feed gases. The measured conditioning efficiency of ions over electrons was several thousand times higher, with ion mass as a secondary effect. In early FY07, coated pieces of flat and grooved chamber wall will be inserted into the PEP-II ring to determine

the effect of photon scrubbing on SEY. The samples will be transported, after exposure and under vacuum, to the XPS chamber for yield measurement.

The **Linear Coherent Light Source** (LCLS) injector is scheduled to commission with a metal photocathode having a quantum photoefficiency (QE) of > $2x10^{-5}$ at the exciting laser wavelength of 255 nm. Cathodes are now prequalified for installation by measuring the QE in the SMS Cathode Qualification System, after processing the cathode to maximize the QE. Then, after installation at the injector, only a modest bake-out is be required to remove atmospheric-adsorbed water and hydrocarbons. The first LCLS cathode is now prequalified and installed in the Sector 20 rf gun.

In vacuo process cleaning of the copper cathode surface is done by bombardment with 1-3 keV H_2 ions, which previous laboratory measurements showed does not increase surface roughness. Several hours of initial bombardment is needed to remove the amorphous machining layer from the surface then, after air exposure, only a brief re-bombardment is required to restore good QE.

8. FY06 PROGRESS IN THE TEST EXPERIMENT PROGRAM by Roger Erickson

The test experiment program in FFTB was concluded and the majority of the small experiment work was done in End Station A. The FFTB run (T-485) was fitted between SPPS and E-167 runs. There were several brief periods of ESA experimental activity in November, January and April, and in the June –August period several experiments were installed and took data.

T-469, DIRC R&D Program: D.W.G.S. Leith, J. Va'vra

The experiment used an End Station A beam, with ~1 particle per pulse, to study the performance of a fused silica bar Cherenkov detector, a development of the DIRC particle identifier in BaBar. It uses a spare fused silica bar from BaBar, but incorporates multipixel photomultiplier tubes, and electronics affording resolutions ~ 1 mm in space and ~100 ps in time coordinates.

The DIRC system at BaBar affords excellent particle identification in the relevant particle energy range. In possible future applications at much higher luminosity, limitations to the technique are expected to arise from beam induced backgrounds in the large water tank that serves as an optical coupler between the fused silica and the photomultiplier tubes. In addition, the Cherenkov cone reconstruction resolution is limited by the optical dispersion in the fused silica (the variation in the light propagation speed with wavelength). Both of these concerns are being addressed in this test. By reducing the effective pixel size from 3 cm to 6 mm, the volume of the coupling fluid can be reduced by one to two orders of magnitude. This requires parallel to point optical focusing. The new pixellated photomultipliers also have excellent timing characteristics, and coupling that with fast-timing, multi-channel electronics to achieve a time resolution of <100 ps, the optical dispersion in the long fused silica bar may be corrected by measuring each photon's time of propagation.

The 3.6-mete- long fused silica bar has been mounted on a movable stage at the downstream end of End Station A, where the low intensity secondary beam was delivered. Light from the end of the bar was focused, by a 50 cm focal length mirror, on to an array of six photomultipliers of various designs. The optical coupling from the fused silica to the photon detectors was achieved by using mineral oil. Detectors were from Burle (multichannel plates) and Hamamatsu (foil dynodes). About 200 channels of preamplifiers using Elantek chips, and custom developed constant fraction discriminators, provided tight timing signals to a TDC system. The timing fiducial was derived from the linac timing system, and was monitored for drift by using a counter in the beam with ~ 35 ps resolution.

The experiment ran this year with a set of improved photon detectors. An additional Burle/Photonis MCP was added, with an improved design of the electron transport. One PMT was replaced by a new Hamamatsu MaPMT with better timing capability, and whose anode size and spacing was selected to optimize angular resolution. The number of available instrumented channels was increased by 15%. Newly developed improvements on the TDC calibration were implemented. In addition, the beam was understood better, was better instrumented, and had lower backgrounds. In this configuration, the data sample collected was more than double what had been obtained before.

The correlation between time of arrival of the light and the chromatic dispersion has been observed already. Analysis is proceeding to optimize a procedure to use the measurements to sharpen the angular resolution and hence the particle segregation capability. Future work is expected to explore the extension of pixellated PMT performance in red light where optical dispersion is less significant, but Cherenkov light output is lower.

T-474, T-475, T-480, T-488, **ILC Test Beam Experiments in End Station A**: **M. Woods**

The SLAC Linac can deliver to End Station A (ESA) a high-energy test beam with similar beam parameters as for the International Linear Collider (ILC) for bunch charge, bunch length and bunch energy spread. ESA beam tests run parasitically with PEP-II with single damped bunches at 10Hz, beam energy of 28.5 GeV and bunch charge of $(1.5\text{-}2.0)\cdot 10^{10}$ electrons. Four experiments were approved and took data in FY06. A 5-day commissioning run was performed in January 2006, followed by a 2-week run (Run 1) in April and a 2nd 2-week run (Run 2) in July. These tests included: i) BPM (T-474) and Synchrotron Stripe (T-475) energy spectrometer prototypes to study systematic effects for precision energy spectrometer measurements, where the ILC goal is to achieve an accuracy of 100 parts-per-million; ii) collimator wakefield studies (T-480) for determining the optimal material and geometry of ILC collimators. These collimators are needed to eliminate beam halo that could cause unacceptable backgrounds for the ILC detectors, but they can also potentially ruin the small beam emittance; iii) characterizing the performance of prototype beam position monitors (BPMs) for the ILC Linac as part of T-474; and iv) a study of background effects for the IP feedback BPMs at the ILC (T-488). Beam tests were also performed to characterize beam-induced electro-magnetic interference (EMI) along the ESA beamline and to study an EMI failure mode in the electronics for the SLD vertex detector, and bunch length diagnostics were tested that have applicability for ILC and LCLS.

Brief summaries of the ESA setup and beam tests follow:

i. ESA infrastructure. We installed and commissioned a new beamline, including 2 wire scanners, a beam containment collimator and 4 machine protection ion chambers, a data acquisition system for the experiments running Labview on a PC reading out VME and Camac crates; and bunch length diagnostics using high frequency diode and pyroelectric detectors.

ii. T-474 BPM energy spectrometer. Two rf bpm triplets were installed and commissioned. New bpm processing electronics for these and 5 additional existing rf bpms were also installed and commissioned. One of the new rf bpm triplets, BPM3-5, uses prototype ILC Linac bpms. For Run 2, an interferometer system was commissioned to monitor transverse motion of the BPM3-5 triplet.

iii. T-475 Synchrotron Stripe energy spectrometer. A prototype quartz fiber detector was installed at a synchrotron light port in the A-line and commissioning data taken.

iv. T-480 Collimator wakefields. The collimator wakefield box used previously at the ASSET region in the Linac was relocated to ESA. 8 sets of collimators were manufactured in the UK and wakefield kicks from all 8 sets have been measured. The BPM system developed for T-474 is used for the BPM diagnostics.

v. T-488 IP BPM studies. This experiment studies background effects in an IR environment for the fast feedback bpms that will stabilize collisions at the ILC IP. The experiment was approved in May and first data was taken in Run 2. The setup included a mockup of nearby beamline components in the ILC design.

vi. EMI studies. We acquired broadband antennas measuring frequencies up to 7.5GHz, with signals to a 1.5GHz bandwidth scope, to characterize electro-magnetic interference (EMI) along the ESA beamline. In particular this was done near ceramic gaps that were installed to facilitate studies for bunch length diagnostics and EMI studies. In Run 2 we installed electronics from the SLD Vertex Detector that had a failure mode during SLD operation, suspected to be due to beam-induced EMI. We were able to reproduce the failure mode, demonstrate that it was due to direct beam-induced EMI pickup at the electronics board and characterize the EMI levels at which it failed.

The ILC test beam program in ESA is described in SLAC-PUB-11988 (also available as EUROTeV-Report-2006-060), which was prepared for a paper and poster contribution at EPAC06. Two other papers and posters were also contributed to EPAC06 for T-480 and T-488. There are 22 institutions collaborating on the ILC test beam program in ESA. Analysis of the data taken in FY06 is ongoing. The program will continue in FY07 with the addition of a magnetic chicane, undulator magnet and new BPMs for the energy spectrometer tests (T-474 and T-475), new collimators for wakefield measurements (T-480) and a new bunch length measurement experiment using Smith-Purcell radiation (T-487).

T-485, Magnetism with Ultrashort Magnetic Field Pulses: H. Siegmann, S. J. Gamble, M. Burkhardt

The experiment made use of the extremely high magnetic fields around the tightly focused FFTB beam to explore the switching characteristics of ~10 nanometer thick magnetic films at so far

unexplored time scales. A previous experiment (T-478) exposed similar films using beam pulse lengths of ~5 picoseconds and ~100 femtoseconds. The goal of the T-485 run this fiscal year was to confirm the results from T-478, thereby making them suitable for publication. Namely, T-485 attempted to obtain a better characterization of the profile of the SLAC electron beam than was measured during T-478. This characterization was necessary to determine if certain features in the T-478 data were due to an unexpected magnetic response of the system to a clean Gaussian pulse, or to an expected magnetic response to an irregular beam.

The physics being explored is that of the ultrafast switching of ferromagnetic spins, which is expected to yield information important for fast magnetic recording. The samples are premagnetized along an easy direction and mounted in a vacuum chamber on a motorized arm in the beamline. Single pulses of the FFTB beam are then sent directly through the samples. Since the magnetic field of the electron beam falls off with radius, different portions of the sample are exposed to different field strengths, peaking near the impact region of the beam. The high fields obtained within the 5 picosecond or 100 femtosecond duration of the bunches allow for the study of ultrafast magnetization dynamics on time scales far beyond any other laboratory setting. The initial T-478 results displayed unexpected behavior of the system in two ways. First, the magnetic spins exposed to both the picosecond and femtosecond bunches did not conform to the expected switching pattern when the angle of the initial magnetization and the applied field from the FFTB beam was larger than 120 degrees. The observed anomalies in the behavior suggest a possible breakdown of the conventional magnetization dynamics equations in the high field-high switching angle regime. Second, the samples exposed to the picosecond pulses show small physical holes in the magnetic layers directly at the point of impact of the beam, where the top few layers have been removed in the exposure process. Remarkably, however, these holes are absent on the same samples when exposed to the femtosecond beams of identical charge. This means that the heat transfer to the sample is less efficient when the pulses get shorter. This result is of great interest for any ultrafast spectroscopy.

The T-485 run was not able to accomplish its goal. During the run an anomalously high number of X-rays were present in the beam pipe originating from a source which could not be determined during the length of the beam time. This rendered it impossible to measure the beam profile, as the X-rays flooded the detectors and consequently the signal from the wire scanners became lost in the noise. Furthermore, no femtosecond beam could be produced during the T-485 run. When the compressed beam was requested from the control room, the routine “wake loss scan” was not performed, which the users did not know until after the end of the run. A later analysis showed that the number of electrons in the beam present at the time of the attempted compression was insufficient to successfully complete the final stage of compression, and the actual state of the beam at the time of sample exposure is completely unknown. Between the two failures of beam characterization and lack of compression, all of the T-485 data is unfortunately completely useless.

T-486, Askaryan Effect in Ice: Calibration of ANITA Payload

In previous experiments at SLAC, the Askaryan Effect, the emission of coherent Cherenkov emission of radio energy from electromagnetic showers, was characterized in sand and salt. The ANITA project, a balloon flight over Antarctica, is intended to detect Askaryan emission from

extreme energy neutrinos in the ice cap there. This will be an important step in testing the prediction that there is a high energy cutoff of the hadronic cosmic ray spectrum (the GZK effect), at ~10^{20} eV, that also distorts the neutrino spectrum. Since the origin of these ultrahigh energy particles is not understood, this will bring valuable evidence to the study.

The balloon gondola, a framework supporting 30 specially designed horn antennas and their associated signal triggering, digitizing and recording electronics, was assembled in End Station A and supported at the back of the end station in a way simulating a balloon flight. The fragile solar photovoltaic panels were not installed. The Cherenkov radio emission was generated by stopping the 28.5 GeV electron beam in a block of ice approximately 15 feet thick. The top surface of the ice was cut to a downward slope of 6 degrees to the horizontal. This caused the Askaryan Cherenkov radiation to be refracted out in a beam aimed at the general position of the payload. The gondola was moved and rotated to accumulate measurements of signal strength from all antennas and for a range of angles and offsets between the radio beam and the horns. Systematic checks were made by varying the beam intensity, taking data with the ice covered with thermal insulation and also with insulation removed, and changing the surface texture of the ice. Calibration signals from an emitting antenna aimed at the gondola were recorded between beam runs.

Because the system is required in Antarctica within weeks, and further testing, integration and optimization is scheduled, only preliminary verification of the test data has been possible so far. The results show that the signal strength is close to that expected, and constitutes the first observation of the Askaryan effect in ice. The variations between antennas, and the acceptance cone of each antenna, are also acceptable, and the data will permit the calibration constants for the flight to be obtained.

9. FY06 PROGRESS FOR THE EXO DOUBLE-BETA-DECAY R&D PROGRAM by Peter Rowson

A SLAC group (M. Breidenbach, C. Hall, D. MacKay, A. Odian, C. Prescott, P.C. Rowson and K. Wamba) have been collaborating with the Stanford Physics Department group of G. Gratta, and with others, in an R&D program to test the feasibility of a novel large-scale double-beta-decay experiment. This experiment, known as EXO (for Enriched Xenon Observatory) proposes to use a large quantity (>1 ton) of Xenon enriched in the Xe^{136} isotope as both a decay and detection medium. The double beta decay process,

$$Xe^{136} \rightarrow Ba^{136++} + e^- + e^- \ (+ 2\nu)$$

can proceed in the two neutrino($2\nu\beta\beta$) mode expected from the Standard Model (and which has already been observed in several nuclei other than Xe^{136}), or possibly in the neutrinoless ($0\nu\beta\beta$) mode. The $0\nu\beta\beta$ process is expected to occur only if neutrinos are Majorana particles, and at a rate proportional to the square of an "effective" neutrino mass, and hence its observation would serve a mass measurement and as the first demonstration that Majorana neutrinos occur in nature. Xenon's excellent calorimetric properties (necessary to distinguish the broad beta spectrum of the

electron energy sum in the $2\nu\beta\beta$ process from the line spectrum in the two-body $0\nu\beta\beta$ decay), readily achievable high purity, and lack of worrisome radioactive isotopes make this element an attractive candidate for a low background experiment. In addition, we propose to operate the rare decay search in a coincidence mode, by identifying the Barium daughter nucleus of double beta decay on an event-by-event basis. Barium identification is accomplished by a laser florescence technique that is sensitive enough to observe a single ion and, in principle, to distinguish the various Barium isotopes. The site for such an experiment must be deep underground to minimize cosmic ray backgrounds

To date, the R&D efforts at SLAC and Stanford have focused on a liquid xenon (LXe) TPC design, where the Barium identification would be accomplished by removing the ion from the LXe using a electrostatic probe, and then delivering the ion to an as-yet-unspecified laser system. The campus group has successfully constructed and operated a laser-illuminated ion trap for Barium and has observed single Barium ions. In addition, they have demonstrated state-of-the-art energy resolution in LXe (which occurs at electric fields >4 kV/cm) and have preliminary results showing resolution enhancement when the 175 nm scintillation light produced in xenon, in addition to ionization, is collected.

The logistical problems connected with the procurement of a large amount (~10 tons) of isotopically enriched Xe^{136} were dealt with under the Nuclear-Non-Proliferation programs of DOE. To date, we have obtained 200 kg of xenon isotopically enriched to 80% in Xe^{136} for use in a prototype experiment. The prototype, which does *not* employ Barium identification, is presently being built. The experiment, known as "EXO200", will be placed in the DOE operated underground facility WIPP (Waste Isolation Pilot Plant) in Carlsbad NM. EXO200 will collect useful data for TPC performance, should definitively observe $2\nu\beta\beta$ in Xe^{136} for the first time, and should accumulate the large number of $2\nu\beta\beta$ decays needed to characterize this important background. . In addition, a design goal is that the prototype has sufficient sensitivity to test with one or two years of data the recent and very controversial claims from the Moscow-Heidelberg Ge^{76} experiment that they have observed $0\nu\beta\beta$ events.

SLAC Activities : R&D

At SLAC, a xenon purification system was constructed that is operated at ultra-high vacuum along with a xenon purity monitor (XPM). The purifier employs a heated Zirconium metal getter to remove non-noble gas contaminants (nominally to the 0.1 ppb level), as well as distillation capability (to remove Argon). The XPM drifts electrons produced from a UV-laser-illuminated cathode in LXe across a gap and measures the transport efficiency. The XPM was upgraded this year to include a longer drift region (60 mm was increased to 109 mm) for improved sensitivity to impurities We have confirmed electron lifetimes as high as 4 ms in purified LXe in this way (more typically, results are ~1 ms), and have reproduced electron drift velocities available in the literature. In addition, we have recently replaced our cold-finger/liquid-nitrogen (LN) cooling system for the XPM with a refrigerator that cools HFE-7000, a hydroflouroether, into which the XPM is submerged. The HFE may serve as both a coolant and a radiation shield for the prototype detector, and also alleviates safety concerns regarding large volumes of LN at the WIPP underground facility. The new HFE-based system is working well.

Aseries of experiments was performed to test the feasibility of electrostatic ion extraction from xenon. The "probe-test cell" incorporated a movable electrostatic probe, and an instrumented (PMTs, Si barrier detectors) volume for LXe or gaseous Xe containing a pair of HV electrodes. One of the electrodes holds a weak U^{230} source which undergoes two α decays and emits Th^{228} and Ra^{222} ions into the Xe. We have seen that the probe tip, if set to negative potential, collects radioactive ions (thorium and radium α decays confirm presence of the species). The apparatus was used to measure ion mobility in LXe, an important issue as the barium ions will be produced in an electric field, and this work has been published in NIM : http://xxx.lanl.gov/PS_cache/cond-mat/pdf/0503/0503560.pdf . A"cryoprobe" equipped with internal plumbing that functions as a Joule-Thompson expansion cooler using high pressure argon gas, was first designed and tested at SLAC. The probe tip cooled to below the freezing point of xenon, and ions are trapped in xenon ice. By this means, we demonstrated that captured ions may be released by thawing the xenon ice, preventing irreversible attachment to a bare metal or dielectric probe tip. A second approach using a "hot probe" is under study at SLAC. We have seen in the literature how an appropriately chosen metal surface (eg, platinum) can have a work function that favors the release of adsorbed metal atoms (eg barium) in a ionized state when heated to modest, ~500C, temperatures. This work now continues at Stanford, along with a series of alternative ion-capture experiments, in an apparatus designed ultimately to test the laser identification and ion capture simultaneously for the first time.

The SLAC group had coauthored a paper, submitted to Phys.Rev.B, on observations of ionization and scintillation correlation effects in LXe performed by the Stanford campus group (available in the LANL E-print server at http://xxx.lanl.gov/PS_cache/hep-ex/pdf/0303/0303008.pdf

SLAC Activities : EXO200

A substantial effort is now focused on development of the 200 kg prototype for installation at WIPP, "EXO200". The EXO200 TPC detector will incorporate a ~17 cm drift region, a maximum electric field of ~3 kV/cm, and a detection plane consisting of wire grids and/or pads and LAAPDs

The design of the EXO200 apparatus is complete, and many major components are already being fabricated. The custom made modular cleanrooms that will house the experiment at WIPP are already complete and installed in the Stanford HEPL facility, with the large low-radioactivity-copper cryostat installed including its low-radioactivity shielding lead. The refrigeration systems, and xenon handling systems, which were designed by the SLAC team, are nearly complete. In September, the first cooldown of the cryostat to ~175K was successfully tested, and checkout continues. Extensive testing of the entire system at HEPL is planned prior to disassembly of the six cleanroom modules, which will be loaded with the apparatus by that time for shipment to WIPP.

A major effort is underway now to complete construction of the xenon pressure vessel and the TPC electrode structure that it will contain. This effort is co-lead by the SLAC physicist and mechanical engineering team, along with our colleagues at Stanford. Machining of the copper pressure vessel has begun at Stanford. Assembly of the vessel and TPC will be done in a separate cleanroom at HEPL that is presently nearly complete.

A test setup for the numerous (~600) large area amplification photodiodes (LAAPDs) used for 175 nm light collectionin the EXO 200 TPC is now operating at HEPL

The SLAC group has, thanks to assistance from local electrical engineering manpower, designed and started production of the ~200 channels of low noise charge sensitive preamps, and associated digitization, control modules as well as rack-mounting and cooling hardware for EXO200.

A SLAC group lead the effort to produce a complete detector monte carlo, and in addition, event reconstruction software to be used for the prototype. A first pass version is ready now and has been extensively used.

The design of a full scale device incorporating Barium identification will follow pending the results of our R&D and prototyping effort.

10. FY06 Progress in Theoretical Physics by Michael Peskin

The research of the Theoretical Physics Group ranges from the development of fundamental theories such as M-theory, string theory, and higher dimensional theories at very short distances to detailed calculations and tests of theories directly relevant to high-energy physics experiments at SLAC and elsewhere. This section summarizes the current activities of the Theory Group and a few of its important achievements in FY2006.

Physics at the International Linear Collider – The Theory Group is intensively involved in all aspects of physics related to the development of the next-generation linear electron-positron collider (ILC). Much of the work involves understanding how to use the unique capabilities of the linear collider environment, such as beam polarization, highly efficient heavy-quark tagging, and the possibility of backward-scattered photon beams, to test aspects of new physics at very high energies that would otherwise be inaccessible. It includes analyses of linear collider experiments on the most familiar models of the next energy scale in physics, including studies of the measurement of the parameters of the spectrum of supersymmetric particles of possible strong interactions coupling to the Higgs sector and the top quark. It also includes exploration of a wide variety of newly-proposed models, some of which are discussed in later sections. Each phenomenon has a specific experimental realization at the linear collider, and we are making an effort to understand the systematic picture of how these effects can be found and distinguished.

Over the past year, we have made important progress in two aspects of linear collider physics. First, we have understood much more precisely than before how measurements of the masses and cross sections of new particles at the ILC will impact our understanding of the particle physics origin of the dark matter that makes up 80% of the mass in the universe. It has been understood for some time that experiments at the ILC can propose candidates for the origin of the dark matter. The new studies make clear that the ILC can also measure the properties of these particles sufficiently well to provide microscopic predictions of the cosmic density of these particles that can be directly compared to astrophysical observations. The data from the ILC can also be used to determine the cross sections of the dark matter particles that are used in astrophysical detection experiments. In this way, the combination of ILC data with results from dark matter direct detection experiments and from GLAST and other gamma ray observatories can directly measure the distribution of dark matter in the galaxy.

Second, we have understood with much greater clarity how the measurements of cross sections and branching fractions for new particles can resolve potential ambiguities in the determination of the underlying parameters of a model of new physics. These measurements make essential use of the important capabilities of the ILC for polarized beams and full-event reconstruction. This

analysis points to a capability for the ILC that goes far beyond the discovery of new particles to the clarification of physics at a very deep level.

Physics at Bottom Factories – The Theory Group is intensively involved in all aspects of physics related to the physics of *B* factories, and the *BABAR* experimental programs in *B* physics and two-photon collisions. Members of the group have devised new methods for measuring the parameters of CP violation in the Standard Model from analyzing detailed aspects of specific rare *B* decay modes. We have also studied models of CP violation beyond the Standard Model, and the reactions involving 'penguin' diagrams that are expected to probe for these effects most sensitively. In the past year, we have been pleased to see methods developed in our group for the characterization of B meson decays using polarization of final-state vector bosons being used to make high-precision measurements of the fundamental CP-violating phases.

Development of Quantum Chromodynamics – Although there is strong evidence that Quantum Chromodynamics (QCD) is the fundamental theory of the strong interactions, there is much room for improvement in the methods by which QCD is applied to compute predictions for specific processes. Members of the Theory Group have devised improved computational methods for QCD both for high-precision studies and for the extension of QCD calculations to new regimes. These include the development of 'commensurate scale relations' which aid in removing scale and scheme ambiguities from QCD calculations, and the development of renormalization schemes that are analytic in the quark masses. In the past year, these methods have been applied to define gauge-invariant vertex functions for gluons and other non-Abelian gauge bosons that seem to have powerful applications both to QCD and to models of grand unification. Members of the Theory Group have also been pursuing insights into the strong-coupling region of QCD from the gauge theory-gravity duality that has recently been proposed in string theory. We have shown that relatively simple hypotheses applied to five-dimension theories of gravity lead to successful predictions for the mass spectrum of mesons and baryons in the real strong interactions. These theories also lead to successful predictions for the form factors of mesons and for the prediction of exclusive large-momentum-transfer strong interaction processes.

Computational Perturbative Quantum Chromodynamics – The most challenging aspect of improving methods for QCD is that of devising methods for high-order Feynman diagram calculations. Members of the Theory Group have been devising methods to simplify the computation of diagrams involving essentially massless quarks and leptons participating in high-energy collisions. In terms of technical difficulties of QCD computations, the frontier now lies in the calculation of two-loop or NNLO corrections, and in one-loop (NLO) calculations with a large number of quarks and gluons in the final state. These corrections are essential to interpret the Tevatron and the eventual Large Hadron Collider (LHC) data to the few-percent level, and to understand the backgrounds to new physics signals at the LHC. Over the past few years, members of the group have taken a leading role in the community in developing methods for the computation of QCD processes at NNLO. More recently, the work of our group has mainly been devoted to computing one-loop diagrams with many final-state particles, making use of new computational methods based on string theory in twistor space. In the past year, members of our group have used these methods to compute all one-loop QCD amplitudes contributing to quark and gluon scattering processes involving up to 5 particles in the final state. These methods actually compute infinite families of one-loop diagrams, so in certain specific polarization states the answers are now known for arbitrarily many final-state particles. These methods seem to be extendable to reactions involving the production of massive particles, including W, Z, and the top quark. At the same time, these methods give new insight into the computation of multiloop

diagrams. In the context of N=4 supersymmetric Yang-Mills theory, a highly symmetric model that plays the role here of a simplified model of QCD, members of our group have been able to compute certain four-loop (NNNNLO) amplitudes. The generalization of these calculations to QCD is now being studied.

Superstring Theory and M-Theory – Members of the Theory Group have been involved in studies of superstring theory and its possible relevance to elementary particle physics. Superstring theory may give a context for the solution of the cosmological constant problem, the question of why the observed cosmological constant is tens of orders of magnitude smaller than straightforward estimates in quantum field theory. Supersymmetry forces the cosmological constant to be zero, but only if it is an exact symmetry of Nature, not one that is spontaneously broken. It is a very important question whether there is an intermediate solution in which supersymmetry is broken but in such a way that the theory still controls the magnitude of the cosmological constant. A new direction of approach to this problem is related to the fact that the observed universe seems to contain a small positive cosmological constant. The first solution of string theory with a positive cosmological constant was constructed by members of our group in 2003. Since then, we have been developing more powerful methods for string model construction, and these have revealed a wealth of new solutions to string theory with positive cosmological constant. In the past year, members of our group have made progress in this program on several fronts. First, we have found new geometrical methods that lead to new families of string theory solutions. Second, we have been able to demonstrate that certain solutions of string theory which are known to be unstable resolve themselves into new solutions with positive cosmological constant. Third, we have understood better the possibility of transitions between string solutions and computed rates for the decay of one solution of a family into another. This latter calculation has interesting similarities to the analysis of black hole solutions in string theory.

Other studies in our group have clarified the structure of black hole and other gravitational solutions of string theory. Members of our group have analyzed the effect of stringy corrections to the equations of Einstein's gravity in smoothing the internal singular structure of black holes. These corrections turn out to be important for precision counting of black hole states and the microscopic understanding of black hole entropy.

Models of New Particles associated with Electroweak Symmetry Breaking – A central question in particle physics for many years has been the nature of the Higgs bosons or other particles that cause the spontaneous breaking of electroweak symmetry. As we look forward now to the start of physics at the LHC, it seems particularly important to put all of the options for the nature of the Higgs sector on the table. In the past year, members of the Theory Group have opened several new directions in this study. We have proposed models with multiple Higgs bosons that, in different variants, leads to theories in which Higgs bosons are especially heavy and to theories in which Higgs bosons have new types of associated partners. In the context of supersymmetric models with grand unification, we have proposed models in which the Higgs boson is composite. In these models, the multiple possible bound states provide the various levels of spontaneous symmetry breaking that grand unification requires. We have examined models in which the supersymmetric partners of the Higgs bosons provide the cosmic dark matter, and we have studied the implications of these models both for dark matter searches and for the observation of new particles at the LHC.

New Theoretical Methods – Other new theoretical methods being developed by the Theory Group include: applications of object-oriented programming techniques to simulation problems in

physics; new methods for solving lattice Hamiltonian systems; light-cone Fock state methods in non-perturbative QCD and non-perturbative studies of QCD in light cone quantization.

Iterative renormalization-group-like methods for diagonalizing the Hamiltonians of many-body systems have been applied to 2-dimensional antiferromagnets. In the past year, we have shown that these methods can produce very accurate values of the ground state energy of these systems in strong-coupling situations, and that these methods can be used to analyze the complex phase diagrams of these materials.

11. FY06 Progress in the Klystron Department by Chris Pearson

The SLAC Klystron and Microwave Department is primarily involved in the development and manufacturing of klystrons and other high power microwave components for use on present and future HEP and BES programs. The department is also responsible for the operation and maintenance of these klystrons and supporting RF systems.

Klystron Manufacturing

During FY06, the department's manufacturing group produced ten 5045 klystrons for the SLAC Linac, four of the 1.2 MW CW klystrons used in the SLAC B-factory storage rings, and one XL4 klystron for the LCLS injector. The group also produced a variety of R&D RF and vacuum electronic devices (some of which are described in paragraphs below), including a new RF Gun for LCLS, a new RF window for ILC L-band accelerator structure and component testing, and various components used for Advanced Accelerator RF Breakdown Research.

The 5045 klystrons are 65 MW peak pulsed power S-band klystrons which are the RF power source for the SLAC 2-mile accelerator (These klystrons are also the RF source for the SPEAR3 injector). Although this klystron (developed at SLAC in the 1980's) has been in production for many years, the lifetime and reliability of this klystron continues to improve. Current mean time between failures is 65,000 hours. There are now more than 25 gallery klystrons with over 100,000 operating hours. The department also manufactures the sub-booster klystrons providing drive power to the 242 5045 gallery klystrons.

The B-factory storage ring klystrons (see photo) are also manufactured by the SLAC Klystron Department. The PEP-II project requires 14 (16 in '07) storage ring klystrons. These high power CW klystrons, originally purchased from commercial sources, are now being replaced by more reliable higher power (1.2 MW) klystrons designed and manufactured specifically for this application by the Klystron Department. Theses klystrons are the worlds highest power CW klystrons. Currently, 7 of these klystrons are operating in PEP-II allowing higher luminosities to be achieved. This klystron will also be used to supply RF power for SSRL Spear-3. By 2007, a total of 12 of the SLAC-built tubes will be supplying RF power in support of SPEAR3 and PEP-II.

The Klystron Department also manufactures the XL-4, a 60 MW X-band klystron. This klystron, originally designed as a power source for the extensive NLC high gradient accelerator studies and the NLCTA, is now in service providing power for various R&D programs including the Accelerator Development High Gradient Program currently running experiments at ASTA and

End Station B. This high power X-band klystron will also be used as an RF power source for the LCLS X-band Compression Linearizer.

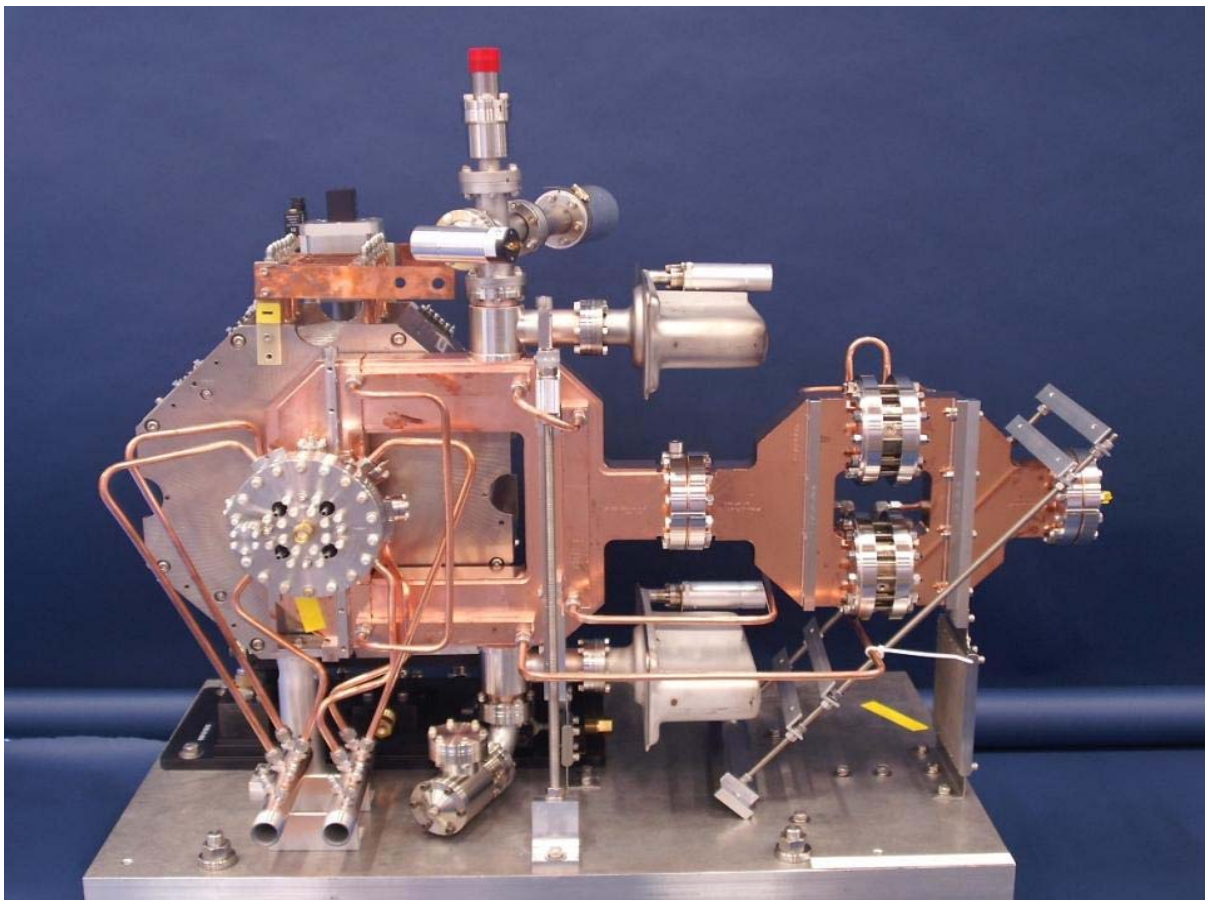

The LCLS RF Gun mechanical design and fabrication is an example of a high power RF vacuum electronic component that benefits from the Klystron Department's engineering and fabrication expertise. With the thermo-mechanical analysis and mechanical design of the RF gun completed in FY05, attention turned to fabrication. Parts for two complete gun assemblies were manufactured with the second set serving as a spare during the fabrication phase. Since the fabrication of the first gun was successful, the second set of parts is being finished as a complete second gun assembly. Cold test of the first gun RF structure was very successful with the likely gun operating temperature falling within 2°C of the design operation temperature without use of deformable tuners in the coupling cell. Cathode tuning tests and cell field balance vs. mode spacing agreed very well with RF simulations. Final mechanical assembly of the gun and solenoid assembly was done in the MFD Vacuum Group building 31 clean room due to their superior facilities for handling large clean assemblies like the RF gun. The completed gun assembly (see photo) was moved to the Klystron Department's Test Lab ASTA bunker where it will undergo vacuum bake out and start high power RF testing prior to the end of FY06.

Klystron R&D

Initial work on an X-band Sheet Beam Klystron for NLC and the successful test of the 95 GHz Sheet Beam Klystron at the end of FY2005 (Photo) have led to several development efforts for new sheet beam klystron designs. During FY2006 engineers in the Klystron Department have been looking at various Sheet-Beam Klystron (SBK) technologies for applications across a range of frequencies from L-band to W-band. Due to the three-dimensional geometries involved, emphasis has been placed on the application and development of analysis tools for these SBK devices. Specifically, 3D particle tracking and electromagnetic codes have been in development that can operate on single and multi-CPU platforms under Windows and LINUX operating systems. For the SBK geometry, the most challenging aspect is to correctly design the focusing and transport optics (an image from an electron gun simulation is shown at left). It is believed by the Klystron engineers that the RF circuit is simple to design and control. This is especially true for the L-band SBK under investigation as a possible plug-compatible device for an International Linear Collider (ILC) system. The LSBK would provide a smaller, lighter, and less-expensive, alternative to the multiple beam klystrons that were originally proposed for the ILC. The image in the figure below shows a comparison of size and weight of the two designs. The design and modeling of the LSBK is currently being funded by internal SLAC funds but a decision by the ILC Global Committee is expected that will provide ILC funds to support the fabrication and testing of the new RF source.

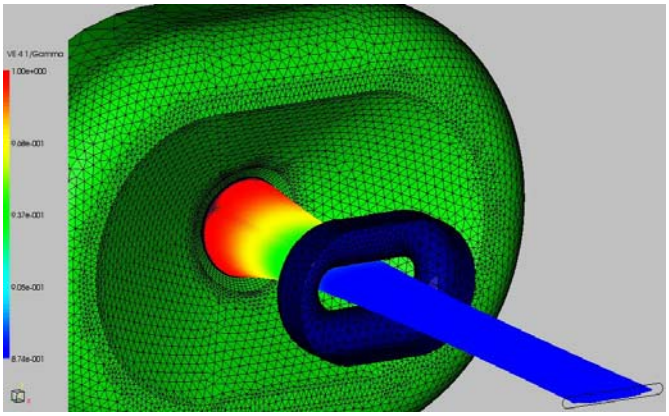

ILC Multiple Beam Klystron vs. Sheet Beam Klystron

MBK's:

~5000 lbs.
91" - 98" long
35"- 45" wide

Solenoid Power
4kW - 8kW

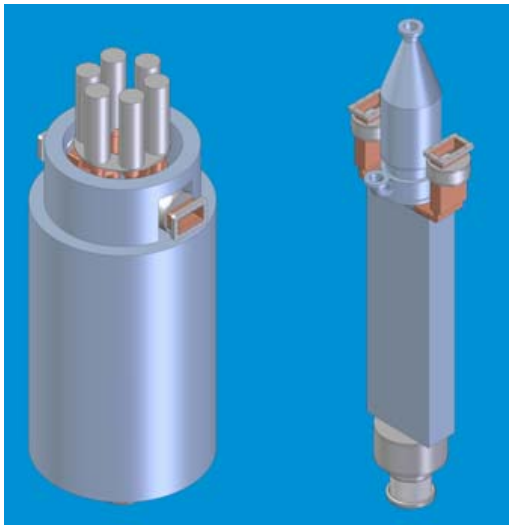

L-band SBK:

921 lbs.
106" long
28" wide

No Solenoid
Power Required!

Compton X-Ray Experiment

This year (May) concluded efforts with the Compton experiment in ASTA in favor of new high power microwave experiments.

During the time period from October to May a new interaction chamber was completed, configured and installed into the beamline. Besides more flexibility, this chamber permitted 180 degree collisions between a high power laser beam and an electron beam. The reflecting mirror in the beam path had a 1 cm hole which permitted the electron beam to pass unobstructed into a spectrometer while allowing a laser beam to focus at an interaction point. Temporal alignment between the laser and electron beams to within a few picoseconds was accomplished using a 6 GHz real-time scope.

During the last days of operation it was discovered that the remote mirror mount was faulty causing an excessive bremstrahlung X-ray background level. This had the effect of masking the desired X-rays. A final run using a thin Ce:YAG target showed some evidence for X-ray production but, unfortunately, results were not conclusive.

Klystron Microwave Engineering and Maintenance

The Klystron Microwave Engineering and Maintenance group assists the laboratory with all aspects of RF needs, from low noise, low power control systems to the operation of the megawatt CW PEP klystrons. The group's primary focus is the maintenance and operation of the low level and high power RF systems in the SLAC Linac and PEP-II storage rings. The group also contributes RF engineering assistance to many other smaller projects throughout SLAC, including Spear, End Station Experiments, and ILC.

During FY06 the group has managed the construction, testing, processing, and installation of two additional high powered RF cavities for the new PEP RF stations. These RF stations will supply additional power allowing greater luminosities to be achieved in the SLAC B-factory, and are scheduled to be operational for the next experimental run starting in January '07. Additional work concerning PEP includes the design and implementation of beam diagnostic equipment using MatLab for high level applications.

A significant portion of the group's effort this year has been directed at the design and construction of the LCLS low level RF system. This system requires timing stability of better than 100 femtoseconds. In addition, high Q, Terawatt laser systems need to be synchronized to the accelerator RF to this 100 fs level. The group's expertise in this type of RF system is critical to the success of the project.

12. FY06 SCIENCE AND TECHNOLOGY PROGRESS IN THE RADIATION PROTECTION DEPARTMENT by Sayed Rokni

The Radiation Protection Department (RPD) performs applied research in areas related to radiation safety and shielding analyses. Results of these research efforts are published in refereed journals, SLAC internal technical notes and are presented at various national and international workshops and conferences. In FY06, RPD's research was focused on production, attenuation and interactions of radiation with matter and on the development, maintenance and benchmarking of radiation production, interaction and transport computer codes.

Measurement of neutron energy spectra; benchmarking with different Monte Carlo radiation transport codes

Measurements of high-energy neutron spectra are an important research goal for the RPD since neutrons dominate the requirements for lateral shielding at high-energy accelerator facilities. Analysis of experimental data obtained in 2004 at the CERN-EU High Energy Reference Field (CERF) facility was completed last year. In that experiment, a 120 GeV/c mixed hadron beam interacted with a copper target creating a stray radiation field which was attenuated by a lateral shield of either 80 or 160 cm thick concrete or 40 cm thick iron. High-energy neutron spectra were measured with a NE213 organic liquid scintillator located outside of the shielding. The measurement locations covered an angular range with respect to the beam axis between 13 and 110 degrees. Energy spectra in the energy range from 32 to 380 MeV were obtained by an unfolding method using a newly upgraded response matrix.

Energy spectra of neutrons were then calculated with the Monte Carlo radiation generation and transport codes FLUKA, MARS and PHITS for different measurement locations for benchmarking purposes. For many locations, the measured neutron fluence was within the results obtained from the different codes within the experimental uncertainties. Comparing the predictions of the three codes to each other, it was observed that FLUKA and PHITS predicted similar fluences, while the energy spectra calculated with MARS were slightly lower. In order to investigate differences, simulations were also performed for a simplified cylindrical geometry. Results demonstrated that the differences partially can be explained by differences in the high-

energy hadron production in the copper target. Results of these studies were documented and presented at two international workshops.

Proposed measurements of induced radioactivity and residual dose rates at the End Station A (ESA)

The first FLUKA benchmark measurements of induced radioactivity at electron accelerators were performed at SLAC in the year 2000 with samples of different materials irradiated laterally to a copper target in the Beam Dump East facility. Results were compared to predictions from detailed FLUKA simulations showing that some of the measured special activities were underestimated by the calculations by factors of 2.5. Possible reasons for the discrepancies were investigated but a conclusive answer could not be given due to the large uncertainties, both with regards to the measurements and to the simulations. In FY06, staff from the Radiation Protection groups at CERN and SLAC prepared and submitted a new proposal for an experiment at ESA to avoid many of these uncertainties. Additionally, by extending the benchmark to residual dose rates, the propose experiment allows for a far more thorough check of the FLUKA predictions for activation at electron accelerators. This proposal also takes into account the important increase in predictivity brought about in this field by recent improvements in the code.

Development of the FLUKA Computer Code

RPD staff contributed to a major new revision of the FLUKA Monte Carlo code which has been released in 2006 (version 2006.3). In addition to many new features and improvements, both in the user interface (input by name, use of parentheses) and especially in the physics (in particular better prediction capability concerning activation), photoproduction of muon pairs - already tested in previous versions with many approximations - is now fully implemented. The User Manual, available as Report SLAC-R-773, has been updated.

13. Progress in SSRL Operations by Piero Pianetta

FY2006 User Experimental Run

In the FY2006 user run, the facility proved to be exceptionally reliable, providing very stable beam for a very high fraction (96.2%) of the scheduled time. This is an exceptional achievement for a new storage ring. The user run commenced on November 28, 2005 and continued through August 7, 2006, and the SPEAR3 storage ring operated at 3 GeV/100 mA and provided 60+ hour life times. (The average uptime over the past five years was 96%.) During the FY2006 run, scientists on 345 different proposals received beam time in a total of 1,002 experimental starts involving approximately 1,700 users, with approximately 900 users on-site or remote accessing beam line equipment. Approximately 66% of the users came from universities and other laboratories in the United States, 15% from DOE and US government laboratories, 5% from US industry, and 14% from international institutions.

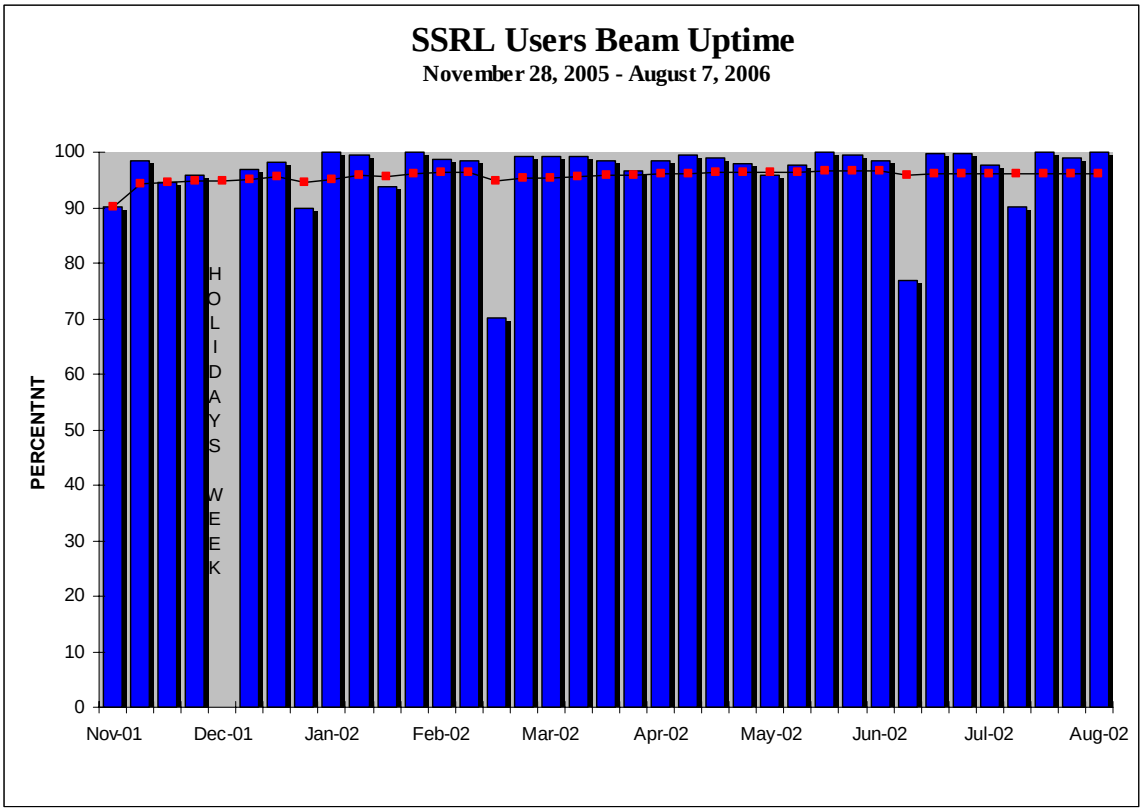

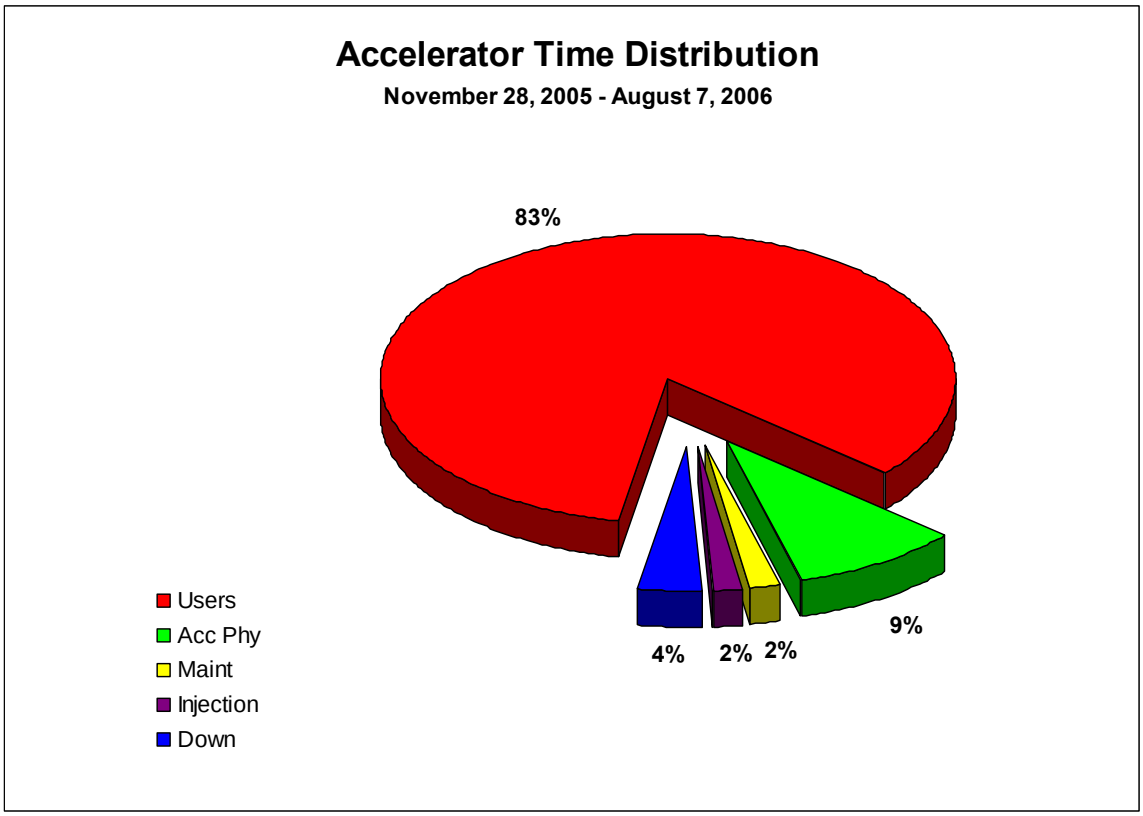

Distribution of Proposals Receiving Beam:

Materials Science	14%
Physics	5%
Chemistry	16%
Polymers	2%
Medical Applications	5%
Biology/Life Sciences	45%
Earth Sciences	3%
Environmental Sciences	5%
Optics	1%
Engineering	3%
Other	1%

- **SPEAR3 Accelerator Improvements**

The accelerator improvements for SPEAR3 are focused in four areas: 1) characterizing and improving accelerator performance and reliability at 100 mA to maximize beam quality for users; 2) developing and implementing a new lattice optics configuration that accommodates a magnetic chicane having two small vertical beam size waists (the double-waist chicane optics, or DWC optics) in the east long straight section; 3) characterizing and optimizing accelerator operation at 500 mA; and 4) preparing for the implementation of top-off injection with beam line stoppers open.

Injector – Work continued in FY2006 to improve the reliability and operation of the injector at 3 GeV. The injection timing system was modified to equalize booster ramping efficiency for all bucket timings. Work continued to characterize and stabilize gun and linac operation. A feedback system was implemented to stabilize the booster White Circuit. Booster performance was assessed and plans for its realignment were made. A study of the stability of all injector power supply systems was initiated. Additional improvements include rebuilding the BTS injection line (to remove several vacuum windows), upgrading transport line beam position and intensity monitors, enhancing the stability and monitoring of powered devices, completing a pulsed signal monitoring system, implementing an EPICS control system access to injector component control and readback variables, and installing a second klystron for the gun/linac system. The design of simpler and more robust booster kicker pulsers has begun and plans for developing a laser-heated-cathode rf gun are in progress. The Accelerator Physics group is studying booster beam capture efficiency and has proposed a minor lattice modification that could improve performance. Studies of other booster improvements, including the powering of unused sextupole magnets and the possible addition of a subharmonic rf cavity, are under way. The injector improvement project will continue in FY2007 and beyond.

Turn-Turn Beam Position Monitors (BPMs) – Commissioning and development of the user software interface for the turn-turn BPM system is continuing in FY2006. The test tone calibration system will be commissioned and the true performance of the processors is being quantified. The turn-turn BPMs will then be integrated into the orbit feedback system.

Synchrotron Light Monitor (SLM) – The SLM beam line received first light in January 2006. The optical bench components were commissioned and the beam line component alignment was refined. The first measurement of beam bunch length was performed during the user run and low alpha experiments were performed in which the bunch length was shorted to 6.5 ps with 100 mA stored current in SPEAR. The upgrade and realignment of the BL2 pinhole camera system was completed in early spring of 2006.

Beam Scrapers – The new horizontal and vertical beam scrapers were commissioned and used to characterize beam lifetime, injection apertures, and minimum apertures for future insertion devices. The scrapers will continue to be a valuable diagnostic for beam size, lifetime and aperture studies.

LION Development – Commissioning of the Long Ion Chamber (LION) system continued during the FY2006 user run. Tests of the system with high injected beam current were carried out in early spring 2006. The LION system must be connected to the Beam Containment System before the injected beam current limit can be raised to enable faster 500-mA fill times.

High-Current SPEAR3 Tests – SSRL received authorization from the DOE Site Office to conduct SPEAR3 operation with currents up to 500 mA, above the official safety envelope value of 100 mA allowing routine running of SPEAR3 with beam lines closed for accelerator studies. A successful test of the Double Waist Chicane lattice (see below) at 500 mA was conducted in February 2006 with no observed problems.

Orbit Control – The first phase of the fast orbit feedback system, using only the 54 Bergoz averaged-orbit BPMs, was completed. A test of the system demonstrated successful feedback operation with a bandwidth approaching 100 Hz. Further work was done to optimize the SVD-derived inverse response matrix and digital filters as well as to maximize the frequency response

of the orbit corrector power supplies. Work continued in order to provide an operator interface and data acquisition applications for the new fast orbit feedback system.

The orbit monitor processing system has a temperature dependence that has been demonstrated to cause orbit instability when the feedback system is active. A project to build temperature-controlled rooms and install finer temperature regulation in the processor equipment racks was completed in time for testing before the end of the run. Initial tests showed that the cooling system reduced the processor temperature variation from several degrees Celsius to less than a degree, thus decreasing the processor temperature-related orbit instability. Further tests during the 2007 run will quantify the degree of improvement.

Hydrostatic level sensors (HLS) were installed a few strategic areas in the SPEAR3 tunnel to monitor the vertical motion of tunnel floor and some beam line components. If this system proves to be useful for detecting component motion, more sensors will be added in the future and their signals will be used in the orbit feedback system.

Double Waist Chicane (DWC) Lattice – The DWC optics, temporarily installed without chicane magnets during the FY2005 shutdown, was tested successfully for the first time in December 2005. While the lifetime was a few percent less than that for the normal lattice, this was anticipated in the optics studies and is acceptable. This lattice was characterized and optimized so that it will be used with the new BL12 undulator and beam line which was installed during the 2006 summer shutdown. It has already been demonstrated to work without problems at 500 mA and with the "dispersion leak" optics variation that reduces the emittance from 18 nm-rad to 12 nm-rad. The design and fabrication of vacuum chamber and chicane magnets needed for the full DWC implementation are being completed during the 2006 shutdown. Most of the components have been installed, together with the BL12 in-vacuum undulator. The installation of the beam line that utilize the downstream chicane straight section is underway.

Top-Off Injection – The design of the system needed for top-off injection with beam line stoppers open was begun in FY2006. This injection mode, with minimal interruption to users, will enable more frequent beam injection to limit beam current variation, minimizing the variation of thermal power on beam line optical components and improving beam stability for users. Work has begun to improve the injector systems to accomplish this injection mode (see above). An extensive study of beam loss modes was initiated to determine what radiation safety components will be required to inject beam into SPEAR3 with open beam line radiation stoppers. Significant changes to the Personnel Protection System, including the Septum Interlock, will be needed to implement the top-off system. This work will enable the first phase of top-off injection - a mode that will maintain beam current constancy in SPEAR3 to a few percent. A second phase of top-off development that would enable maintaining SPEAR3 beam current constancy to less than 1% will most likely require large-scale improvements to the electron gun and possibly to the booster. These changes will not commence until FY2007.

SPEAR3 Performance and Lattice Upgrades – The accelerator physics and engineering groups continued to study and tune the SPEAR3 accelerator to maximize its performance and stability. This work includes investigating the sources of beam instability (power supplies, rf system component vibration and temperature-related motion, etc) and ongoing efforts to characterize beam dynamical behavior as a function of lattice and insertion device parameters. With regards to the latter, a detailed study of the deleterious effects of the new BL13 EPU on beam properties, and possible cures, is in progress in collaboration with physicists at other light sources. The results of this study will be incorporated into the design of the BL13 EPU system.

An investigatory study of the possibility of circulating short bunch electron bunches (<~1 ps) in the SPEAR3 storage ring was initiated. A new isochronous lattice configuration was developed that would preserve the short bunch length, and provide the option of circulating the bunches for some small number of revolutions (<1000), as opposed to storing the beam, will be analyzed.

Gun Test Facility – The GTF continued to support the LCLS injector group through FY2006. Experiments performed included novel *in situ* methods to improve the cathode performance,

experiments to eliminate the correlated energy spread produced by the gun, and beam-based screen resolution measurements. New diagnostics will continue to be developed including the electro-optic bunch length measurement as well as testing new diagnostics such as digital cameras and bunch charge monitors. The laser will continue to be used to test transverse pulse shaping techniques, the LCLS streak camera and methods to improve the laser pointing stability.

Additional ultrafast electron diffraction experiments were also planned. Improved detectors were tested and the pulse length reduced to improve the temporal resolution. The useful operating range of the gun for electron diffraction has also been explored.

- **Beam Line and Facilities Improvements**

BL1, 2, 3, 8 (bend beam lines) – Upgrade activities on bend magnet beam lines 1, 2, and 8 were limited to those essential to keep the beam lines operating with higher SPEAR3 current. In particular, during the 2006 shutdown, the BL2 beam position monitor was upgraded for improved stability and the BL8 beam position monitor shielding was upgraded for 500 mA operations. BL3 will remain closed.

BL4 – The BL4 upgrade continued with the fabrication of components and is scheduled for installation during FY2007. The BL4 upgrade is partially funded by DOE BER.

BL5 – The BL5-1 M_3 refocusing mirror system has been installed and commissioned as has the shielding for 500 mA operation. No other significant upgrades are scheduled.

BL7 – The 500-mA upgrade installation was completed with the temporary BL7-2 LN monochromator and the beam line was commissioned. Assembly of the BL7-2 sagittal focusing monochromator will be completed and the monochromator will be installed and commissioned at the beginning of the FY2007 run.. BL7 and BL 7-3 upgrades are largely funded by NIH NCRR.

BL10 – While no significant upgrades are planned, some cooling enhancements of zero order beam masks downstream of the BL10-1 monochromator have been scheduled.

New beam lines under development:

BL12 – The in-vacuum ID was delivered and installed in the ring as were the remaining dipole magnets and associated vacuum chamber required to produce the SPEAR3 orbit chicane. The hutches are being erected. The remaining optical components will installed during October 2006. It is anticipated that the beam line will start commissioning by November 2006. The computing infrastructure required to support this beam line is being installed. A large-area CCD detector was procured with an October 2006 delivery date. This beam line is funded by the California Institute of Technology through a gift from the Gordon and Betty Moore Foundation.

BL13 – The ID fabrication will continue. The beam line front end design will be completed and fabrication will commence. The M_0 mirror system will be designed and the optic ordered. Design of the in-alcove beam transport system will start. Rather than order a new monochromator for BL13, it has been decided to relocate the BL5-1/5-2 spherical grating monochromator, associated slits, and refocusing optics to BL13. This relocation is planned for the summer 2007 shutdown. During the remainder of FY2006, the BL5-1/5-2 gratings and grating cooling system will be analyzed for applicability to BL13. If new gratings are required, the gratings will be ordered in FY2006.

SSRL Instrumentation and Control Software

XAS Instrument Control System Software and Computing Developments **– T**he new ICS software has been installed on BL7-3. This system will run on the Microsoft Windows operation system and will form the basis for the upgrade of other beam lines as the new standard SSRL beam line control system. The system will be based on VXI instrumentation, controlled using a National Instruments USB2 interface.

It is anticipated that the new ICS software running on the Microsoft Windows XP operating system controlling CAMAC hardware using the existing Grand Interconnect hardware will be installed on a least one experimental station.

Development of the SSRL dedicated beam line network will continue. The initial design, consisting of several VLANs has been implemented initially on BL7. Experience gained during the operation of the new beam will fine tune the design which will be extended to all beam lines in the coming years.

Legacy OpenVMS based programs will still be available, but will be run from a server style computer, displaying on the workstation at the beam line. Projects will be initiated to either port or replace such applications to an operating system independent model.

Computers and Networking – The SSRL network has been extended to Building 130. Deployment of SAN storage technology is ongoing. Further planning for the fiber-optic network backbone upgrade to 10 Gbit/s data rate will be performed and the availability and cost will be analyzed. The beam line network cabling and infrastructure system will be reorganized to meet cable plant improvement requirements. Some central windows servers will be upgraded and a Windows 2003 Server will be deployed. Central services will be available on Itanium-based servers. In collaboration with the SLAC networking group, a possible upgrade of the wireless network infrastructure will be planned. New web-based SSRL user administration applications will be developed and deployed to the public.

Facilities and Infrastructure – Following the recommendations of the final safety review for the LN distribution system, an oxygen deficiency monitor network is being added and integrated into the Building 120 fire alarm upgrade project. Implementation of insulated piping to the LN-cooled monochromators will then begin. The funding for the SLAC SLI SORIP infrastructure project has been received The air handler supplying cool air for the SPEAR3 power supply building (Building 118) does not have the cooling capacity necessary to support SPEAR3's planned growth. It will be replaced with a higher capacity unit and additional ductwork will be installed.

- **Facility Research and Development**

Inelastic Scattering and Advanced Spectroscopy Facility for SPEAR3 – An Inelastic X-ray Scattering and Advanced Spectroscopy Facility is being developed that will eventually be located at a new SPEAR3 insertion device beam line. Various techniques complementary to the current spectroscopy programs at SSRL will be carried out at this facility. They include X-ray Raman scattering (XRS), resonant inelastic X-ray scattering (RIXS), selective X-ray absorption (S-XAS) and X-ray emission spectroscopy (XES). XRS will widen the range of absorption spectroscopy on low Z samples, traditionally performed in the soft X-ray range, to systems and sample conditions where the penetration of a hard X-ray probe is essential. XRS can thus provide unique new insight for, *e.g.*, studies of carbonaceous systems related to fossil fuels and hydrogen storage under *in situ* conditions, water and aqueous systems in ambient and extreme conditions, high pressure phases of gases and the formation of methane hydrates. RIXS spectroscopy is a novel technique to study in detail the local electronic structure and spin states of, *e.g.*, 3d transition metal compounds with hard X-rays. As compared to conventional K-edge spectroscopy, it can better isolate lowest unoccupied molecular orbital (LUMO) resonances and has less lifetime broadening along the energy transfer axis. Furthermore it provides L-edge/M-edge like information. S-XAS, such as site-selective EXAFS, combines the chemical sensitivity of XES with EXAFS to provide more detailed structural information in mixed valence systems. S-XAS can also be used to extend the *k*-range of EXAFS beyond an absorption edge that otherwise would limit the data collection, hence yielding more accurate determination of neighbor distances. XES contains chemical and structural information complementary to XANES. All of these techniques are valuable in the study of a wide range of systems including man-made and biological catalysts as well as correlated systems.

Internal DOE-BES funding was allocated for instrumentation development in FY2005. Additional funding was obtained through non-DOE grant awards. First, as part of the SSRL Structural Molecular Biology program proposal to NIH-NCRR and DOE-BER (described in the KP11 FTP) funding was awarded to: a) make the unit compatible to perform emission scans as required for XES and RIXS and b) purchase analyzer crystals for the various proposed applications related to biological 3d transition metal systems. Second, in collaboration with Prof. Anders Nilsson (PI), an NSF proposal (NSF CHE-0518637 1096374-2-QANAB) focusing on research on water in ambient and extreme conditions was submitted and funded. Funds were used to upgrade the XRS spectrometer with parts for a second multicrystal component which will double the efficiency to a total of 14 analyzers.

Three Si(553) analyzers were purchased for work on Cu Kβ XES and the upgrade of the spectrometer for XES in addition to XRS capabilities was undertaken. This required the purchase and integration of two vertical stages for simultaneous scanning of goniometer and detector in order to obtain X-ray emission spectra. In addition, a stand-alone alignment unit based on a Newport table was built on which the complete XES setup is placed. This unit can be attached to the BL6-2 hutch table, allowing for a fast turn around with other users at BL6-2. SSRL thus has developed and implemented XES (resonant and nonresonant) as well as XRS capabilities at BL6-2**.** In addition to the XRS work, XES on Mn and Cu Kβ lines can currently be performed. The potential of the technique was demonstrated with the observation of a clear spectral shift for compounds with H_2O versus OH^- ligands. Commissioning work on the new XES spectrometer was also performed at APS where, in addition, experiments on Zn and Mn proteins were carried out. Multiple beam-time proposals for SSRL-based XRS and XES work were submitted in November. Finally, the process of submitting a science-based proposal to the DOE for an undulator-based facility was initiated. Several potential users from groups are actively engaged in contributing to the scientific case for this proposal. Plans for development of dispersive optics for pump-probe type XRS, XES and RIXS experiments will be initiated as will implementation of *in situ* and high pressure instrumentation for XRS studies. The development of the science-based funding proposal to DOE for an undulator-based facility will be completed and the proposal will be submitted by the end of FY2006.

Molecular Environmental and Interface Science – Molecular Environmental and Interface Science (MEIS) research at SSRL focuses on the fundamental interfacial, molecular- and nanoscale processes that control contaminant and nutrient cycling in the biosphere with the goals of elucidating local and global elemental cycles and anthropogenic influences on the environment. Knowledge of these processes is required to develop contaminant remediation technologies and environment-friendly industrial processes. Mass and energy flow through surfaces and reactant transformations, often driven by solar inputs, occurring on nanoparticles, and mediated by bacteria, are major research themes in this field, and offer discovery opportunities for novel remediation technologies and energy capture, conversion, and storage materials/processes. Key areas of investigation at SSRL include: (a) structural chemistry of water and dissolved solutes, (b) structural chemistry and reactivity of environmental nanomaterials (biominerals, oxide and sulfide minerals, biofilms, and organic materials), (c) reactions at environmental interfaces, including sorption, precipitation and dissolution processes that affect the bioavailability of heavy metals and other contaminants, and (d) microbial transformations of metals and anions. SSRL-based MEIS research utilizes synchrotron-based X-ray absorption spectroscopy (XAS), wide-angle X-ray scattering (WAXS), small-angle X-ray scattering (SAXS), X-ray standing wave (XSW) spectroscopy, and photoemission spectroscopy (PES). These techniques provide unique capabilities to probe structure/composition/function relationships in complex environmental systems.

The Brown Group has continued studies at SSRL in the following areas (1) abiotic and biotic oxidation pathways of pyrite (FeS_2) and cinnabar (HgS) surfaces; (2) formation of ternary surface complexes of dicarboxylic acids and metal ions on metal oxide surfaces; (3) studies of the reactivity of nanoparticles of hematite and cinnabar to heavy metal contaminant ions; (3) interactions of metal ions with biofilm- and organic polymer-coated metal oxide surfaces under *in*

situ conditions; (4) XAFS spectroscopy studies of heavy metal contaminated soils and mine wastes, including mercury speciation in mine wastes from the California Coast Range, zinc and arsenic speciation in soils from the Carnoules region of southern France, and uranium speciation in soils and sediments from Chihuahua, Mexico; and (5) XAFS, micro-XAFS, and micro-XRD studies of uranium in the Hanford Vadose Zone.

In the area of environmental nanomaterials (Bargar), research focused on synthesizing and characterizing bacteriogenic Mn oxides having different sizes and properties. To support a SSRL-based post doc for this research, a 5-year interdisciplinary proposal was submitted to the NSF-CRC program (Chemistry Division), in collaboration with three other institutions (UC Berkeley, Princeton, and Oregon Health and Sciences University). Research will be initiated to study structure/reactivity relationships of bacteriogenic nanoparticulate UO_2 (post doc supported by DOE-BER EMSP) as part of a collaborative multi-disciplinary investigation of the fundamental chemical factors controlling the long-term release of uranium at remediated field sites. A two-day user training workshop entitled, "Synchrotron X-ray Scattering Techniques in Materials and Environmental Sciences: Theory and Application" was held in May 2006.

The instrument development goals achieved in FY2006 were to integrate the X-Y-Z scanning stage and detectors for rapid XRF imaging measurements. User commissioning for the μ-XAS and μ-XRF systems will be initiated in winter/spring 2006 and completed during June/July 2006. The procurement for an area X-ray detector for μ-XRD measurements has been initiated.

Strongly Correlated Materials – The program of angle-resolved photoemission spectroscopy (ARPES) study of strongly correlated electronic materials continues to be very active and productive in its two main tasks: scientific research and advanced instrumentation development and operation in support of the research. The goal is get critical information about the strongly correlated materials that cannot be obtained by any other means.

During this period, the instrumentation development takes two forms: i) Develop and design a new beam line that will bring the ARPES capability to a new level. A scientific case has been made for a new beam line. ii) Upgrade current experimental end-station to have better sample temperature control, and photoelectron detection efficiency. Instrumentation development has been very important to the success of the program, and significant progress has been made on both fronts during the period. We will have a new experimental chamber, an improved low temperature sample manipulator, and an improved spectrometer/detector. These improvements will also lower the cost of the proposed future upgrades of the beam line. These instrumentation innovation efforts have benefited not only the research program described below, but also other user programs at SSRL and ALS.

Research wise, the primarily focus is the many-body interactions that are important to the mechanism for high-temperature superconductivity; however, we have also extended the work to other correlated oxides.

Work has been performed to systematically investigate the evolution of Fermi surface and quasiparticle dynamics through a topological transition in correlated oxide $Sr_{2-x}La_xRuO_4$. In collaboration with a group at University of St. Andrews, we have performed a joint study which combines de Haas-van Alphen (dHvA) and ARPES to track the carrier doping evolution of the correlated electron system as the material is doped through a critical point in the band structure. We investigated the relationship of proximity to this critical point and an evolution from Fermi liquid to non Fermi liquid behavior. The significantly improved momentum resolution enables this investigation.

We uncovered evidence for small lattice polaron formation by looking at the Frank-Condon type of broadening in $Ca_2CuO_2Cl_2$ and $Sr_2CuO_2Cl_2$. Small lattice polaron formation and its interplay with magnetic interactions in undoped and underdoped materials have been theoretically

suggested for a long time, direct spectroscopic evidence for this behavior does not exist yet. By performing a temperature dependent investigation, we expect to make progress on this subject.

Important progress was made to understand the electronic structure of a novel multilayer cuprate material where the CuO_2 layers are self-doped. These materials exhibit a number of surprises as they are very high temperature superconductors although simple valence counting would have put them in the insulating regime. We have uncovered a novel form of self-doping and a number of surprises associated with it.

Important progress was made in understanding the role of B_{1g} phonon coupling and superconducting transition temperatures in multilayer materials such as $Bi_2Sr_2CaCu_2O_8$ and $Bi_2Sr_2Ca_2Cu_3O_{10}$. We found that this mode coupling is much stronger in materials with multilayers of CuO_2 planes in their unit cells and with higher T_c, while this coupling is much weaker in cuprates with single CuO_2 layer and lower T_c.

Important progress was made in uncovering a phantom Fermi surface and its nesting instability in $Ca_3Ru_2O_7$. The delicate interplay between various degrees of freedom and their intricate roles in the rich physical phenomena is at the heart of physics in complex oxides. In $Ca_3Ru_2O_7$, high resolution ARPES data reveal well defined quasiparticle bands of unusually low weight, emerging in line with the metallic phase of the material below ~30K. At the structural phase transition temperature of 48K, we find clear evidence for an electronic instability, gapping large parts of the underlying Fermi surface that appears to be nested. Metallic pockets are found to survive in the small, non-nested sections, constituting a low-temperature Fermi surface with two orders of magnitude smaller volume than in all other metallic ruthenates.

Important progress was made in understanding Fermi surface and quasiparticle excitations of Sr_2RhO_4. We find well-defined quasiparticle excitations with a highly anisotropic dispersion, suggesting a quasi-two-dimensional Fermi liquid like ground state. A quantitative analysis of the ARPES derived band structure is in excellent agreement with dHvA and specific heat data. This work presents one of the rare quantitative comparison (the other being Sr_2RhO_4) between ARPES, transport and thermodynamic data down to few percent level.

We have observed doping dependent coupling of electrons to bosonic modes in the single-layer Bi-cuprate $Bi_2Sr_2CuO_6$. We compare for the first time the self-energies in an optimally doped and strongly overdoped, non-superconducting single-layer Bi-cuprate, $Bi_2Sr_2CuO_6$. Besides a strong overall weakening we also find that weight of the self-energy in the overdoped system shifts to higher energies. We have presented evidence that this might well be related to the coupling of c-axis phonons which are un-screened at optimal doping, being particularly sensitive to the rapid change of the c-axis screening in the doping range.

Chemical Physics of Surfaces and Liquids – The main focus of this research program is to use X-ray and electron spectroscopies to address important questions regarding chemical bonding on surfaces and in aqueous solutions. Photoelectron spectroscopy (PES), X-ray emission spectroscopy (XES), X-ray absorption spectroscopy (XAS) and X-ray Raman spectroscopy (XRS) provide an atom specific projection of the electronic structure. Problems related to systems in catalysis, energy technologies, electrochemistry and molecular environmental science are studied using XES, XAS, XRS and density functional theory (DFT) calculations. Probing hydrogen bonding and the structure of liquid water in aqueous systems are new and novel applications of X-ray spectroscopic techniques. Instrument development is an important part of the activity to provide new spectrometers, and enable measurements at high gas pressures and at liquid interfaces.

Detailed studies of water adsorbed on TiO_2 and Fe_2O_3 at ambient pressures using the differential pumped XPS systems continued, as have hydrogenation studies of carbon nanotubes for investigations of the potential of carbon based materials as hydrogen storage materials. Studies of water at high pressures and temperatures, different pH and in various aqueous solutions have

provided new information to address structure, hydrogen bonding and electronic structure of water in the bulk and in the influence of ions.

Molecular Adsorbates on Surfaces. XPS and XAS studies were performed on water adsorbed on Cu surfaces at ambient conditions. At pressures of 1 Torr, water dissociates to form a co-adsorbed oxygen-OH-water overlayer on Cu(110). The relative concentration of the different species depends strongly on temperature and relative humidity. On Cu(111) the interaction of water with the surface at 1 Torr and room temperature is extremely weak, resulting in a bare surface with no adsorbed water. These results show that in order for water to wet a Cu surface, it is necessary to form OH groups on the surface allowing for strong hydrogen bonding between water and OH.

Catalysis. Using a combination of density functional theory calculations and XES and XAS for nitrogen on Cu and Ni surfaces, a detailed picture has been obtained of the chemisorption bond. It is suggested that the adsorption bond strength and hence the activity of transition metal surfaces as catalysts for chemical reactions can be related to certain characteristics of the surface electronic structure, in particular the center of the d band is important.

Water in Aqueous Systems. New models of the structure of liquid water based on XAS and XRS experiments which go against the existing understanding based on theoretical simulations were proposed. New experiments with XRS have demonstrated important isotope effects between H_2O and D_2O which indicate that the discovered asymmetry in hydrogen bonding in water could be related to quantum effects in the motion of the hydrogen atoms. New experiments of water using photoelectron spectroscopy have been performed using both valence and core levels providing insights into the electronic structure rearrangements due to hydrogen bonding.

Instrument Development. A new UHV surface science end-station was completed and installed at BL5. A highly efficient soft X-ray spectrometer optimized for C, N and O K-edges has been designed and is under construction and a differentially-pumped high-pressure cell using cryogenic technology that can be inserted into this UHV system is being assembled.

Development of Resonant Coherent X-ray Scattering – The scientific motivation for the development program outlined below is the investigation of the critical fluctuations of a magnetic domain structure at the magnetic-paramagnetic phase transition. This research falls into the general area of critical fluctuations at phase transitions for which theory predicts that the order parameter diverges at the transition temperature. For magnetic phase transitions this implies that the domain size should diverge, *i.e.*, right at the transition temperature a single magnetic domain should extend –momentarily– over the entire sample. However, this has never been observed experimentally. One of the major reasons for this lack of experimental proof is that impurities and defects limit/influence these fluctuations. This limitation can be overcome by studying critical fluctuations in ultra-thin films with quasi 2-dimensional magnetization. Such ferromagnetic films can be prepared essentially defect free by epitaxial growth with thicknesses of only a few monolayers. A further advantage of studying a thin film is that the fluctuations are expected to be much slower in thin films than in bulk materials. To investigate the nature of these critical fluctuations, the following four experiments will be undertaken:

1. *Resonant Small Angle Scattering of Incoherent Soft X-rays*
   Resonant scattering at the dichroic L_3 absorption edge of magnetic transition metals will yield statistical information about the magnetic domain structure such as average domain size and domain shape. Hence, when investigating the temperature dependence of this statistical information close to the transition temperature, the average domain size of the critical magnetic fluctuations can be derived.

2. *X-ray Photon Correlation Spectroscopy (alias Dynamic 'Light' Scattering)*
   By scattering of coherent photons, information about the dynamics of the fluctuations can be derived from the time dependence of the scattering intensities. A third generation synchrotron light source like SPEAR3 will enable time resolving dynamics occurring on the microsecond time regime.

3. *Ultra-Fast, High-Resolution, Lensless Imaging of Magnetic Domain Structures*
   One potential application of SLAC's upcoming X-ray free electron laser LCLS will be ultra-fast, high-resolution lensless imaging. This will allow recording of femtosecond snap shots of the magnetic domain structure at and in the vicinity of the magnetic phase transition. A series of such images will enable distinguishing "real" magnetic fluctuations from defect-pinned fluctuations.

4. *Ultra-fast X-ray Photon Correlation Spectroscopy*
   At LCLS, a beam splitter and a delay line will be used to obtain two femtosecond short X-ray pulses separated by a variable delay ranging from a femto- to a few picoseconds. Using both these pulses for lensless imaging of the magnetic domain structure will reveal the dynamics of the magnetization fluctuations on a femto- to picosecond time scale.

Commissioning of the rebuilt BL5-2 continued, which also included commissioning of the dedicated end station for coherent soft X-ray scattering. Double pinhole test scattering patterns were recorded to characterize the coherence properties of the beam line. In addition, a novel implementation for coherence measurements based on a non-redundant array of pinhole structures was developed and successfully applied.

The feasibility of phase contrast imaging in resonant soft X-ray holography was demonstrated by imaging of a magnetic domain structure. The important implication of this achievement is that sample damage can be reduced significantly by using phase instead of amplitude scattering contrast.

In addition, multiple reference beam Fourier transform holography has been developed. Since an image is obtained simultaneously from each reference beam, the effectiveness of the imaging technique increases linearly with the number of reference holes. This allows to further reduce the required dose for imaging on the nano-scale, which is in particular important for radiation sensitive samples like organic materials.

The thin film preparation chamber assembled during FY2005 has been commissioned. First ultrathin magnetic films for the investigation of critical magnetic fluctuations have been grown. In preparation for these experiments, temperature control, earth field compensation, and an optical MOKE system to characterize the magnetic properties of the thin films were developed.

Small and Wide Angle Scattering Studies of Soft Matter & Colloids – A proposal for a new SAXS/WAXS Materials Science beam line at SSRL has been developed in response to the burgeoning demand for the technique in a host of modern nano-scale science applications. The beam line's design takes advantage of the accrued knowledge of the decades of experimental scattering from synchrotron sources in the field of materials science. Detailed plans concerning its physical specifications and configuration are already in place: with a double crystal monochromator (interchangeable between silicon [111] crystals and multilayers) and a horizontal and vertical focusing toroidal mirror and five meter path length downstream of the sample environment. This will provide a beam ~10^{13} photons able to probe correlation lengths within physical media up to half a micron in size at time resolutions of 100 ms or less, thereby opening up a facility for a whole new range of science. Some of this new science that would be made accessible by this geometry would include many pore size distributions (spatially) and matrix complexations (temporally) that are currently beyond the abilities of modern facilities.

Nanoparticles for Environmental Sorption Control. This project focused on the nano-scale structural chemistry and environmental chemical dynamics of bacteriogenic manganese oxide (MnO) nanoparticles. Investigations at BL1-4 addressed the relationships between particle size and MnO structure and stability and the factors controlling the colloid chemistry of MnO nanoparticles in aquatic systems. Insofar as Mn plays unique and important roles in local and global elemental cycles, including those of C, S, N, Fe and numerous other trace metals, the knowledge gained from this project will contribute towards our understanding of the dynamics that control the chemistry of our soils, natural waters, and atmosphere. Initial measurements of

bacteriogenic Mn oxide particle sizes in bacteria/mineral mixtures were made allowing the feasibility and test techniques for dispersing particles to be assessed.

Reflection Geometry SAXS. The capabilities of the new experimental hutch permitted collection of the first SAXS data in a reflection geometry, studying controlled growth of silicon nanotubes intended for nano-scale thermoelectric applications. In an effort to access the pores and achieve significant alignment, a method was developed for producing vertical pores out of the plane of a substrate. Cubic mesoporous titania was believed to have produced an ultra-flat hexagonal pattern from its 111 face that could be used to surface nucleate vertical growth in the silica 2D hexagonal system SBA-15 and hence the creation of accessible, aligned pores. Early data, in the reflection geometry, permitted characterization of the packing arrangement and aspect ratio of these nanotubes, which revealed difficulties in the synthesis, leading to misaligned tubular structures, which remain to be corrected.

Nanoporous Metallic Media. Nanoporous metals were fabricated electrochemically by selective dissolution or 'dealloying'. When immersed in a suitably aggressive reagent (*e.g.* nitric acid), the more active metal was removed leaving behind a 'sponge-like' bicontinous network of the noble element. We have studied AgAu and CuPt alloys, which formed nanoporous Au or Pt, respectively. SAXS has been used to characterize the pore sizes and the pore morphology as a function of dealloying time (1 minute to 3 days). We found that with increasing dealloying time the average ligament spacing increases and the morphology develops into a bicontinous network which then coarsens. In a related study, diffraction has been used to characterize the strain that develops during dealloying.

Structural Properties of Novel Materials – Several major subgroups of materials are explored in this area, including the local structure of non-crystalline materials, thin films, and nanoporous materials.

Non-crystalline Materials – A second experimental run was performed on the structure of liquid water. Several experimental improvements were made, including using an energy of 19.6 keV instead of 12 keV, which increases the maximum momentum transfer to 19.7 $Å^{-1}$. Secondly, a smaller, 600 micron orifice was used in the water jet. The smaller water diameter results in better energy resolution within the diffracted beam analyzer, which allows for better resolution between the elastic and Compton components of the diffracted beam. We also implemented a thermal bath for the recirculated water beam enabling us to measure the scattering both at room temperature (23 C) and at 5 C, very close to the density maximum of 4 C.

The analysis of the scattering from water is underway. Some of the challenges needing to be met during the analysis include the correct separation of the elastic and Compton components of the scattered beam. The advantage of increased energy resolution improves but does not eliminate the overlap between the elastic and Compton components. In a small region of momentum transfer (roughly between 2 and 6 $Å^{-1}$) there is overlap of the two peaks. Analytical techniques are being developed to consistently separate the two components. A second challenge is the correct form of the independent scattering. A molecular form factor has been calculated for water vapor, but it is expected that there will be subtle changes in the shape of the form factor for liquid water. We intend to use the excess electron density at small atomic separation to modify the form factor for liquid water. We plan to submit the work for publication during this period as well as write the doctoral dissertation.

Thin Film Structure – Studies on organic semiconductors have been extended to sexithiophene and substituted oligothiophenes, such as *p*-tolyl-trithiophene-*p*-tolyl, and studies will be initiated of other semiconducting conjugated polymers, such as poly[5,5'-bis(3-dodecyl-2-thienyl)-2,2'-bithiophene], PQT-12, which has a high field-effect mobility.

Nanoporous Metals – Nanoporous metals can be fabricated electrochemically by selective dissolution, or 'dealloying'. When immersed in a suitably aggressive reagent, the more active metal is removed leaving behind a 'sponge-like' bicontinous network of the noble element. Alloys of interest include AgAu, CuAu, CuPt, which form nanoporous Au or Pt for example. X-ray

scattering methods (SAXS and GIXS) have been used to carefully characterize the pores and the near-surface structure in these materials.

Charge Density Wave Materials – Rare earth (*R*) tellurides (RTe$_2$ and RTe$_3$) are ideal materials in which to study charge density waves (CDW), since the CDW gap is large and large crystals can be grown. High-resolution X-ray diffraction has been used to study the nature of the incommensurate and commensurate CDWs in RTe$_2$ and RTe$_3$ with initially R=La and Ce. From the diffraction data, the atomic displacements, which permit a deeper understanding of the observed thermodynamic and transport properties of these materials, have been obtained.

Ultra-trace and Microanalysis – A micro-focus X-ray mirror system using Kirkpatrick-Baez (KB) optics was commissioned in the back hutch of BL6-2 and first real data studying interplanetary dust particles were collected. Initially, this required a profound understanding of the alignment of the newly upgraded upstream beam line optics illuminating the virtual source of the KB system. This adjustable virtual source slit allows mapping to be carried out at variable focal spot sizes between approximately 2 and 15 microns. Photon fluxes fall in the $10^8 – 10^{10}$ photon/second range depending on the X-ray spot size, and the accessible energy range covers readily the elements Mg through Br. An aluminum-coated BN window allows simultaneous imaging of the sample with a high resolution optical microscope during the X-ray measurements. A helium gas shower is mounted above the sample to minimize radiation damage (due to ozone generation) as well as spectrum "contamination" by argon fluorescence from air. This shower creates a gentle flow of He without introducing vibrations to the sample mount. The X-ray hutch itself has been temperature-stabilized minimizing possible X-ray beam and/or sample drift during measurement. In addition, the data collection software SUPER was upgraded allowing the collection of the entire emitted fluorescence spectrum for each pixel rather than collecting only predefined single channel analyzer windows for selected elements of interest. This is crucial in particular for studying samples containing a variety of elements such as interplanetary dust particles. In those cases overlapping fluorescence lines in particular from neighboring elements can easily lead to false images of the elemental distribution. Efforts were made to evaluate different software packages for quantitative analysis of the individual fluorescence spectra. A software package developed at the ESRF called PyMca is currently being employed for quantitative analysis. The KB-based experiments in FY2005 were very successful, given the short amount of beam time available for characterization of the optical setup. In addition to optics characterization, elemental maps and trace element spectra were obtained for several thin sections of micrometeorites. These samples included round-robin samples provided by the Bulk Chemistry subteam leader of the Stardust Preliminary Examination Team. Our microprobe has been used in the preliminary examination of the samples returned by the Stardust NASA mission which swept through the tail of a comet (comet Wild 2) resulting in the first successful sample return mission since the Apollo program.

In FY2006, the KB optic-based microfocus facility has opened up for external user groups. A first user group from Canada has already been on line in January 2006, studying Fe distribution in fruit fly brains as a model for human Alzheimer disease. In addition, SSRL scientists performed preliminary test measurements for upcoming user groups studying Cu distribution in mice liver as a model for the Wilson disease, as well as of transition metal distribution in arthropod tools, such as spider fangs or worm teeth.

In addition to the work on the microprobe, a new TXRF chamber was designed, built and commissioned on BL6-2 mostly for studying small samples from the Genesis mission. Despite its hard landing, this mission returned fragmented samples of solar wind collected at the Lagrangian point for over two years. TXRF, due to the ability to distinguish between surface contamination (from Utah desert) and the true implanted solar wind, is an especially effective technique for studying these types of samples. In particular, the sample holder of this new setup was tailored for mounting small (cm^2) size samples without adding any contamination. In close collaboration with the PI of the Genesis mission, flight-spare samples and flown Sapphire samples have been analyzed with high detection sensitivity. These indicate that while some of the returned sample pieces have significant surface roughness and contamination, effectively reducing the sensitivity of the measurement, others are sufficiently clean and smooth to enable us to measure bulk solar

wind of dominant species (*e.g.* Fe). Further examination of samples will determine whether minority species will be able to be quantified.

Finally, the proposal to NIH (1 R01 EB004321-01) with the title "A multi-keV X-ray microscopy facility for bio-imaging" for development of a zone plate-based, multi-keV Transmission X-ray Microscope (TXM) facility was funded in May 2005 by the Bioengineering Research Partnerships program of NIBIB. The total award was distributed over four years and started in May 2005. The purchase order for the basic TXM instrument from Xradia Inc. was placed in September 2005. This instrument will provide important and currently at SSRL unavailable capabilities for the study of biological systems *in-situ*, such as the imaging of elemental distributions within single cells or tissues with high spatial resolution. The full field microscope will operate using photon energies between 5 – 13 keV and exploits the advantages of hard X-rays for 2D and 3D absorption and phase contrast microscopy such as large penetration depth, a large depth of focus, analytical sensitivity and compatibility with wet specimens. Together this will allow high resolution *in-situ* imaging, tomography and spectromicroscopy without extensive sample preparation. The TXM will be delivered from Xradia Inc. in October of 2006. We are currently building a new X-ray hutch on BL6-2 for this high-resolution microscope. It is anticipated that commissioning will begin in fall of 2006 and by the end of 2006 resolution test structures will be imaged in 2D and 3D with a spatial resolution below 60 nm in absorption contrast.

XAS Studies as a Probe of Electronic Structure / Contribution to Function – X-ray absorption spectroscopy (XAS), at the ligand and metal K- and metal L-edges, is used to determine the electronic and geometric structure of metal-based centers in inorganic and bioinorganic systems. The goal is to understand the involvement of the metal center in catalytic cycles important in industrial and biological catalysis. The experimental approach is complemented by Density Functional Theory (DFT) calculations, photoemission spectroscopy measurements, valence bond simulations and the development of data analysis tools, as well as by other non-synchrotron-based methodologies including MCD, resonance Raman and EPR spectroscopies, where applicable. The combined approach enables significant insight into geometric and electronic structure and their contributions to reactivity. Currently, studies are focused on systems containing copper, iron, titanium, manganese, molybdenum, and tungsten, with the anticipation of extending these studies to other transition metal sites.

Copper –The geometric and electronic structures of two mononuclear CuO_2 complexes $[Cu(O_2)\{HB(3\text{-}Ad\text{-}5\text{-}^{i}Prpz)_3\}]$ (**1**) and $[Cu(O_2)(\beta\text{-diketiminate})]$ (**2**) have been evaluated using Cu K- and L-edge XAS studies in combination with valence bond configuration interaction (VBCI) simulations and spin unrestricted broken symmetry density functional theory (DFT) calculations. These systems are related to oxygen activation at a single copper center, as in dopamine β-monooxygenase and peptidylglycine α-hdroxylating monoxygenase. Cu K- and L-edge XAS data indicated the Cu(II) and Cu(III) nature of **1** and **2**, respectively. Total integrated intensity under the L-edges showed that the ψ^*_{LUMO} in **1** and **2** consists of 20% and 28% Cu character, respectively, which is indicative of a very covalent ground state in both complexes, although more so in **1**. This is consistent with VBCI simulations, which also indicated that the ground state in **2** has more d^8 character. DFT calculations showed that the ψ^*_{LUMO} in both complexes is dominated by O_2^{n-} character, although the O_2^{n-} character is higher in **1**. It was also shown that the strong donor ligand in **2** is responsible for tuning the molecule towards more Cu(III)-peroxide like character in contrast to trispyrazolyl borate in **1** which leads to a Cu(II)-superoxide species.

Heme-Copper Oxidases – The geometric and electronic structure of the untethered heme-peroxo-copper model complex $[(F_8TPP)Fe^{III}\text{-}(O_2^{2-})\text{-}Cu^{II}(TMPA)](ClO_4)$ (**1**) has been investigated using Cu and Fe K-edge EXAFS spectroscopy and DFT calculations in order to describe its geometric and electronic structure. The Fe and Cu K-edge EXAFS data indicated a Cu···Fe distance of ~3.72 Å. Spin unrestricted DFT calculations for the $S_T = 2$ spin state were performed on $[(P)Fe^{III}\text{-}(O_2^{2-})\text{-}Cu^{II}(TMPA)]^+$ as a model of **1**. The peroxo unit is bound end-on to the copper, and side-on to the high spin iron, for an overall $\mu\text{-}\eta^1\text{:}\eta^2$ coordination mode. The Fe^{III}-peroxide η^2-bond has two components that arise from the donor interactions of the peroxide π^*_σ and π^*_v orbitals with the Fe

d_{xz} and d_{xy} orbitals, which give rise to σ and δ bonds, respectively, while for the Cu site the primary bonding interaction is between the peroxide π^*_σ and Cu d_z^2 orbitals. The π^*_σ interaction of O_2^{2-} with both Cu (η^1) and Fe (η^2) provides an effective superexchange pathway for strong antiferromagnetic coupling between the metal centers.

Non-Heme and Heme Iron

Cyanides – Distinct spectral features at the Fe L-edge of the two compounds $K_3[Fe(CN)_6]$ and $K_4[Fe(CN)_6]$ have been identified and characterized as arising from contributions of the ligand π* orbitals due to metal-to-ligand back-bonding Analysis of the L-edge spectral shape, total intensity and energy shift have been used to quantify the contributions of σ-donation and π-back-donation to metal cyanide bonding. The methodology developed demonstrates the application of Fe L-edge XAS as a direct probe of metal-to-ligand back-bonding.

Heme vs. Non-Heme Fe – Fe porphyrin compounds, or hemes, form the basis for electron transfer in a number of biological systems, with the most well-known being the cytochromes, which effect electron transfer by shuffling between low spin Fe(II) and Fe(III). The delocalization of the Fe d-orbitals into the porphyrin ring has been difficult to study spectroscopically because of the dominant porphyrin π →π* transitions, which obscure the metal based d-d bands. Recently, we have developed a novel methodology that allows for the interpretation of the multiplet structure of Fe L-edges in terms of differential orbital covalency (i.e. differences in delocalization of the different d orbitals) using a valence bond configuration interaction (VBCI) model. Applied to heme systems, this methodology allows experimental study of the delocalization of the Fe d-orbitals into the porphyrin ring. This methodology has been applied to study two model systems $[Fe(tpp)(ImH)_2]Cl$ and $[Fe(tpp)(ImH)_2]$ (low spin Fe(III) and Fe(II), respectively) and have compared their multiplet structure to those of the two low spin non-heme compounds $[Fe(tacn)_2]Cl_2$ and $[Fe(tacn)_2]Cl_3$. The Fe L-edge spectra are very sensitive to the effects of π donation and π back-donation. The e^1 hole (in heme, D_{4h}; t_{2g}, in O_h) in the ground-state electron configuration of low spin Fe(III), creates a dominant spectroscopic feature which was quantified in terms of π donation. The L-edge spectrum of $[Fe(tpp)(ImH)_2]$ exhibits additional transitions caused by back-bonding, which was also quantified. It was found that heme acts as a substantial □-donor to Fe(III) but only a minimal □-acceptor to Fe(II), indicating the electron transfer involves a hole-based super-exchange mechanism.

Siderophores – In order to overcome the immense difference between environmentally and nutritionally available Fe, many microorganisms produce low-molecular weight iron-chelators called siderophores. Our recently developed L-edge methodology, described above, provides a way of studying the bonding in these compounds. Fe L-edge data on a small set of compounds, $K_3[Fe(oxalate)_3]$, $[Fe(pha)_3]$ and $K_3[Fe(catecholate)_3]$ have been obtained. Results show that both the Fe K- and the L-edges shift to lower energy across the series: $K_3[Fe(ox)_3] < [Fe(pha)_3] < K_3[Fe(cat)_3]$. This shift indicates a decrease in effective nuclear charge and an increase in electron donation by the ligands. The total intensity of the Fe L-edge transitions decreases across the series, implying that the Fe-O bonds of $K_3[Fe(cat)_3]$ are the most covalent of the compounds. By simulating the shape of the spectra, it has been possible to calculate the σ and π contributions to bonding in the compounds, providing insight into the factors which affect the differences in their thermodynamic stability.

Iron-Sulfur – Ligand K-edge XAS has been used to obtain a quantitative description of Fe-S bonding in Fe-S model complexes and protein active sites. The results of these studies have been correlated to the extent of H-bonding and differences in redox potentials. To develop a quantitative description of hydrogen bonding in Fe-S systems, a series of P450 model complexes, where the amount of hydrogen bonding was systematically varied, were examined by S K-edge XAS. The data show a dramatic decrease in pre-edge intensity with increasing H-bonding to the ligated thiolate. DFT calculations reproduced these effects and showed that the observed changes are in fact solely due to H-bonding to the thiolate ligand. The energy of the H-bonding interaction was estimated to be -2.5 kcal/mol in the gas phase. The rather small H-bonding energy appears to contrast the large change in ligand-metal bond covalency (30%) observed in the data. A bond

decomposition analysis of the total energy was developed to correlate the pre-edge intensity change to the change in Fe-S bonding interaction on H-bonding. This analysis showed that the Fe-S interaction energy is greatly reduced due to H-bonding. This effect is greater for the reduced than the oxidized state, leading to an ~350 mV increase in the redox potential. It was found from a VBCI model that E^o should vary linearly with the covalency of the Fe-S bond in the oxidized state, which can be determined directly from S K-edge XAS. The above study was extended to a hydrogen bonded $[Fe_4S_4]^{2+}$ cube, which had an elongated core structure in contrast to the compressed core structures of most $[Fe_4S_4]^{2+}$ cubes. A decrease in pre-edge intensity was observed for the H-bonded cube. DFT calculations indicated that the change in Fe-S covalency observed experimentally had almost equal contributions from the cluster elongation and the H-bonding interaction. These calculations also indicated that the elongation of the $[Fe_4S_4]^{2+}$ cube changes the spin topology of the ground state due to redistribution of the ligand superexchange interactions in the cluster.

The geometric and electronic structure of the active site of the nonheme iron enzyme nitrile hydratase (NHase) has been studied using S K-edge XAS and DFT calculations. Using thiolate (RS^-), sulfenate (RSO^-) and sulfinate (RSO_2^-) ligated model complexes to provide benchmark spectral parameters, the results showed that the S K-edge XAS is sensitive to the oxidation state of S-containing ligands and that the spectrum of the RSO^- species changes upon protonation as the S-O bond is elongated (by ~0.1 Å). These signature features were used to identify the three cysteine residues coordinated to the low-spin Fe^{III} in the active site of NHase as $CysS^-$, CysSOH and $CysSO_2^-$ in both the NO-bound inactive form and the in the photolyzed active form. These results were correlated to geometry optimized DFT calculations. The pre-edge region of the XAS spectrum is sensitive to the Z_{eff} of the Fe and revealed that the Fe in the $[FeNO]^6$ NHase species has an effective nuclear charge very close to that of its photolyzed Fe^{III} counterpart. DFT calculations revealed that this results from the strong π back-bonding in to the π anti-bonding orbital of NO, which shifts charge from the formally t_2^6 low-spin ferrous center.

Titanium Cyclopentadienyl Catalysts – Ti-TEMPO complexes (TEMPO = 2,2,6,6-tetramethylypiperidine-N-oxyl) provide a means for generating Ti(III) complexes by homolysis of the Ti-O bond. The rate of Ti-O bond homolysis depends on the ancillary ligation to the titanium, and it has been determined that bis-Cp-Ti-TEMPO (Cp=cyclopentadienyl) complexes readily undergo homolytic cleavage, while the mono-Cp-Ti-TEMPO complexes do not. Recently, Ti K- and Cl K-edge XAS studies have been applied to a series of Ti-TEMPO complexes ($TiCl_3$TEMPO, $TiCl_2$CpTEMPO, $TiClCp_2$TEMPO). The XAS results indicate that these complexes are best described as Ti(IV)-TEMPO anions. The Cl K-edges show that the replacement of Cl by Cp weakens the remaining ligands, demonstrating a spectator ligand effect which is one factor that contributes to Ti-TEMPO bond homolysis. However, correlation of the XAS results to DFT calculations shows that stabilization of the three-coordinate product by Cp makes a more significant contribution to the energetics of Ti-O(TEMPO) bond homolysis.

PES Studies of Electronic Structure Contribution to Function – The shake-up satellite structure present in core and valence photoemission spectroscopy (PES) data is being used in combination with a valence bond configuration interaction (VBCI) model to experimentally quantify electronic relaxation (i.e. the change in electronic structure of metal complexes upon oxidation) and its contributions to reduction potentials and kinetics of electron transfer. Variable-energy PES (VEPES) experiments provide the tool to maximize the metal contribution, while minimizing that of the ligand, to the valence band region through cross section effects (delayed maximum and Cooper minimum) and resonance enhancement. VEPES data on a series of model iron complexes – high spin $[FeCl_6]^{4-/3-}$ and low spin $[Fe(CN)_6]^{4-/3-}$, $[Fe(tacn)_2]^{2+/3+}$, $[FeTpp(HIm)_2]^{1+/0}$, $[FeTpp(Py)_2]^{1+/0}$ – were measured and analysis initiated.

Materials Research

Research carried out by SSRL faculty and staff and associated Stanford faculty and students covers a broad set of disciplines: (1) Complex Materials; (2) Magnetic Materials; (3) Scientific and Educational Gateway Program (through FY2006); (4) Novel Materials and Model Systems for the Study of Correlated Phenomena; (5) Nano-scaled Magnetism in the Vortex State of High-T_c Cuprates; (6) Nano-scale Electronic Self-Organization in Complex Oxides; (7) Nano-Magnetism; (8) Behavior of Charges, Excitons and Plasmons at Organic/Inorganic Interfaces; and (9) Development and Mechanistic Characterization of Alloy Fuel Cell Catalysts. Areas (4) through (8) are collaborative efforts of the SSRL X-ray Laboratory for Advanced Materials and the Stanford University Geballe Laboratory for Advanced Materials.

1. Complex Materials

Z.-X. Shen, S. Doniach, M. Greven, R.B. Laughlin, X.J. Zhou, K. Tanaka, H. Li, L. Lu, K. Downum, Y. Cho, J. Hancock, D. Santiago, D. Schroeter, L. Zhou, X. Zhou, B.A. Bernevig

The team has conducted comprehensive experiments using photoemission (Shen), scattering (Greven and Shen), and theoretical investigation (Laughlin and Doniach) on complex materials, and has made substantial progress in this period. There also are synergetic interactions with the nano-science programs of Greven, especially in the area of single crystal growth, and Shen's core program on strongly correlated materials.

A major focus of the program is the electron-doped materials that have presented an important challenge to the systematic understanding of high-temperature superconductors. The Greven group has continued its successful effort on the electron-doped superconductor $Nd_{2-x}Ce_xCuO_4$ (NCCO), built on its early success in growing high-quality single crystals. Recent results include the first determination of spin-correlations in superconducting samples, which constitutes significant progress toward a full understanding of the normal state of the electron-doped superconductors. Since superconductivity in high-T_c cuprates appears in close proximity to the antiferromagnetic phase, it is essential to understand the nature of nearby magnetic ground states. Through careful X-ray and neutron diffraction work, Greven discovered that the oxygen reduction process, required to render NCCO superconducting, transforms a fraction of the crystals into cubic $(Nd,Ce)_2O_3$, and that the field-effects observed by others and ascribed to a quantum phase transition of NCCO are not intrinsic, but due to this secondary phase. Consequently, the question of genuine magnetic field effects in NCCO has remained a very interesting, unresolved research topic. By studying the magnetic field effect on the spin excitations, Greven was recently able to obtain new data consistent with the absence of field-induced magnetic order [Motoyama *et al.*, preprint]. Moreover, these measurements constitute the first neutron scattering study of the effects of a magnetic field on the superconducting magnetic gap in NCCO. The discovery of spurious magnetism in NCCO is a good example of the benefits of a synergistic growth and scattering effort like that by Greven.

Greven continued the novel use of inelastic X-ray scattering to investigate the collective charge excitations in the model high-temperature superconductor Hg1201, the single-layer material with the highest value of T_c, and of the parent compound La_2CuO_4. This latter work, carried out at the APS and made possible by newly available large Hg1201 crystals grown by Greven, led to the discovery of a remarkably rich structure of electron-hole pair excitations in the cuprate superconductors.

Greven's work on the structural phase diagram and charge-order phenomena in the layered manganite was extended to cover a wider range of doping as well as neutron scattering. These results will allow a comprehensive understanding of the structural and magnetic phase diagram.

The angle-resolved photoemission spectroscopy (ARPES) component of the program (Shen) has two primary tasks, research, and operation of the beam line 10.0.1 end-station at the ALS in support of this research. That activity also benefited a broader community performing ARPES experiments using the end-station.

The focus during this period of time is to understand the nature of collective modes coupled to cuprate superconductors. Data with very high signal-to-noise level, together with a numerical method developed in collaboration with Ward Plummer's group (Oak Ridge National Laboratory), enabled a glimpse of the phonons and their coupling to electrons in cuprates. This represents the first experimental evidence for multi-boson coupling in cuprates.

Another area of major progress during the period is the new insight on the polaronic behavior of single hole in undoped cuprate. Based on ARPES data from La_2CuO_4 and phonon spectra from neutron scattering, theoretical calculation by Gunnarsson's group (Max Plank Institute) show that the spectra are consistent with the material being in the polaronic regime, which is consistent with our earlier finding for copper oxide chloride.

Shen's group also has made important technical progress in applying synchrotron radiation for high resolution spectroscopy experiments. The resolution and flux density at the ALS have been a critical factor for the program in generating a significant database. On the other hand, this also raises the technical problem of space charging. Shen's group has systematically characterized this problem and our finding is generally useful in guiding high resolution photoemission experiments in third generation synchrotron radiation facilities.

A major advance by Shen's group during this period is the discovery of nodal quasiparticle and nodal antinodal anisotropy in layered colossal magnetoresistive manganites. This finding provides deep new insights on the "pseudogap" phenomena in cuprates. The pseudogap behavior has for a long time been considered to exist only in superconducting materials, and thus is directly related to high-temperature superconductivity. Finding this same behavior in ferromagnetic state suggests that the relationship between "pseudogap" and superconductivity is more subtle. In particular, this finding supports the notion that there are two "pseudogaps", and the larger pseudogap is in fact a reflection of a competing state to superconductivity. Thus, both superconducting and pseudogap phases are manifestation of the same underlying physics that give rise to the rich and intricate phenomena seen in these complex oxides.

The work of the Laughlin group in 2005 was conducted mainly by David I. Santiago and Zaira I. Nazario. The Laughlin group has studied the phase diagram in cuprates high T_c superconductors. Recent experimental measurements suggest the coexistence of various phases of matter in different regions of the pseudogap regime. Guided by such experiments the group has studied the properties of a spin-density-wave antiferromagnetic mean-field ground state with d-wave superconducting (DSC) correlations. This work concentrates in the case when antiferromagnetic order is turned on weakly on top of the superconductivity, which corresponds to the onset of antiferromagnetism at a critical doping. In such a case a small gap proportional to the weak antiferromagnetic gap opens up for nodal quasiparticles, and the quasiparticle peak would be discernible.

The program looked broadly at the many-body problem in condensed matter system, beyond the high-T_c superconductors and transition metal oxides. Work on the superfluid to Mott insulator transition in bosonic systems has been done, where the phase diagram of a single component Bose Einstein Condensate (BEC) in an optical lattice at zero temperature was obtained. In that work, the discontinuous nature of the transition between the superfluid and the Mott insulator (under certain conditions) was elucidated, as well as its independence on commensuration of the number of bosons with the lattice. Recently, measurements which could be interpreted as such a transition have been performed by Mark Kasevich's group of Stanford University. While, being superfluids, BECs share many properties with superfluid helium, they have never been seen to share the existence of roton excitations which are present in helium. Superfluid helium is close to becoming a solid. The roton minimum is a consequence of enhanced density fluctuations at the reciprocal

lattice vector of the stillborn solid. Thus rotons have not been observed in BECs in atomic traps since they are not near a solid phase, but if they are tuned near a transition to a Mott insulating phase, a roton minimum will develop at a reciprocal lattice vector of the lattice. Equivalently, a peak in the structure factor will appear at such a wave vector. The smallness of the roton gap or the largeness of the structure factor peak are experimental signatures of the proximity to the Mott transition.

Laughlin's group has also done some work on metal-insulator transitions. Specifically, the work was motivated by V_2O_3 and f-electron systems which have phase diagrams in which a line of first order metal-insulator transition ends at a critical point above which the two phases are indistinguishable. Bob Laughlin's Gossamer technique was extended to show that the Gossamer metal in a single band model will describe a metallic phase that becomes arbitrarily hard to differentiate from an insulator as one turns the Coulomb correlations up. Thus one can go continuously from the metal to the insulator.

Laughlin's group also has done some work on quantum criticality that should be published this year. In collaboration with Jan Zaanen, they have an article on spin-orbit coupling and interesting quantum interference effects that will also be published in this period. The Doniach group expects to continue work on the relation between superconductivity and electron correlations in intercalated graphite. Recent work on superconductivity in doped graphite intercalated compounds has suggested that, despite theoretical work to model this by conventional electron phonon coupling BCS theory, these theories have been unable to explain why different intercalates have very different T_c's. T_c spans at least one order of magnitude when going through different intercalates and it is believed possible to study the relative effects of t-J correlation coupling versus electron-phonon coupling on these various T_c's.

The Doniach group has been focusing on looking at electron correlations in graphite. Although this has traditionally been considered in the context of band theory, recent experiments by Kopelevich and collaborators show strong evidence of a semi-metal - insulator transition in applied magnetic fields of order 1 kG. The experimentalists found that a scaling relation suggested by Das and Doniach in 2001 for the superconductor – "bose metal" state of thin film superconductors also applies to the graphite data. The effects of correlations in graphite have been studied using a t-J model, following ideas proposed by Baskaran for the superconductor MgB_2.

2. Magnetic Materials Research

J. Stöhr, H. Siegmann, H. Ohldag, Y. Acremann

The general goal of this program is to develop new techniques and approaches for the study of modern magnetic materials in the form of thin films, multilayers and nanostructures and explore the origin of magnetic phenomena associated with such materials.

Work has continued on the phenomenon of *exchange bias* by means of X-ray microscopy and spectroscopy. In particular, soft X-ray dichroism absorption spectroscopy was used to investigate the direction of interfacial exchange coupling in a ferromagnetic / antiferromagnetic Co/FeF_2 bilayer. This system behaves quite differently from conventional exchange bias and, depending on sample preparation, it can exhibit either positive or negative exchange bias. Two different kinds of interfacial uncompensated Fe moments were found in FeF_2. A smaller pinned portion couples antiparallel to the ferromagnet and can lead to positive or negative exchange bias depending on the size of the cooling field. A larger portion couples more strongly and parallel to the ferromagnet. It increases the degree of antiferromagnetic order in FeF_2 near the interface and plays an important role in the observed coercivity increase at high temperatures. The work was recently published: H. Ohldag, H. Shi, E. Arenholz, D. Lederman and J. Stöhr, *Phys. Rev. Lett*. **96,** 027203 (2006).

The program on ultrafast magnetic switching with electron beams and the program on lensless magnetic imaging with X-rays, reported last years, have now been funded separately as part of the Stanford Ultrafast Science Center (PULSE) and the work is reported under that program.

A new subprogram has started, based on the exploration of new ways of exciting magnetic materials by ultrafast magnetic field pulses. Rather than using electron beams ultrafast laser pulses have been explored for launching fast and strong current pulses. The idea is to generate ultrafast magnetic field pulses by current flow through a strip-line, as illustrated in Figure 1. The current pulse is triggered by an ultrafast laser which either opens an electro-optical (Auston) switch or creates ultrafast photoemission into vacuum on one side of the stripline which is grounded on the other side. Such a scheme has the advantage of being compatible with ultrafast X-ray imaging.

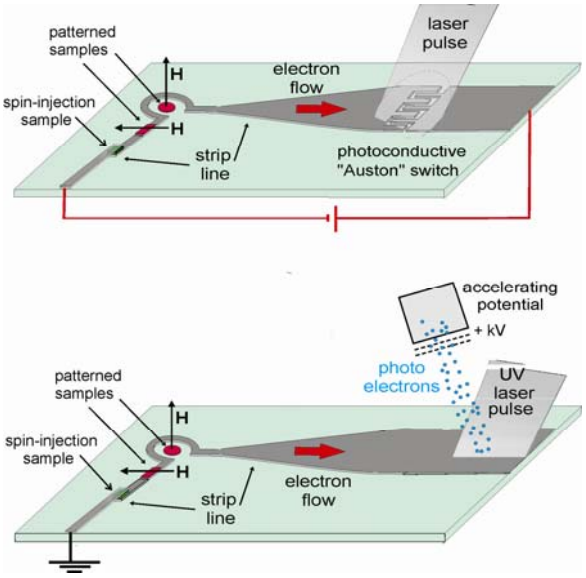

Figure 1. Arrangement for generating short and strong current pulses traveling down a strip line. In the upper picture the current pulse is generated by a photoconductive switch, in the lower picture by a photoemission pulse.

The scheme illustrated in Figure 1 using laser pulse probe experiments will be explored and will characterize the achievable pulse length and field strength. Samples will be fabricated with our new magnetic thin film deposition system and by use of lithographic manufacturing techniques.

The design of a scanning transmission X-ray microscope for BL13 at SSRL will also continue.

3. Scientific and Educational Gateway Program

A. Nilsson, A. Mehta and R. R. Chianelli

This continuing, joint effort with the University of Texas at El Paso (UTEP) serves both the Mexican-American and Mexican communities in undergraduate and graduate education by engaging student scholars in science and engineering research programs at all levels. The program provides travel support for Mexican-American and Mexican students and supporting faculty, science and technological support by an SSRL scientific staff member, who also assists participants in beam line operations and laboratory facilities use, and a scientific staff member at UTEP, who develops and implements computational tools and software for analysis of synchrotron data. These staff members train students in methods of data reduction and analysis and, jointly with SSRL staff scientists, develop collaboratory tools for remote access to instrumentation and data measured at SSRL. This program has been quite effective, as shown by the number of UTEP students participating in FY2001-2005 (almost 50 students). These students and staff underwent training and carried out experiments on existing SSRL peer-reviewed proposals coordinated across five separate beam lines. The students continue to enhance their

training by taking highly successful proposal writing classes at UTEP (Chianelli). SSRL staff work closely with the UTEP faculty and staff to train and support the new students and their research efforts. Part of the period in FY2005 saw the synchrotron start-up for the now successfully completed SPEAR3 upgrade. In addition, an electrical accident further delayed the schedule. However, this allowed time for the students to concentrate on data analysis with the help of SSRL and UTEP staff. Progress during this period was excellent with many students and faculty further developing their proficiency in the use of synchrotron techniques and producing publications based on previous collected data. Several students achieved in-depth understanding of synchrotron radiation and its application by attending the Stanford-Berkeley Summer School.

The level of synchrotron related skills increased substantially for both the students and faculty, which will be reflected by refereed publications and meeting presentations of the group. Particularly skills were improved in the areas of SAXS and carbon edge XANES. Progress was made in six core areas in FY2005; (1) The Chianelli group continued to address structure/function relations in transition metal sulfide (TMS) hydrodesulfurization (HDS) nanocatalysts. The first "Gateway" Ph.D. (Myriam Perez) graduated and accepted a post-doctoral position at SSRL; (2) Diffraction studies on Maya Blue demonstrated that the pigment is a surface complex of the indigo dye with palygorskite clay; (3) Data analysis on both the SAXS and WAXS data from asphaltenes, crude oils from Mexico and Venezuela and TMS catalysts was completed; (4) The Gardea group continued to investigate the metal binding properties of the "hyperaccumulators"; (5) The Pingitore group continued to study trace elements in human bone. The incorporation of Sr, Zn, Pb, *etc.* in human bone is a topic that impacts archaeology, nuclear waste/terrorism, biomedicine, and environmental pollution. All of these projects yielded significant publications in 2005 and in press for 2006.

The SPEAR3 installation allowed time to develop the full scientific impact of the program. This is shown by the significant increase in the demonstrated impact of synchrotron studies on the scientific understanding of the problems discussed above. Students and faculty are well trained to participate in "bringing on line" the new SPEAR3 experiments and testing the new significant capabilities.

Approximately 60 students will have been involved in synchrotron programs at SSRL involving multiple techniques, diffraction (SAXS and WAXS), scattering techniques including anomalous dispersion scattering, XAFS (hard and soft X-ray) and protein crystallography. Many of these students will become a regular part of the synchrotron user community and some will have synchrotron use become a major part of their careers. Many these students will have obtained experience at other DOE facilities. Up to four students will have completed or nearly finished a Gateway Ph.D. and become full members of the synchrotron community. Several faculty members at UTEP and related Mexican institutions will have become new synchrotron users. Major scientific progress will have been reported from the Gateway program as discussed above. The progress will be of such quality that the program will not only have made a major impact on training minority scientists but the students will have produced significant and competitive scientific contributions.

4. Novel Materials and Model Systems for the Study of Correlated Phenomena

I.R. Fisher, M.R. Beasley, T.H. Geballe, M. Greven, N. Barisic, G. Chabot-Couture, A.S. Erickson, G. Koster, L. Litvak, Y. Matsushita, N. Ru, P. SanGiorgio, K.Y. Shin, G. Yu, X. Zhao, X. Zhou

This program directly addresses scientific questions at the heart of understanding correlated electron behavior in complex materials. This work explores the conditions of occurrence and mechanisms behind these effects, and examines the consequences for bulk properties and collective phenomena. The approach is to identify and synthesize model systems that enable

exploration of particular interactions in isolation. The essence of the proposed research therefore lies in the design, growth and characterization of novel materials.

The original title of this subtask was "Nanoscale ordering in complex oxides: model systems for local probes." The title was updated during the recent renewal to better reflect the focus of our current research.

Negative-U Impurities -- Over the course of the last three years a multistep synthesis route has been established to produce high-quality single crystals of the unusual superconductor $(Pb_{1-x}Tl_x)Te$, and work has gone forward on detailed measurements to characterize the thermodynamic, transport and spectroscopic properties of these samples. The Tl impurities appear to act as negative-U centers in this material, and this research explores the role that these impurities play in both the superconducting and normal state properties. Early measurements established that a critical concentration of Tl impurities is required to cause superconductivity in PbTe. For Tl concentrations beyond this critical value the Fermi level appears to be pinned, such that the Tl impurities act in a self-compensating manner. It seems that the superconductivity is intimately linked to the presence of a mixed Tl valence, the presence of which also is reflected in the normal state transport of the material. In particular, during FY2005 evidence was found for a charge Kondo effect associated with degenerate valence states of the Tl impurities. This observation, supports the notion of an electronic pairing mechanism in superconducting Tl-doped PbTe, perhaps accounting for the unusually high T_c value. Ongoing research seeks to further investigate this effect in Tl-doped PbTe and related materials, testing various predictions of the theoretical models that have been proposed.

In FY006, the superconducting properties of Tl-doped PbTe have been explored in more detail. Heat capacity measurements for the highest Tl concentrations indicate that the superconducting anomaly is close to the BCS result ($\Delta C/\gamma T_c \sim 1.43$), which within the charge Kondo model would imply that the renormalized electrons are indeed participating in the superconductivity. However, this quantity appears to show a marked decrease as the impurity concentration decreases, the origin of which effect is uncertain and warrants further investigation. Additional insight can be expected from a close collaboration with C. Gough and E. M. Forgan (Birmingham, UK) exploring the penetration depth via microwave conductivity and muon spin rotation. Initial experiments from early this year indicate that the T-dependence of the superfluid density is close to BCS predictions, but with some unusual field dependence. The continuing normal state magnetotransport measurements show an unexpected trend towards a linear T-dependence of the resistivity that we are continuing to study. These data are currently being modeled by J. Schmalian (Ames Laboratory) and P. Coleman (Rutgers) in terms of a pair-diffusion process associated with the negative-U properties of the Tl-impurities. Initial EXAFS measurements (in collaboration with F. Bridges, UCSC) are suggestive of two Tl-Te distances, consistent with the proposed disproportionation, but are limited in resolution due to the proximity of a nearby Pb absorption edge. Experiments are also planned at the NHMFL Microkelvin Laboratory (with Yoon Seuk Lee, U. Florida) to look for reentrant behavior at low temperatures, a key prediction of Schmalian's charge Kondo model. Additional external collaborations will probe the effect of pressure on the superconducting and normal state properties (S. Brown, UCLA), the optical conductivity (Z. Schlesinger, UCSC) and core level spectroscopy (C. Fadley, UCSD).

- ***Charge-Density Waves in Layered Rare Earth Tellurides*** -- We recently identified the layered rare earth (R) tellurides RTe_3 and RTe_2 as model systems to study Fermi surface reconstruction in incommensurate CDW compounds, a topic that has significant bearing on current questions in the field of cuprates and other strongly correlated oxides. These are particularly attractive model systems because (a) the electronic structure is especially simple and the band filling can be tuned by chemical substitution; (b) the CDW gap is large and can be measured by a variety of powerful techniques; (c) we can explore the consequences of the CDW formation on the magnetic properties of the material; and (d) we are able to grow high-quality

single crystals, enabling sensitive probes of the Fermi surface including dHvA and ARPES, and real space probes including STM.

Initial angle resolved photoemission experiments in collaboration with Z.X. Shen clearly revealed the CDW gap, showing gapped and ungapped regions of the Fermi surface. Our ongoing experiments further explored the Fermi surface nesting and CDW formation in both RTe_3. Further experiments probing the FS reconstruction in RTe_3 were conducted by a student supported by this grant during an extended visit to A.P. Mackenzie's research group in St. Andrews, Scotland. These measurements revealed multiple frequencies all of which vary with angle according to 1/cos(theta), consistent with minimal z-axis dispersion. The measurements are currently being compared with ARPES data with the aim of fully determining the reconstructed FS. Other experiments have been performed at SSRL, following award of beam time. Initial high-resolution diffraction experiments have revealed an extremely well-ordered modulated structure with minimal harmonic content. These measurements are continuing with the ultimate goal of finding a model for the atomic displacements in the CDW state, and hence determining whether the material consists of short regions of commensurate modulations with regular discommensurations, or is indeed a truly incommensurate structure.

Experiments at SSRL have established that the CDW in RTe_3 has remarkably little harmonic content. Work is currently in process to model the atomic displacements in an effort to differentiate between a truly incommensurate distortion and a modulation consisting of a dense array of discommensurations. Further diffraction experiments were planned to follow the T-dependence of the CDW wave-vector, motivated in part by theoretical models of S. Kivelson (Stanford) predicting a possible phase transition between unidirectional (stripe) and bidirectional (checkerboard) order. Additional experiments and analysis will finalize our dHvA study, while magnetotransport measurements will pursue our recent observation of superzone gap formation in the heavy rare earth members of the series (*i.e.* an additional gapping of the FS at T_N). Work has also continued to explore the role of Te vacancies in RTe_{2-x} in determining the optimal nesting wave-vectors and resulting CDW modulation in this single-layer variant. Most excitingly, there is now confidence the alternating single and double layer compound R_2Te_5, intermediate between the single layer RTe_2 and bilayer RTe_3 compounds has been successfully synthesized. Experiments are probing how band filling affects the CDW formation in this family of compounds, providing a useful window on the role of dimensionality (stripe vs checkerboard) in CDW systems. Numerous internal and external collaborations continue to probe other physical properties of these materials, including STM (A. Kapitulnik, Stanford), optical conductivity (L. DeGiorgi, ETH, Zürich), NMR (V. Brouet, Université de Paris Sud, France) and positron annihilation (S. Dugdale, Bristol, UK).

Ferromagnetism in the Mott Insulator Ba_2NaOsO_6 -- The interplay between orbital and spin degrees of freedom can play a pivotal role in many correlated electron effects. Perhaps the clearest example of this is to be found in ferromagnetic Mott insulators – a rarified and unusual class of materials. In a single band Hubbard model, hopping between adjacent sites leads to an antiferromagnetic ground state. However, orbital degeneracy can favor ferromagnetic exchange due to the additional energy that can be gained from Hund's rule coupling of electrons in two different orbitals. In such a case, the appearance of ferromagnetism is thought to be accompanied by a complex form of anti-ferro orbital order, the precise nature of which depends strongly on details of the specific lattice and material. This is an exciting and topical area in correlated electron physics. However, there are precious few candidate materials. Furthermore, those that have been studied belong exclusively to the 3d transition series.

Ba_2NaOsO_6 presents a wonderful opportunity to study the interplay of orbital and spin ordering in the unusual environment of a $5d^1$ ferromagnet. A method has recently been determined to grow relatively large single crystals of this material that enable a host of exciting experiments. Initial thermodynamic and transport measurements, performed early in FY2006, demonstrate that this material is indeed a ferromagnetic Mott insulator, but with an ordered moment that is substantially less than 1 μ_B (*i.e.*, the ordered state consists of a complicated spin structure with a net ferromagnetic moment). The reason for this is becoming evident. At room temperature,

Ba_2NaOsO_6 occupies an undistorted double-perovskite structure, in which the OsO_6 coordination polyhedra are neither rotated with respect to the lattice, nor distorted from a perfect octahedral symmetry. In this case, the three t_{2g} orbitals are indeed degenerate, and ferromagnetic exchange can be anticipated. However, the FCC lattice cannot be decorated with three "color" orbitals in such a way that each site always has nearest neighbors of a different color. For adjacent sites of the same color the superexchange is perforce antiferromagnetic. Hence, in the absence of any additional structural phase transition, it can be anticipated that the resulting ground state of Ba_2NaOsO_6 is a complex mixture of spin and orbital order, with a strong ferromagnetic component, but which falls short of 1 μ_B. An active proposal is in place with the Advanced Photon Source (together with Z. Islam, APS, ANL) to study the spin and orbital ordering in this compound later in the year. Other ongoing experiments will probe the high-field magnetization (with L. Balicas, NHMFL), exploring the possibility of a metamagnetic transition to the fully saturated state.

Electronic Inhomogeneities in Correlated Electron Materials -- One of the goals of this program is to synthesize model systems for the study of nanoscale electronic inhomogeneities that result from the coulomb interactions in correlated electronic materials, and ultimately to study these inhomogeneities using scanning probes. Toward this end, thin films of the Mott insulator CuO have been grown, in which such nanoscale inhomogeneities have been previously reported. This is perhaps the simplest conceivable copper oxide related to the high temperature cuprate superconductors. Epitaxial thin films of stable monoclinic CuO have been grown previously on MgO substrates. More recently CuO has been grown epitaxially with square symmetry in the plane (*i.e.*, either cubic or tetragonal overall). The composition is confirmed by UPS spectra taken *in-situ* in an adjacent chamber. The structure has been confirmed using *in-situ* RHEED and by Photo-Electron Diffraction. Ion-beam assisted deposition (IBAD) has been tried to further enhance our ability to get a cubic structure, but this has not so far been successful, due presumably to differential sputtering of oxygen and cupper. Very recently, it has also shown that CuO can be grown using Pulsed Laser Deposition. The detailed properties of films grown by these two methods now need to be compared.

In parallel with this effort, thin films of ZrO_2 have been deposited using pulsed laser deposition (PLD) for use as high-K dielectrics for field-effect doping applications. The student working on this project has left the university. In light of this, focus will revert to the CuO work and this part of the project will not be continuing.

A square-planar (rock salt) form of CuO has now been deposited successfully and physical study of these films is being pursued. Standard transport and optical measurements are being carried out, and various scanning probes are being applied in collaboration with colleagues here at Stanford. These include Scanning Hall probes, MFM, STM and scanning potentiometry to look for inhomogeneities. In addition, on the materials side, studies will begin on approaches to dope these films. This might be done through introducing oxygen deficiency or by using strongly electro-positive (or negative) over-layers.

Superconductivity and Magnetism: Pair Density Waves and $SrRuO_3$ -- Studies of the superconductor/ferromagnetic proximity have drawn a remarkable level of interest, primarily because it is proving to be an effective model system for the study of the interaction between superconductivity and magnetism. One of the most striking predictions from theory is the existence of decaying pair density waves in the ferromagnetic side of an SF proximity bilayer due to the exchange field in the F material. Evidence for this effect is mixed. In order to get more detailed information regarding SF proximity structures, in collaboration with the group of Kookrin Char at Seoul National University, tunneling density of states studies are in progress on the F side of Nb/permalloy SF bilayers as a function of the thickness of the F layer. It is found that the striking result that the tunneling density of states as a function of thickness (viewed as deviations from the normal density of states) is of constant form with amplitude that scales exponentially over four orders of magnitude as a function of the F layer thickness. No evidence for pair density oscillations was found. More recently, a detailed comparison of these results with the available

theory has been carried out. It is found that the theory can account for these data only if patently unreasonable values are used of the exchange field and the spin-flip scattering rate. This work has now been accepted for publication. One possible reason for this serious discrepancy is that we are using very strong ferromagnets whereas the theory assumes weak magnetism. In order to clarify the situation, a second strong ferromagnet (Ni) is presently being studied for the F material.

Thin films of $SrRuO_3$, a rare example of a 4d itinerant ferromagnet continue o be deposited and studied. With the group of Lior Klein, the magneto-transport in $SrRuO_3$ is being examined to test recent theories of the effect of the Berry phase in magnetic systems. We did not confirm the predictions. Studies also continue of various physical properties of the films including spin accumulation at domain walls during electric transport, the magnetic anisotropy of the material and the superconducting properties of $Nb/SrRuO_3$ SF hybrids. In SF hybrids there is only magnetic coupling between the S and F layers (*i.e.*, there is no proximity effect coupling).

Given present results on the tunneling density of states on Nb/permalloy SF proximity bilayers, it is very important to study other F materials to see if these results are universal or specific to permalloy. Studies with Ni as the F material were mentioned above. The next obvious step would be to move systematically to lower exchange fields. Following others, the Ni-Cu alloy system will be used. Scanning Hall probe studies of these bilayers will also be carried out to establish directly the orientation and spatial homogeneity (or not) of the magnetization of the F layers.

As was mentioned last year, it is also planned to use the *in situ* FTIR system to study the optical conductivity of $SrRuO_3$ at high temperatures. Lower temperature measurements carried out by us with Zack Schlesinger at UCSC showed that a coulomb-like pseudo-gap appears to open at low frequencies as temperature increases. This seems to be part and parcel of the bad metal behavior of this material (*i.e.*, increasing resistivity with increasing temperature beyond the Ioffe-Regal limit). Recent theories of highly incoherent electrons using dynamical mean-field theory predict such a gap should open. Clearly these predictions need to be tested.

Advanced Superconductors -- The mercury-based materials $HgBa_2Ca_{n-1}O_{2n+2+\delta}$ are model high-temperature superconductors due to their relatively simple structure, because they appear to be least affected by chemical disorder, and because of their record superconducting transition temperatures (*e.g.,* for n = 3, T_c = 134 K at ambient pressure and 164 K at 31 GPa). Consequently, these materials are the most desirable high-temperature superconductors for experimental study. Comparison with results for lower-T_c materials will eventually allow us to separate materials-specific properties from properties shared by all superconducting cuprates. However, the synthesis of this homologous series has remained a serious challenge until recently, and rather few experiments have been done on the Hg family of superconductors. In a major breakthrough, we succeeded in growing single crystals of Hg1201 (n=1) as large as 50 mm^3, more than two orders of magnitude larger than the previous world record. Neutron diffraction (at NIST) and synchrotron X-ray work (at SSRL) confirmed the single-grain nature of our samples, with a typical mosaic of 0.04 degrees for the smaller X-ray samples. The new crystals have allowed us to begin systematic transport, magnetometry, and resonant inelastic X-ray scattering (RIXS) experiments (at the APS), and to initiate numerous collaborations, both at Stanford and elsewhere, with scientists using complementary experimental techniques. For example, optical spectroscopy measurements by Dr. C.C. Homes (BNL) are consistent with a newly-discovered scaling law for the superfluid density. It is noted that these RIXS experiments led to the important discovery of a subtle incident photon energy dependence of the K-edge RIXS cross section, which needs to be explored in future experiments in order to arrive at satisfactory qualitative and quantitative understanding of the charge-transfer excitations in complex oxides. It furthermore led to the surprising observation of a remnant charge-transfer gap in optimally-doped Hg1201.

The superconducting properties of the new Hg1201 (n=1) crystals are being refined further, through a heat treatment in an oxygen atmosphere, in order to obtain very underdoped and also overdoped samples. This long-term project, which also involves transport measurements and magnetometry, is challenging since uniform oxygen control far away from optimal doping is a non-trivial task, especially for large crystals. The initial RIXS work on optimally-doped Hg1201

will be expanded in order to determine that nature of the electron-hole pair excitations in underdoped samples. Furthermore, the growth of the multilayer (n>1) members of the Hg family of superconductors continue to be studied. Due to the high Hg partial pressure during the growth, this task is more challenging than the growth of the n=1 system. This effort will enable increasingly detailed and valuable experiments on the Hg-based model superconductors, such as X-ray and neutron scattering, optical spectroscopy and Raman scattering, ARPES, STM, as well as thermal and charge transport. Quantitative experimental results for the Hg-based family of materials can be expected to serve as benchmarks for tests of theories of high-T_c superconductivity. Efforts will continue to grow sizable crystals of Y-Bi2212 for inelastic neutron scattering and complementary experimental work.

The effects of chemical inhomogeneities were previously investigated in the bismuth-based family of copper oxide superconductors, $Bi_2Sr_2Ca_{n-1}Cu_nO_{2n+1+\delta}$. The double-layer variant (n = 2; "Bi2212") of this homologous series has been of great interest to the ARPES and STM communities, but systematic neutron scattering work has not been possible due to the lack of sizable crystals. It was found that the maximum attainable value of T_c can be increased to a new record value of 96K for a small amount of Y doping, *i.e.,* Ca-site disorder, which, in effect, leads to a stoichiometric Bi:Sr ratio of 2:2 and hence zero Sr-site disorder. These results have the important implication that the degree and the type of disorder are very important experimental parameters that can and should be controlled: a new generation of experiments on such optimized samples is clearly called for. Efforts have continued to grow sizable crystals for inelastic neutron scattering and complementary experimental work.

5. Nanoscaled Magnetism in the Vortex State of High-T_c Cuprates

S. Zhang, A. Bernevig, T. Hughes, R. Li, X. Qi

This work explores fundamental physical processes which give rise to novel collective phenomena and self-assembled nanostructures resulting from high magnetic fields or complex synthesis processes. The complex nanostructures include antiferromagnetism inside the vortex cores and checkerboard charge order of the Cooper pairs in high T_c superconductors.

A major accomplishment of our research program is the theory of the "pair density wave" (PDW), which describes the checkerboard charge order of Cooper pairs in high T_c superconductors. Due to strong correlations or Fermi surface nesting, electrons can form a self-organized crystal like a Wigner crystal, or a charge-density-wave. In these charge-ordered states, the elementary unit cell contains only a single electron. On the other hand, the PDW state is a charge ordered state of the Cooper pairs, rather than single electrons. We showed that such a state could be favored in underdoped cuprates, where local pairing force is strong, but the kinetic energy of the holes is reduced. A global phase diagram was proposed to describe the competition between the antiferromagnetic state, the d-wave superconducting state and the PDW states. Most remarkably, the PDW state only exists at certain magic, rational doping fractions, *e.g.* at x=1/8, 1/16, 3/16, where the denominator is a power of 2. At these magic filling fractions, the Cooper pairs form a checkerboard structure.

Some of these theoretical predictions were soon confirmed experimentally. Earlier STM experiments at Stanford and Berkeley have uncovered microscopic charge ordering on the surface of high T_c cuprates. More recent STM experiments unveiled a more precise 4x4 checkerboard charge pattern on the surface of CaNaCuOCl crystals. Close to a doping level x=1/8, the charge ordering pattern is only consistent with the charge ordering of the hole pairs, in accordance with our theoretical proposal. Another remarkable transport experiment was carried out by Ando's group, in which they systematically measured the resistivity as a function of doping, and identified certain "magic doping fractions" at x=1/16, 3/16, 1/8 and 3/8, where the resistivity displays a maximum, indicating charge ordering tendencies. This observation is again consistent with our predicted global phase diagram.

The work on the pair-density-wave and charge ordering received broad attention in the high T_c community. It was featured in the "News and Views" section of *Science*, in an article entitled "Crystalline Electron Pairs." The PI was invited to speak at numerous international conferences, including the Gordon Conference and the Aspen winter conference. The two students working on the projects have successfully completely their Ph.D.s and are continuing their scientific careers through postdoctoral positions elsewhere.

6. Nanoscale Electronic Self-Organization in Complex Oxides

A. Kapitulnik, H. Manoharan, K.A. Moler, Z.-X. Shen, H. Bluhm, A. Fang, A.A. Geraci, C.W. Hicks, L. Mattos, K. Todd

Nanoscale ordering in complex oxides, where the valence electrons self-organize in ways qualitatively different from those of conventional metals and insulators, is one of the most important outstanding problems in physics today. Our research is inherently multi-disciplinary as is presented below.

ARPES Program

The nanoscience funding has enabled leverage of our core program on strongly correlated materials, as the students and postdoctoral associates are taking experimental shifts for each other. In addition to oxide materials, effort continues to explore nanoscale science in related materials. Collaboration has continued with Ian Fisher's group on charge density wave materials, and effort has been expanded on materials made of carbon nanoclusters.

Electronic Structure of Charge Density Wave State Rare Earth Tellurides – These materials manifest many competing phases with different electrical properties, and are ideal model systems for phase change materials – complex Tellurides used extensively as memory medium. In collaboration with the Fisher group, the ARPES investigation of the Tellurides from the tri-Tellurides to the di-Tellurides has been extended. Through ARPES, insights were gained on the electronic structure and the underlying reason for the charge density wave formation.

Electronic Structure of Solids Made of Carbon Nano-Clusters – We have made good progress towards understanding the electronic structure of molecular solids made of C_{60}. As was reported before, something was discovered that has been speculated for a long time but never observed before: dramatic change in the electronic structure with molecular orientation. In collaboration with the Osterwalder group of the University of Zürich, molecular rotations using photoelectron diffraction has been directly confirmed.

Solids made of carbon nano-clusters such as fullerenes and diamondoids have been studied. Preliminary data have been obtained on the diamondoids. These are interesting carbon nanoclusters with diamond structure but having their dangling bonds satisfied by hydrogen. They have the benefits of both diamond and nanomaterials and thus great potential for applications.

Magnetic Imaging Program

Using novel scanning techniques, studies continued of several high-T_c systems. In particular the study was emphasized of the interplay between magnetism and superconductivity. In addition, it was realized that much insight could be gained by continuing these studies with higher spatial resolution and lower temperatures. Much of FY2006 have therefore been devoted to the development of a He-3 based scanning Hall probe microscope with a new generation of Hall probes with 100 nm spatial resolution. Below are some of our advances in the past year:

The Mesoscopic Magnetic Imaging of Very Underdoped Cuprate – The existence of partial flux quanta was demonstrated, resulting from wandering pancake vortex stacks, in very underdoped YBCO.

Nanoscale Ferromagnetism, Antiferromagnetism, and Superconductivity in $ErNi_2B_2C$ – Hendrik Bluhm from the Moler group in collaboration with Suchitra Sebastian from Ian Fisher's group studied the interplay of ferromagnetism, antiferromagnetism, and superconductivity in $ErNi_2B_2C$. The coexistence of these three phases leads to fascinating nanostructured ferromagnetism. The first high-quality local magnetic images were obtained of this nanostructure, reaching two main conclusions. First, the twin boundaries in the antiferromagnetic state strongly pin vortices. This may be a new model system for planar pinning structures. Second, a spontaneous vortex lattice has been theoretically predicted to exist at low temperatures in the ferromagnetic state. It has been demonstrated that it does not.

It was demonstrated that a spontaneous vortex lattice does not exist in ENBC. Instead, we found a nano-scale magnetic texture. Upon completion of our He-3 based scanning Hall probe microscope, we expect to use the dramatically improved spatial resolution to make substantial progress on identifying the nature of this nano-scale magnetic texture, which results from the coexistence of multiple competing phases.

Magnetic Signatures of Time Reversal Symmetry Breaking in Sr_2RuO_4 – Per Bjornsson from the Moler group magnetically imaged the ab-plane surface of single crystals of the unconventional superconductor Sr_2RuO_4, including one sample with an array of micro-holes, using scanning SQUID and Hall probe microscopy in a dilution refrigerator at low applied magnetic fields. The images show dilute trapped vortices, as would be expected in conventional type-II superconductors, and no other magnetic features. No direct signs of the spontaneous magnetization were found that would be expected in a time reversal symmetry breaking (TRSB) superconductor. These measurements set upper limits on the presence of TRSB signatures in this material. Prof. Yoshi Maeno from the University of Kyoto spent three months in our lab collaborating on the further search for TRSB signatures. Characterization of this fascinating material will continue.

High Resolution STM Studies

This year a variable-temperature UHV STM was operated in pursuit of proposal goals. A new method was also developed to apply local stress to materials. Much development time has been spent on integrating these tools, including atomic dosing and manipulation, with the complex materials that are the focus of this research.

Nanoscale Ordering in Correlated Magnetic Materials – Using STM data acquired at IBM, Laila Mattos from the Manoharan group in collaboration with theorists Greg Fiete and Barbara Jones analyzed several artificial Kondo lattices and observed a coherence effect in which the Kondo temperature is enhanced in the center of lattices which are resonant with a 2D surface Fermi wavelength. In addition, a correlation hole (the "Kondo hole") in a central vacancy was demonstrated through this analysis. A manuscript was written and will be submitted to *Nature Physics* in the first quarter of 2006.

Local Electronic Structure in Novel Superconductors – A new method for applying pressure to thin superconducting samples was developed. In this apparatus, a piezo induces either uniaxial or biaxial stress in the plane of conducting layers of the compound under investigation. Strain gauges confirmed 70% strain transmission from the piezo to the surface of the samples. This method was applied to BSSCO to distort the unit cell with uniaxial compression and attempt to tune across phase boundaries, but pointed to the utility of using thin films rather than single crystals due to strain relaxation through the thickness of the sample. Achievable equivalent pressures were estimated at 30 to 90 atm.

Following an effort to learn how to prepare surfaces, tunneling spectroscopy measurements have begun on PbTe to explore the proposed charge-Kondo ground state in these materials synthesized by the Fisher group. Temperature-dependent spectra will be obtained that aim to get through the Kondo formation regime, but that cannot yet achieve the lowest temperatures (~1 K) necessary for superconductivity. No local tunneling spectroscopy measurements exist for these materials at any temperature; hence a priority has been placed on this achievement.

Piezo stress measurements are now being applied to $SrRuO_3$ and $Y_2B_4C_8O_{20-x}$ (Y-248) thin films grown by the Geballe group. The Y-248 sample is expected to have a superconducting T_c of ~81K, and an attempt will be made to detect a shift in T_c as stress is applied via our piezo apparatus. The $SrRuO_3$ sample displays a ferromagnetic phase transition at ~150K, which can be observed as a kink in the resistivity at the transition temperature. Measurements on epitaxially strained $SrRuO_3$ thin films have demonstrated that the T_c of this transition can be lowered to 30K in an 80 Å thick film (on $SrTiO_3$ substrate). Work will begin to observe and then tune this phase transition via piezo control.

Electronic Structure of Solids Made of Carbon Nano-Clusters –UHV STM imaging and spectroscopy was performed on solids and monolayers formed from a new form of carbon nanoclusters: diamondoids, nanometer-sized diamond molecules. These samples were provided through an agreement with Chevron who discovered them in crude oil. Doped diamondoid crystals and layers have the promise of being interesting electronic materials, and possibly superconductors following C_{60}. Data have been obtained from crystal molecule layers of diamondoids of the first 4 orders—namely 1, 2, 3, and 4 cages per molecule. Local spectroscopy revealed a variation in the bandgap, and sensitivity of the electronic structure to the rotational orientation of the molecules. These observations are very interesting in light of analogous measurements of ARPES on C_{60} by the Shen group. The Shen group is also collaborating with us and measuring ARPES on diamondoid layers. Our STM measurements are now being compiled in a manuscript for submission planned by April 2007.

Preliminary STM measurements on diamondoid solids reveal hints of vibrational structure revealed by inelastic tunneling spectroscopy. This will be investigated as the phonon structure can then be compared to C_{60} films and crystals and used for future studies of doping, metallicity, and possibly superconductivity.

STS of Ordered Structures on High-T_c Materials

In the past year the STM-STS system upgrade was completed for better stability and noise performance. As a first project to see the impact of the improved system, $Bi_2Sr_2CaCu_2O_{8+\delta}$ single crystals cleaved in UHV were again studied and measured at low temperatures. The study continues of ordered and inhomogeneous structures on BSCCO:2212 and there are plans to extend it to the single layer material BSCO:2201 produced by the group of M. Greven. The study of CDW in tellurides made by the group of I. Fisher will also be carried forward. This project will continue over the next few years.

Ordered Structures in the LDOS of BSCCO – Exploration continued of the newly remodelled system In particular, a very high-resolution study was performed of the gap structure in real space. 128x128 pixels on ~60 square samples yielded many interatomic spectroscopic points. Analysis of the coherence peak size which is much more pronounced, suggests that resonances due to bound states near the gap size can contribute to the coherence peak height. To further explore this possibility, very fine energy resolution was achieved by using the ability to minimize the voltage modulation needed to obtain the conductance data, as well as the integration time on the measuring lock-in. The results have been spectacular. Focusing on the superconducting gap, patches were found of what appear to be two different phases in a background of some average gap, one with a relatively small gap and sharp large coherence peaks and one characterized by a large gap with broad weak coherence peaks. These spectra were compared with calculations of the local density of states for a simple phenomenological model in which a $2\xi_0 x 2\xi_0$ patch with an enhanced or suppressed d-wave gap amplitude is embedded in a region with a uniform average d-wave gap.

Studies of $TbTe_3$ – In collaboration with Ian Fisher's group, and as complementary studies to ARPES, high resolution STM studies were performed of $TbTe_3$. The data show the topography of a $TbTe_3$ surface clearly revealing the CDW ordering. Close inspection of the topography indicates that the CDW periodicity is found in either three- or four-row repetition, averaging to a nesting-$|\mathbf{q}|$ vector of size 0.29, as is also found in the accompanying Fourier transform.

STS Studies of the CDW State of $CeTe_3$ – With the improved STM-STS system it is planned to study $CeTe_3$ to complement the initial studies of *$TbTe_3$*. Here the gap is expected to be larger (~400 meV) in optimally nested regions of the Fermi Surface (FS), whereas other sections with poorer nesting should remain ungapped. Using this instrument, both the CDW and the signal from the ungapped part of the Fermi surface will be observed.

Optical Tests for Time Reversal Symmetry Breaking in Sr_2RuO_4 – The construction has been completed of the first-ever zero-area fiber optical Sagnac interferometer for measuring absolute magneto-optic Kerr rotation at cryogenic temperatures. A single strand of Polarization-Maintaining fiber is fed into a liquid helium cryogenic probe, eliminating the need for optical viewports and makes the apparatus immune to temperature change. With an optical power of $10\,\mu W$ at 1550 nm wavelength, Kerr measurements are demonstrated on $SrRuO_3$ thin films with a shot-noise limited sensitivity of $1\times10^{-7}\,rad/\sqrt{Hz}$ from $250K$ down to $5K$ without any modulation of the magnetic state of the sample. Typical drift is measured to be $1\times10^{-7}\,rad/Hour$. This system is ready to be incorporated into a He-3 cryostat for measurements on Sr_2RuO_4.

7. Nano-Magnetism

J. Stöhr, H. Siegmann, Y. Acremann, V. Chembrolu, J. P. Strachan, X. Yu

The general goal of this program is to explore spin currents and the associated quantum mechanical exchange interaction for the excitation and switching of the magnetization in magnetic nanostructures. In particular, this program is based on the use of unique time-dependent X-ray imaging techniques with tens of nanometers spatial and tens of picoseconds temporal resolution.

The manufacture of nanoscale spin injection samples has been accomplished and X-ray imaging techniques have been developed with 30 nm spatial and 100 ps temporal resolution. Using time-dependent scanning transmission X-ray microscopy the changes induced in a buried magnetic sensor layer of 100 x 150 nm^2 dimension have been directly imaged by spin currents. These results reveal unique new curled magnetization states which arise from the interplay of spin and charge currents, as illustrated in Figure1.

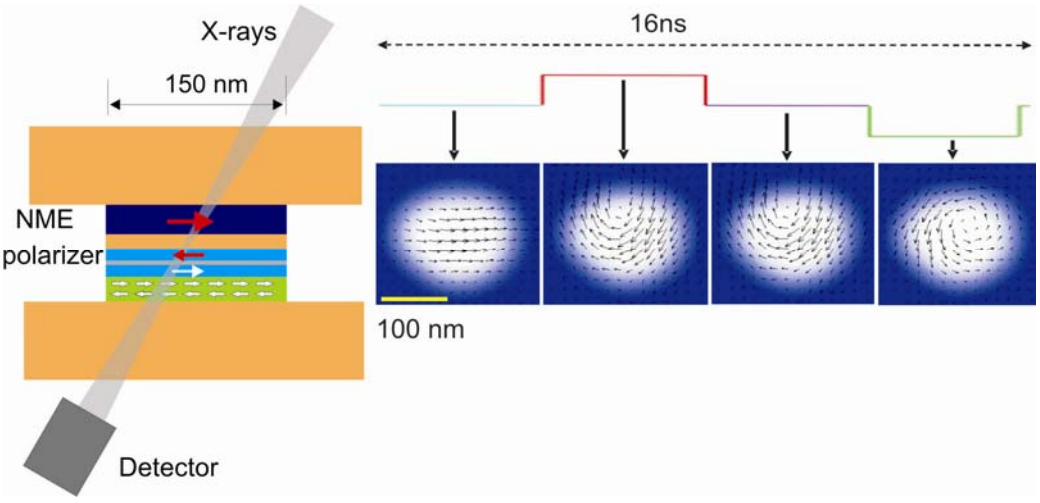

Figure 1. Left: Schematic of the pillar structure, showing the ferromagnetic layers in blue, the antiferromagnetic pinning layer in green and the Cu leads and spacer layers in orange. The bottom two FM layers are coupled into a fixed antiferromagnetic arrangement by a Ru spacer layer and

their magnetization direction is pinned by exchange coupling to the green antiferromagnet shown at the bottom. The incident X-ray beam is incident 30^0 from the surface normal and is focused by a zone plate to a size of about 30 nm. The transmission through the structure as a function of sample position is monitored by an X-ray detector.
Right: Measured time dependent magnetization directions indicated by arrows within the 4 nm thick $Co_{0.86}Fe_{0.14}$ sensor layer inside the 100 nm x 150 nm nanopillar. Images at four times are shown. By varying the delay time of the X-ray probe pulse relative to the current pulse entire motion pictures were recorded.

Motion pictures with 200 picosecond time resolution and 30 nm spatial resolution reveal a fast, subnanosecond switching process based on the lateral displacement of a magnetic vortex, as illustrated at four selected times in Figure 1. While the motion of vortices is omnipresent in nature their role in magnetic switching has previously remained unrecognized or unappreciated. Our measurements show how the injected spin current laterally displaces magnetic vortices created by the curled Oersted field of the accompanying charge current. The new fundamental switching process is intriguing in that it is accelerated by the curly Oersted field yet it may result in metastable final states which are undesirable in technological applications.

Now that the experiment technique has been established and demonstrated different magnetic configurations and sample geometries will be explored. Of particular interest are sample geometries where the electrical part of the current does not directly flow through the sensor layer but the effect of only the spin polarized electrons that diffuse into the sensor layer can be studied. This will be explored with new types of samples which do not have the form of a pillar but are planar. One of the main questions is whether the switching time in such "spin-current only structures" will be decreased by the absence of the Oersted field which accompanies the charge current.

8. Behavior of Charges, Excitons and Plasmons at Organic/Inorganic Interfaces

M.D. McGehee, N. Melosh, M. Brongersma

As electronic device dimensions shrink to nanometer scales and the range of desirable applications grows, two trends are emerging. First, the range of materials under serious development is growing, and many device structures consist of both organic and inorganic building blocks. Second, many physical phenomena that were heretofore only observed within academic experiments are becoming important for technologically relevant devices. Consequently, there are a large number of technical issues that need to be solved before these new possibilities become technologically viable. These include reproducible device performance on this length scale, sample heterogeneity, interface state control, defect properties, thermal transport and surface roughness. In addition, physical phenomena such as electron tunneling, Förster coupling, and plasmon-excitation quenching begin to severely impact device behavior at length scales less than 10 nm. This is particularly true within the emerging subset of structures that utilize both organic and inorganic materials, such as solar cells, electronic paper, molecular electronics, and organic light emitting displays. Within this rather broad collection of challenges, our team has identified the need to understand excited state behavior within organic species close to inorganic surfaces as a key problem for future applications of these materials.

Excited state phenomena within organic materials are often complicated by the multiple length scales, morphology, multiple competing decay processes, and inorganic surface interactions that affect the overall behavior of the system. Current studies of realistic devices are complicated by simultaneous excitation decay via a number of different processes within different regions of the sample. These decay processes, in which the charge or energy of an excited state in a molecule is transferred to an adjacent metal electrode, depend strongly upon the molecule to metal spacing.

In order to address these issues systematically, our team examines exciton transfer and decay within organic systems on a hierarchy of length scales. Melosh studies exciton transport and molecular wave function coupling to metal electrodes on the molecular level (~1 nm). McGehee examines exciton and charge transport within conducting polymer films close to metallic electrodes or dielectric films (5-100 nm). Brongersma investigates how excitons couple to surface plasmon waves on metal surfaces within the 10-500 nm range. Collectively, these measurements provide a better overall understanding of the behavior and importance of charges, excitons and plasmons within electrically active organic-inorganics than would be possible from a single study alone.

Charge Transport in Conjugated Polymers: The structure has been characterized and the charge carrier mobility measured of films of regioregular poly (3-hexylthiophene) P3HT as a function of molecular weight, casting solvent, annealing temperature and surface treatment. The primary characterization technique was X-ray diffraction at SSRL. It has been seen that when low molecular weight polymers and low boiling point solvents are used, crystals form rapidly in the bulk of the film. Consequently the crystals do not align with each other and the conjugated parts of the polymer chains do not stack up against each other at the grain boundaries. The charge carrier mobility can be as low as 10^{-6} cm^2/Vs. On the other hand, when higher molecular weight polymer and higher boiling point solvents are used, crystallization tends to occur only at the surface of the gate dielectric. Consequently, the crystals all tend to have the same orientation and charge carriers can easily hop from one crystal to another. The mobility in this case can be as high as 10^{-1} cm^2/Vs. These studies highlight how critical it is to optimize the structure of organic semiconductor films when assessing new molecules for applications. The initial demonstration used P3HT as the light absorbing and energy donating material. This polymer is actually a poor choice because it is not a good light emitter and therefore is not a good energy donor by the Förster mechanism. Better emitters have been used and it was found that energy transfer becomes effective over distances as large as 30 nm. Unfortunately, the energy levels of the polymer used were not suitable for splitting excitons at the interface between the two polymers. A goal for this year is to obtain suitable polymers from the Molecular Foundry and Jean Fréchet's group at UC Berkeley so that solar cells that utilize energy transfer over 30 nm distances can be made.

Exciton Transport in Conjugated Polymers: Almost all organic photovoltaic cells are based on either planar or bulk heterojunctions of two semiconductors. After light is absorbed, excitons must get to the interface between the two semiconductors to dissociate by electron transfer. In some cases, such as in dye-sensitized cells or polymer-fullerene bulk heterojunctions with very high fullerene concentrations, excitons are formed right at the interface and exciton transport is therefore not a limiting factor on the performance of the cells. In many other cases, such as in polymer-nanowire or polymer-titania cells, excitons need to travel at least five nanometers, if not more. For this reason exciton diffusion is a very important process to understand and optimize. Exciton diffusion must also be avoided in light-emitting diodes so that excitons do not reach quenching sites. The exciton diffusion length has been measured in several polymers and it was found that the values are less than reported in the literature. Common sources of error in diffusion length measurements are neglecting interdiffusion between the donor and acceptor, interference effects and resonance energy transfer. Since the diffusion length in most polymers is 6 nm or less, ways have been explored to enhance exciton transport. One is to use resonance energy transfer from a donor to an acceptor with a slightly smaller energy gap. It has been shown that exciton harvesting form P3HT, a polymer commonly used in the best polymer solar cells, can be improved by a factor of three by transferring energy to a low band gap polymer. This improvement in exciton harvesting triples the efficiency of solar cells made with P3HT. It has also been shown that resonance energy transfer occurs in many previously studied donor-acceptor blends, including polymer-fullerene blends with low fullerene concentrations.

Determining the Orientation of Organic Molecules at Buried Interfaces: It has recently been shown that crystals nucleate at the interface with the dielectric in polymer thin film transistors by analyzing XRD rocking curves and observing that the crystals could only be as well oriented as they are if they nucleate off of the interface. This technique will be used to address the general

question of how conjugated polymers pack at interfaces. This topic is particularly relevant to organic-inorganic solar cells. It is hypothesized that in some cases polymers, such as P3HT, pack with their side chains pointing towards a titania surface. For reasons not yet understood, in other cases the polymer packs with its conjugated backbone attached to the titania. It is thought that the cells with the backbone attached to the titania work much better because there is no barrier to electron transfer.

Omni-Directional Emitters and Plasmon Coupling: Brongersma demonstrated in a series of experiments and electromagnetic simulations that metal/light emitting molecule/metal optical microcavities can be engineered to produce an omnidirectional emission resonance. The two metal layers in this cavity have a clear optical function, but at the same time they also serve as electrical contacts for current injection. This is quite desirable from an electronics viewpoint as metals exhibit a low resistance. However, in current light emitting devices metals are generally avoided and more resistive transparent conductors such as Indium Tin Oxide are used as they allow for more efficient light extraction. Brongersma is interested in further exploring the use of metals in light emitters and exploiting the unique properties of surface plasmon-polaritons to increase the out-coupling efficiency, decrease the lifetime of emitters, and modify the angular emission distribution. In this study, he showed that for a cavity thickness equal to one-quarter of the surface plasmon resonance wavelength, $\lambda_{sp}/4$, a completely flat dispersion relation for surface plasmon-polaritons can be realized. Dipolar emitters placed in such a cavity radiatively decay into surface plasmon-polariton modes that subsequently couple to far-field radiation in all directions. This omni-directional resonance contrasts sharply with the typically highly directional resonant enhancements from waveguided modes in planar dielectric optical microcavities. In order to experimentally verify the predicted behavior, the angular emission from a blue-emitting polymer within a gold cavity was measured. In these experiments the omni-directional behavior was indeed observed and the work is currently being submitted to Applied Physics Letters. These studies may be of importance for the field of solid state light emission, which is rapidly gaining in importance in a number of applications such as traffic lights, room lighting, and displays. In particular, the observed isotropic emission is important in applications where a large viewing angle is desired.

Surface Plasmon Spectroscopy: The Melosh group has focused on investigating the optical properties of molecular films within metal-molecule-metal junctions and their behavior during electrical cycling. The goal is to resolve the dispute about molecular re-arrangements under high bias that may lead to different molecular conductivity, which has special importance for molecular electronics and understanding electron transfer near metal electrodes. A new technique has been developed, 'Surface plasmon spectroscopy' (SPS) to probe the optical absorption of molecular layers between metal electrodes. This method enables us to 'see' inside a 1-3 nm thick molecular film between two opaque metal electrodes. Based upon the Kretschman surface plasmon excitation architecture, this method relies upon the reflectivity change due to coupling into surface plasmons to measure the real and imaginary parts of the molecular film's dielectric constant. By repeating this measurement at multiple wavelengths the optical absorption spectrum can be obtained from the imaginary component of the dielectric constant.

It was discovered that the absorption of molecules on a *single* metal surface is almost identical to solution phase, however thin organic films placed between metal electrodes exhibit significant absorption maxima shifts (15-30 nm). These shifts are believed to be due to Stark effects within the junctions, and need to be included in electron transport calculations. Typically these junctions consist of an Au or Al bottom electrode 20-30 nm thick, a thin molecular layer 5-30 nm thick, and a top Au metal contact 15-30 nm thick. However, to simultaneously test the electrical response and optical absorptivity, new top metal contact methods are necessary to prevent pin-hole shorts through the molecular layer.

The limits of Surface Plasmon Spectroscopy will be pushed further in order to determine its maximum sensitivity and resolution. Measurements will be extended to include single molecular thick films of dye molecules R6G and 'active' molecules such as spiropyrans and [2]-rotaxanes. These active molecules change their optical, and presumably electronic, state upon either UV-

absorption or electrical redox chemistry, respectively. Studying the molecular reconfigurations using SPS within these systems will help us understand the nature of molecular electronic behavior in direct contact with electrodes, an important topic for emerging applications utilizing organic species together with inorganic structures.

In addition to direct optical studies, the change in optical properties will be examind as electrical bias is applied to metal-molecule-metal junctions. Molecules may include model systems such as alkanes, or conjugated systems like oligo-phenylethylene vinylene (OPEs). In order to take full advantage of these molecules, the PALO technique must be extended to be able to deposit the top float-on electrode onto a Au bottom electrode, which currently results in shorting. We believe this is due to the high mobility of the Au atoms under large applied bias, thus we are going to investigate methods to lift on Al top electrodes onto Au bottom electrodes.

Surface Plasmon Sources: Brongersma will continue his research in the area of Metal-Molecule-Metal junctions. In addition to using these junctions as light sources, he is interested in exploring the possibility to fabricate a surface plasmon-polariton source. To this end, new simulation tools will be developed that can quantify the emission out of the side of the junction and into surface plasmon-polariton modes. The Metal-Molecule-Metal junctions will be attached to a metal (plasmonic) waveguide that can guide the surface plasmon-polaritons over short (~ 10 μm) distances. Interestingly, the metal waveguide can again serve a dual purpose and act as the electrical contact to the source as well. The end goal is to fabricate a stable, low-noise, high intensity, and compact plasmonic source. These type of pigtailed sources could be of practical importance and can be used to ensure efficient coupling from light sources to optical waveguides and fibers.

Soft Contact Metal Deposition: In order to address electrical shorting in our evaporated metal devices, a new technique was developed to softly deposit the top metal contacts onto an organic film. Depositing the top metal contact for molecular electronics is always difficult, especially for near-atomically flat films. Sputter or e-beam deposited metals always damage the organic sample to some extent, while other 'soft' methods like lift-off float-on electrodes wrinkle excessively and stamped contacts are atomically quite rough. Our procedure, "Polymer Assisted Lift Off" (PALO), utilized a thin polymer as a backing to support pre-evaporated metal electrodes, which gave them mechanical strength and hydrophobicity. Using a nonadhesive metal deposited onto an ultra-flat substrate (mica or Si), the electrodes could be 'lifted-off' onto a water surface due to the hydrophobicity of the polymer (*e.g,* PMMA) layer. This floating set of electrodes could then be transferred onto a thin organic film without damage. A paper on the PALO method is under review by *Advanced Materials*.

Large electrode arrays were created with the PALO technique, with wire widths as small as 1 micron to as large as 3 mm, with lengths up to 3 cm. This is an extraordinary dimension for 20 nm thick metal films, (an aspect ration of 1.5 million!) especially without any wrinkling or buckling of the metal. This is a result of the thermodynamic driving force of the polymer layer to force the water from between the two surfaces, and the favorable maximization of the metal –water surface area. To demonstrate the utility of this technique, we performed studies of electron tunneling through carboxy alkanes with a PALO top contact. These devices demonstrated the same electron tunneling behavior as literature STM and nanopore measurements. Even with 4 mm^2 contact areas, no shorting is observed.

9. Development and Mechanistic Characterization of Alloy Fuel Cell Catalysts

A. Nilsson, P. Strasser, H. Ogasawara

The main focus of this research program is the investigation of mechanistic aspects of fuel cell catalysis on metal surfaces. One of the main challenges for the Hydrogen Fuel Initiative is to develop cost efficient electrocatalysts with high durability for the next generation of fuel cells. An essential aspect of this project is to develop synchrotron radiation based X-ray diffraction and

spectroscopy methods that allow *in-situ* probing of the intermediates in the catalytic cathode process where both species identification, geometric and electronic structure properties is fully characterized. In parallel to the fundamental synchrotron work, theory-guided combinatorial synthesis and high throughput electrochemical screening methodologies for fuel cell cathode catalysts will be developed and applied in order to link mechanistic hypotheses and catalyst testing under realistic conditions in high dimensional compositional and process parameter spaces.

Oxygen Reduction by Water on Surfaces: The adsorption of water on oxygen covered metal surfaces reduces oxygen to OH forming a OH-water co-adsorbed phase. This OH-water co-adsorbed phase is an important intermediate in fuel cell catalysis. XAS, XPS and STM studies were performed on the OH-water co-adsorbed phase on Pt(111) and Ru(001) surfaces. While the OH species is fully hydrogen bonded to surrounding water molecules on Pt(111), the OH species on Ru(001) is in a non-donor broken hydrogen bonded configuration.

***Wetting at Water on Surfaces*:** The fuel cell reaction occurs in confined spatial regions called triple phase boundaries where the gas, electrolyte containing water and catalytic metal particle contact. A wetting behavior of metal surface plays an important role in how triple phase boundaries. We demonstrated on Pt and Cu surfaces that the wetting is related to the difference in substrate electronic structure.

Instrument Development: An electron spectrometer equipped with three differential pumping stages was installed on surface science end-station at SSRL BL5-1 for the *in-situ* investigation of fuel cell reaction. A differentially pumped ambient-pressure reaction cell using cryogenic technology is being assembled.

Structural Molecular Biology

The primary purpose of work described here is to develop synchrotron radiation facilities and provide access for the national scientific community through a strong user support program. Such synchrotron resources are a powerful and versatile tool for research in structural molecular biology, and provide tools very relevant to addressing the U.S. Department of Energy mission needs. The scientific and technological focus of this program includes the applications of synchrotron radiation to macromolecular crystallography, small-angle X-ray scattering (SAXS) and X-ray absorption spectroscopy (XAS). These efforts are led at SSRL by Professors K.O. Hodgson, B. Hedman and W.I. Weis, and Drs. S.M. Soltis and H. Tsuruta.

Key aspects of the program being provided by the BER funding include:

- Continued availability to, and support of users on, state-of-the-art beam lines and instrumentation on the upgraded 3rd-generation SPEAR3 storage ring for SMB research for a significant fraction of a given year (~9 months or more per year)).
- Enhanced user support and training for SMB scientists using up to 10 existing stations at SSRL (of which eight are on high-intensity, multipole wiggler beam lines).
- Full operation and user research program on all three stations on the Beam Line 9 facility dedicated to SMB research.
- Continued development and implementation of advanced optics, experimental facilities, detectors, computer resources and software to enable optimal advantage to SMB users of the capabilities of the new 3rd generation SPEAR3 storage ring.
- Continuation of capital improvement projects in areas such as beam line enhancements, data acquisition systems including detectors, electronics, controls and computer hardware for SMB stations.

- Continued synergistic research and user support in the SMB area with the NIH National Center for Research Resources (NCRR)-funded Biomedical Technology Program (BTP) and the National Institute of General Medical Sciences (NIGMS)-funded macromolecular crystallography operations support and Structure Determination Core of the Joint Center for Structural Genomics.

BER Funded Staffing and New Opportunities for SMB R&D

The BER-funded scientific and technical staff at SSRL currently effectively support users of up to ten existing stations, including the three BER-funded Beam Line 9 SMB stations (BL9-1 and BL9-2 for macromolecular crystallography and BL9-3 for X-ray absorption spectroscopy). This is done in coordination with other specialized activities supported by NIH NCRR and NIH NIGMS. Ph.D. level research staff, currently all or in part supported by BER, are A. Cohen, R.P. Phizackerley, C. Smith, S.M. Soltis (in crystallography), S. DeBeer George, B. Hedman, K.O. Hodgson (in X-ray absorption spectroscopy), and H. Tsuruta (in small-angle X-ray scattering). Support is also continued for one summer month of salary support for Professor W.I. Weis (a term member of the SSRL faculty with primary appointment in the Department of Structural Biology on Stanford campus; a leading expert in multiple-wavelength anomalous dispersion (MAD) phasing who contributes significantly to continued developments and applications in this important area).

Professor A. Brünger has a joint appointment between SSRL (⅓) and the Stanford School of Medicine (⅔). His activities focus on computational and methodological macromolecular crystallography, and are having a very positive impact on providing new capabilities for SSRL users and staff. Funding continued in FY2005 and FY2006 for support of a graduate student research assistant (S. Kaiser) to work with Dr. Brünger on SSRL SMB-related developments.

Five-Year SMB Program Plan for Beam Line and Instrumentation Developments and for User Operations Support – A competitive five-year renewal proposal for the DOE-BER and NIH-NCRR funded SMB Resource at SSRL was submitted formally to NIH on June 1, 2004. As per discussion and agreement between the DOE-BER and NIH-NCRR program staff, this renewal formed the basis for a joint evaluation of the synergistically funded and managed SMB program at SSRL. The proposal contained developments directed specifically to the BER-funded program, which focuses mainly on developments and implementation of new instrumentation and beam line facilities to enable the SMB user community to benefit in the most optimum way from the new capabilities provided by the new SPEAR3 accelerator. The Special Study Section Committee, which performed a site visit at SSRL in November 2004, provided an exceptionally strong endorsement of the SSRL SMB program as a whole, and recommended that the BER funds requested for personnel, travel, materials and supplies and other non-equipment expenses, be provided at the budget level requested in the proposal. For equipment, it was recommended that all proposed items in the BER budget be funded with the one modification: a reduction in scope of a data storage system, from 300 TB to 100 TB. A FWP, modified according to the Study Section Committee recommendations and with a revised budget, was submitted to DOE-BER on 4/25/05. The proposed Operations Funding and Capital Equipment Funding in this FWP have since been revised and is consistent with programmatic guidance. The NIH-NCRR grant award for the five-year period of the SSRL SMB program has been made.

Structural Molecular Biology Program at SSRL

During the FY2006 run, the SPEAR3 accelerator continued to be exceptionally reliable, providing very stable beam for a very high fraction (96.2%) of the scheduled time, at up to 60+ hr life times. The new rapid fills, taking 1-3 mins each, became routine and greatly enhanced the use of beam time and the thermal stability of the optics. The FY2006 user run extended over a ~8 month period from ~November 28 through August 7, 2065. Outstanding utilization and performance were seen over the run period. About 50% of the proposals assigned time was for structural molecular biology-related research. Demand for beam time continues to be greater than the available beam time.

SSRL is planning a normal ~9 month/year run cycle, delivering (as do the other three DOE synchrotrons) about 5,000 user hours per year (*i.e.*, about 630 scheduled user shifts per year). SSRL has the goal of maintaining or increasing this by as much as 10% over the coming 3-5 years, paced by the needs for operational shutdowns for new beam line insertion devices and other planned upgrades and the availability of adequate base facility operating budgets from DOE BES (which are anticipated given the budget outlook for DOE-SC in the coming 10 years).

The strong demand for all the stations at SSRL continues. Over all the stations at SSRL, the overdemand averaged ~160%. Among the most severe in the overdemand category remain the crystallography stations, with a combined overdemand of ~230% for beam lines BL9-1, BL9-2 and BL11-1. The SAXS wiggler station BL4-2 was in overdemand by 176% despite having become a dedicated beam line for this technique and science, whereas BL9-3 (for XAS) was in overdemand by 267%, one of the highest in all of SSRL. The fraction of beam time on X-ray stations allocated to structural molecular biology research continues to be ~35-40% while the fraction of SMB users is ~45%. Since the majority of this beam time is awarded on a peer-review competitive basis among all SSRL proposals, SMB proposals continue to compete very well at SSRL.

User Satisfaction – As continuing part of user activities at SSRL, each user group is asked at the end of their run to complete an "End-of-run summary form". This form provides an opportunity for pointing out specific problems/issues and offering suggestions as to means of improvement. It also asks several questions to get a reading on overall satisfaction. The forms are analyzed by the SSRL staff and summaries by the SSRL Users Organization Executive Committee. The users rate in five categories (Unsatisfactory to Excellent). In the area of "Overall Scientific Experience" 24% overall were very good and 68% were excellent in FY2005 the FY2006 statistics are being compiled as of the writing of this document. These summaries included all the open SMB beam lines and users and, while subjective, indicate a significant measure of user satisfaction with the operation and service of the facility.

Beam Line 9 Upgrade Project – At the end of the FY2005 run, there remained, to replace the BL9-1 and BL9-2 monochromators as well as about 80% of the beam line masks, slits, filters, and windows. Additionally, motivated by the expected improvement in beam focus, the BL9-2 branch line needed to be realigned 0.4 mrad to the insertion device centerline. At the beginning of the 2005 shutdown, the initial focus was the installation, alignment, plumbing, cabling, and motion control tests of the in-alcove hardware. The BL9 in-alcove installation was completed successfully by November 2005, when attention turned to the out-of-alcove hardware installation. The BL9-1 and BL9-2 monochromators and the rest of the branch line hardware components for all three lines were installed and alignment was completed by January 2006. The low-conductivity water (LCW) system and associated machine protection system (MPS) sensors were replaced. Branch line commissioning began in late January. Staggered starts of user operations of all three branch lines (in order BLs 9-3, 9-2 and 9-1) took place during the month of February, and they are now in full use by the general user community. The upgraded optical components have already led to a demonstrated increased performance of 2X and 3X for BL9-1 and 9-2, respectively, over earlier operating conditions with SPEAR3. All branch lines for BL9 are now ready for SPEAR3 500-mA operations, which are anticipated to commence during specific periods in the next year's run cycle.

Beam Line 4 Upgrade Project – The BL4 500-mA upgrade project is yet to be completed due to overall budget constraints. Despite the comparative lack of resources (due mainly to the constrained DOE BES core budget that is sharing the upgraded cost of the BL and the significant cut in those funds in FY2006), many BL4 components including the LN_2-cooled monochromators, the monochromator slits, the graphite filters, the Be windows, and the branch line beam stoppers are in various stages of fabrication and assembly or are complete awaiting installation. In the coming months the mirror systems, mirror slits, fan allocation masks, pivot masks, and hutches will become the major focus of the BL4 upgrade effort.

One major and unexpected development in the BL4 upgrade project was the decision in FY2005 to relocate BL4 from its current location in Building 131 to adjacent to BL11 in Building 130.

This decision rests on several factors: (a) Rebuilding BL4 in a new location permits installation activities to commence while BL4-2 continues to serve the Bio-SAXS user community. This will minimize the BL4 down time since the existing BL4 need not be decommissioned until much of the new BL4 is already installed. (The relocated and upgraded BL4 will reuse only the existing BL4 insertion device, front end, hutch instrumentation, and much of the instrumentation and control suite.) (b) The new BL4 location incorporates a portion of the SPEAR3 concrete shield wall that already has been upgraded to current seismic standards. In contrast, the SPEAR3 concrete shield wall at the old BL4 location was scheduled for seismic retrofit in several years. Since the retrofit of this wall necessitates removal of nearby beam line hardware, relocation of BL4 avoids future disruptions of the beam line during this seismic retrofit. (c) The relatively unencumbered geometry of the new BL4 location simplifies the installation while affording the opportunity to optimize the beam line layout for improved performance, functionality, and user ergonomics. BL4-2 will continue in its new location to serve at 100% the general user community in the area of biological small-angle X-ray scattering/diffraction. Installation and re-commissioning of the new BL is anticipated to be complete in FY2007.

Beam Line 7 Upgrade Project – The end of FY2005 and the beginning of 2006 saw a flurry of activity and associated progress on the BL7 500-mA upgrade project such that the beam line at this point is a few working weeks away from the start of commissioning. Much of early FY2005 was spent assembling the remaining BL7 masks and optical systems in preparation for installation. The masks and mirrors to be installed inside the SPEAR3 shielding enclosure received the highest priority for attention to ensure that all such components were ready for installation during the tight summer 2005 installation envelope. The optical configuration of each branch line employs an in-alcove M_0 mirror for power filtering, harmonic rejection, and beam vertical focusing (BL7-1) or beam collimation (BL7-3). These single crystal silicon mirrors are side cooled through contact to water-cooled copper pads using a gallium-indium eutectic as a thermal transfer medium. During this same time period, the remaining "out-of-alcove" optical elements, masks, slits, windows, and vacuum transport systems were assembled. Several key elements, such as the BL7-3 LN_2-cooled monochromator, were assembled in prior years and stored for later installation. Among the key components assembled in FY2005 was the BL7-1 side scattering monochromator. This focusing monochromator employs a side-cooled, cube-root cut Si crystal assembly, like BL9-1 and BL11-1.

By the start of the SPEAR3 summer shutdown in August the vacuum assembly of the beam line optics and beam transport components was largely complete and the effort turned to the rapid disassembly and removal of the obsolete BL7 components and radiation enclosures (hutches). Within approximately one month from the start of the shutdown, the site of BL7 was stripped bare of virtually all optics, support hardware, and hutches, and this removal of the old hardware paved the way for installation of the new beam line. The most important installation milestone was the completion of the installation, alignment, plumbing, cabling, and motion control tests of the in-alcove optics and beam transport hardware prior to the close up and restart of SPEAR3 at the beginning of November 2006. While the in-alcove components were being installed, new radiation containment hutches were constructed in the out-of-alcove area. This task is nearing completion at this point, and the installation of the out-of-alcove beam line optics and beam transport is near completion. When complete, this rebuild will provide 100% general user access to BL7-1 for macromolecular crystallography, with the same infrastructure as provided for all other MC beam lines at SSRL, and BL7-3 will be dedicated to dilute solution biological X-ray absorption spectroscopy (100% general user), alleviating some of the oversubscription of BL9-3 and thereby providing more time for other techniques, such as microXAS imaging and single crystal XAS on BL9-3. The upgrade of BL's 7-1 and 7-3 is mainly funded from NIH NCRR.

Macromolecular Crystallography

For macromolecular crystallography, advances in instrumentation and beam line technologies continued in FY2006. During the FY2006 run, five MC beam lines were in operation with the new SPEAR3 lattice running at a current of 100 mA (BL11-1, BL9-2, BL9-1, BL1-5 and 50% of the available time on the shared station, BL11-3). The Stanford Auto-Mounting (SAM) system was

available on these beam lines. The SAM system incorporates a robot that can mount up to 288 samples without the user having to enter the experimental hutch and operates in an integrated environment within the Blu-Ice experiment control software that can be used to select and screen samples in a totally automated fashion. During FY2006, the SAM system was used routinely by a significant percentage of the user community. A high priority will be placed on optimizing the beam line in-hutch instrumentation for 500-mA SPEAR3 performance. Specifically, the newly rebuilt BL7-1 is being commissioned and made operational for the general user community (and as mentioned – this phase took place for BL9-1 and BL9-2 early in FY2006).

Beam Line 12 – New Capacity and New Experiments – The California Institute of Technology received a $12.7M gift from the Gordon and Betty Moore Foundation to fund the construction of a new high-intensity, state-of-the-art synchrotron beam line for MC research at SSRL. Under a cooperative research agreement, the use of the beam line will be shared between macromolecular crystallography general user community (60%) and scientists at the California Institute of Technology (40%). BL12 will make use of a powerful in-vacuum hybrid undulator source. The 67-period undulator with a 6 mm gap operating on SPEAR3 will produce a brightness of ~10^{18} p/s/mrad^2/mm^2/0.1%bp at an energy of 12 keV, approaching that of the APS UA undulator. The beam line will provide a very narrow energy band pass for optimized MAD experiments and is being designed to accommodate the study of microcrystals. With this very bright source, it is projected that samples with dimensions on the order of ~5-10 μm on an edge, and otherwise weakly diffracting crystals, will be able to be routinely studied.

The design and construction of BL12 is progressing well, with commissioning currently scheduled for early FY2007. The undulator ID was delivered in late June and has been installed in SPEAR3. The four dipole magnets required to produce the SPEAR3 orbit chicane for the new ID and the associated new SPEAR3 vacuum chamber have been installed. The quadrupole magnet triplet required to focus the SPEAR3 beam into a double waist for the BL12 ID was fabricated and installed during the summer 2005 SPEAR3 shutdown. The new SPEAR3 magnetic lattice incorporating the double waist was commissioned at 100 mA during the fall. More recently this lattice was successfully injected and run at 500 mA. The beam line front end has been installed. The three mirrors required for the beam line optical concept are currently being installed. The LN_2-cooled monochromator hardware has been installed and testing will commence shortly. Modifications to Building 131 and the SPEAR3 concrete shielding enclosure required to extract the beam were initiated and completed during the summer 2005 SPEAR3 shutdown. Overall, the beam transport systems are on schedule for completion by November 2006.

The hutch instrumentation is conceptually established, with the standard SSRL crystallography equipment and software being utilized wherever possible. The crystal mounting robot, cryostream and fluorescence detector systems will be replicated with some improvements. Modifications to the sample table and detector positioner to increase the stability of the sample handling system are being developed. The designs for systems needed for the visualization and manipulation of micro-samples have also been developed and are based on currently available technologies. A Mar325 CCD detector has been ordered for the beam line. BL12 will provide a state-of-the-art facility for SSRL's general users to carry out extremely rapid data collection and to routinely study challenging systems such as large complexes, viruses, micro-crystals, and weakly diffracting samples with large unit cells. Funding for general user operation for this beam line was included in the submission (and recommended) of the five-year peer-reviewed proposal to DOE BER, but has not yet been realized. It is our hope that funding for this purpose can be added beyond inflationary increases in the operations budget in FY2007.

Remote Data Collection – Since June 2005, macromolecular crystallography users have had the option to conduct remote user access data collection diffraction experiments from their home institutions and other remote locations by means of advanced software tools that enable control of the beam lines. Remote experimenters have access to the same tools as local users, and have the capability to mount, center, and screen crystalline samples, and to collect, analyze, and backup diffraction data. Automated sample mounting is accomplished with the SAM system. Beam line

and experimental control is carried out using Blu-Ice/DCS and additional remote monitoring of the experiment and data backup is supported with several web-based applications. The highly graphical applications and computational resources at SSRL are accessed through a client/server application that uses minimal resources on the client side and has a typical response close to that obtained at the beam line. This remote capability is now available on beam lines 1-5, 9-1, 9-2, 11-1, and 11-3, and starting in FY2006, 7-1.

Many of the applications required to perform a crystallography experiment are highly graphical in nature, and typically do not perform well through standard remote login techniques over large geographical distances. This problem has been addressed with the use of a terminal server application provided by NoMachine. This server is accessible to remote users through a free client application that is easily installed on their home computers. This system enables the user to run all command line and X-Window based applications available at the beam lines, including the Blu-Ice control software and data processing suites. SAM cassettes with preloaded samples are shipped to SSRL and a staff member loads up to three cassettes into the dispensing dewar at the assigned beam line and authorizes the user group to access the control system in a secure mode. Through a NX client remote desktop, the experimenter selects and mounts the samples from inside a cassette using the Blu-Ice software to access the SAM system. After a sample is mounted, it may be centered in the X-ray beam automatically, or if desired, the experimenter may manually adjust the crystal position by clicking on the video image, displayed at the home institution, of the sample within Blu-Ice. The SAM system can be configured for fully automated operation to screen large numbers of crystals while unattended. From within Blu-Ice, multiple samples can be selected for screening, and parameters for acquiring test diffraction data can be configured. An automated screening sequence is typically comprised of mounting the sample, aligning the sample loop to the X-ray beam, taking a diffraction image and video image at a phi angle of 0 and 90 degrees, and returning the sample into the cassette. This sequence is repeated for all selected samples. Automated scoring of the diffraction quality of each sample can be carried out. The scoring results are written to a spreadsheet to assist the user in selecting the best sample for data collection. The user can then start data collection on the best crystal, or a series of ranked crystals.

Users are becoming increasingly interested in operating the beam line and accessing computational resources remotely. Out of 65 beam time requests that were received during the June and July scheduling period, there were 18 requests (27%) for partial or full remote access. For the first FY2006 scheduling period, 25 requests (46%) for remote access have been received. To date, remote access has been used for more than 35 experimental user runs representing 20 research groups as far away as Australia and New Zealand. During the commissioning phase, NIAID members on a site visit at The Scripps Research Institute in La Jolla observed the remote screening of ~150 SARS related protein crystals on BL11-1. This screening run aided in the structure determination of a conserved domain from the severe acute respiratory syndrome coronavirus [K.S. Saikatendu, *et al.*, *Structure*, **13**, 1665 (2005)].

Other improvements to the macromolecular beam lines and equipment include:

Automated Crystal Annealing – Using automated crystal annealing techniques has been shown to decrease mosaicity and improve diffraction for some macromolecular crystal systems. SSRL now offers two methods for users (on-site and remote) to anneal samples, implemented through the Blu-Ice software and GUI. During data collection, a cold nitrogen gas stream flows over the crystalline sample to maintain it at cryogenic temperature. The crystal is annealed by letting the sample warm up to near room temperature, and then quickly cooling the sample back down to ~100 K. This may be initiated from the Blu-Ice GUI by either of two methods: *stream blocking* or *flow control*. The annealing time for both methods is set by the user and requires confirmation to prevent accidental annealing. The *stream blocking* method uses a thin paddle to physically block the nitrogen gas stream near the sample position. This device may be controlled through the Blu-Ice GUI or manually by pushing a button located on top of the unit. The paddle position is encoded so that the control system may check if the paddle is fully retracted out of the gas stream. The device is also spring-loaded so that the paddle will retract if power to the device is lost. The

main advantage of the *stream blocking* method is that the nitrogen stream is quickly blocked and unblocked, rapidly warming and cooling the sample. The second method for annealing, *flow control*, uses the nitrogen flow control settings of the beam line Oxford Cryojet to turn off the nitrogen stream from within the Cryojet dewar. Because there is a long transfer line between the Cryojet dewar and the sample position, the flow rate of the nitrogen stream at the sample position is changed more gradually than with the *stream blocking* method. The main advantage of the *flow control* method is that only the cold nitrogen stream is stopped and a warm nitrogen stream remains protecting the sample from icing.

A Universal Sample Container for Robots – The availability of robotic sample mounting systems continues to increase at synchrotron sources. Most of these are compatible with standard Hampton-style magnetic cryo-pins. However, many types of containers are used for sample pin transportation and storage. Currently at synchrotron beam lines in the US there are three main sample storage containers used: the SSRL cassette, the ALS puck, and the Molecular Structure Corporation (MSC) magazine. In an effort to minimize compatibility problems for users, a collaboration was initiated by SSRL with the ALS, the APS SBC-CAT and the industrial company, MSC to develop a "universal puck". The universal container resembles a standard ALS puck. The key differences between the universal container and the original ALS puck are that the universal container incorporates features of the SSRL cassette and provides the same clearance around the sides and bottom of the sample pin as an MSC magazine. Both the universal container enclosure and the base contain magnets and the assembly will be held together by magnetic force. All compatibility issues have been addressed, and the approach is believed to provide complete transferability between all three systems.

The enclosure piece of the universal container will be used inside the SSRL SAM dispensing dewar. To adapt the enclosure piece to the standard SAM setup an adaptor cassette has been developed. Four universal containers may be inserted into one adaptor cassette. The adaptor is then inserted inside the SSRL robot dispensing dewar using the cassette transport handle. Within the SSRL dispensing dewar the three cassette locations will each be capable of interchangeably holding an SSRL cassette or an adaptor cassette containing four universal containers. Once the development is complete, SSRL users will have the option to use SSRL cassettes (with a 288 total capacity) or universal containers (with 192 samples) and the SAM system will be programmed to sort samples between these two options.

Beam Line Simulator – Funding has been secured from a combination of DOE BER, NIGMS and NIH NCRR to build a macromolecular crystallography off-line facility for crystal screening and beam line instrumentation and software development. This facility will contain the electronics, computing, software, and hardware required to mimic a typical SSRL crystallography beam line (albeit with much lower flux). A Rigaku MicroMax X-ray generator source that was procured by the Joint Center for Structural Genomics (JCSG) group with funding from NIGMS will be installed on this facility. JCSG will also fund the robotic system and both JCSG and SMB Core staff will participate in the construction of the beam line simulator. A BER-funded high-precision computer-controlled table is in production. The control electronics and the final beam definition system have been acquired with funding from NIH NCRR, while NIGMS funds are used to procure a kappa goniometer, Cryo-Jet Cryo-cooler, detector positioning system and associated electronics. BER funding is also providing the enclosure and the infrastructure. Benefits of this off-line resource include: 1) an increase in the rate of new developments without using precious synchrotron beam time, 2) the availability of an additional screening facility, 3) provision for an X-ray source for screening when SPEAR3 is down and 4) use as a training location where new staff and users can receive hands-on instruction.

X-ray Absorption Spectroscopy

BL9-3, dedicated to general user biological XAS, accepts 2 mrad of the wiggler fan as a side station on the 16-pole 2-T hybrid wiggler BL9. BL9-3 provides extremely high intensity over a

broad X-ray energy range, with focused beam from ~4 keV to ~35 keV. The LN_2-cooled monochromator has two sets of Si(220) crystal pairs that can be brought in and out of the beam without breaking vacuum, providing a choice of two different azimuthal orientations of the 220 planes with different glitch patterns, allowing a choice for a given element/energy range. Its M_1 optic (after the monochromator) is configured such that the table does not move vertically during scanning, providing excellent stability and thus data quality. With SPEAR3, the focal spot is ~0.4 x 3 mm FWHM, producing a measured flux of ~2.2×10^{12}/100 mA at 9000 eV with 1x4 mm apertures. A factor of five will be gained at 500 mA. With careful adjustment of the collimating M_0 mirror, the beam line produces an energy resolution close to the theoretical limit. It is a superb BioXAS station and has enabled studies at μM concentration levels, bringing the experimental capabilities closer to physiological metal level in biological systems.

The upgrade for SPEAR3 500-mA operation was described above. The major impact of this upgrade has been to improve the beam line shielding and install beam line masks, slits, filters, and windows for the higher heat load. A significant additional improvement resulting from this upgrade is that the new pivot mask and beam line breakout in the SPEAR3 shield wall have made it possible to operate the BL9-3 M_0 mirror at lower incidence angle (thus higher energy cutoff). The operating range was during the FY2004 and FY2005 runs limited to ~5-23 keV. The new operating range at lower mirror angle will allow focused operations >30 keV. In the future, if user demand so requires and with additional shielding, fully unfocused operations will be possible with the upper energy cutoff determined by the Si(220) monochromator crystal limit of ~45 keV. A second improvement is that the liquid nitrogen feed lines for cooling the monochromator crystals were re-designed to allow remote operation by improving the routing of the lines. The previous lines required entry into the optics hutch (closing all three BL9 branch lines) to route the lines manually to avoid catching on other BL components and causing damage. This change will provide a significant improvement in efficiency for user-requested monochromator crystal changes.

In the 2004 submission, it was proposed and strongly endorsed that the current capabilities for measurements in the 2-5 keV range be moved from BL6-2, and that BL3-3 (a bending magnet beam line) be rebuilt for this purpose. It has more recently been realized that rather than upgrade the BL3-3 soft X-ray station in its current location, this branch line could be incorporated as a branch line on a new bending magnet line, BL14. This would allow for a more optimal optics layout and hutch setup, as the location provides for a "green-field" approach, at what is estimated to be the same cost. The optical concept for the station envisions a collimating mirror followed by a double crystal monochromator and a refocusing mirror. This beam line will be located in Building 130 between the new location of BL4 and BL13. Detailed design for this new beam line began FY2006.

Other development projects in FY2006 include:

Installation and Commissioning of a Hard X-ray Fluorescence MicroXAS Imaging System – A fluorescence microXAS imaging system, based on Kirkpatrick-Baez (KB) mirror optics, was made available to users on BL6-2 during FY2006. The KB optics were purchased from Xradia Inc. The KB optics is mounted on an optical rail inside a helium box. This He path reduces air absorption and scattering of the primary X-ray beam, providing higher flux and less signal background. The setup contains a high-precision slit aperture mounted downstream of the first, vertically focusing KB mirror, which enables varying the intercepted beam size of the optics. This allows trading focused flux for spot size by probing different areas and locations of the mirror surface. The commissioning began with the characterization of the X-ray beam at the location of the virtual source slit downstream of the KB optics. It was found that the beam line focus at this position was very close to the theoretical beam size obtained by ray tracing calculations. Depending on the size of the virtual source, a smallest focus size of about (2 (horz) x 3 (vert)) μm^2 with approximately 5×10^8 photons/sec/100 mA was measured by scanning a 100 μm diameter tungsten wire through the X-ray focus. The largest focus size is about (15 (horz) x 11 (vert)) μm^2, which is limited by the size of the beam line focus at the virtual source position.

Samples are mounted on a high-resolution x,y,z,theta sample stage allowing for sub-micron step sizes using a goniometer head with various sample mounting options for different types of samples. The sample itself can be observed by a high resolution long distance optical microscope with manual adjustable zoom, which is attached to a video camera/video server. A pellicle coated with about 100 nm of aluminum allows observing the sample in beam direction as the beam is scanned across the sample surface. This optical microscope is attached to a CCD camera/video server read-out and will simultaneously enable to optically locate and monitor certain areas of interest of the sample, which can then be easily moved in and out of the focal position. Currently the entire emitted fluorescence spectrum is detected as a function of position on the sample by an existing single element Si(Li) detector. In addition, a high resolution X-ray camera was developed in FY2005. This camera uses a very thin Gadox (P43) scintillator. An optical lens creates a magnified image of the X-ray beam on the scintillator onto a video camera with a magnification of about 2.5:1. This camera is important for characterizing the shape of the X-ray beam at various locations in the X-ray hutch. This camera improves and facilitates the optical alignment of the entire beam line as well as of the fluorescence microXAS imaging instrument. The K-B optic was funded by DOE BES and additional equipment and partial staff effort is provided from the SMB XAS program.

Instrumentation Development path is enclosed in a helium atmosphere. The existing setup achieves this by using flexible tubing which connects to a Plexiglas slit box (which includes a fluorescent screen for beam alignment) and then to the sample box. The setup requires manual adjustment of the slits and can only accommodate one sample at a time. Since at these energies external calibrations are necessary, frequent changes are required between the sample(s) of interest and the reference calibrant. This requires that the user enters the experimental hutch, changes the sample, and then allows the helium atmosphere to re-equilibrate. Although the setup is functional, significant improvements have been defined and a design is underway that will enable higher quality data, enhanced ease of use and more efficient beam time utilization.

Motorized slits in a KF-40 flanged vacuum- and helium-compatible configuration have been procured as a replacement for the manual slit system. The slits will be coupled to the beam line exit port and the sample box space using vacuum-compatible bellows, which will reduce potential helium leakage. Down-stream of the slits, a 6-way cross will be used to house a motorized linear motion feed-through, which will have both a fluorescent screen for sample alignment and reference calibrants for external calibration. A view port on one side of the cross will allow for viewing the beam size and position using an Applied Scientific Instruments LC150 camera, with a display at the work area. The opposite port will house a photodiode for fluorescent measurements from the reference calibrant. The design of the sample box space is still in progress, and will include both a shutter system (to minimize beam induce radiation damage) and a sample cooling system. During this year sample cooling options have been explored and tested, including a contact-cooled sample block (to -90º C), a Peltier-cooled setup, and a LHe flow cryostat with internal photo-diode detectors. In addition, improvements are being made to the existing detector electronics. This modified setup will be used on BL6-2, and will eventually be moved to BL14, when this beam line has been built (see below).

XAS Instrument Control System Software and Computing Developments – The SSRL developed Instrument Control System (ICS) forms the primary interface between control hardware and data collection software. The ICS software provides a consistent, convenient yet flexible interface to a large variety of different types of beam line hardware. These include, but are not limited to motors (D.C. and stepper), real-time clocks, counters, analog-to-digital converters and digital-to-analog converters. ICS supports devices controlled using CAMAC, VXI/VME, PXI, network, and RS232 based technologies. At present ~70 different devices are supported. The ICS software also includes a comprehensive set of subroutines for client programs that provide easy-to-use access to all devices in both a synchronous and asynchronous manner. During FY2005 several improvements, modifications and new instrument interfaces were added to the ICS software. It should be noted that all such changes have been made in such a way so that they can be easily ported to the new ICS software (see below) with a minimum effort. New device interfaces added

during FY2005 include: Lakeshore Temperature Controller, V535 VXI Stepper Motor Controller, Proteus XES Stepper Motor Controller, Newport XPS D.C. Servo Controller, Ortec Analog-to-Digital Converters, M550 CAMAC LVDT Reader, and a Vortex & XIA DXP Detector Electronics Interface. During the year, development was started on ICS interfaces for both the Radiant Vortex-EX and XIA DXP detector electronics. The Vortex software was used very successfully on BL9-3, both by SSRL staff and visiting scientists. It is anticipated that development of both the interfaces will continue in FY2006 and beyond.

Although the current production version of ICS (V.1.22) provides a robust, reliable and fully featured software interface, it can only be used on Alpha CPU based computers running the OpenVMS operating system. Unfortunately, Alpha CPU based technology is in the process of being phased out. A transition to different platforms is being conducted in three main areas: (1) the development of an Operating System Independent version of the ICS software; (2) the migration of SSRL Data Acquisition Software to the new Operating System Independent model; and (3) new computer systems to support legacy software during the transition away from Alpha based CPU computers. Significant progress was achieved in all three areas, and the new ICS software was commissioned on BL7-3 in the spring of 2006. ***s for XAS in the 2-5 keV Energy Region*** – An improved setup for XAS measurements in the 2-5 keV range is currently in development, in preparation for the new capabilities to be provided by a new bending magnet beam line, as proposed in the program proposal. In this energy range, X-rays have a very short path length in air and thus the entire beam

Also, significant progress was made in the design and development of a dedicated beam line network. Specifically a dedicated firewall machine was purchased, a Fortinet Fortigate 1000 (with a combination of DOE-BER and SMB DOE-BES funds). This firewall machine will be installed as a "fail-over" partner to an existing Fortigate 1000 firewall that already protects the SPEAR3 and Injector control systems. In addition, progress was made on the design of the Virtual Local Area Networks, or VLANs, that the firewall will provide. The design of the network is being undertaken with the assistance of the SLAC computer security team. It is anticipated that BL7-3 will be the first beam line to take full advantage of the new network architecture.

Small Angle X-ray Scattering/Diffraction

SAXS/D Beam Line 4-2 Operations – The SSRL small-angle X-ray scattering/diffraction facility on BL4-2 is dedicated to small angle X-ray scattering studies on biological systems. During the FY2006 run, the excellent beam characteristics created by the combination of the new low-emittance storage ring and the 20-pole wiggler, provided users with enhanced capabilities. Especially notable was the high stability of the photon beam as a direct result of the top-up injection scheme, which typically took 2-3 minutes three times a day, and helped stabilize the overall performance of the optics components. The stored electron ring current changed less than 20% between fills at 60+ hr lifetimes and the practically constant thermal load on the optics components resulted in the high beam stability. A number of user/staff research projects benefited strongly from these beam characteristics. It is also important to point out that several new exciting scientific projects were also initiated during FY2005, suggesting further growth in beam time demand and continuing need for advanced instrumentation for conducting challenging experiments.

SAXS/D Hardware Upgrades – In order to take advantage of the high-brightness SPEAR3 beam, a new instrument was built in FY2004. The main goals of this development were to 1) extend the range of instrument to both large characteristic length as well as to higher structural resolution, and 2) allow multiple instrument configurations during short beam time by automation. The new instrument incorporates the ability for automatically changing the sample-to-detector distance and a pair of built-in collimator/analyzer crystals in Bonse-Hart geometry for ultra-small angle X-ray scattering (USAXS) studies. The former feature allows users to select a desired sample-to-detector distance, thereby angular range, among five pre-designed distances, 0.5, 0.9, 1.4, 2.0, and 2.5 m. The Bragg spacings, $d=1/(2\sin\theta/\lambda)$, in Å covered by these distance ranges are: 4.6-270, 8.7-520, 13-790, 18-1100, 23-1400, respectively, assuming the use of a 9 keV X-ray beam and a 5-mm-diameter beam stop.

Development projects include:

Camera Improvements – For the new camera, developments focused on automated camera distance change and related improvements: (1) Several hardware improvements were made to facilitate distance changes. Three stages on a common optical rail, individually supporting the most upstream flange of the scattering path, the sample stage and the slit assembly, were linked together in such a way that a single motorized motion moves all at the same time, eliminating manual translation of the sample stage. (2) A new collimator assembly was built, consisting of two in-vacuum slits built by Advanced Design Consulting, two flexible bellows and vertical and horizontal translation stages. The distance between the two slits is adjustable between ~0.5 to 1.2 m, so that the up-stream slit can be used as a beam defining slit for shorter sample-to-detector distances. (3) The vertical translation stage for the sample position was replaced with one that provides a longer range. (4) Smaller hardware improvements for the camera setup include the design of a new static measurement cell holder, which features dry nitrogen paths around each sample cell slot to prevent moisture condensation so that measurements can be performed at temperatures significantly lower than room temperature, *e.g.,* 4°C. The ability to simultaneously achieve quasi-anaerobic conditions by nitrogen purging can be useful for those samples that are sealed in the standard sample cell, but normally require handling in a glove box filled with nitrogen gas. (5) The sample alignment video microscope was equipped with miniature vertical and horizontal translation stages and the cross hair can now be aligned with the direct beam position in the Blu-Ice software sample monitor window so that the user simply clicks on the exact location of the specimen to bring it into the beam (cross hair) automatically. (6) A split ion chamber for monitoring vertical beam position drift was built and installed. It is mounted on a precision motorized slide for vertical translation so that one quick vertical scan provides exact beam position at the most upstream location within the BL4-2 experimental hutch. All split ion chamber signals (top and bottom plates, difference and sum of them) can be monitored in Blu-Ice to keep track of direct beam position in case of unexpected beam positional shifts. The integrated ion chamber signal will be used as an incident beam intensity monitor when the new in-vacuum solution cell (see below) is used since the standard ion chamber, which records incident beam intensity immediately up-stream of the sample position, has to be removed when the in-vacuum cell is used.

Design and Construction of a New In-vacuum Solution Sample Cell – The first-generation in-vacuum cell performed well, but required substantial effort to align in the X-ray beam due to a few geometrical constraints. A new in-vacuum solution sample cell has been designed to eliminate these shortcomings while also providing additional new features. An X-ray capillary is mounted on a thermostated jacket, which is attached to a motorized vertical slide for alignment as well as for inserting and retracting the capillary cell in and out of the beam. The new in-vacuum cell will be permanently integrated with the pin-hole camera setup at the most upstream section of the scattering path, eliminating the need for installation and alignment in the beam each time it is needed. The small dimension of the enclosure (~2” in the beam direction) makes it possible to obtain higher angle scattering data by the use of a standard flat window solution cell holder immediately upstream of the in-vacuum cell. This way it is possible to quickly switch between the in-vacuum capillary cell and other sample holders. The black anodized enclosure of the new in-vacuum cell has six standard optic fiber receptacles for simultaneous light scattering and absorption measurements as well as illumination. A large glass window on the side is used for illumination and sample monitoring via a video camera, and a specifically designed port on the opposite side is used for exchanging the X-ray capillaries. The new in-vacuum cell is currently in assembly and will be commissioned in actual solution scattering experiments in FY2006. A Hamilton sample dispenser and a remote-controlled valve have been recently acquired. These are programmable devices either by the built-in controller of the dispenser or any computer via RS232 protocol. In FY2006 we will combine these devices with the new in-vacuum cell, a development aimed at high-throughput solution X-ray scattering studies. We intend to obtain a programmable sample changer, which would allow users to select one sample solution among many in the

standard 96-well plate and send it to the capillary cell. The dispenser would enable dilution series to be measured.

Software Developments and Improvements of the Computational Environment – Running SAXS/D experiments on BL4-2 previously required the use of separate beam line control and data acquisition software packages, which lacked communication between them. In order to solve this problem, we installed and customized the Distributed Control System (DCS) and the accompanying graphical user interface (GUI) Blu-Ice (developed for macromolecular crystallography by the SSRL SMB MC group) for small-angle X-ray scattering data collection at BL4-2 in FY2004. The DCS/Blu-Ice package brings a number of notable benefits including: (1) proven stability, (2) in-house origin and the large knowledge base at SSRL within the SMB group, (3) IP based client/server model that allows integration of the integrated control system (ICS), which is SSRL's other beam line control software, with data acquisition, (4) remote viewing and/or control of the experiment, (5) script based language and object oriented architecture that permit customization of existing features and addition of new functionalities and capabilities, and (6) X-windows based graphical user interface package (*i.e.* Blu-Ice) that can be run on multiple computer operation systems such as Microsoft Windows, Linux, Unix, and OS X (Macintosh).

Additional customizations and numerous improvements have been made to DCS and Blu-Ice to enable beam line staff members to condition the beam line and users to acquire data more efficiently. These improvements include: (1) automation of slit optimization, (2) automation of sample position search, (3) automation of camera length change, (4) automation of sample positioning, (5) new capabilities for multiple sample measurement, (6) new features to conditionally allow users to modify data acquisition conditions. Modifications were also made to a section of DCS so that data acquisition conditions can be recorded for later use in data analyses. Both the incident and transmitted beam intensities, integrated over the actual CCD exposure time, are now recorded synchronously, and they are written in the header portion of each 16-bit TIFF image files generated by the BL4-2 MarCCD165 detector. The same information and other experimental parameters are stored in a separate text file for future use.

Frequent sample-to-detector distance change is important for SAXS/D experiments to cover a wider range of scattering angles during a single slot of beam time. Additions to the Blu-Ice software in FY2005 have implemented automatic checking of vacuum levels and other sensors that are activated during camera length changes. If the sensors detect a fault, the camera length change will not proceed until corrections are made. The sample scan GUI was completely reworked. The users can find samples from the sample view image, set data acquisition parameters for each sample (up to a total of 10 samples), and, with one click, start data acquisition on all the samples. For each sample, the user can find the sample position in three alternative ways. Once the sample position is determined, the position parameters are automatically entered into a scan parameter table, and the user, for each sample, can set exposure time, number of exposures, and time intervals between each exposure, allowing for dynamic studies. This new GUI has made data acquisition using the MarCCD165 detector much more intuitive and effective at the same time, and has made user experiments more productive.

Bio-SAXS/D Linux File Server Improvements – During the FY2005 summer shutdown, we acquired a new and faster Linux PC as well as a larger capacity RAID disk array (860 GBytes), both purchased using DOE-BER funds, to completely replace the original BL4-2 computer in order to be ready for increased overall data throughput at BL4-2. The new file server also runs a Samba server program so that any SSRL Windows XP PC can read and write data files on the Linux computer directly over the network.

Molecular Environmental and Interface Science

Synchrotron radiation (SR)-based techniques provide unique capabilities relevant to environmental remediation science, and have emerged as major science and technology R&D tools in this field. The high intensity of SR sources coupled with X-ray photon-in/photon-out detection allows noninvasive *in situ* analysis of dilute, hydrated, and radioactive samples. SR techniques can be used to characterize the structural chemistry of non-crystalline solids, nanoparticles, environmental interfaces, bacteriogenic minerals, complex organic materials, and of metals sequestered within bacteria, plants, and dissolved in solution. Further, because of their high degree of collimation, SR X-rays can be focused to beams of micron dimension, allowing spatially resolved characterization of chemical species in microstructured samples, chemical microgradients, and microenvironments that often fundamentally control the behavior and release of contaminants in the environment, in waste forms, and in contaminated vessels.

- ***BER Funded Staffing and New Opportunities for MEIS R&D***

The goal of this program is to provide user support for BER ERSD-funded environmental remediation scientists and their collaborators at SSRL. This is accomplished through an integrated approach involving direct hands-on support, technique development, education and outreach efforts, and instrument development. Software support for instrumentation control and data acquisition is provided through a parallel effort for biological applications in the SSRL SMB XAS program, with BER-funded personnel.

User Support and Instrument Development – The key element of this user-support program is an ERSD-funded scientific staff member (Dr. Samuel Webb), who provides advice to users regarding experiment planning, hands-on training assistance at beam stations, and consultation regarding data analysis. Major techniques supported include X-ray absorption spectroscopy (XAS), X-ray diffraction (XRD), microbeam X-ray fluorescence chemical imaging (μ-XRF), and microbeam XAS/XRD. Another major element of the program is the development of innovative techniques for ERSD research. Presently, a microbeam spectroscopy/diffraction facility is being develop, optimized for experiments on U, Np, Pu, Tc, and other radionuclides that require high-energy X-rays, as well as for nonradioactive contaminants such as Cr, As, Se, Cd, Hg, and Pb. The microbeam facility is comprised of a Kirkpatrick-Baez (K-B) mirror pair, which focuses incident SR X-rays to a 2 micron spot, and various detectors, and includes sample positioners, video cameras, slits and ion chambers, all of which are mounted on an ambulatory optical bench. This facility will significantly enhance access to SR microbeam techniques for ERSD researchers, particularly to those national laboratory and academic programs located in the Western US.

Environmental Remediation Science Support Program at SSRL

BER-ERSD projects were conducted on beam stations BL11-2 and BL2-3 (XAS) and BL2-1 and BL11-3 (SR-XRD). A dedicated project scientific staff member, Dr. Samuel Webb, was hired to provide user support for BER-funded researchers, to help commission the microbeam system, and to implement the user support program at the microbeam system. Dr. Webb has 8 years of experience in the field of XAS-based environmental sciences, including three years as a postdoc at SSRL in Dr. Bargar's group, a demonstrated mastery of the experimental techniques required for the position, and a demonstrated strength in user support.

User Education and Outreach –A web site was created for the SSRL-based environmental remediation science community (http://www-ssrl.slac.stanford.edu/mes/remedi/index.html) to provide key information and links to resources for these users, including contact information, information on submitting proposals and obtaining beam time, beam station resources at SSRL, science highlights, and a primer on the application of synchrotron techniques to environmental remediation science. A workshop entitled, "Applications of Synchrotron X-ray Scattering Techniques in Materials and Environmental Sciences," was held on May 16 and 17, 2006.

Instrument Development – Activities centered on the design, implementation, and initial testing of an X-ray microprobe for μ-XAS, μ-XRD, and μ-XRF measurements. The microprobe is optimized for experiments on radionuclides of interest to BER researchers including U, Np, Pu, Am, and Tc, and it also provides experimental capability for a range of heavy metals, including Cr, As, Pb, and Sr. Initial hardware design, fixture fabrication, and assembly were completed in FY2005 and user operation began in FY2006. A high-resolution fast X-Y-Z scanning stage (required for μ-XRF imaging) and state-of-the-art digital spectroscopy amplifiers (DXP, Inc., required for both μ-XRF and μ-XAS capabilities) were procured and will be implemented during the current FY. The microprobe produces a focused beam of 2 μm diameter, which is close to the theoretical limit, and a flux of $3x10^7$ photons/s at 20 keV (100 mA current). A great deal of attention was focused on the mechanical stability of the system. The effective beam spot drift rates were reduced to 6.3 nm/h (horizontal) and 125 nm/h (vertical), well below the measured spot size of the beam. μ-EXAFS measurements on a 10 μm-diameter Mo wire (20 keV) show a high degree of reproducibility and low noise, suggesting that the mechanical stability of the system is adequate for planned measurements.

Capital Equipment – An X-ray area detector for μ-XRD measurements has been ordered and is expected to be commissioned in FY2007.

14. SCIENCE EDUCATION by Mike Woods

Education and promoting development of the next generation of scientists and engineers is a key part of SLAC's mission. The primary means for achieving this is by providing research opportunities at SLAC's facilities and centers for experiments in Particle Physics, Particle Astrophysics and Photon Science. A large number of graduate students are supervised by SLAC and Stanford faculty and a much larger number work with faculty at user institutions. In addition, SLAC provides educational opportunities for K-12 students and teachers, community college students and undergraduates. SLAC hosts or participates in several events each year that promote science and science education, such as SLAC Kids' Day and the DOE Science Bowl. SLAC also continued its successful Public Lecture Series, making the forefront science research carried out at SLAC accessible to the local community.

Precollege (K-12 Students and Teachers, Community College Students)
SLAC began participation in the DOE LSTPD teacher professional development program in 2006 with 1 high school teacher taking an 8-week summer internship. That teacher will be a lead teacher for an LSTPD program (to be renamed as DOE ACTS) at SLAC in FY07 that will offer a 4-week workshop for 9 middle school science teachers. Some high school students are hired for specific projects during the summer. SSRL, for example, hired 4 high school students in summer 2006.

Undergraduate Students
In summer 2006, 22 undergraduate students from around the country had summer research internships at SLAC, through DOE's Science Undergraduate Laboratory Internships (SULI) program. These students are housed on Stanford campus and carry out individual projects with SLAC scientists who mentor the students. SLAC's summer science program for undergraduates, now funded through SULI, has operated at SLAC for over 30 years. Two Stanford graduate students were co-directors for this year's program. There is a lecture series as part of the program and students prepare presentations and papers on their research work. The 22 student papers are collected into a SLAC Report. SLAC also supported one Pope Fellowship in summer 2006, which

is an internship for an undergraduate student at one of the user institutions whose faculty and students participate in SLAC's research program. In addition to these SLAC programs, a number of user groups bring undergraduate students to SLAC each summer, while a few more students are hired by SLAC staff scientists directly to work on specific tasks. SSRL, for example, had 9 undergraduates as direct hires for the summer and 23 working on synchrotron-based experiments as members of user groups in FY06.

Graduate Students

SLAC is a host for the research of large numbers of graduate students every year. These students work with SLAC and Stanford faculty, or with faculty from other institutions who carry out research at SLAC as users of the facilities, both in the Particle and Particle Astrophysics (PPA) programs and in the Photon Science (PS) programs. PPA currently has 57 Stanford graduate students pursuing Ph.D.s with SLAC faculty and there are an additional 9 1st year graduate students working at SLAC as rotation students for at least one quarter. About 30 graduate students are advised by SSRL or Stanford department faculty and work in a field related to Photon Science as part of their thesis work. SLAC graduate students represent a large range of scientific disciplines and are matriculated in several of the Schools of Stanford University, with home departments including Physics, Applied Physics, Materials Science and Engineering, Electrical Engineering, Chemistry, Structural Biology, Geological and Environmental Sciences, Molecular & Cellular Physiology, Neurology, and Neurological Sciences. Users bring a large number of graduate students to SLAC for their research, in particular for the BaBar experiment at PEP-II and for SSRL. SSRL hosted approximately 285 user graduate students in FY06, and the number was similar for particle physics and accelerator physics experiments at BaBar, PEP-II and the FFTB, NLCTA and ESA test facilities. Many of the user groups include non-US students who come to SLAC with faculty from their home institutions, in particular for the BaBar experiment at PEP-II.

Postdoctoral Scientists

SLAC is a major training ground for young postdoctoral scientists working either as SLAC or Stanford University employees or coming here as members of user teams. Postdocs benefit from intense training and immersion in the scientific opportunities provided by SLAC's facilities, working together with SLAC's faculty and staff scientists. Photon Science experiments at the SSRL and the Sub-Picosecond Pulse Source (SPPS) facilities hosted approximately 175 postdocs in FY06. The BaBar experiment at PEP-II and accelerator physics and test beam experiments at PEP-II, NLCTA, FFTB and ESA also hosted about 200 postdocs in FY06.

Affirmative Action Programs for Students

SLAC has a number of programs designed to enhance diversity in the sciences, including the following programs for students: the Youth Outreach Program (YOP) providing summer employment for local disadvantaged youths between ages 16-22; the National Consortium for Graduate Degrees for Minorities in Engineering and Science, Inc. (GEM) and the Work Study Program (WSP). 3 students participated in the YOP during FY06; 5 participated in GEM; and 4 participated in WSP. GEM students at SLAC come for summer employment for two or three consecutive summers. WSP students from local high schools and community colleges are provided part-time employment during the academic year and full-time employment during the summer.

Summer Schools

A large number of workshops are held at SLAC each year and provide opportunities for graduate students (and in some cases undergraduate students) to attend and present posters, talks and papers. Two summer schools were held at SLAC in 2006, which are targeted specifically to graduate students and young postdocs. This year, the topic for the 34th SLAC Summer Institute was "Exploring with the LHC" and it attracted 204 participants. The 5th joint Stanford-Berkeley Summer School on "Synchrotron Radiation and Its Applications in Physical Science" attracted 38 participants.

Events

SLAC's 5th Annual Kids@SLAC Day was held in August and attracted 250 children aged 9-16 years old. This fun and informative event provided an opportunity for kids to learn about what is done at SLAC, and to spark interest for potential science-related careers. A science talk on black holes, astrophysics and fundamental particles was given by KIPAC's Phil Marshall. Kids could attend several workshops, choosing from Optics, Mechanics, Astrophysics, Rockets, Waves, Electronics, Catapults, Monster Muscles, Paleontology, Radiation, Magnetics, Biology, Electric Motors, Vacuum and Welding.

SLAC hosted a regional DOE Science Bowl for high school students for the second time and again it was a great success. 25 high school teams from 16 schools competed. 60 SLAC staff and faculty participated as organizers, moderators, time keepers, score keepers and team escorts. Awards were presented by SLAC's Nobel Laureate Martin Perl.

SLAC staff volunteer to assist local schools and students in a number of ways, including invited presentations, demonstrations, and judging at Science Fairs. Four staff scientists judged Bay area regional science fairs in FY06. One staff member also serves on the board of *Expanding Your Horizons*, a science program for girls in Grades 6-12.

Public Lectures

The SLAC Public Lecture Series opens the doors to the inner workings of SLAC for the local nonscientific community. Lecturers describe what SLAC is all about: the research, the facilities, and the people that make this a world-class research institute. Refreshments are provided after the talks and attendees can chat with staff scientists and faculty, who are on hand to answer questions. Five lectures were offered to the public in FY06 to capacity audiences of over 300 people each. The topics for these lectures were the Big Bang, hidden dimensions, arsenic, the Archimedes palimpsest and comets.

Tours

Public Tours of SLAC are available to the general public and schools, for everyone 12 and older and are provided free as a public service. Tours include an overview of SLAC science, a view of the giant detectors required to observe subatomic particles and a stroll down the Klystron Gallery, the world's longest building. Approximately 1000 middle school students and an additional 1000 high school students toured SLAC in FY06. This includes Scout troops, groups from summer programs, and other youth groups. SSRL also hosts and guides student tours that are part of the curricula for undergraduate classes at Stanford and other Bay Area universities. Many public tours of SLAC are given, and for Stanford's commencement day, approximately 500 people toured SLAC.

15. FY06 SCIENTIFIC AND TECHNICAL INFORMATION MANAGEMENT by Patricia Kreitz and Sharon West

This year, InfoMedia (formerly Technical Publications) processed a total of 974 scientific and technical information (STI) documents and made all appropriate copies publicly accessible. During this year, SLAC and OSTI implemented a reporting methodology for multipart documents and SLAC began XML harvesting. For this year's assessment, all of SLAC's FY06 STI was reported in XML format and the totals for FY05 now reflect the total number of STI reported to OSTI that year, in both SGML and XML formats.
SLAC identifies STI publication products as preprints, preprint leaks, and reprints, as defined below.

Preprint	*Original manuscript submitted to SLAC for publication. When preprints are published, preprint numbers are assigned and electronic announcement records are harvested by OSTI that include a link to the electronic version.*
Preprint Leak	*Manuscript submitted to SLAC after publication elsewhere, but the original manuscript is available to SLAC. When preprints leaks are published preprint numbers are assigned and electronic announcement records are harvested by OSTI that include a link to the electronic version.*
Reprint	*Manuscript first published elsewhere—typically a journal—and the original manuscript is not available to SLAC. SSRL makes up the bulk of reprints due to the proprietary nature of that work. When reprints are processed, reprint numbers are assigned and electronic announcement records are harvested by OSTI, but a link to the text from the SLAC publications server is not provided.*

This year there was a 19% decrease from last year's total STI documents processed. For preprint reporting, this number is due to insufficient resources to perform extended outreach. For reprints, there seems to be a time delay between the actual journal publication date and the hands-on parsing of that metadata into the publishing system so these documents can be registered and reported. InfoMedia continues to work to streamline and improve these processes and supporting systems to ensure numbers better reflect current year reprint activity.

Table 1. Total OSTI Announcements Reported

	FY01	FY02	FY03	FY04	FY05	FY06
Total STI reported to OSTI	886	1,156	1,244	1,580	1,207	974

Table 2. OSTI Preprint Announcements

	FY01	FY02	FY03	FY04	FY05	FY06
Preprints	260	305	299	417	418	463
Preprint Leaks	69	207	435	438	370	263
Total Submitted to OSTI	329	512	734	855	788*	726
Leaks as Percentage of Total:	*21%*	*40%*	*59%*	*51%*	*47%*	*36%*

**The balance of 402 preprint records from FY05 and all FY06 preprint records were reported via the XML harvesting method.*

Table 3. OSTI Reprint Announcements

	FY01	FY02	FY03	FY04	FY05	FY06
SSRL Reprints	57	499	176	528	318	180
SLAC-HEP Reprints	500	145	334	207	101	68
Total Submitted to OSTI	557	644	510	735	419**	248

*** FY05 and FY06 reprint announcements were reported via the XML harvesting method.*

FY06 Accomplishments

Reduced Leaked Documents

There was an 11% reduction in the total number of preprint leaks processed this year. This decrease is due in part to previous year's outreach efforts as well as continuous improvement efforts to the leak and document workflow processes.

Implemented XML Harvesting and Improved STI Accessibility

- Developed automated two-way XML harvesting metadata collection and tracking system.
- Implemented XML harvesting.
- Continued effort to clean up repository of viable multi-part PDF files for legacy document harvesting.
- Developed requirements for new robust document management repository.

FY07 Plans

Harvesting of SLAC's Legacy Documents

SLAC plans to provide OSTI access to their scanned legacy documents, which were previously reported in hardcopy format. Preparation for this harvest includes verifying PDFs from scanned documents are optimum file sizes, and ensuring the OSTI ID numbers supplied by OSTI are cross-referenced in SLAC's databases. OSTI is currently in the process of developing lists of these OSTI IDs as a start.

Outreach Efforts

In support of SLAC's STI mandates, the SLAC Director will send a site-wide reminder to all SLAC authors, staff and users about their responsibility to register and submit their written work to InfoMedia to ensure that appropriate STI can be collected, managed, and reported.

16. FY 06 FOURTH GENERATION SOURCE DEVELOPMENT – THE LINAC COHERENT LIGHT SOURCE PROJECT by Mark Reichanadter

Project Authorization Milestones – The Project received approval of Critical Decision 3-B (Approve Start of Full Construction), in February 2006.

Environment, Safety and Health – A general safety coordinator and an expert construction safety coordinator provide safety expertise and support the LCLS organization throughout 2006. LCLS has in place a functioning Integrated Safety Management System (ISMS) through 2006. The LCLS project recordable incident rate is currently 0.63[2]. This compares favorably to general industry rates of 6.8 and that of the Department of Energy with is 2.1 for similar work. LCLS released the final draft of the Fire Hazards Analysis (FHA) for internal and DOE review and comments in June 2006. The FHA was approved and issued on schedule, in mid-July 2006.

Management – The LCLS management team was strengthened by adding two Associate Project Directors (Civil Construction and Engineering). Also, the LCLS procurement organization, 100% dedicated to LCLS but reporting to the SLAC Business Services Division Director, has been augmented by securing two procurement consultants with significant experience in DOE procurements and civil construction. The LCLS also hired a full-time Controls Manager who is responsible for integrating the existing SLAC controls infrastructure with the LCLS controls systems.

2006 marked the start of the delivery of the LCLS Long-Lead Procurements (LLP). In particular, LLP for the LCLS undulator titanium strongbacks, magnet poles and magnet blocks, the Injector Drive Laser, Sector 20 Laser Facility and a Magnetic Measurement Facility (complete with measurement and fiducialization equipment) were all procured in 2006. In addition, there were several refurbishment projects to prepare the SLAC site for the LCLS. These included the S24 stairway upgrade, BSY vertical wall upgrade, FFTB equipment and shielding removal, and excavation of activated soil in preparation for the start of LCLS construction in September 2006.

The LCLS project reports monthly performance, variances and contingency allocation against an approved baseline. Configuration management is in place which complies with DOE O 413.3. Monthly performance status is reported to DOE via the Project Assessment and Reporting System (PARS). LCLS conducted an Earned-Value Management System (EVMS) review with DOE's Office of Engineering, Construction and Management in order to validate the LCLS EVMS.

LCLS Scientific/Technical Progress – For 2006, the LCLS is primarily a 'design-procure-construct' project and has passed the 30% completion point. The Architect/Engineer has submitted the Title-II design package to SLAC for review at the "100% of Complete" stage. LCLS has contracted with a Construction Manager/General Contractor (CM/GC) who will prepare the construction bid packages and contract with trade contractors to build the LCLS civil construction. All bid packages for the LCLS have been solicited and approximately 70% have been awarded. LCLS has taken 'beneficial occupancy' of the Sector 20 Laser Facility and the Magnetic Measurement Facility.

For the main construction effort, SLAC-LCLS has cleared the Research Yard for the start of the main construction effort. This included the FFTB equipment removal and shielding, demolition of B113 and partial demolition of B102. A number of utilities were also removed or rerouted. In September 2006, the CM/GC has begun the main LCLS construction effort.

[2] The number of injuries sustained by an average crew of 100 individuals over one year.

LCLS has also begun installing the Injector and Linac beamlines and the Injector beam commissioning will begin early in 2007. The LCLS Drive Laser has been installed in the Sector 20 Laser Facility and preliminary commissioning activities are underway. The LCLS RF Gun has been fabricated and is now in final assembly and test. The new X-band klystron was tested at >50 MW with no performance problems identified. RF gun solenoid magnetic measurements are in progress, as are many of the LCLS 135 MeV injector beamline components.

The 2006 shutdown is under way during which installation is occurring of a large portion of the LCLS Injector beamline in SLAC's Linac and the LCLS Injector enclosures. At the completion of the installation, LCLS will begin preparing the LCLS Injector for commissioning.

Undulator production is under way using two undulator assembly vendors each of whom is approved to proceed with the assembly of undulators 3-16. At the end of 2006, a total of 12 undulators (30%) have been completed. The first production undulator has been acceptance tested and pretuned (K_{eff} set) on the Dover measurement bench in SLAC's Magnetic Measurement Facility (MMF).

A Single Undulator Test (SUT) was constructed at ANL, consisting of an integrated undulator system module from the floor up to verify undulator system and performance measurement. The SUT successfully tested all motion control and performance criteria against the physics requirements.

A prototype rf beam position monitor (BPM) has been installed in the ANL injector test stand and has undergone a series of beam tests. Although tests are not complete, a significant amount of information has been obtained and the design appears robust.

For LCLS photon systems, several new staff members have been added to the XTOD and XES teams. Prototypes of both the gas and solid attenuator systems have been developed that meet the physics requirements of the LCLS. LCLS-TN-06-1 "The Physics Analysis of a Gas Attenuator with Argon as a Working Gas," describes the use of argon gas to extend the gas attenuation for photon energies up to 8 keV. A "prototype" has been constructed with 3 small chambers, orifices, and data acquisition system to experimentally verify the pressure calculations. The design goal of 20-torr operation was met with stable operation with boil-off nitrogen up to a pressure of 60 torr observed. The measured pressure distribution and required gas flow are in good agreement with calculation.

The conceptual design of the X-ray slit subsystem has been developed. It is more compact than the previous design and has very few parts in the vacuum. Investigation into the feasibility of making the slit blocks as desired has begun. Thus far, they appear to be feasible to manufacture as conceived.

The XTOD group conducted damage experiments measuring the depths of any craters observed. The gas detector data from TTF provided measured fluence for each sample shot during the damage experiment. Clear correlation between the crater depths measured on the SiC sample with the gas detector fluences was observed. Pulse-to-pulse fluence was found to vary by 200% (lowest to highest). Applying the model to our single shot data taken at lower fluences has shown the damage threshold for SiC to be at about the melt dose which is consistent with expectations and indicates that these materials will perform under design conditions in the LCLS beam.

For the FEL Offset Mirror System, calculations were performed of the predicted FEL characteristics after reflection from state-of-the-art X-ray mirrors. The calculations predict some broadening of the FEL beam after reflection from mirrors of these types. A set of specifications consistent with this performance is being prepared for use in obtaining vendor quotes and developing physics requirements for the mirrors.

Cornell University is collaborating on the LCLS 2D detector project as this project ramps up during its second year.

The experimental capabilities desired by the AMO group have been substantially defined: a chamber with a pulsed or continuous gas jet, with multiple electron time-of-flight spectrometers, ion spectrometer for charge state determination and ion imagining, and one or two X-ray fluorescence spectrometers.

Detailed information on the Project status and issues may be found in the Monthly Reports, posted at http://www-ssrl.slac.stanford.edu/lcls/internals/monthlyreports/ .